

# Inertial Effects in Suspension Dynamics

Thesis by

Ganesh Subramanian

In Partial Fulfillment of the Requirements

for the Degree of

Doctor of Philosophy



California Institute of Technology

Pasadena, California

2002

(Defended April 15, 2002)

© 2002

Ganesh Subramanian

All Rights Reserved

## Acknowledgements:

To begin with, I wish to acknowledge my advisor, John Brady, for his encouragement and support through this odyssey. My academic discussions with him have always been illuminating and his acute physical insight will continue to be a source of inspiration. I also thank my group: Mike and Sundar for guiding me through the initial days of uncertainty, and Ileana, in particular, for keeping my spirits up and the flame burning as the journey was nearing its end.

Among people at Caltech, Murtuza, Amit and Anu have been very helpful at different stages in my PhD. I am indebted to Prakash and Vidya for inculcating in me, a love for Indian classical music. Outside of Caltech, my friends Satish and Aravind have been pillars of support. Satish especially has always been a willing confidant; his short stay in California is one I will always cherish.

Finally, I wish to thank my parents and sister to whom I owe everything.

## Abstract

This work analyses the role of small but finite particle inertia on the microstructure of suspensions of heavy particles subjected to an external flow. The magnitude of particle inertia is characterized by the Stokes number ( $St$ ), defined as the ratio of the inertial relaxation time of a particle to the flow time scale. Fluid inertia is neglected so that the fluid motion satisfies the quasi-steady Stokes equations. The statistics of the particles is governed by a Fokker-Planck equation in position and velocity space. For small  $St$ , a multiple scales formalism is developed to solve for the phase-space probability density of a single spherical Brownian particle in a linear flow. Though valid for an arbitrary flow field, the method fails for a spatially varying mass and drag coefficient. In all cases, however, a Chapman-Enskog-like formulation provides a valid multi-scale description of the dynamics both for a single Brownian particle and a suspension of interacting particles. For long times, the leading order solution simplifies to the product of a local Maxwellian in velocity space and a spatial density satisfying the Smoluchowski equation. The higher order corrections capture both short-time momentum relaxations and long-time deviations from the Maxwellian. The inertially corrected Smoluchowski equation includes a non-Fickian term at  $O(St)$ .

The pair problem is solved to  $O(St)$  for non-Brownian spherical particles in simple shear flow. In contrast to the zero inertia case, the relative trajectories of two particles are asymmetric. Open trajectories in the plane of shear suffer a downward displacement in the velocity gradient direction. The surface of the reference sphere ‘repels’ nearby trajectories that spiral out onto a new stable limit cycle in the shearing plane. This limit cycle acts as a local attractor and all in-plane trajectories from an initial offset of  $O(St^{\frac{1}{2}})$  or less approach the limit cycle. The topology of the off-plane trajectories is more complicated because the gradient displacement changes sign away from the plane of shear. The ‘neutral’ off-plane

trajectory with zero net gradient displacement acts to separate trajectories spiralling onto contact from those that go off to infinity. The aforementioned asymmetry leads to a non-Newtonian rheology and self-diffusivities in the gradient and vorticity directions that scale as  $St^2 \ln St$  and  $St^2$ , respectively.

# Contents

<b>1</b>	<b>Introduction</b>	<b>1</b>
	<b>Bibliography</b>	<b>8</b>
<b>2</b>	<b>Multiple scales analysis of the Fokker-Planck equation for a single Brownian particle in simple shear flow</b>	<b>11</b>
2.1	Introduction . . . . .	11
2.2	Problem formulation . . . . .	14
2.3	Brownian motion in simple shear flow . . . . .	19
2.3.1	Exact solution . . . . .	20
2.3.2	Multiple scales analysis . . . . .	24
2.4	Comparison of exact and multiple scales solutions . . . . .	36
2.4.1	Multiple scales solution for a Maxwellian initial condition . . . . .	36
2.4.2	Multiple scales solution for a delta function initial condition . . . . .	42
2.4.3	The athermal limit . . . . .	45
2.5	Conclusions and discussion . . . . .	48
	<b>Bibliography</b>	<b>51</b>
<b>3</b>	<b>Chapman-Enskog formulation for the Fokker-Planck equation</b>	<b>53</b>
3.1	Introduction . . . . .	53

3.2	Equivalence of the Chapman-Enskog and multiple scales formalisms for a single Brownian particle in an external flow . . . . .	55
3.3	Chapman-Enskog method for a configuration dependent drag force in one dimension . . . . .	59
3.4	Chapman-Enskog method for inertial suspensions . . . . .	64
3.4.1	Introduction . . . . .	64
3.4.2	Problem formulation . . . . .	67
3.4.3	Multiple scales analysis . . . . .	71
3.4.4	Higher order inertial corrections . . . . .	88
3.5	Conclusions . . . . .	91
	<b>Bibliography</b>	<b>93</b>
<b>4</b>	<b>Trajectory analysis for inertial non-Brownian suspensions: In-plane trajectories</b>	<b>95</b>
4.1	Introduction . . . . .	95
4.2	Equations for particle trajectories . . . . .	97
4.3	Nature of inertial velocity corrections for small Stokes numbers . . . . .	103
4.4	Relative in-plane trajectories of two spheres in simple shear flow . . . . .	109
4.4.1	Open trajectories with initial offsets much greater than $O(St^{\frac{1}{2}})$ . . . .	115
4.4.2	The effect of hydrodynamic coupling on the in-plane gradient displacement . . . . .	127
4.4.3	In-plane Limiting trajectory . . . . .	130
4.4.4	Far-field analytical expression for in-plane gradient displacement . . .	136

4.4.5	Calculation of in-plane self-diffusivity in the velocity gradient direction ( $D_{zz}^{ip}$ ) . . . . .	140
4.4.6	Behavior within the limiting trajectory . . . . .	147
	<b>Bibliography</b>	<b>160</b>
<b>5</b>	<b>Trajectory analysis for inertial non-Brownian suspensions: Off-Plane trajectories</b>	<b>163</b>
5.1	Introduction . . . . .	163
5.2	Relative off-plane trajectories . . . . .	166
5.2.1	Off-Plane open trajectories . . . . .	166
5.2.2	Off-plane spiralling trajectories . . . . .	170
5.3	Perturbation analysis for off-plane trajectories . . . . .	176
5.3.1	Open trajectories with initial gradient offsets much greater than $O(St^{\frac{1}{2}})$ .178	
5.3.2	Open trajectories with initial gradient offsets of $O(St^{\frac{1}{2}})$ . . . . .	186
5.3.3	Far-field analytical expressions for lateral displacements $\Delta z$ and $\Delta x$ .	199
5.3.4	Scaling of self-diffusivities in the velocity gradient ( $D_{zz}$ ) and vorticity ( $D_{xx}$ ) directions . . . . .	209
5.4	Comparison with direct numerical simulation of pair trajectories . . . . .	212
5.5	Microstructure and rheology . . . . .	216
	<b>Bibliography</b>	<b>219</b>
<b>6</b>	<b>Conclusions</b>	<b>222</b>
	<b>Bibliography</b>	<b>225</b>

<b>A</b>	<b>Appendices for Chapter 2</b>	<b>226</b>
A.1	Free Brownian motion . . . . .	226
A.1.1	Exact solution . . . . .	227
A.1.2	Multiple scales analysis . . . . .	229
A.1.3	Failure of the naive multiple scales scheme . . . . .	233
A.2	Two-time-scale expansions of the exact solutions . . . . .	235
A.3	Inertial corrections to equation (2.36) for $b_{m,n}^{(0)}$ . . . . .	240
A.4	Identity of exact and multiple scales solutions of section 2.4.2 . . . . .	244
A.4.1	Identity of leading order solutions . . . . .	244
A.4.2	Identity of $O(St)$ velocity-dependent corrections . . . . .	250
A.5	Solution to the inhomogeneous Smoluchowski equation . . . . .	259
A.5.1	Green's function for the Smoluchowski equation . . . . .	259
A.5.2	A Green's function identity . . . . .	260
<b>B</b>	<b>Appendices for Chapter 3</b>	<b>263</b>
B.1	The $O(St)$ Chapman-Enskog solution, $\bar{P}_M^{(1)}$ , for general $M$ . . . . .	263
<b>C</b>	<b>Appendices for Chapter 4</b>	<b>266</b>
C.1	The $O(1)$ and $O(St)$ velocity fields . . . . .	266
C.2	$O(St)$ solution in the outer layer O1 . . . . .	270
C.3	Non uniform nature of the $O(St)$ corrections for zero-Stokes closed trajectories	272
C.4	In-plane open trajectories with initial offsets of $O(St^\beta)$ ( $0 < \beta \leq 1/2$ ) . . . . .	274
<b>D</b>	<b>Appendices for Chapter 5</b>	<b>279</b>
D.1	Gradient displacement $\Delta z$ in the limit $x^{-\infty}, z^{-\infty} \gg 1$ . . . . .	279

## List of Figures

1.1	Parameter plot delineating the domain of validity (shaded region) of our work.	4
2.1	Iso-probability contours in simple shear flow for $St \geq 0$ .	33
4.1	One-dimensional approximation for the relative velocity of approach for two spheres. Initial condition: $u_0 = 5, y_0 = 1$ .	108
4.2	One-dimensional approximation for the relative approach velocity of two spheres. Initial condition: $u_0 = 0.1, y_0 = 1$ .	108
4.3	Finite $St$ open trajectory with $O(1)$ initial offset.	115
4.4	Stresslet velocity field induced by a sphere in shear flow.	128
4.5	Finite $St$ limiting trajectory in the plane of shear.	131
4.6	The critical offset ( $m_1^c St^{\frac{1}{2}}$ ) values obtained from numerical integration of the in-plane trajectory equation (4.25) are plotted as a function of $St^{\frac{1}{2}}$ .	136
4.7	Tracer particle (darker shade) undergoing a random walk due to successive uncorrelated pair-interactions.	141
4.8	Trajectory spiralling into the limit cycle for $St = 0.2$ .	154
4.9	Trajectory spiralling into the limit cycle for $St = 0.2$ .	154
4.10	Trajectory spiralling out onto the limit cycle for $St = 0.2$ .	155
4.11	Trajectory spiralling into the limit cycle for $St = 0.1$ .	156
4.12	Trajectory spiralling into the limit cycle for $St = 0.1$ .	156
4.13	Trajectory spiralling out onto the limit cycle for $St = 0.1$ .	157
4.14	Trajectory spiralling into the limit cycle for $St = 0.02$ .	157

4.15	Trajectory spiralling into the limit cycle for $St = 0.02$ . . . . .	158
4.16	Trajectory spiralling out onto the limit cycle for $St = 0.02$ . . . . .	158
4.17	Phase plane of trajectories for $St = 0$ in simple shear flow. . . . .	159
4.18	Phase plane of trajectories for finite $St$ in simple shear flow. . . . .	159
5.1	Zero $St$ off-plane open trajectory for $x^{-\infty} = 0.5$ and $z^{-\infty} = 0.15$ . . . . .	164
5.2	Off-Plane open trajectory for $x^{-\infty} = 0.5$ , $z^{-\infty} = 0.15$ and $St = 0.1$ . . . . .	164
5.3	Off-Plane closed orbit starting through $(x, y, z) \equiv (0.1, -3, 0)$ . . . . .	165
5.4	Inward spiralling off-plane trajectory starting from $(x, y, z) \equiv (0.1, -3, 0)$ for $St = 0.1$ . . . . .	165
5.5	Axisymmetric separatrix envelope enclosing closed orbits at $St = 0$ . . . . .	167
5.6	Modified $St$ spiralling trajectories within the modified separatrix envelope. . . . .	171
5.7	Geometric relation between gradient and vorticity displacements . . . . .	185
5.8	Off-Plane inertial trajectory with $O(St^{\frac{1}{2}})$ initial gradient offset. . . . .	186
5.9	Off-Plane open trajectory for $x^{-\infty} = 0.5$ and $z^{-\infty} = 0.5$ . . . . .	194
5.10	Limiting off-plane open trajectory for $x^{-\infty} = 0.5$ and $z^{-\infty} = 0.12$ . . . . .	195
5.11	Off-plane open trajectory for $x^{-\infty} = 1.5$ and $z^{-\infty} = 0.5$ . . . . .	196
5.12	Off-plane open trajectory for $x^{-\infty} = 1.5$ and $z^{-\infty} = 0.15$ . . . . .	196
5.13	Limiting off-plane open trajectory for $x^{-\infty} = 1.5$ and $z^{-\infty} = 0$ . . . . .	197
5.14	Spiralling off-plane trajectory starting from $(x, y, z) \equiv (1.8, -1, 0)$ . . . . .	197
5.15	Off-plane trajectory starting from $(x, y, z) \equiv (2, -0.5, 0)$ and spiralling off to infinity. . . . .	198
5.16	In-Plane trajectory starting from $(x, y) \equiv (-2.03, 0.9)$ for $St = 2$ . . . . .	216

## List of Tables

4.1	$(\Delta z)_{inplane}$ values with and without the $\mathbf{U} \cdot \nabla_{\mathbf{x}} \mathbf{\Omega}$ contribution: $St = 0.1$ . . . .	129
4.2	Comparison of theoretical and numerical values of the critical offset in the shearing plane. . . . .	135
4.3	Comparison of numerical and analytical values, and the far-field approximation (4.55) of $(\Delta z)_{inplane}$ for $St = 0.1$ . . . . .	140
4.4	Comparison of analytical and numerical values of the in-plane diffusivity for different Stokes numbers. . . . .	147
5.1	$\Delta x$ values for $x^{-\infty} = 0.2$ and $z^{-\infty}$ ranging from 5 to 0.1; $St = 0.1, 0.01$ . . . .	184
5.2	$\Delta x$ values for $x^{-\infty} = 1$ and $z^{-\infty}$ ranging from 5 to 0.1; $St = 0.1, 0.01$ . . . .	184
5.3	Limiting offsets for off-plane trajectories for small $x^{-\infty}$ ; $St = 0.1, 0.01$ . . . .	191
5.4	Values of $\Delta z$ for $x^{-\infty} = 1.5$ and 5, $z^{-\infty}$ ranging from 5 to 0.1; $St = 0.1, 0.01$ . . . .	193
5.5	Comparison of numerical and the far-field approximation (5.42) of $\Delta x$ in the limit $x^{-\infty}, z^{-\infty} \gg 1$ for $St = 0.1$ . . . . .	201
5.6	Comparison of numerical values and the far-field approximation (5.43) of $\Delta z$ in the limit $x^{-\infty}, z^{-\infty} \gg 1$ for $St = 0.1$ . . . . .	204
5.7	Comparison of numerical values and the analytical approximation (5.44) for $\Delta x$ in the limit $x^{-\infty} \gg 1, z^{-\infty} = 0$ for $St = 0.1$ . . . . .	206
5.8	$\Delta x$ and $\Delta z$ values for $x^{-\infty} = 0$ and $z^{-\infty}$ ranging from 5 to 0.1. . . . .	214
5.9	$\Delta x$ and $\Delta z$ values for $x^{-\infty} = 0.2$ and $z^{-\infty}$ ranging from 5 to 0.1. . . . .	214
5.10	$\Delta x$ and $\Delta z$ values for $x^{-\infty} = 0.5$ and $z^{-\infty}$ ranging from 5 to 0.1. . . . .	214

5.11	$\Delta x$ and $\Delta z$ values for $x^{-\infty} = 1$ and $z^{-\infty}$ ranging from 5 to 0.1. . . . .	214
5.12	$\Delta x$ and $\Delta z$ values for $x^{-\infty} = 2$ and $z^{-\infty}$ ranging from 5 to 0.1. . . . .	215
5.13	$\Delta x$ and $\Delta z$ values for $x^{-\infty} = 5$ and $z^{-\infty}$ ranging from 5 to 0.1. . . . .	215

# Chapter 1

## Introduction

A suspension is a multiphase system where the dispersed phase comprising solid particles is suspended in a fluid medium. Suspensions are important in a variety of natural and industrial settings including landslides, drilling fluids, fluidized beds, etc; a great majority of processes in the chemical industry entail the handling and transport of multiphase materials. The suspended particles in these systems interact through hydrodynamic, interparticle and Brownian forces. The interplay between these forces leads to a macroscopic flow behavior that is complex and often strikingly different when compared to a Newtonian fluid like water. Indeed, it is now known that concentrated suspensions cannot be treated using a classical Newtonian formulation with an effective viscosity. Even with a Newtonian suspending fluid, suspensions at high enough particle concentration exhibit pronounced non-Newtonian behavior with normal stress differences and a shear-rate-dependent viscosity (Jeffrey & Acrivos 1976, GadalaMaria & Acrivos 1980, Singh 2000, Zarraga et al 2000). Thus, an understanding of suspension properties is of great interest both from a fundamental point of view and with regard to enhancing the efficiencies of the aforementioned industrial processes.

In many of the above applications inertial effects are important, in some cases even dominant. The study of inertial effects is motivated not merely by their quantitative significance, but because inertia of either phase often qualitatively alters suspension behavior. For instance, fluid phase inertia, characterised by the Reynolds number ( $Re$ ), may lead to particle migration and thence to concentration inhomogeneities in an initially uniform sus-

pension, an effect that was originally shown for the case of Poiseuille flow (Segre & Silberberg 1962ab, Ho & Leal 1974). Particle inertia leads to the preferential concentration of particles in regions of high strain rate in dilute particle-laden turbulent flows, and this in turn has a significant effect on the fluid phase turbulence (Eaton & Fessler 1994). In general, inertial effects in suspensions have been shown to induce non-Newtonian behavior (Lin et al 1970, Tsao & Koch 1995). Ideally, it is desirable to study the separate roles of particle and fluid inertia in suspension flows. Since the ratio of particle to fluid inertia scales as the ratio of the densities of the respective phases, it is possible to study particle inertia independent of fluid inertial effects for suspensions of heavy particles; for instance, considering 10 micron particles in air ( $\eta \sim 10^{-5} Pa.s$ ,  $\rho_p/\rho_f \sim 1000$ ) and a typical shear rate  $\sim 10s^{-1}$ , one has  $St = 0.1$  and  $Re = 10^{-4}$ . This work considers the role of particle inertia in determining the microstructure and rheology of heavy suspensions. Inertial forces in the fluid are therefore neglected ( $Re = 0$ ) and the suspending fluid satisfies the Stokes equations. The statistics of the particles are given by a probability density function that satisfies a Fokker-Planck equation in phase space. A dimensionless measure of particle inertia is the Stokes number ( $St$ ), defined as the ratio of the inertial relaxation time of a particle to the flow time scale.

In contrast to the extensive body of knowledge available for inertialess flows of suspensions ( $Re, St = 0$ ) (Happel & Brenner 1965, Brady & Bossis 1988, Kim & Karrila 1991), there is relatively limited work in situations where particle-phase inertia is important. While considerable work has been done on particle-laden (gaseous) turbulent flows, the systems studied are typically dilute and as a result, the primary focus is on turbulence modification by the suspended particles rather than on interparticle interactions (Eaton & Fessler 1994, Fessler et al 1994, Kulick et al 1994, Rousson & Eaton 2001). There exists a large body of work, both theoretical and computational, on rapid granular flows that represent the infinite  $St$  limit.

Particle inertia is dominant in these cases and the effect of the interstitial (suspending) fluid is often neglected. Interparticle collisions are the main mechanism of momentum transport at high concentrations, and the statistics of the particles are therefore modeled by analogy with a molecular hard-sphere gas, the difference being that the collisions between the macroscopic particles are dissipative (Jenkins & Savage 1983, Lun et al 1984, Jenkins & Richman 1985ab, Campbell 1990). In the last decade, Koch and co-workers have developed a theory for zero  $Re$ , finite (but large)  $St$  suspensions that accounts for the effects of interstitial fluid (Tsao & Koch 1995, Sangani et al 1996).

This present work is valid for zero  $Re$ , small but finite  $St$ , and in addition, we allow for Brownian effects by letting the Peclet number ( $Pe$ ), defined as the ratio of the Brownian diffusion time scale to the flow time scale, be finite. The reason for the latter is that the high  $Pe$  limit (i.e., strongly sheared suspensions) is known to be singular (Brady & Morris 1997); Brownian diffusion and advection effects balance in asymptotically thin ( $O(Pe^{-1})$ ) boundary layers near particle-particle contact, and the resulting asymmetry of the boundary layer microstructure leads to persistent non-Newtonian effects that decay very slowly ( $\approx Pe^{-0.22}$ ) as  $Pe \rightarrow \infty$ . Our analysis allows one to investigate the effect of particle inertia (finite  $St$ ) on this limiting behavior. The domain of validity of our work is shown in Fig 1.1 in the parameter space spanned by  $Re$ ,  $St$  and  $Pe$ . The ratio  $St/Pe$  is independent of the flow and small compared to unity<sup>1</sup>, implying that Brownian effects need only be considered for small  $St$ .

The thesis is divided in two parts. The first part, comprising Chapters 2 and 3, introduces and develops a multiple scales (Chapman-Enskog) formalism to solve the Fokker-Planck equation for small but finite  $St$  (and arbitrary  $Pe$ ) in non-equilibrium situations.

---

<sup>1</sup>This ratio  $St/Pe = Sc_p^{-1}$ , where  $Sc_p$  is the Schmidt number and the subscript  $p$  is used to indicate that the kinematic viscosity in the definition of  $Sc_p$  is based on the particle density;  $Sc_p \gg 1$  whence the conclusion follows (also see Chapter 2).

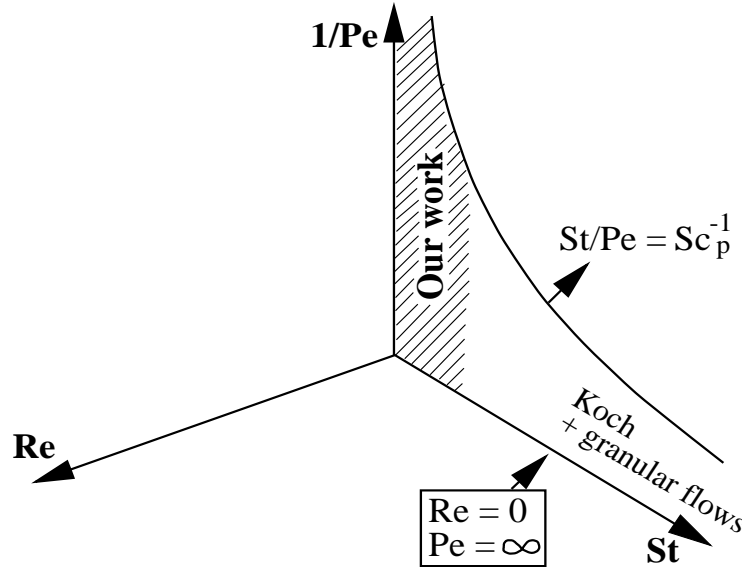


Figure 1.1: Parameter plot delineating the domain of validity (shaded region) of our work.

In Chapter 3, we derive an inertially corrected Smoluchowski equation accurate to  $O(St)$  that includes the first effects of particle inertia. The suspension (spatial) microstructure is characterised by the pair-distribution function that satisfies the well-known Smoluchowski equation in the inertialess limit ( $St = 0$ ). The solution to the corrected equation therefore accounts for changes in the suspension microstructure for finite  $St$ , thus serving to determine inertial modifications of the suspension flow properties. Chapters 4 and 5 are devoted to applying the formalism in order to obtain explicit results for simple shear flow of a dilute non-Brownian suspension of spherical particles. Each of chapters 2, 3, 4 and 5 have associated appendices that are labeled A, B, C and D, respectively.

In Chapter 2, we begin by performing a multiple scales analysis of the Fokker-Planck equation for a single Brownian particle in a simple shear flow. This simplistic case contains all three time scales present in the full problem of a finite  $St$  suspension subjected to an external flow field, and yet allows for an exact solution thereby enabling the validation of the proposed formalism. The three time scales are: the inertial relaxation time of the

particle ( $\tau_p$ ), the time scale for Brownian diffusion ( $\tau_D$ ) and the time scale imposed by the shear flow ( $\dot{\gamma}^{-1}$ ,  $\dot{\gamma}$  being the shear rate). The governing Fokker-Planck equation describes the evolution of the probability density on time scales of  $O(\tau_p)$  or longer; for small  $St$ , it therefore accounts for both the rapid momentum relaxations in  $O(\tau_p)$  and the slower spatial diffusion processes on time scales of  $O(\dot{\gamma}^{-1})$  or  $O(\tau_D)$ . The disparate time scales of momentum and spatial relaxations motivate the use of a multiple scales method for the problem. However, it is shown that the customary multiple scales procedure (which has been successfully used, for instance, in the analysis of linear and non-linear oscillators to yield amplitude/phase modulated periodic solutions, and for non-linear wave equations to yield similarly modulated travelling wave solutions; see Kevorkian & Cole (1995)) does not work for the Fokker-Planck equation since the independent variables in this case span both position and velocity space, and including only one of the two (as in the naive multiple scales approximation) leads to spurious relaxation terms. We therefore employ a modified version of the formalism originally used by Wycoff & Balazs (1987) for the Kramers equation<sup>2</sup>; in our case, this entails expanding the probability density in an infinite series of Hermite functions of the fluctuation velocity, defined as the difference between the velocity of the Brownian particle and the velocity of the ambient simple shear flow at its instantaneous location. The expansion coefficients in the infinite series are found to satisfy Smoluchowski-like equations with inertial corrections at successive orders in  $St$ . The coefficient of the zeroeth order Hermite function represents the number density and satisfies a corrected Smoluchowski equation containing an off-diagonal diffusive component at  $O(St)$ .

For a finite  $St$  suspension in an external flow, the time scale for momentum relaxations becomes configuration dependent on account of hydrodynamic interactions, and

---

<sup>2</sup>The Fokker-Planck equation in one dimension is better known as Kramers equation in the physics literature after Kramers, who originally used it to calculate the escape rate of a Brownian particle from a deep potential well (Kramers 1940).

the multiple scales formalism introduced in Chapter 2 is no longer applicable in its original form (i.e., in the form used for a single particle). In Chapter 3 we formulate a generalized Chapman-Enskog expansion that still shares the same basic structure as the original multiple scales formalism, but accounts for the complex form of the momentum relaxations in a suspension. The expansion of the probability density is now in terms of tensorial Hermite functions; the coefficient of the zeroth order term, however, still represents the number density, and we derive a corrected Smoluchowski equation for the same, including the  $O(St)$  inertial terms. In addition to (expected) corrections to the leading order velocity field and diffusivities, the equation derived is shown to contain a non-Fickian term at  $O(St/Pe^2)$ . Though applicable only in the limit  $St \ll 1$ , the range of validity of the Chapman-Enskog formulation is expected to increase with increase in the particle volume fraction ( $\phi$ ) because, for fixed  $St$ , the increase in the suspension viscosity with increasing  $\phi$  reduces the effective particle inertia.

In Chapters 4 and 5, we examine a monodisperse non-Brownian suspension of heavy spherical particles in simple shear flow. In order to obtain analytical results, only pair-wise hydrodynamic interactions are considered; the quantitative accuracy of our calculations will therefore be restricted to the case of dilute suspensions. With these assumptions, the rheological problem reduces to analysing the relative trajectories of two inertial (finite  $St$ ) spheres in shear flow. The expression for the relative velocity, to  $O(St)$ , is obtained from the Smoluchowski equation derived in Chapter 3 in the limit  $Pe \rightarrow \infty$ . A subsequent path integration along the  $O(St)$  modified trajectories will, in principle, determine the pair-distribution function that then serves to characterize the finite  $St$  microstructure. For  $St = 0$ , the pair-trajectories are fore-aft symmetric and were originally determined by Batchelor & Green (1972a). The fore-aft symmetry implies that a pair-interaction leads to

no net displacement in the transverse direction. Although the zero-Stokes open trajectories support an isotropic distribution, the existence of a region of closed trajectories in simple shear flow leads to an indeterminate pair-distribution function (Batchelor & Green 1972b). A well-posed steady problem can only be obtained by the inclusion of (say) Brownian motion or three-particle interactions. Particle inertia destroys the fore-aft symmetry of the zero-Stokes trajectory space, giving rise to net transverse displacements in the velocity gradient and vorticity directions (of simple shear flow) following each pair-interaction, in turn leading to diffusive behavior for long times. The differing strengths of interaction along the gradient and vorticity directions result in an anisotropic self-diffusivity tensor, the gradient and vorticity components of which scale as  $St^2 \ln St$  and  $St^2$ , respectively. Unlike the inertialess limit where the indeterminacy of the rheological problem is related to the dependence of the long-time distribution on the particular initial condition (in the region of closed trajectories), the indeterminacy for finite  $St$  arises from the absence of such a long-time limit. For finite  $St$  the region of closed trajectories is destroyed, but there exists instead a planar limit cycle that acts as a local attractor; the associated basin of attraction has an infinite volume. As a result, (almost) any initial condition<sup>3</sup> for long times leads to a progressive accumulation of particles on the attracting cycle, resulting in a temporally growing distribution. As is the case for  $St = 0$ , one again needs to include additional mechanisms in order to obtain a well-posed rheological problem.

It is finally noted that notwithstanding use of the corrected Smoluchowski equation derived in Chapter 3, the second part of the thesis comprising Chapters 4 and 5 is more or less self contained and maybe read independently of the first.

---

<sup>3</sup>One may obtain a finite long-time pair-distribution function for initial conditions that correspond to a zero probability in the basin of attraction of the limit cycle. These exotic initial conditions, however, do not correspond to any reasonable physical scenario.

## Bibliography

- [1] Batchelor, G.K. & Green, J.T. 1972a The hydrodynamic interaction of two small freely-moving spheres in a linear flow field. *J. Fluid Mech.* **56**, 375-400.
- [2] Batchelor, G.K. & Green, J.T. 1972b The determination of the bulk stress in a suspension of spherical particles to  $O(c^2)$ . *J. Fluid Mech.* **56**, 401-427.
- [3] Brady, J.F. & Bossis, G. 1988 Stokesian dynamics. *Ann. Rev. Fluid Mech.* **20**, 111-157.
- [4] Brady, J.F. & Morris, J.F. 1997 Microstructure of strongly sheared suspensions and its impact on rheology and diffusion. *J. Fluid Mech.* **348**, 103-139.
- [5] Campbell, C.S. 1990 Rapid granular flows. *Ann. Rev. Fluid Mech.* **22**, 57-92.
- [6] Eaton, J.K. & Fessler, J.R. 1994 Preferential concentration of particles by turbulence. *Int. J. Multiphase Flow* **20**, Suppl. S, 169-209.
- [7] Fessler, J.R., Kulick, J.D. & Eaton, J.K. 1994 Preferential concentration of heavy-particles in a turbulent channel flow. *Phys. Fluids* **6**(11), 3742-3749.
- [8] GadalaMaria, F. & Acrivos, A., 1980 Shear-induced microstructure in a concentrated suspension of solid spheres. *J. Rheol.* **24**(6), 799-814.
- [9] Happel, J. & Brenner, H. 1965 *Low Reynolds number hydrodynamics, with special applications to particulate media*. Prentice-Hall.
- [10] Ho, B.P. & Leal, L.G. 1974 The creeping motion of liquid drops through a circular tube of comparable diameter. *J. Fluid Mech.* **71**, 361 - 383.

- [11] Jeffrey, D.J. & Acrivos, A. 1976 Rheological properties of suspensions of rigid particles. *AIChE J.* **22**(3), 417-436.
- [12] Jenkins, J.T. & Richman, M.W. 1985a Grads 13-moment system for a dense gas of inelastic spheres. *Arch. Ration. Mech. Anal.* **87**(4), 355-377.
- [13] Jenkins, J.T. & Richman, M.W. 1985b Kinetic-theory for plane flows of a dense gas of identical, rough, inelastic, circular disks. *Phys. Fluids* **28**(12), 3485-3494.
- [14] Jenkins, J.T. & Savage, S.B. 1983 A theory for the rapid flow of identical, smooth, nearly elastic, spherical-particles. *J. Fluid Mech.* **130**, 187-202.
- [15] Kevorkian, J. & Cole, J.D. 1995 *Multiple Scale and Singular Perturbation Methods*. Springer-Verlag.
- [16] Kim, S. & Karrila, S.J. 1991 *Microhydrodynamics: Principles and Selected Applications*. Butterworth-Heinemann.
- [17] Kramers, H.A. 1940 Brownian motion in a field of force and the diffusion model of chemical reactions. *Physica* **7**, 284-304.
- [18] Kulick, J.D., Fessler, J.R. & Eaton, J.K. 1994 Particle response and turbulence modification in fully-developed channel flow. *J. Fluid Mech.* **277**, 109-134.
- [19] Lin, C.J., Peery, J.H. & Schowalter, W.R. 1970 Simple shear flow round a rigid sphere: inertial effects and suspension rheology. *J. Fluid Mech.* **44**, 1-17.
- [20] Lun, C.K.K., Savage, S.B. & Jeffrey, D.J. 1984 Kinetic theories for granular flow - Inelastic particles in couette-flow and slightly inelastic particles in a general flowfield. *J. Fluid Mech.* **140**, 223-256.

- [21] Rouson, D.W.I. & Eaton, J.K. 2001 On the preferential concentration of solid particles in turbulent channel flow. *J. Fluid Mech.* **428**, 149-169.
- [22] Sangani, A.S., Mo, G., Tsao, H.K. & Koch, D.L. 1996 Simple shear flow of dense gas-solid suspensions at finite Stokes numbers. *J. Fluid Mech.* **313**, 309-341.
- [23] Segre, G. & Silberberg, A. 1962a Behavior of macroscopic rigid spheres in Poiseuille flow. Part 1. Determination of local concentration by statistical analysis of particle passages through crossed light beams. *J. Fluid Mech.* **14**, 115-135.
- [24] Segre, G. & Silberberg, A. 1962b Behavior of macroscopic rigid spheres in Poiseuille flow. Part 2. Experimental results and interpretation. *J. Fluid Mech.* **14**, 136-157.
- [25] Singh, A. 2000 Rheology of non-colloidal suspensions. PhD Thesis, Indian Institute of Science, Bangalore, India.
- [26] Zarraga, I.E., Hill, D.A. & Leighton, D.T. 2000 The characterisation of the total stress of concentrated suspensions of non-colloidal spheres in Newtonian fluids. *J. Rheol.* **44**, 185-220.
- [27] Tsao, H.K. & Koch, D.L. 1995 Simple shear flows of dilute gas-solid suspensions. *J. Fluid Mech.* **296**, 211-245.
- [28] Wycoff, D. & Balazs, N.L. 1987a Multiple time scales analysis for the Kramers-Chandrasekhar equation. *Physica* **146A**, 175-200.

## Chapter 2

# Multiple scales analysis of the Fokker-Planck equation for a single Brownian particle in simple shear flow

### 2.1 Introduction

The Fokker-Planck equation (also known as the Kramers-Chandrasekhar equation) is the fundamental equation governing the statistics of a Brownian particle in phase space. Restricting consideration to position coordinates alone gives a coarser description characterized by the well-known Smoluchowski equation (Smoluchowski 1915). The derivation of the Smoluchowski equation from the Fokker-Planck equation involves neglecting processes that occur on the scale of the particle inertial relaxation time ( $\tau_p$ ). It is this separation of time scales between the rapid relaxation of the velocity distribution towards a Maxwellian and the much slower evolution of the spatial coordinates that allows the formulation of a successful multiple scales scheme when the inertial relaxation time is the shortest time scale present. This was originally done for a slowly varying potential force field by Wycoff & Balazs (1987a) by expanding the probability density in an infinite series of Hermite functions (of the velocity), with coefficients determined as functions of position and time from the multiple scales procedure. The analysis was carried out for situations where the length scale characterising the potential is much greater than the mean free path of the Brownian particle, the latter being the characteristic distance travelled by the particle (moving with its thermal velocity) in a time interval of  $O(\tau_p)$ .

In this chapter we extend the formalism of Wycoff & Balazs to a Brownian particle in a simple shear flow. The velocity field is given by  $\mathbf{u}_{shear}(\mathbf{y}) = \dot{\gamma}\bar{y}\mathbf{1}_x$ , and gives rise to a nonconservative hydrodynamic force field owing to the vorticity of the imposed flow. Here  $\dot{\gamma}$  is the shear rate,  $\mathbf{1}_x$  is the unit vector in the flow direction and  $\bar{y}$  is the coordinate in the gradient direction. In addition to the inertial ( $\tau_p$ ) and configurational ( $\tau_D = a^2/D$ , where  $D$  is the diffusivity) relaxation times, the shear rate introduces a new time scale  $\dot{\gamma}^{-1}$ , and the assumption made here is a separation of the inertial and flow time scales. Therefore, the method remains valid for arbitrary relative magnitudes of  $\tau_D$  and  $\dot{\gamma}^{-1}$ , that is, arbitrary values of the Peclet number  $Pe = \dot{\gamma}\tau_D$ . In contrast to equilibrium problems, the pertinent variable for the Hermite functions (in the expansion of the probability density) is no longer the absolute velocity of the Brownian particle but rather the difference between its absolute velocity and the velocity of the unperturbed flow field at its current location. As it is convected by the flow, the particle can only equilibrate about the instantaneous flow velocity and the ‘equilibrium’ distribution is therefore a local Maxwellian about the ambient flow velocity. The main purpose of this chapter is to develop a consistent multiple time scales scheme for such non-equilibrium problems and to compare explicitly the exact and multiple scales solutions for the case of simple shear flow.

The solution of the Fokker-Planck equation poses a formidable challenge in all except the simplest cases. It is therefore desirable to reduce the original phase-space description to one in position space since the concomitant decrease in the number of independent variables makes the reduced system more tractable. The multiple scales procedure helps achieve this reduction and provides a systematic way of obtaining corrections to the Smoluchowski description (valid for inertialess particles) to account for the effects of particle inertia. These corrections assume particular significance when hydrodynamic interactions between parti-

cles are taken into account, for in this case, the corrected Smoluchowski equation governs the effect of the inertia of the particulate phase on suspension microstructure. The limit of vanishing Brownian motion is also of special interest since a non-colloidal, inertialess suspension possesses a symmetric microstructure with a Newtonian rheology. The multiple scales method would enable one to study the effects of inertia on this microstructural symmetry and its consequences for suspension rheology.

In section 2.2, we formulate the mathematical problem and give the governing equations. The method of multiple scales is then introduced; when applied directly to the Fokker-Planck equation, however, the method works only for the case of free Brownian motion. We proceed to modify the multiple scales formalism along the lines of Wycoff & Balazs (1987a), taking into account the spectrum of the Fokker-Planck operator in velocity space (for a linear drag force), in order to extend its validity to a general force field. In section 2.3.1, we detail the exact solutions for two initial conditions for Brownian motion of a single spherical particle in simple shear flow, together with their small Stokes number expansions. The initial velocity distributions considered are a Maxwellian and a delta function, the former corresponding to a particle initially at equilibrium, and the latter relating to the Green's function for the problem. Using the method developed in section 2.2, the general form of the multiple scales hierarchy for simple shear flow is derived in section 2.3.2, and the inertial corrections to the Smoluchowski equation are obtained. The corrected equation is solved to obtain the number densities for the two initial conditions, which are then compared to the corresponding exact expressions. In section 2.4, we compare the exact and multiple scales solutions for the phase space probability densities for the aforementioned initial conditions, and in addition, consider the form of the multiple scales hierarchy in the limit when thermal effects are negligible. Finally in section 2.5, we summarize the results and comment

on modifications in the procedure necessary when considering hydrodynamically interacting particles.

## 2.2 Problem formulation

The Fokker-Planck equation for a single particle in shear flow is

$$\frac{\partial P}{\partial \bar{t}} + \mathbf{u} \cdot \frac{\partial P}{\partial \mathbf{y}} + \frac{\dot{\gamma} \bar{y}}{m} \mathbf{1}_x \cdot \frac{\partial P}{\partial \mathbf{u}} = \frac{6\pi\eta a}{m} \frac{\partial}{\partial \mathbf{u}} \cdot (\mathbf{u}P) + \frac{kT}{m} \left( \frac{6\pi\eta a}{m} \right) \nabla_{\mathbf{u}}^2 P. \quad (2.1)$$

Here,  $P(\mathbf{y}, \mathbf{u}, \bar{t}) d\mathbf{y} d\mathbf{u}$  is the probability that the Brownian particle is in the elemental volume  $[(\mathbf{y}, \mathbf{y} + d\mathbf{y}), (\mathbf{u}, \mathbf{u} + d\mathbf{u})]$  at time  $\bar{t}$ ,  $m$  is the mass of the particle,  $a$  is its radius,  $\eta$  is the viscosity of the suspending fluid and  $T$  is the absolute temperature. Using the non-dimensionalizations:  $\bar{t} = m/(6\pi\eta a)t$ ,  $\mathbf{y} = a\mathbf{x}$  and  $\mathbf{u} = (\dot{\gamma}a)\mathbf{v}$ , (2.1) becomes

$$\frac{\partial P}{\partial t} + St \mathbf{v} \cdot \frac{\partial P}{\partial \mathbf{x}} = \frac{\partial}{\partial \mathbf{v}} \cdot (\mathbf{v} - y\mathbf{1}_x)P + \frac{1}{Pe St} \nabla_{\mathbf{v}}^2 P. \quad (2.2)$$

In equation (2.2), the Stokes number  $St = m\dot{\gamma}/(6\pi\eta a)$  is the ratio of the inertial relaxation time ( $\tau_p = m/6\pi\eta a$ ) to the flow time scale, and is a measure of the inertia of the Brownian particle, while  $Pe = (6\pi\eta a^3\dot{\gamma})/kT$  is a measure of the importance of thermal effects. Thus in the limit  $St \ll 1$ , we have  $\dot{\gamma}^{-1} \gg \tau_p$ , which illustrates the separation of time scales. Equations (2.1) and (2.2) entail the assumption that the hydrodynamic force experienced by the suspended particle can be taken as equal to the pseudo-steady Stokes drag. This is a valid assumption when the density of the particle is much greater than that of the fluid (i.e., when  $St \gg Re$ , where  $Re = \rho a^2 \dot{\gamma} / \eta$  is the Reynolds number, and is a measure of the inertial forces in the suspending fluid of density  $\rho$ ). In this limit the vorticity generated at the surface of the particle diffuses out into the bulk much faster than the particle inertia

relaxes so that the particle, in effect, encounters a steady flow field and use of the steady Stokes drag is appropriate on all time scales starting from  $\tau_p$ . In fact, equation (2.1) can also be written as the equivalent Langevin equation,

$$m \frac{d\mathbf{u}}{dt} = -6\pi\eta a(\mathbf{u} - \dot{\gamma}\bar{y} \mathbf{1}_x) + \mathbf{F}^B(t), \quad (2.3)$$

where  $\mathbf{F}^B(t)$  is the Brownian force modelled as a delta-correlated white noise with amplitude determined from the fluctuation dissipation theorem (Chandrasekhar 1954):

$$\langle \mathbf{F}^B(t) \rangle = 0, \quad \langle \mathbf{F}^B(t) \mathbf{F}^B(t') \rangle = 2kT(6\pi\eta a)\delta(t - t').$$

The configuration space Smoluchowski equation for a Brownian particle in shear flow corresponding to the Fokker-Planck equation (2.1) is

$$\frac{\partial g}{\partial t} + \frac{\partial}{\partial \mathbf{y}} \cdot (\dot{\gamma}\bar{y} \mathbf{1}_x g) = D \nabla_{\mathbf{y}}^2 g, \quad (2.4)$$

where  $g(\mathbf{y}, \bar{t})$  is the positional probability density at time  $\bar{t}$  and  $D = kT/(6\pi\eta a)$  is the Stokes-Einstein diffusivity. The Langevin equation of motion equivalent to (2.4) is given by (2.3) with  $m = 0$ . When the time  $\bar{t}$  is scaled with the shear rate (representative of the slower spatial relaxation processes), the non-dimensional Smoluchowski equation becomes

$$\frac{\partial g}{\partial t} + \frac{\partial}{\partial x}(yg) = \frac{1}{Pe} \nabla_{\mathbf{x}}^2 g. \quad (2.5)$$

Unlike the Fokker-Planck equation, the Smoluchowski equation depends only on  $Pe$ , and therefore it should be possible to solve the former in a perturbative fashion for small  $St$  but arbitrary  $Pe$  with the leading order positional density given by the solution to (2.5). It is

our goal to obtain corrections to (2.5) for small Stokes numbers.

The multiple scales formalism is suited to the description of dynamical systems characterised by concurrent processes occurring on widely separated time scales. The evolution of the momentum and spatial coordinates of a Brownian particle in shear flow for small Stokes numbers presents one such instance, and suggests the applicability of the formalism in this case. When applied to equation (2.2), the multiple scales method allows for the simultaneous evolution of the probability density on a hierarchy of time scales depending on  $St$ , the rates of evolution on the different time scales being asymptotically separated for small  $St$ . In principle, an infinite number of time scales is needed for an accurate description valid for all times. This need not always be the case, however; in free Brownian motion, the relaxation processes are characterised by the scales  $\tau_p$  and  $\tau_D$ , and accordingly, one only needs two independent variables in order to capture the time dependence of the exact solution to arbitrary order in the relevant small parameter  $\epsilon = (\tau_p/\tau_D)^{\frac{1}{2}}$ . In section 2.3.2 it will be seen that the addition of a third time scale viz.  $\dot{\gamma}^{-1}$  for shear flow necessitates the inclusion of an infinite hierarchy.

In the multiple scales formalism, the probability density is written in the form  $P(\mathbf{x}, \mathbf{v}, \{t_i\})$  ( $t_i = St^{i-1}t$ ), where  $t_1$  changes on the scale of  $\tau_p$  and the  $t_i$ 's for  $i \geq 2$  represent the slower spatial relaxations. For small  $St$ ,  $P$  is expanded as a power series in  $St$ , as is the time derivative

$$\frac{\partial}{\partial t} = \sum_{i=1}^{\infty} St^{(i-1)} \frac{\partial}{\partial t_i}, \quad (2.6)$$

thereby splitting the original time variation in equation (2.2) into variations on each of the scales  $t_i$ , which are then treated as independent variables. The solution at any given order does not completely determine  $P$  to that order, however, but instead allows for an arbitrary dependence on the slower time scales. This dependence is typically determined by secularity

constraints (consistency conditions) at higher orders, which dictate that the solutions should not exhibit an unbounded growth on any of the time scales. Applying this approach directly to equation (2.2) works only for the case of free Brownian motion since the resulting operator (at leading order) involves only the momentum variables, and therefore does not preserve the properties of the original Fokker-Planck operator for a position dependent force field (see Appendix A1.3).

In order to devise an indirect way of applying the multiple scales procedure that remains valid for a general force field, we again start with equation (2.2). If for a moment one neglects the  $O(St)$  spatial derivative on the left-hand side, the simplified equation

$$\frac{\partial P}{\partial t} = \frac{\partial}{\partial \mathbf{w}} \cdot (\mathbf{w}P) + \nabla_{\mathbf{w}}^2 P = L_H(\mathbf{w})P \quad (2.7)$$

is obtained, where  $\mathbf{w} = (PeSt)^{\frac{1}{2}}(\mathbf{v} - y\mathbf{1}_x)$  is the scaled fluctuation velocity. It is well known that the operator  $L_H$  has a denumerable infinity of eigenvalues and a complete set of eigenfunctions (Titulaer 1978) given by

$$\lambda_{n_1, n_2, n_3} = - \sum_{i=1}^3 n_i,$$

$$\psi_{n_1, n_2, n_3}(\mathbf{w}) = e^{-\frac{|\mathbf{w}|^2}{2}} \prod_{i=1}^3 H_{n_i} \left( \frac{w_i}{2^{\frac{1}{2}}} \right),$$

where  $H_n(x)$  denotes the  $n^{\text{th}}$  Hermite polynomial defined as  $H_n(x) = (-1)^n e^{x^2} d^n(e^{-x^2})/dx^n$ .

The general solution to equation (2.7) is therefore

$$P(\mathbf{w}, t) = \sum_{n_1, n_2, n_3} \left( b_{n_1, n_2, n_3} e^{-(n_1+n_2+n_3)t} \right) \psi_{n_1, n_2, n_3}(\mathbf{w}), \quad (2.8)$$

where the coefficients  $b_{n_1, n_2, n_3}$  are determined from initial conditions so as to satisfy the

normalization constraint viz.  $\int P d\mathbf{w} = 1$ . For small but non-zero  $St$ , the solution to equation (2.2) has the same general form as (2.8) to leading order. However, in addition to the exponential decay  $e^{\lambda t}$  (on the scale of  $\tau_p$ ), the coefficient of  $\psi_{n_1, n_2, n_3}$  now involves a slowly varying function of space and time characteristic of the spatial relaxation processes. Thus to leading order, the solution to equation (2.2) can be written as

$$P^{(0)}(\mathbf{x}, \mathbf{v}, t) = \sum_{n_1, n_2, n_3} \left[ b_{n_1, n_2, n_3}(\mathbf{x}, t^{slow}) e^{-(n_1 + n_2 + n_3)t} \right] \psi_{n_1, n_2, n_3}(\mathbf{w}), \quad (2.9)$$

where  $t_{slow}$  denotes temporal dependence on asymptotically slower time scales of  $O(\dot{\gamma}^{-1})$ . The leading order coefficient corresponding to the zero eigenvalue, viz.  $b_{0,0,0}$ , satisfies the Smoluchowski equation (2.5), and for long times (2.9) takes the asymptotic form  $b_{0,0,0}(\mathbf{x}, t^{slow}) \psi_{0,0,0}(\mathbf{w})$ , that is, a Maxwellian velocity distribution about the shear flow times the solution to the configuration-space Smoluchowski equation. As we shall show, the higher order corrections for finite  $St$  ( $P^{(i)}$ 's,  $i \geq 1$ ) involve a spectrum of decay rates corresponding to  $\psi_{n_1, n_2, n_3}$  and not just a single exponential as in (2.9). Therefore, the complete solution to equation (2.2) can be written as

$$P(\mathbf{x}, \mathbf{v}, t) = \sum_{n_1, n_2, n_3} \sum_{i=0}^{\infty} (St)^i \left[ \sum_{s=0}^{\infty} \phi_{n_1, n_2, n_3, s}^{(i)}(\mathbf{x}, t^{slow}) e^{-st} \right] \psi_{n_1, n_2, n_3}(\mathbf{w}), \quad (2.10)$$

where  $\phi_{n_1, n_2, n_3, \Sigma n_i}^{(0)} = b_{n_1, n_2, n_3}$  is the only non-zero element for  $i = 0$ . Neglecting all exponentially decaying terms in (2.10) would give the so-called Bogliubov solution valid for long times. Having characterised the form of the solution in velocity space, one may now apply the multiple scales formalism to determine the dependence of the  $\phi$ 's on the longer time scales (denoted by  $t_{slow}$  above).

In section 2.3.2, where we carry out the multiple scales analysis, (2.10) is used for

the general solution to equation (2.2), and a recurrence relation between the  $\phi$ 's is derived. In terms of the multiple scales notation defined above, the exponential decay in (2.10) occurs on the  $t_1$  (fast) scale, while the dependence of the  $\phi$ 's on the slower time scales is represented in terms of the set  $\{t_j\}_{i=2}^{\infty}$ . As would be expected based on the previous discussion, the recurrence relations together with the appropriate initial conditions are in themselves not sufficient to completely determine the  $\phi$ 's. In fact, it will be found that at each order the elements  $\phi_{\{n_i\},s}$ , with  $s = \sum n_i$ , are left undetermined. The additional requirements for determinacy are derived in the form of consistency conditions which serve as definitions of the operators  $\partial/\partial t_i$  (rather than as secularity constraints) in a manner similar to the Chapman-Enskog expansion (Chapman & Cowling 1970, Titulaer 1978). It must be emphasised that the above procedure necessitates treating  $St$  on the two sides of equation (2.2) differently. While  $St$  on the left-hand side is treated as a small parameter, that on the right-hand side (as part of  $PeSt$ ) is merely treated as a scale factor for the fluctuation velocity, i.e., the magnitude of  $PeSt$  dictates the variance of the leading order Maxwellian.

### 2.3 Brownian motion in simple shear flow

In this section we compare the exact and multiple scales solutions for simple shear flow. It suffices to consider the two-dimensional case since the third dimension (viz. the coordinate in the vorticity direction and the corresponding velocity component) does not couple to the others and continues to evolve as in free Brownian motion. Equation (2.2) written out explicitly for two dimensions is

$$\frac{\partial P}{\partial t} + St \left( u \frac{\partial P}{\partial x} + v \frac{\partial P}{\partial y} \right) = \frac{\partial}{\partial u} (u - y)P + \frac{\partial}{\partial v} (vP) + \frac{1}{PeSt} \left( \frac{\partial^2 P}{\partial u^2} + \frac{\partial^2 P}{\partial v^2} \right). \quad (2.11)$$

We demonstrate the applicability of the multiple scales procedure to (2.11) by considering two distributions of initial velocities, a Maxwellian and a delta function centered at the origin. In the absence of an equilibrium spatial distribution, the natural initial distribution of particle positions to impose (and which simplifies the analysis) is that of a delta function. This singularity in the spatial condition, however, leads to a divergent series in  $St$ . A comparison with the exact solution can nevertheless be made and serves to verify the applicability of the multiple scales procedure<sup>1</sup>.

### 2.3.1 Exact solution

The exact solution to equation (2.11) (wherein the shear flow constitutes a linear force) is a multivariate Gaussian in phase space (Risken 1989, Miguel & Sancho 1979) with the elements of the variance matrix being functions of time. The Green's function of (2.11) for a Brownian particle at  $(x, y) \equiv (0, 0)$  with velocity  $(u', v')$  at  $t = 0$ , from which the solution for a Maxwellian distribution of initial velocities can be obtained, is

$$G(\mathbf{x}, \mathbf{v}, t | \mathbf{0}, \mathbf{v}', 0) = \frac{1}{(2\pi)^2 \Delta^{\frac{1}{2}}} \exp \left[ -\frac{\mathbf{c} : \mathbf{X}\mathbf{X}}{2\Delta} \right]. \quad (2.12)$$

In (2.12),

$$\mathbf{X} = \begin{bmatrix} x - St u' k_1 - St^2 v' k_3 \\ y - St v' k_1 \\ u - u' k_2 - St v' k_4 \\ v - v' k_2 \end{bmatrix},$$

---

<sup>1</sup>This is illustrated in Appendix A where the exact and multiple scales solutions for free Brownian motion are compared for a delta function initial condition.

and

$$\begin{aligned}
k_1 &= (1 - e^{-t}), \\
k_2 &= e^{-t}, \\
k_3 &= [t(1 + e^{-t}) - 2(1 - e^{-t})], \\
k_4 &= [1 - (1 + t)e^{-t}],
\end{aligned}$$

are functions that characterize relaxation from the initial conditions. The determinant of the variance matrix  $\langle \mathbf{XX} \rangle$  is  $\Delta$  and  $\mathbf{c}$  is the matrix of cofactors. The elements of the variance matrix are:

$$\begin{aligned}
\langle xx \rangle_d &= \frac{St}{Pe} \left[ 2t - (1 - e^{-t})(3 - e^{-t}) + St^2 \left( \frac{2}{3}t^3 - 4t^2 + 8t - \frac{3}{2} \right) \right. \\
&\quad \left. + St^2 e^{-t}(-4t^2 - 8t + 8) - St^2 e^{-2t}(t^2 + 5t + \frac{13}{2}) \right], \\
\langle xy \rangle_d &= \frac{St^2}{Pe} \left[ (t^2 - 4t + \frac{11}{2}) - 8e^{-t} + e^{-2t}(\frac{5}{2} + t) \right], \\
\langle yy \rangle_d &= \frac{St}{Pe} [2t - (1 - e^{-t})(3 - e^{-t})], \\
\langle uu \rangle_d &= \frac{1}{PeSt} \left[ (1 - e^{-2t}) + 2St^2(t - \frac{11}{2}) + St^2 e^{-t}(4t + 8) - St^2 e^{-2t}(t^2 + 3t + \frac{5}{2}) \right], \\
\langle uv \rangle_d &= \frac{1}{2Pe} [1 - 4e^{-t} + e^{-2t}(3 + 2t)], \tag{2.13} \\
\langle vv \rangle_d &= \frac{1}{PeSt}(1 - e^{-2t}), \\
\langle ux \rangle_d &= \frac{1}{Pe} [(1 - e^{-t})^2 + St^2(4 - 4t + t^2) + St^2 e^{-t}(-8 - 4t + 2t^2) + St^2 e^{-2t}(4 + 4t + t^2)], \\
\langle vx \rangle_d &= \frac{St}{Pe} \left[ \frac{1}{2} + 2e^{-t}(1 - t) - e^{-2t}(\frac{5}{2} + t) \right], \\
\langle uy \rangle_d &= \frac{St}{Pe} \left[ (2t - \frac{9}{2}) + e^{-t}(6 + 2t) - e^{-2t}(\frac{3}{2} + t) \right], \\
\langle vy \rangle_d &= \frac{1}{Pe}(1 - e^{-t})^2,
\end{aligned}$$

where the subscript ‘ $d$ ’ indicates the associated delta function initial condition. From the variances it is evident that for large times  $\langle xx \rangle_d \sim t^3$  and  $\langle uu \rangle_d \sim t$ . In shear flow,  $u \sim y$  and  $\langle yy \rangle_d$ , being diffusive on time scales of  $O(\dot{\gamma}^{-1})$  or larger, grows linearly with time, which implies  $u \sim y \sim t^{1/2}$ . This in turn implies that  $x \sim ut \sim t^{3/2}$  for long times. The other asymptotic scalings can similarly be derived; for instance,  $\langle xy \rangle_d \sim O(t^{3/2} \cdot t^{1/2}) \sim O(t^2)$ . The effect of inertia is, in part, to modify the behavior for small times as seen by the presence of exponentially decaying terms on the scale of  $\tau_p$ . The profusion of algebraic terms at short times is indicative of inertial couplings between convectively and diffusively growing terms.

Using (2.12), one can derive the solution for a Maxwellian initial condition as simply

$$P^m(\mathbf{x}, \mathbf{v}, t) = \int d\mathbf{v}' G(\mathbf{x}, \mathbf{v}, t | \mathbf{0}, \mathbf{v}', 0) \exp \left[ -Pe St \frac{|\mathbf{v}'|^2}{2} \right].$$

We tabulate, to  $O(St)$ , the long-time expressions for the spatial variances in this case for comparison with solutions of the corrected Smoluchowski equation derived below (see (2.40)); these are given by

$$\begin{aligned} \lim_{t \rightarrow \infty} \langle xx \rangle_m &= \int d\mathbf{v} d\mathbf{x} (xx) \lim_{t \rightarrow \infty} P^m(\mathbf{x}, \mathbf{v}, t) = \frac{St}{Pe} \left[ 2t + St^2 \left( \frac{2t^3}{3} - 3t^2 - 2 \right) \right], \\ \lim_{t \rightarrow \infty} \langle xy \rangle_m &= \int d\mathbf{v} d\mathbf{x} (xy) \lim_{t \rightarrow \infty} P^m(\mathbf{x}, \mathbf{v}, t) = \frac{St^2}{Pe} (t^2 - 3t), \\ \lim_{t \rightarrow \infty} \langle yy \rangle_m &= \int d\mathbf{v} d\mathbf{x} (yy) \lim_{t \rightarrow \infty} P^m(\mathbf{x}, \mathbf{v}, t) = \frac{St}{Pe} (2t - 2), \end{aligned} \quad (2.14)$$

where the long-time limit is taken to eliminate all exponentially decaying terms<sup>2</sup>. It should also be noticed that the higher order algebraic terms in the variances in (2.13) and (2.14) are not identical to those for a delta function initial condition (see Titulaer 1978), which shows that the effects of inertial relaxations from a particular initial condition persist for long times;

<sup>2</sup>The exact expression for  $\langle yy \rangle_m$  is  $(St/Pe)(2t - 2 + 2e^{-t})$ , and is easily found since the variance in the  $y$  direction is identical to that for free Brownian motion for any initial condition.

the leading order temporal growths are the same, of course.

The solution for the second initial condition where the Brownian particle is initially at rest at the origin is simply

$$P^d(\mathbf{x}, \mathbf{v}, t) = G(\mathbf{x}, \mathbf{v}, t | \mathbf{0}, \mathbf{0}, 0).$$

In order to compare with solutions obtained from the multiple scales analysis, we expand the exact solutions as a two-time-scale series by scaling all exponential terms with  $\tau_p$  (in accordance with Wycoff & Balazs (1987a)) and all algebraic terms with  $\dot{\gamma}^{-1}$ , thereby expressing the exact solutions in terms of  $t_1 (= t)$  and  $t_2 (= St t_1)$ . Since equation (2.11) contains  $Pe$  only in the combination  $Pe St$ , the exact solution for small  $St$  and arbitrary  $Pe$  can be expanded in the form<sup>3</sup>

$$\begin{aligned} P(\mathbf{x}, \mathbf{v}, t_1, t_2; St, Pe) &= \sum_{i,j=0}^{\infty} St^i (Pe St)^j P^{(i,j)}(\mathbf{x}, \mathbf{v}, t_1, t_2), \\ &= P^{(0,0)} + Pe St (P^{(0,1)} + St P^{(1,1)} + St^2 P^{(2,1)}) \\ &\quad + (Pe St)^2 (P^{(0,2)} + St P^{(1,2)}) + (Pe St)^3 P^{(0,3)} + O(St^4), \end{aligned}$$

which would be convergent for arbitrary  $Pe$  as  $St \rightarrow 0$ . The two-time-scale expansions for the exact solutions  $P^m$  and  $P^d$  to  $O(St)$  are tabulated in Appendix A2. In the next section, we perform the multiple scales analysis to  $O(St)$  to determine  $P^{(0,0)}$  and  $P^{(0,1)}$  in the above series.

---

<sup>3</sup>Note that such a series involving only integral powers of the parameters  $Pe$  and  $St$ , suggesting an analytic dependence, is plausible only in the absence of bounding surfaces. A finite (or semi-infinite) domain may lead to the existence of boundary layers wherein the distribution function substantially deviates from the local equilibrium solution. The analyticity with respect to the parameter is usually lost in such cases.

### 2.3.2 Multiple scales analysis

In this section we follow the analysis of (Wycoff & Balazs 1987a) in developing the general structure of the multiple scales perturbation scheme. It is convenient to use the rescaled fluctuation velocity  $\mathbf{w}$  ( $= (Pe St)^{\frac{1}{2}}(\mathbf{v} - y\mathbf{1}_x)$ ) so that  $St$  is the only parameter in equation (2.11). To this end, we also need to use the rescaled position variables  $(\hat{x}, \hat{y}) = (Pe St)^{\frac{1}{2}}(x, y)$  and equation (2.11) becomes

$$\frac{\partial \bar{P}}{\partial t} + St \hat{y} \frac{\partial \bar{P}}{\partial \hat{x}} + St \left( w_1 \frac{\partial \bar{P}}{\partial \hat{x}} + w_2 \frac{\partial \bar{P}}{\partial \hat{y}} \right) = \frac{\partial}{\partial w_1} (w_1 \bar{P}) + \frac{\partial}{\partial w_2} (w_2 \bar{P}) + \left( \frac{\partial^2 \bar{P}}{\partial w_1^2} + \frac{\partial^2 \bar{P}}{\partial w_2^2} \right), \quad (2.15)$$

where  $\bar{P}(\hat{\mathbf{x}}, \mathbf{w}, t) = P(\mathbf{x}, \mathbf{v}, t)/(Pe St)^2$  is the rescaled probability density (to satisfy the integral constraint  $\int \bar{P} d\hat{\mathbf{x}} d\vec{w} = 1$ ). Using the general form (2.10) of section 2.2, we write

$$\begin{aligned} \bar{P}(\hat{\mathbf{x}}, \mathbf{w}, \{t_j\}; St, Pe) = & \frac{1}{(2\pi)} \sum_{m,n=0}^{\infty} \sum_{i=0}^{\infty} (St)^i \left[ \sum_{s=0}^{\infty} \phi_{m,n,s}^{(i)}(\hat{x}, \hat{y}, t_1) e^{-st_1} \right] \\ & H_m \left( \frac{w_1}{2^{\frac{1}{2}}} \right) H_n \left( \frac{w_2}{2^{\frac{1}{2}}} \right) \exp \left[ -\frac{w_1^2 + w_2^2}{2} \right], \quad (2.16) \end{aligned}$$

where  $t_1$  is used to denote that the  $\phi$ 's are independent of the fast time scale  $t_1$ . The analysis being restricted to two dimensions, we use  $(m, n)$  in place of  $\{n_i\}$  to label the eigenfunctions.

In addition, we set

$$\frac{\partial}{\partial t} = \sum_{r=1}^{\infty} St^{(r-1)} \frac{\partial}{\partial t_r}, \quad (2.17)$$

where the  $t_r$ 's are treated as independent variables. Substituting (2.16) and (2.17) into (2.15), we collect like powers of  $St$  and equate the coefficients of  $e^{-st_1}$  in these terms to zero for each  $s$ , since this is the only way the relation would hold for arbitrary  $St$  and  $t_1$ . This leads to a

recurrence relation for the  $\phi$ 's given as

$$\begin{aligned} & \sum_{r=2}^{i+1} \frac{\partial}{\partial t_r} \phi_{m,n,s}^{(i+1-r)} + (m+n-s)\phi_{m,n,s}^{(i)} + \frac{1}{2^{\frac{1}{2}}} \left( \frac{\partial \phi_{m-1,n,s}^{(i-1)}}{\partial \hat{x}} + \frac{\partial \phi_{m,n-1,s}^{(i-1)}}{\partial \hat{y}} \right) + \hat{y} \frac{\partial \phi_{m,n,s}^{(i-1)}}{\partial \hat{x}} \\ & + 2^{\frac{1}{2}} \left\{ (m+1) \frac{\partial \phi_{m+1,n,s}^{(i-1)}}{\partial \hat{x}} + (n+1) \frac{\partial \phi_{m,n+1,s}^{(i-1)}}{\partial \hat{y}} \right\} + \frac{\phi_{m-1,n-1,s}^{(i-1)}}{2} + (n+1)\phi_{m-1,n+1,s}^{(i-1)} = 0. \end{aligned} \quad (2.18)$$

Thus when formulated in terms of fluctuating velocities, the above recurrence relation no longer possesses nearest neighbor symmetry as was found in Wycoff & Balazs (1987ab). This is seen more readily when (2.18) is rewritten in terms of the tensorial coefficients  $\phi_{N,s}^{(i)}$ 's, where  $\phi_{N,s}^{(i)}$  contains all  $\phi_{m,n,s}^{(i)}$  with  $m+n=N$ . While all other elements can be written in terms of  $\phi_{N,s}^{(i)}$ ,  $\phi_{N+1,s}^{(i)}$  and  $\phi_{N-1,s}^{(i)}$ ,  $\phi_{m-1,n-1,s}^{(i-1)}$  results in an additional term proportional to  $\phi_{N-2,s}^{(i)}$ , which clearly destroys the symmetric structure.

If  $\tilde{a}_{m,n}(\hat{x}, \hat{y})$  are the coefficients of  $H_m H_n$  in a similar expansion of the initial distribution function, then the initial condition becomes

$$\tilde{a}_{m,n}^{(i)}(\hat{x}, \hat{y}) = \sum_{s=0}^{\infty} \phi_{m,n,s}^{(i)}(\hat{x}, \hat{y}, 0), \quad (2.19)$$

where  $\tilde{a}_{m,n}^{(i)} = 0 \forall i \geq 1$  when the initial condition is independent of  $St$ . Equations (2.18) and (2.19) together with suitable consistency conditions (derived below) are used to obtain the  $\phi$ 's. We now tabulate the solutions at successive orders.

For  $i=0$ , one obtains from (2.18)

$$\begin{aligned} \phi_{m,n,s}^{(0)} &= 0 \quad \forall \quad s \neq m+n, \\ \phi_{m,n,m+n}^{(0)} &= b_{m,n}^{(0)}(\hat{x}, \hat{y}, t_A), \end{aligned} \quad (2.20)$$

where  $b_{m,n}^{(0)}$  is an arbitrary (slowly varying) function of space and time that will be made determinate by consistency conditions at higher orders. The initial condition for  $b_{m,n}^{(0)}$  is

$$b_{m,n}^{(0)}(\hat{x}, \hat{y}, 0) = \tilde{a}_{m,n}^{(0)}(\hat{x}, \hat{y}). \quad (2.21)$$

That the only zero non-zero element at this order occurs for  $s = m + n$  implies that to leading order, the solution of (2.15) is

$$\bar{P}^{(0)}(\hat{\mathbf{x}}, \mathbf{w}, t) = \frac{1}{(2\pi)} \sum_{m,n} b_{m,n}^{(0)} e^{-(m+n)t_1} H_m\left(\frac{w_1}{2^{\frac{1}{2}}}\right) H_n\left(\frac{w_2}{2^{\frac{1}{2}}}\right) \exp\left[-\frac{w_1^2 + w_2^2}{2}\right],$$

which is of the same general form as (2.9), now for two dimensions.

For  $i = 1$ , equation (2.18) takes the form

$$\begin{aligned} & \frac{\partial}{\partial t_2} \phi_{m,n,s}^{(0)} + (m+n-s)\phi_{m,n,s}^{(1)} + \frac{1}{2^{\frac{1}{2}}} \left( \frac{\partial \phi_{m-1,n,s}^{(0)}}{\partial \hat{x}} + \frac{\partial \phi_{m,n-1,s}^{(0)}}{\partial \hat{y}} \right) + \hat{y} \frac{\partial \phi_{m,n,s}^{(0)}}{\partial \hat{x}} \\ & + 2^{\frac{1}{2}} \left\{ (m+1) \frac{\partial \phi_{m+1,n,s}^{(0)}}{\partial \hat{x}} + (n+1) \frac{\partial \phi_{m,n+1,s}^{(0)}}{\partial \hat{y}} \right\} + \frac{\phi_{m-1,n-1,s}^{(0)}}{2} + (n+1)\phi_{m-1,n+1,s}^{(0)} = 0. \end{aligned}$$

Putting  $s = m + n$ , one obtains the consistency condition for  $b_{m,n}^{(0)}$  at this order,

$$\frac{\partial b_{m,n}^{(0)}}{\partial t_2} + \hat{y} \frac{\partial b_{m,n}^{(0)}}{\partial \hat{x}} + (n+1)b_{m-1,n+1}^{(0)} = 0. \quad (2.22)$$

For other values of  $s$ , one obtains the entire first order solution:

$$\phi_{m,n,m+n+1}^{(1)} = 2^{\frac{1}{2}} \left\{ (m+1) \frac{\partial b_{m+1,n}^{(0)}}{\partial \hat{x}} + (n+1) \frac{\partial b_{m,n+1}^{(0)}}{\partial \hat{y}} \right\},$$

$$\phi_{m,n,m+n}^{(1)} = b_{m,n}^{(1)}(\hat{x}, \hat{y}, t_1),$$

(2.23)

$$\phi_{m,n,m+n-1}^{(1)} = -\frac{1}{2^{\frac{1}{2}}} \left( \frac{\partial b_{m-1,n}^{(0)}}{\partial \hat{x}} + \frac{\partial b_{m,n-1}^{(0)}}{\partial \hat{y}} \right), \quad (2.24)$$

$$\phi_{m,n,m+n-2}^{(1)} = -\frac{1}{4} b_{m-1,n-1}^{(0)},$$

$$\phi_{m,n,s}^{(1)} = 0 \quad \forall s \neq m+n, m+n+1, m+n-1, m+n-2,$$

where  $b_{m,n}^{(1)}$  will similarly be determined by the consistency condition at the next order.

Assuming a  $St$  independent initial condition, equation (2.19) yields

$$b_{m,n}^{(1)}(\hat{x}, \hat{y}, 0) = \frac{1}{2^{\frac{1}{2}}} \left( \frac{\partial b_{m-1,n}^{(0)}}{\partial \hat{x}} + \frac{\partial b_{m,n-1}^{(0)}}{\partial \hat{y}} \right) + \frac{b_{m-1,n-1}^{(0)}}{4} - 2^{\frac{1}{2}} \left\{ (m+1) \frac{\partial b_{m+1,n}^{(0)}}{\partial \hat{x}} + (n+1) \frac{\partial b_{m,n+1}^{(0)}}{\partial \hat{y}} \right\}. \quad (2.25)$$

For  $i = 2$ ,

$$\begin{aligned} & \frac{\partial}{\partial t_3} \phi_{m,n,s}^{(0)} + \frac{\partial}{\partial t_2} \phi_{m,n,s}^{(1)} + (m+n-s) \phi_{m,n,s}^{(2)} + \frac{1}{2^{\frac{1}{2}}} \left( \frac{\partial \phi_{m-1,n,s}^{(1)}}{\partial \hat{x}} + \frac{\partial \phi_{m,n-1,s}^{(1)}}{\partial \hat{y}} \right) + \hat{y} \frac{\partial \phi_{m,n,s}^{(1)}}{\partial \hat{x}} \\ & + 2^{\frac{1}{2}} \left\{ (m+1) \frac{\partial \phi_{m+1,n,s}^{(1)}}{\partial \hat{x}} + (n+1) \frac{\partial \phi_{m,n+1,s}^{(1)}}{\partial \hat{y}} \right\} + \frac{\phi_{m-1,n-1,s}^{(1)}}{2} + (n+1) \phi_{m-1,n+1,s}^{(1)} = 0. \end{aligned} \quad (2.26)$$

Using  $s = m+n$ , this reduces to

$$\frac{\partial b_{m,n}^{(1)}}{\partial t_2} + \hat{y} \frac{\partial b_{m,n}^{(1)}}{\partial \hat{x}} + (n+1) b_{m-1,n+1}^{(1)} = \frac{\partial b_{m,n}^{(0)}}{\partial t_3} - \left( \frac{\partial^2 b_{m,n}^{(0)}}{\partial \hat{x}^2} + \frac{\partial^2 b_{m,n}^{(0)}}{\partial \hat{y}^2} \right), \quad (2.27)$$

which needs to be translated into separate consistency conditions for  $b_{m,n}^{(1)}$  and  $b_{m,n}^{(0)}$ . For this purpose, we first consider the case  $m = 0$  for which equations (2.22) and (2.27) simplify to

$$L b_{0,n}^{(0)} = 0, \quad (2.28)$$

$$L b_{0,n}^{(1)} = \frac{\partial b_{0,n}^{(0)}}{\partial t_3} - \left( \frac{\partial^2 b_{0,n}^{(0)}}{\partial \hat{x}^2} + \frac{\partial^2 b_{0,n}^{(0)}}{\partial \hat{y}^2} \right), \quad (2.29)$$

where  $L = \partial/\partial t_2 + \hat{y}\partial/\partial \hat{x}$ . The first equation gives  $b_{0,n}^{(0)} = F(\hat{x} - \hat{y}t_2)$ , which forces a secular term (on the  $t_2$  scale) in  $b_{0,n}^{(1)}$ . This would suggest setting the right-hand side of (2.29) to zero to eliminate the secularity. For  $m \geq 1$ , however, the (coupled) hyperbolic system of equations for  $b_{m,n}^{(0)}$  at leading order, viz. (2.22), allows for the existence of secular solutions, and this is evidently independent of any constraint we might subsequently impose on the right-hand side of (2.27). Therefore, secularity arguments work only for  $m = 0$ . But if we treat the consistency conditions as definitions for the operators  $\partial/\partial t_i$  ( $i \geq 2$ ) themselves, rather than the arguments on which these act (in a manner similar to the Chapman-Enskog expansion), one finds that the consistency conditions at this order reduce to

$$\frac{\partial b_{m,n}^{(1)}}{\partial t_2} + \hat{y} \frac{\partial b_{m,n}^{(1)}}{\partial \hat{x}} + (n+1)b_{m-1,n+1}^{(1)} = 0, \quad (2.30)$$

$$\frac{\partial b_{m,n}^{(0)}}{\partial t_3} = \frac{\partial^2 b_{m,n}^{(0)}}{\partial \hat{x}^2} + \frac{\partial^2 b_{m,n}^{(0)}}{\partial \hat{y}^2}. \quad (2.31)$$

The multiple scales hierarchy thus retains its structure at successive orders, i.e., the consistency condition for  $b_{m,n}^{(i)}$  obtained at a given order will now be identical to that for  $b_{m,n}^{(i+1)}$  at the next order and so on. For other values of  $s$  in (2.26), one obtains the complete second order solution,

$$\begin{aligned} \phi_{m,n,m+n+2}^{(2)} &= (m+1)(m+2) \frac{\partial^2 b_{m+2,n}^{(0)}}{\partial \hat{x}^2} + 2(m+1)(n+1) \frac{\partial^2 b_{m+1,n+1}^{(0)}}{\partial \hat{x} \partial \hat{y}} + (n+1)(n+2) \frac{\partial^2 b_{m,n+2}^{(0)}}{\partial \hat{y}^2}, \\ \phi_{m,n,m+n+1}^{(2)} &= -2^{\frac{1}{2}} 2(n+1) \frac{\partial b_{m,n+1}^{(0)}}{\partial \hat{x}} + 2^{\frac{1}{2}} \left\{ (m+1) \frac{\partial b_{m+1,n}^{(1)}}{\partial \hat{x}} + (n+1) \frac{\partial b_{m,n+1}^{(1)}}{\partial \hat{y}} \right\}, \\ \phi_{m,n,m+n}^{(2)} &= b_{m,n}^{(2)}(\hat{x}, \hat{y}, t_1), \\ \phi_{m,n,m+n-1}^{(2)} &= -\frac{1}{2^{\frac{1}{2}}} \frac{(m+1)}{2} \frac{\partial b_{m,n-1}^{(0)}}{\partial \hat{x}} + \frac{1}{2^{\frac{1}{2}}} \frac{(3-n)}{2} \frac{\partial b_{m-1,n}^{(0)}}{\partial \hat{y}} - \frac{1}{2^{\frac{1}{2}}} \left( \frac{\partial b_{m-1,n}^{(1)}}{\partial \hat{x}} + \frac{\partial b_{m,n-1}^{(1)}}{\partial \hat{y}} \right), \\ \phi_{m,n,m+n-2}^{(2)} &= \left( \frac{b_{m-2,n}^{(0)}}{8} - \frac{b_{m-1,n-1}^{(1)}}{4} \right) + \frac{1}{4} \left( \frac{\partial^2 b_{m-2,n}^{(0)}}{\partial \hat{x}^2} + 2 \frac{\partial^2 b_{m-1,n-1}^{(0)}}{\partial \hat{x} \partial \hat{y}} + \frac{\partial^2 b_{m,n-2}^{(0)}}{\partial \hat{y}^2} \right), \end{aligned} \quad (2.32)$$

$$\phi_{m,n,m+n-3}^{(2)} = \frac{1}{2^{\frac{1}{2}}4} \left( \frac{\partial b_{m-2,n-1}^{(0)}}{\partial \hat{x}} + \frac{\partial b_{m-1,n-2}^{(0)}}{\partial \hat{y}} \right),$$

$$\phi_{m,n,m+n-4}^{(2)} = \frac{1}{32} b_{m-2,n-2}^{(0)},$$

$$\phi_{m,n,s}^{(2)} = 0 \quad \forall s \neq m+n, m+n+1, m+n+2, m+n-1, m+n-2, m+n-3, m+n-4.$$

Equation (2.19) gives the initial condition for  $b_{m,n}^{(2)}$  as

$$\begin{aligned} b_{m,n}^{(2)}(\hat{x}, \hat{y}, 0) = & - \left[ (m+1)(m+2) \frac{\partial^2 b_{m+2,n}^{(0)}}{\partial \hat{x}^2} + 2(m+1)(n+1) \frac{\partial^2 b_{m+1,n+1}^{(0)}}{\partial \hat{x} \partial \hat{y}} + (n+1)(n+2) \right. \\ & \left. \frac{\partial^2 b_{m,n+2}^{(0)}}{\partial \hat{y}^2} \right] - \left[ -2^{\frac{1}{2}} 2(n+1) \frac{\partial b_{m,n+1}^{(0)}}{\partial \hat{x}} + 2^{\frac{1}{2}} \left\{ (m+1) \frac{\partial b_{m+1,n}^{(1)}}{\partial \hat{x}} + (n+1) \frac{\partial b_{m,n+1}^{(1)}}{\partial \hat{y}} \right\} \right] \\ & - \left[ -\frac{1}{2^{\frac{1}{2}}} \frac{(m+1)}{2} \frac{\partial b_{m,n-1}^{(0)}}{\partial \hat{x}} + \frac{1}{2^{\frac{1}{2}}} \frac{(3-n)}{2} \frac{\partial b_{m-1,n}^{(0)}}{\partial \hat{y}} - \frac{1}{2^{\frac{1}{2}}} \left( \frac{\partial b_{m-1,n}^{(1)}}{\partial \hat{x}} + \frac{\partial b_{m,n-1}^{(1)}}{\partial \hat{y}} \right) \right] \\ & - \left[ \left( \frac{b_{m-2,n}^{(0)}}{8} - \frac{b_{m-1,n-1}^{(1)}}{4} \right) + \frac{1}{4} \left( \frac{\partial^2 b_{m-2,n}^{(0)}}{\partial \hat{x}^2} + 2 \frac{\partial^2 b_{m-1,n-1}^{(0)}}{\partial \hat{x} \partial \hat{y}} + \frac{\partial^2 b_{m,n-2}^{(0)}}{\partial \hat{y}^2} \right) \right] \\ & - \frac{1}{2^{\frac{1}{2}}4} \left( \frac{\partial b_{m-2,n-1}^{(0)}}{\partial \hat{x}} + \frac{\partial b_{m-1,n-2}^{(0)}}{\partial \hat{y}} \right) - \frac{1}{32} b_{m-2,n-2}^{(0)}. \end{aligned} \quad (2.33)$$

Combining equations (2.22) and (2.31),  $b_{m,n}^{(0)}$  satisfies

$$\frac{\partial b_{m,n}^{(0)}}{\partial t_2} = -\hat{y} \frac{\partial b_{m,n}^{(0)}}{\partial \hat{x}} - (n+1) b_{m-1,n+1}^{(0)} + St \left( \frac{\partial^2 b_{m,n}^{(0)}}{\partial \hat{x}^2} + \frac{\partial^2 b_{m,n}^{(0)}}{\partial \hat{y}^2} \right), \quad (2.34)$$

where we use

$$\frac{\partial}{\partial t_2} = \sum_{i=2}^{\infty} \frac{\partial}{\partial t_i}, \quad (2.35)$$

to the relevant order so that the dependence on the slower time scales is expressed in terms of  $t_2$  alone, which facilitates comparison with the exact solutions (see Appendix A2). Note that the diffusive terms become  $O(1)$  when we revert to the original variables; thus to leading

order

$$\frac{\partial b_{m,n}^{(0)}}{\partial t_2} + y \frac{\partial b_{m,n}^{(0)}}{\partial x} + (n+1)b_{m-1,n+1}^{(0)} = \frac{1}{Pe} \left( \frac{\partial^2 b_{m,n}^{(0)}}{\partial x^2} + \frac{\partial^2 b_{m,n}^{(0)}}{\partial y^2} \right), \quad (2.36)$$

which for  $m = 0$  is the Smoluchowski equation for a Brownian particle in shear flow.

Since the second-order derivatives jump an order in  $St$ , one might expect higher order derivatives down the hierarchy (for instance, fourth-order derivatives at  $O(St^2)$ , sixth-order at  $O(St^3)$  and so on) to also contribute to leading order. This is not the case, however, as we explicitly show the absence of fourth-order derivatives of  $b_{m,n}^{(0)}$  at  $O(St^2)$  and consider this to be symptomatic of the higher orders in the hierarchy. The second-order derivatives of  $b_{m,n}^{(0)}$  at this order then represent the entire  $O(St)$  correction to equation (2.36) if one likewise shows the absence of fourth-order derivatives at  $O(St^3)$ . This entails considering the operators  $\partial/\partial t_4$  and  $\partial/\partial t_5$  and is done in Appendix A3; we finally obtain the  $O(St)$  correction as

$$\frac{\partial b_{m,n}^{(0)}}{\partial t_4} = 2(n+1) \frac{\partial^2 b_{m-1,n+1}^{(0)}}{\partial \hat{x}^2} - (n+1) \frac{\partial^2 b_{m-1,n+1}^{(0)}}{\partial \hat{y}^2} + (m+1) \frac{\partial^2 b_{m+1,n-1}^{(0)}}{\partial \hat{x}^2} + (3n-m-1) \frac{\partial^2 b_{m,n}^{(0)}}{\partial \hat{x} \partial \hat{y}}. \quad (2.37)$$

The consistency conditions at these orders again reveal the recurrent structure of the hierarchy (see Appendix A3), and thus all  $b_{m,n}^{(i)}$ 's satisfy the same equations (but with different initial conditions). Using (2.35) one can combine (2.36) and (2.37) to obtain the equation governing  $b_{m,n}^{(i)}$  to  $O(St)$  as

$$\begin{aligned} \frac{\partial b_{m,n}^{(i)}}{\partial t_2} + \hat{y} \frac{\partial b_{m,n}^{(i)}}{\partial \hat{x}} + (n+1)b_{m-1,n+1}^{(i)} &= St \left( \frac{\partial^2 b_{m,n}^{(i)}}{\partial \hat{x}^2} + \frac{\partial^2 b_{m,n}^{(i)}}{\partial \hat{y}^2} \right) + St^2 \left[ 2(n+1) \frac{\partial^2 b_{m-1,n+1}^{(i)}}{\partial \hat{x}^2} \right. \\ &\quad \left. - (n+1) \frac{\partial^2 b_{m-1,n+1}^{(i)}}{\partial \hat{y}^2} + (m+1) \frac{\partial^2 b_{m+1,n-1}^{(i)}}{\partial \hat{x}^2} \right. \\ &\quad \left. + (3n-m-1) \frac{\partial^2 b_{m,n}^{(i)}}{\partial \hat{x} \partial \hat{y}} \right], \end{aligned}$$

or in the original variables

$$\begin{aligned}
\frac{\partial b_{m,n}^{(i)}}{\partial t_2} + y \frac{\partial b_{m,n}^{(i)}}{\partial x} + (n+1)b_{m-1,n+1}^{(i)} &= \frac{1}{Pe} \left( \frac{\partial^2 b_{m,n}^{(i)}}{\partial x^2} + \frac{\partial^2 b_{m,n}^{(i)}}{\partial y^2} \right) + \frac{St}{Pe} \left[ 2(n+1) \frac{\partial^2 b_{m-1,n+1}^{(i)}}{\partial x^2} \right. \\
&\quad - (n+1) \frac{\partial^2 b_{m-1,n+1}^{(i)}}{\partial y^2} + (m+1) \frac{\partial^2 b_{m+1,n-1}^{(i)}}{\partial x^2} \\
&\quad \left. + (3n-m-1) \frac{\partial^2 b_{m,n}^{(i)}}{\partial x \partial y} \right], \tag{2.38}
\end{aligned}$$

where the initial conditions for  $i = 0, 1$  and  $2$  are given by (2.21), (2.25) and (2.33), respectively. The solutions to these equations together with the expressions for the  $\phi^{(i)}$ 's given by (2.20), (2.24) and (2.32) completely determine  $P(\mathbf{x}, \mathbf{v}, t)$  to  $O(St)$ . The multiple scales method helps reduce the difficulty of the problem from that of directly solving the full Fokker-Planck equation (2.2) to solving equations (2.38) for the  $b_{m,n}^{(i)}$ 's in configuration space alone.

To identify the corrections to the Smoluchowski equation for long times, we rewrite equation (2.16) in the form

$$\bar{P}(\hat{\mathbf{x}}, \mathbf{w}, t_1, t_2; St, Pe) = \sum_{m,n=0}^{\infty} \sum_{i=0}^{\infty} St^i \left[ b_{m,n}^{(i)} e^{-(m+n)t_1} + \sum_{\substack{j=m+n-2i \\ j \geq 0}}^{m+n+i} \phi_{m,n,j}^{(i)} e^{-jt_1} \right] \bar{H}_m \left( \frac{w_1}{2^{1/2}} \right) \bar{H}_n \left( \frac{w_2}{2^{1/2}} \right), \tag{2.39}$$

where  $\bar{H}_n(x) = H_n(x)e^{-x^2}$  and ‘ $'$ ’ is used to denote the exclusion of the  $i = (m+n)$  term from the summation. The spatial density for finite  $St$ ,  $g(\mathbf{x}, t; St)$ , is obtained by integrating out the momentum coordinates in the above equation. Noting that the integrals of the Hermite functions equal zero for all  $m$  and  $n$  except  $m = n = 0$ , we get

$$g(\mathbf{x}, t_2; St) = \int P dudv = (Pe St) \int \bar{P} dw_1 dw_2 = (Pe St) \sum_{i=0}^{\infty} St^i b_{0,0}^{(i)},$$

where we have neglected exponentially decaying terms (arising from the  $\phi$  summations) since they are negligible for all times greater than  $O(\tau_p)$ . Clearly,  $g$  satisfies the same equations as the  $b_{0,0}^{(i)}$ 's, which, to  $O(St)$ , is

$$\frac{\partial g}{\partial t_2} + y \frac{\partial g}{\partial x} = \frac{1}{Pe} \left( \frac{\partial^2 g}{\partial x^2} + \frac{\partial^2 g}{\partial y^2} \right) - \frac{St}{Pe} \frac{\partial^2 g}{\partial x \partial y} + O(St^2). \quad (2.40)$$

The corresponding initial condition (in rescaled variables) is

$$g(\mathbf{x}, 0; St) = (Pe St) \{b_{0,0}^{(0)}(\hat{x}, \hat{y}, 0) + St b_{0,0}^{(1)}(\hat{x}, \hat{y}, 0) + St^2 b_{0,0}^{(2)}(\hat{x}, \hat{y}, 0)\}, \quad (2.41)$$

where the terms on the right-hand side can be obtained to  $O(St)$  from (2.21), (2.25) and (2.33) for  $m = n = 0$ <sup>4</sup>.

Equation (2.40) is the Smoluchowski equation for a Brownian particle in a simple shear flow correct to  $O(St)$ ; the effect of inertia is to introduce an off-diagonal diffusivity  $D_{xy} = -(St/2Pe)$ . Starting from an isotropic spatial density at  $t = 0$ , the shear flow distorts iso-probability contours into ellipses, which stretch and align themselves with the flow as  $t \rightarrow \infty$ . In the limit of long times, the inclination of the major axis of the ellipse with the flow direction is given by  $\theta = (1/2) \tan^{-1}(3/t)$ , and thus tends to zero as  $t \rightarrow \infty$ . For finite  $St$ , not considering the  $O(St)$  corrections to the initial conditions, the effect of the off-diagonal diffusive term is to endow the probability ellipse with an ‘inertia’ which resists the tilting effect of the flow (see Fig 2.1), slowing it by  $O(St)$ ; indeed, for this case  $\theta = (1/2) \tan^{-1}(3/t + 3St/2t^2)$ , and is therefore greater than its inertialess value by  $O(St)$

<sup>4</sup>For  $m = n = 0$ , it is easy to determine the complete expression for  $\partial/\partial t_5$  and to prove the absence of fourth-order derivatives in  $\partial/\partial t_6$ , both of course acting on  $b_{0,0}^{(i)}$  (or  $g$ ). Thus, to  $O(St^2)$ , the equation for  $g$  becomes

$$\frac{\partial g}{\partial t_2} + y \frac{\partial g}{\partial x} = \frac{1}{Pe} \left( \frac{\partial^2 g}{\partial x^2} + \frac{\partial^2 g}{\partial y^2} \right) - \frac{St}{Pe} \frac{\partial^2 g}{\partial x \partial y} - \frac{3St^2}{2Pe} \frac{\partial^2 g}{\partial x^2}.$$

at any given time.

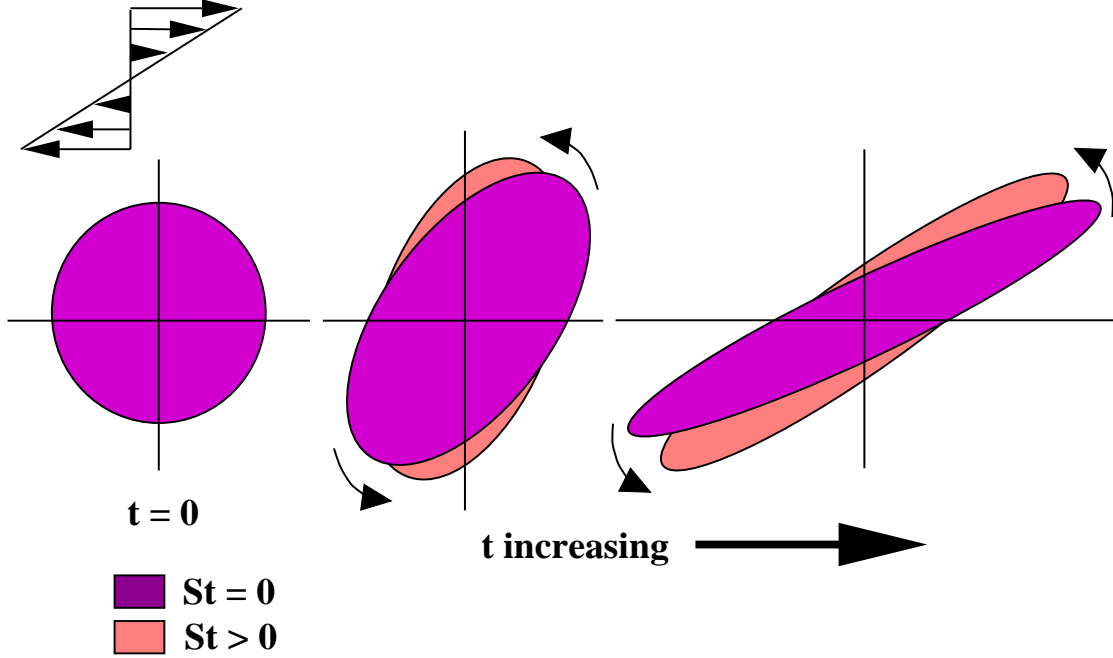


Figure 2.1: Iso-probability contours in simple shear flow for  $St \geq 0$ .

In the limit of vanishing Brownian motion ( $Pe \rightarrow \infty$ ), the inertial corrections vanish for any finite value of  $St$ , and (2.40) simplifies to

$$\frac{\partial g}{\partial t_2} + y \frac{\partial g}{\partial x} = 0,$$

which has the general solution  $F(x - yt_2)$ , leading to a number density that remains constant along a streamline. For long times, the particle is passively convected, with its velocity equal to that of the ambient shear field at its location. This limit holds to all orders in  $St$  for simple shear flow in the absence of Brownian motion; the only inertial effects arise on account of short-time relaxations from initial conditions (see section 2.4.3). This is no longer the case, however, for a general linear flow where the streamlines are curved and a particle of finite mass is unable to faithfully follow the streamlines. For instance in a pure rotational

flow ( $u = Gy, v = -Gx$ ,  $G$  being the angular velocity) for finite  $St$ , the particle will follow a path that spirals outwards due to centrifugal forces in contrast to the purely tangential motion of the fluid elements. The case of simple shear flow of a suspension is similar since the hydrodynamic interactions between particles now cause the particle pathlines to become curved, and thereby deviate from the rectilinear pattern of the ambient field.

The solution to the corrected Smoluchowski equation (2.40) is of the form  $g = g_0 + Stg_1$ , where  $g_0$  is the solution of the leading order Smoluchowski equation, and is obtained from knowledge of the Green's function of (2.40) and the initial condition at leading order. The Green's function is (see Appendix A5)  $G(x, y, t|x', y', t')$  from equation (A.61), and satisfies  $G(x, y, t|x', y', t') = \delta(x - x')\delta(y - y')$ . The  $O(St)$  correction  $g_1 = g_1^h + g_1^p$ , where  $g_1^h$  is the homogeneous solution satisfying the initial condition at  $O(St)$ , and  $g_1^p$  is the particular solution given by<sup>5</sup>

$$g_1^p = -\frac{1}{Pe} \left[ \frac{t_2^2}{2} \frac{\partial^2 g_0}{\partial x^2} + t_2 \frac{\partial^2 g_0}{\partial x \partial y} \right]. \quad (2.42)$$

For the velocity distributions considered, we have from (2.41) (also see sections 2.4.1 and 2.4.2),

$$\begin{aligned} g_0^d(\mathbf{x}, 0) &= \delta(x)\delta(y), \\ g_1^d(\mathbf{x}, 0) &= -\frac{3}{2Pe} [\delta''(x)\delta(y) + \delta(x)\delta''(y)], \\ g_0^m(\mathbf{x}, 0) &= \delta(x)\delta(y), \\ g_1^m(\mathbf{x}, 0) &= -\frac{1}{Pe} [\delta''(x)\delta(y) + \delta(x)\delta''(y)], \end{aligned}$$

where the superscripts  $d$  and  $m$ , as before, indicate the initial conditions corresponding to a

---

<sup>5</sup>See Appendix A5 for details.

delta function and a Maxwellian in velocity space, respectively. The solutions for  $g$ , to  $O(St)$ , for the two cases are

$$\begin{aligned} g^d(\mathbf{x}, t_2; St) &= G_0 - \frac{St}{Pe} \left[ \frac{3}{2} \left\{ \frac{\partial^2 G_0}{\partial x^2} + \left( \frac{\partial}{\partial y} + t_2 \frac{\partial}{\partial x} \right)^2 G_0 \right\} + \left( \frac{t_2^2}{2} \frac{\partial^2 G_0}{\partial x^2} + t_2 \frac{\partial^2 G_0}{\partial x \partial y} \right) \right], \\ &= G_0 - \frac{St}{Pe} \left[ \frac{(4t_2^2 + 3)}{2} \frac{\partial^2 G_0}{\partial x^2} + 4t_2 \frac{\partial^2 G_0}{\partial x \partial y} + \frac{3}{2} \frac{\partial^2 G_0}{\partial y^2} \right], \end{aligned} \quad (2.43)$$

$$\begin{aligned} g^m(\mathbf{x}, t_2; St) &= G_0 - \frac{St}{Pe} \left[ \left\{ \frac{\partial^2 G_0}{\partial x^2} + \left( \frac{\partial}{\partial y} + t_2 \frac{\partial}{\partial x} \right)^2 G_0 \right\} + \left( \frac{t_2^2}{2} \frac{\partial^2 G_0}{\partial x^2} + t_2 \frac{\partial^2 G_0}{\partial x \partial y} \right) \right], \\ &= G_0 - \frac{St}{Pe} \left[ \frac{(3t_2^2 + 2)}{2} \frac{\partial^2 G_0}{\partial x^2} + 3t_2 \frac{\partial^2 G_0}{\partial x \partial y} + \frac{\partial^2 G_0}{\partial y^2} \right], \end{aligned} \quad (2.44)$$

where we have used that  $g_0 = G_0(x, y, t_2)$  (see Appendix A5). Note that the solution for an initial condition of the form  $\delta(x)\delta^{(n)}(y)$  is given by the action of the operator  $(\partial/\partial y + t_2 \partial/\partial x)^n$  on the fundamental solution  $G_0$ , and represents the effect of the ambient vorticity in aligning the ‘multipole’ singularity (initially along the  $y$  axis) with the flow direction with increasing  $t_2$  (Blawdziewicz & Szamel 1993). The number density  $g$  is entirely determined by the three spatial variances viz.  $\langle xx \rangle$ ,  $\langle yy \rangle$  and  $\langle xy \rangle$ . Integrating by parts, one obtains that the terms proportional to  $\partial^2 G_0/\partial x^2$ ,  $\partial^2 G_0/\partial x \partial y$  and  $\partial^2 G_0/\partial y^2$  in (2.43) and (2.44) contribute to the  $O(St)$  corrections to  $\langle xx \rangle$ ,  $\langle xy \rangle$  and  $\langle yy \rangle$  respectively; the resulting expressions for the variances in the two cases are

$$\langle xx \rangle_d = \langle xx \rangle_{G_0} - St(4t_2^2 + 3),$$

$$\langle xy \rangle_d = \langle xy \rangle_{G_0} - St(4t_2),$$

$$\langle yy \rangle_d = \langle yy \rangle_{G_0} - 3St,$$

$$\langle xx \rangle_m = \langle xx \rangle_{G_0} - St(3t_2^2 + 2),$$

$$\langle xy \rangle_m = \langle xy \rangle_{G_0} - St(3t_2),$$

$$\langle yy \rangle_m = \langle yy \rangle_{G_0} - 2St,$$

where  $\langle xx \rangle_{G_0}$ ,  $\langle xy \rangle_{G_0}$  and  $\langle yy \rangle_{G_0}$  are the variances corresponding to  $G_0$  (see Appendix A5). It can easily be verified that the above expressions are identical to (2.13) and (2.14) (neglecting exponentially decaying terms).

## 2.4 Comparison of exact and multiple scales solutions

In the previous section, we calculated the long time limits of the spatial variances generated by the multiple scales analysis for the Maxwellian and delta function initial conditions, and showed that they agreed with those obtained from the exact solutions. Here we compare the complete exact and multiple scales solutions, including the short-time inertial relaxations. We also examine the relaxation of the Brownian particle from a specified initial condition in the athermal limit ( $Pe \rightarrow \infty$ ).

### 2.4.1 Multiple scales solution for a Maxwellian initial condition

The Maxwellian initial condition is given by

$$\begin{aligned} P(\mathbf{x}, \mathbf{v}, 0) &= \{\delta(x)\delta(y)\} \left(\frac{Pe St}{2\pi}\right) \exp\left[-\frac{Pe St(u^2 + v^2)}{2}\right], \\ &= \{\delta(x)\delta(y)\} \left(\frac{Pe St}{2\pi}\right) \exp\left[-\frac{Pe St\{(u-y)^2 + v^2\}}{2}\right], \end{aligned}$$

where the second step is possible due to the presence of  $\delta(y)$ . In terms of the rescaled variables  $(\hat{\mathbf{x}}, \mathbf{w})$ ,

$$\bar{P}(\hat{\mathbf{x}}, \mathbf{w}, 0) = \frac{1}{(2\pi)} \{\delta(\hat{x})\delta(\hat{y})\} \bar{H}_0\left(\frac{w_1}{2^{\frac{1}{2}}}\right) \bar{H}_0\left(\frac{w_2}{2^{\frac{1}{2}}}\right). \quad (2.45)$$

Therefore, (2.21) gives the initial conditions for the  $b_{m,n}^{(0)}$ 's as<sup>6</sup>

$$\begin{aligned} b_{0,0}^{(0)}(\hat{x}, \hat{y}, 0) &= \delta(\hat{x})\delta(\hat{y}) = \frac{\delta(x)\delta(y)}{Pe St}, \\ b_{m,n}^{(0)}(\hat{x}, \hat{y}, 0) &= 0 \quad \forall m+n > 0. \end{aligned} \quad (2.46)$$

For small  $St$ ,

$$b_{m,n}^{(0)}(\hat{x}, \hat{y}, t_2; St) = b_{m,n}^{(0)I}(\hat{x}, \hat{y}, t_2) + St b_{m,n}^{(0)II}(\hat{x}, \hat{y}, t_2) + O(St^2), \quad (2.47)$$

where  $b_{m,n}^{(0)I}$  satisfies the required initial condition, resulting in trivial conditions for all higher order coefficients in the expansion. To leading order, (2.38) for  $i, m = 0$  takes the form

$$\frac{\partial b_{0,n}^{(0)I}}{\partial t_2} + y \frac{\partial b_{0,n}^{(0)I}}{\partial x} = \frac{1}{Pe} \left( \frac{\partial^2 b_{0,n}^{(0)I}}{\partial x^2} + \frac{\partial^2 b_{0,n}^{(0)I}}{\partial y^2} \right). \quad (2.48)$$

Therefore,  $b_{0,0}^{(0)I} = G_0/(Pe St)$  (denoted from here on by  $\bar{G}_0$ ), and  $b_{0,n}^{(0)I}(\hat{x}, \hat{y}, t_2) = 0 \forall n \geq 1$ . Since  $b_{0,0}^{(0)I}$  does not couple to any of the equations for  $b_{m,n}^{(0)I}$  for  $m \geq 1$ , the trivial initial conditions (2.46) imply  $b_{m,n}^{(0)I}(\hat{x}, \hat{y}, t_2) = 0 \forall m \geq 1 \& n \geq 0$ . Thus,  $b_{0,0}^{(0)I}$  is the only non-zero element at the leading order.

At the next order, the  $b_{m,n}^{(0)II}$ 's satisfy trivial initial conditions and are therefore zero for  $m \geq 1$  and  $n \geq 0$ ;  $b_{0,0}^{(0)II}$  (also see equation (2.40)) satisfies

$$Db_{0,0}^{(0)II} = -\frac{1}{Pe} \frac{\partial^2 \bar{G}_0}{\partial x \partial y}, \quad (2.49)$$

---

<sup>6</sup>The factor of  $(Pe St)$  in the initial condition is present in all the  $b_{m,n}^{(i)}$ 's and only serves to normalize the probability density; it does not change the relative orders of the different contributions

where

$$D = \frac{\partial}{\partial t_2} + y \frac{\partial}{\partial x} - \frac{1}{Pe} \left( \frac{\partial^2}{\partial x^2} + \frac{\partial^2}{\partial y^2} \right),$$

and therefore (see (2.42)),

$$b_{0,0}^{(0)II}(\hat{x}, \hat{y}, t_2) = -\frac{1}{Pe} \left[ \frac{t_2^2}{2} \frac{\partial^2 \bar{G}_0}{\partial x^2} + t_2 \frac{\partial^2 \bar{G}_0}{\partial x \partial y} \right].$$

We now consider the  $b_{m,n}^{(1)}$ 's. Using (2.25), the only non-trivial initial conditions are

$$\begin{aligned} b_{0,1}^{(1)}(\hat{x}, \hat{y}, 0) &= \frac{1}{2^{\frac{1}{2}}} \frac{\partial b_{0,0}^{(0)I}}{\partial \hat{y}} = \frac{1}{(2PeSt)^{\frac{1}{2}}} \frac{\delta(x)\delta'(y)}{PeSt}, \\ b_{1,0}^{(1)}(\hat{x}, \hat{y}, 0) &= \frac{1}{2^{\frac{1}{2}}} \frac{\partial b_{0,0}^{(0)I}}{\partial \hat{x}} = \frac{1}{(2PeSt)^{\frac{1}{2}}} \frac{\delta'(x)\delta(y)}{PeSt}, \\ b_{1,1}^{(1)}(\hat{x}, \hat{y}, 0) &= \frac{1}{4} b_{0,0}^{(0)I} = \frac{1}{4} \frac{\delta(x)\delta(y)}{PeSt}, \end{aligned}$$

where we omit the superscript  $I$  for all  $b_{m,n}^{(i)}$ 's ( $i \geq 1$ ), it being understood that they represent the leading order coefficients in a small  $St$  expansion similar to (2.47), and that the higher order corrections do not affect  $P(\mathbf{x}, \mathbf{v}, t)$  to  $O(St)$ . Using (2.38) for  $i = 1$ , the equations governing the non-trivial coefficients are

$$\begin{aligned} Db_{0,1}^{(1)} &= 0, \\ Db_{1,0}^{(1)} &= -b_{0,1}^{(1)}, \\ Db_{1,1}^{(1)} &= 0, \\ Db_{2,0}^{(1)} &= -b_{1,1}^{(1)}, \end{aligned}$$

where  $b_{2,0}^{(1)}$  is non-zero despite a trivial initial condition due to  $b_{1,1}^{(1)}$  acting as the forcing

function. The solutions, in order, to the above equations are

$$b_{0,1}^{(1)}(\hat{x}, \hat{y}, t_2) = \frac{1}{(2PeSt)^{\frac{1}{2}}} \left( \frac{\partial \bar{G}_0}{\partial y} + t_2 \frac{\partial \bar{G}_0}{\partial x} \right), \quad (2.50)$$

$$b_{1,0}^{(1)}(\hat{x}, \hat{y}, t_2) = \frac{1}{(2PeSt)^{\frac{1}{2}}} \left[ (1 - t_2^2) \frac{\partial \bar{G}_0}{\partial x} - t_2 \frac{\partial \bar{G}_0}{\partial y} \right], \quad (2.51)$$

$$b_{1,1}^{(1)}(\hat{x}, \hat{y}, t_2) = \frac{\bar{G}_0}{4}, \quad (2.52)$$

$$b_{2,0}^{(1)}(\hat{x}, \hat{y}, t_2) = -\frac{t_2 \bar{G}_0}{4}. \quad (2.53)$$

In order to determine the complete  $O(St)$  correction, we need to consider the  $b_{m,n}^{(2)}$ 's. Of these, only those coefficients that satisfy initial conditions involving second-order derivatives (and therefore jump an order in  $St$  when expressed in the original variables) contribute to the  $O(St)$  correction. Using (2.33) and (2.25), the initial conditions for these coefficients are

$$\begin{aligned} b_{0,0}^{(2)}(\hat{x}, \hat{y}, 0) &= -\frac{1}{(PeSt)} \left[ \frac{\partial^2 b_{0,0}^{(0)I}}{\partial x^2} + \frac{\partial^2 b_{0,0}^{(0)I}}{\partial y^2} \right], \\ b_{0,2}^{(2)}(\hat{x}, \hat{y}, 0) &= \frac{1}{4(PeSt)} \frac{\partial^2 b_{0,0}^{(0)I}}{\partial y^2}, \\ b_{1,1}^{(2)}(\hat{x}, \hat{y}, 0) &= \frac{1}{2(PeSt)} \frac{\partial^2 b_{0,0}^{(0)I}}{\partial x \partial y}, \\ b_{2,0}^{(2)}(\hat{x}, \hat{y}, 0) &= \frac{1}{4(PeSt)} \frac{\partial^2 b_{0,0}^{(0)I}}{\partial x^2}. \end{aligned}$$

The equations corresponding to these initial conditions are

$$Db_{0,0}^{(2)} = 0,$$

$$\begin{aligned}
Db_{0,2}^{(2)} &= 0, \\
Db_{1,1}^{(2)} &= -2b_{0,2}^{(2)}, \\
Db_{2,0}^{(2)} &= -b_{1,1}^{(2)},
\end{aligned}$$

with the solutions

$$b_{0,0}^{(2)}(\hat{x}, \hat{y}, t_2) = -\frac{1}{PeSt} \left[ \frac{\partial^2 \bar{G}_0}{\partial x^2} + \left( \frac{\partial}{\partial y} + t_2 \frac{\partial}{\partial x} \right)^2 \bar{G}_0 \right], \quad (2.54)$$

$$b_{0,2}^{(2)}(\hat{x}, \hat{y}, t_2) = \frac{1}{4(PeSt)} \left( \frac{\partial}{\partial y} + t_2 \frac{\partial}{\partial x} \right)^2 \bar{G}_0, \quad (2.55)$$

$$b_{1,1}^{(2)}(\hat{x}, \hat{y}, t_2) = \frac{1}{2(PeSt)} \left[ (1 - t_2^2) \frac{\partial}{\partial x} - t_2 \frac{\partial}{\partial y} \right] \left( \frac{\partial \bar{G}_0}{\partial y} + t_2 \frac{\partial \bar{G}_0}{\partial x} \right), \quad (2.56)$$

$$b_{2,0}^{(2)}(\hat{x}, \hat{y}, t_2) = \frac{1}{4(PeSt)} \frac{\partial^2 \bar{G}_0}{\partial x^2} + \frac{1}{2(PeSt)} \left[ t_2 \left( \frac{t_2^2}{2} - 1 \right) \frac{\partial}{\partial x} + \frac{t_2^2}{2} \frac{\partial}{\partial y} \right] \left( \frac{\partial \bar{G}_0}{\partial y} + t_2 \frac{\partial \bar{G}_0}{\partial x} \right). \quad (2.57)$$

Having calculated the relevant coefficients, we consider the expression for the rescaled probability density  $\bar{P}$  as given by (2.39) upto  $O(St^2)$  in the rescaled variables. The original and the rescaled probability densities differ by a factor of  $(PeSt)^2$ ; this does not, however, alter the relative orders of the different terms, and is therefore not included when comparing contributions from the various terms (below). As mentioned earlier, the  $b_{m,n}^{(2)}$ 's jump an order due to the presence of second-order derivatives in their initial conditions. That they contribute to the solution at  $O(St)$  also stems from the fact that the non-trivial coefficients at this order,  $b_{0,0}^{(2)}$ ,  $b_{2,0}^{(2)}$  and  $b_{0,2}^{(2)}$ , multiply a product of two even Hermite functions ( $\bar{H}_2$  and  $\bar{H}_0$  in this case); the  $O(St)$  contribution therefore comes from the presence of the  $O(1)$  constant term in the even Hermite functions. Note that each power of the rescaled velocity variable  $\mathbf{w}$  will render the relevant contribution smaller by  $O(St^{\frac{1}{2}})$  and thus the quadratic term in  $\bar{H}_2$  would be  $O(St)$  smaller than the constant term. For this reason the non-zero coefficients at the first order,  $St b_{1,0}^{(1)}$  and  $St b_{0,1}^{(1)}$ , despite being  $O(St^{\frac{1}{2}})$  contribute

only at  $O(St)$  to the solution (the additional factor of  $St^{\frac{1}{2}}$  coming from the velocity variable in  $\bar{H}_1$ ), while  $St b_{2,0}^{(1)}$  being  $O(St)$  still contributes at the same order. Similarly, the terms containing  $b_{1,1}^{(1)}$  and  $b_{1,1}^{(2)}$  will be  $o(St)$  since they multiply  $\bar{H}_1(w_1/2^{\frac{1}{2}})\bar{H}_1(w_2/2^{\frac{1}{2}})$ . The reason we need to consider them at all is because the equations for the  $b_{2,0}^{(i)}$ 's and  $b_{1,1}^{(i)}$ 's are coupled, and the former contribute to the  $O(St)$  correction.

From (2.24) and (2.32), we observe that the non-trivial elements  $\phi_{m,n,m+n+j}^{(i)}$ ,  $j$  ranging  $m+n-2i$  to  $m+n+i$ , involve at most  $i^{\text{th}}$  order derivatives of  $b_{m,n}^{(0)}$ . The  $\phi^{(4)}$ 's would in general contain fourth-order derivatives of  $b_{m,n}^{(0)}$  and therefore, terms of the form  $St^4 \phi_{m,n}^{(4)}$  would only contribute at  $O(St^2)$  (when taken together with the constant term in the corresponding even ordered Hermite function). On the other hand, the non-zero  $\phi_{m,n}^{(3)}$ 's that contain third order derivatives multiply odd ordered Hermite functions and thus contribute at the same order as the  $\phi_{m,n}^{(4)}$ 's. We now rewrite (2.39) explicitly including only the terms relevant to  $O(St)$ .

$$\begin{aligned}
\frac{P(\hat{x}, \hat{y}, \bar{u}, \bar{v}; St, Pe)}{(Pe St)^2} &= \left( b_{0,0}^{(0)I} + St b_{0,0}^{(0)II} \right) \exp \left[ -\frac{w_1^2 + w_2^2}{2} \right] + St \left[ \left\{ (2^{\frac{1}{2}} w_1) b_{0,1}^{(1)} e^{-t_1} + (2^{\frac{1}{2}} w_2) b_{1,0}^{(1)} e^{-t_1} \right. \right. \\
&\quad \left. \left. - 2 b_{2,0}^{(1)} e^{-2t_1} \right\} - \left\{ w_1 \frac{\partial b_{0,0}^{(0)I}}{\partial \hat{x}} + w_2 \frac{\partial b_{0,0}^{(0)I}}{\partial \hat{y}} \right\} \right] \exp \left[ -\frac{w_1^2 + w_2^2}{2} \right] \\
&\quad + St^2 \left[ \left\{ b_{0,0}^{(2)} - 2 b_{0,2}^{(2)} e^{-2t_1} - 2 b_{2,0}^{(2)} e^{-2t_1} \right\} + 2^{\frac{1}{2}} \left( \frac{\partial b_{1,0}^{(1)}}{\partial \hat{x}} + \frac{\partial b_{0,1}^{(1)}}{\partial \hat{y}} \right) e^{-t_1} \right. \\
&\quad \left. + 2^{\frac{1}{2}} \left( \frac{\partial b_{1,0}^{(1)}}{\partial \hat{x}} + \frac{\partial b_{0,1}^{(1)}}{\partial \hat{y}} \right) e^{-t_1} - \frac{1}{2} \left( \frac{\partial^2 b_{0,0}^{(0)I}}{\partial \hat{x}^2} + \frac{\partial^2 b_{0,0}^{(0)I}}{\partial \hat{y}^2} \right) \right] \exp \left[ -\frac{w_1^2 + w_2^2}{2} \right],
\end{aligned} \tag{2.58}$$

where we have used  $\bar{H}_0(z) = e^{-z^2}$ ,  $\bar{H}_1(z) = 2^{\frac{1}{2}} z e^{-z^2}$ ,  $\bar{H}_2(z) = 2(z^2 - 1)e^{-z^2}$  and retained only the constant term in  $\bar{H}_2$ . It is seen that the terms linear in the velocity variables  $\mathbf{w}$  involve only  $b_{0,0}^{(0)I}$ ,  $b_{0,1}^{(1)}$  and  $b_{1,0}^{(1)}$ , which makes the calculation of the velocity dependent corrections (terms of the form  $(\mathbf{a} : \mathbf{w}\mathbf{x})P^{(0)}$ , where  $P^{(0)}$  is the leading order solution) alone a

much simpler task. On substituting the expressions obtained for the various coefficients, it can be verified that the above series matches up identically to the expansion of the corresponding exact solution ( $P^m$ ) in Appendix A2.

#### 2.4.2 Multiple scales solution for a delta function initial condition

Here, we briefly present calculations similar to that in the previous section, carried out now for a delta function initial condition. The details are given in Appendix A4. We consider the case where

$$\begin{aligned} P(\mathbf{x}, \mathbf{v}, 0) &= \delta(x)\delta(y)\delta(u)\delta(v), \\ &= \delta(x)\delta(y)\delta(u - y)\delta(v), \end{aligned}$$

so that the probability density in rescaled variables can be written as<sup>7</sup>

$$\bar{P}(\hat{\mathbf{x}}, \mathbf{w}, 0) = \frac{\delta(\hat{x})\delta(\hat{y})}{2\pi} \sum_{m,n=0}^{\infty} \frac{(-1)^{m+n} \bar{H}_{2m}(\frac{w_1}{2^{\frac{1}{2}}}) \bar{H}_{2n}(\frac{w_2}{2^{\frac{1}{2}}})}{2^{2(m+n)} m! n!}.$$

For this case, the form of the solution is much more involved, and we restrict ourselves to finding the  $O(St)$  velocity dependent corrections to  $P(\mathbf{x}, \mathbf{v}, t)$ , which only requires the calculation of the  $b_{m,n}^{(0)}$ 's and  $b_{m,n}^{(1)}$ 's to leading order; the superscripts 'I' and 'II' used in section 2.4.1 are therefore omitted (the successful comparison of the number densities for this initial condition suggests the correctness of the complete  $O(St)$  correction). From (2.21), we obtain the initial conditions for the  $b_{m,n}^{(0)}$ 's as

$$b_{2m,2n}^{(0)}(\hat{x}, \hat{y}, 0) = \frac{(-1)^{m+n}}{2^{2(m+n)} m! n!} \delta(\hat{x})\delta(\hat{y}),$$

---

<sup>7</sup>We have used the relation  $\delta(z) = \frac{1}{(2\pi)^{\frac{1}{2}}} \sum_{n=0}^{\infty} \frac{(-1)^n \bar{H}_{2n}(\frac{z}{2^{\frac{1}{2}}})}{2^{2n} n!}$  (see Uhlenbeck & Ornstein 1954).

$$b_{2m+1,2n}^{(0)}(\hat{x}, \hat{y}, 0) = 0,$$

$$b_{2m,2n+1}^{(0)}(\hat{x}, \hat{y}, 0) = 0,$$

$$b_{2m+1,2n+1}^{(0)}(\hat{x}, \hat{y}, 0) = 0.$$

The structure of the consistency condition (2.36) is such that the sets of coefficients

$(b_{2m,2n+1}^{(0)}, b_{2m+1,2n}^{(0)})$  and  $(b_{2m,2n}^{(0)}, b_{2m+1,2n+1}^{(0)})$  form independent subsystems. The trivial initial conditions for the former give

$$b_{2m,2n+1}^{(0)}(\hat{x}, \hat{y}, t_2) = 0, \quad (2.59)$$

$$b_{2m+1,2n}^{(0)}(\hat{x}, \hat{y}, t_2) = 0. \quad (2.60)$$

For the latter, we first obtain the solution for  $m = 0$  (for which the coupling term in (2.36) is absent) and then solve for increasing  $m$  to obtain the general forms

$$b_{2m,2n}^{(0)}(\hat{x}, \hat{y}, t_2) = \frac{(-1)^{m+n}}{(2\pi)2^{2n+m}n!} \sum_{k=0}^m \frac{t_2^{2m-2k} \prod_{l=k}^{m-1} (2n+2m-1-2l)}{2^k k! (2m-2k)!} \bar{G}_0, \quad (2.61)$$

$$b_{2m+1,2n+1}^{(0)}(\hat{x}, \hat{y}, t_2) = \frac{(-1)^{m+n}}{(2\pi)2^{2n+m+1}n!} \sum_{k=0}^m \frac{t_2^{2m+1-2k} \prod_{l=k}^{m-1} (2n+2m+1-2l)}{2^k k! (2m+1-2k)!} \bar{G}_0. \quad (2.62)$$

Using the above expressions in (2.39), it may be verified that the exact and multiple scales solutions are identical to leading order (see Appendix A4.1).

From equations (2.61) and (2.62), the  $\phi_{m,n,s}^{(1)}$ 's for  $s \neq m+n$  can be determined using (2.24). The  $b_{m,n}^{(1)}$ 's satisfy the same set of equations as the  $b_{m,n}^{(0)}$ 's, and from (2.25),

$$b_{2m,2n}^{(1)}(\hat{x}, \hat{y}, 0) = 0, \quad (2.63)$$

$$b_{2m+1,2n}^{(1)}(\hat{x}, \hat{y}, 0) = \frac{1}{2^{\frac{1}{2}}} \frac{\partial b_{2m,2n}^{(0)}}{\partial \hat{x}} - 2^{\frac{1}{2}} (2m+2) \frac{\partial b_{2m+2,2n}^{(0)}}{\partial \hat{x}}, \quad (2.64)$$

$$b_{2m,2n+1}^{(1)}(\hat{x}, \hat{y}, 0) = \frac{1}{2^{\frac{1}{2}}} \frac{\partial b_{2m,2n}^{(0)}}{\partial \hat{y}} - 2^{\frac{1}{2}}(2n+2) \frac{\partial b_{2m,2n+2}^{(0)}}{\partial \hat{y}}, \quad (2.65)$$

$$b_{2m+1,2n+1}^{(1)}(\hat{x}, \hat{y}, 0) = \frac{1}{4} b_{2m,2n}^{(0)}. \quad (2.66)$$

Again,  $(b_{2m,2n}^{(1)}, b_{2m+1,2n+1}^{(1)})$  and  $(b_{2m,2n+1}^{(1)}, b_{2m+1,2n}^{(1)})$  form independent subsystems; they appear in the multiple scales series in the form  $St b_{m,n}^{(1)} e^{-(m+n)t_1} \bar{H}_m \bar{H}_n$ . The former will only contribute terms of the form  $w_1^i w_2^j$ , where  $i+j$  is even. The largest of these corresponds to  $b_{1,1}^{(1)}$  ( $b_{0,0}^{(1)} = 0$ ) and is  $O(St^2)$ . Therefore, we can restrict our attention to the set  $(b_{2m+1,2n}^{(1)}, b_{2m,2n+1}^{(1)})$  when looking at  $O(St)$  corrections. Solving (2.36) for initial conditions given by (2.64) and (2.65), one obtains

$$b_{2m+1,2n}^{(1)} = \frac{2^{\frac{1}{2}}(-1)^{m+n}}{(2\pi)2^{2n+m}n!} \left[ S_1^{(m,n)} \frac{\partial \bar{G}_0}{\partial \hat{x}} - S_2^{(m,n)} \left( \frac{\partial \bar{G}_0}{\partial \hat{y}} + t_2 \frac{\partial \bar{G}_0}{\partial \hat{x}} \right) \right], \quad (2.67)$$

$$b_{2m,2n+1}^{(1)} = \frac{2^{\frac{1}{2}}(-1)^{m+n}}{(2\pi)2^{2n+m}n!} \left[ S_2^{\prime(m,n)} \left( \frac{\partial \bar{G}_0}{\partial \hat{y}} + t_2 \frac{\partial \bar{G}_0}{\partial \hat{x}} \right) - S_1^{\prime(m,n)} \frac{\partial \bar{G}_0}{\partial \hat{x}} \right], \quad (2.68)$$

where

$$\begin{aligned} S_1^{(m,n)} &= \sum_{k=0}^m \frac{t_2^{2m-2k} \prod_{l=k}^{m-1} (2n+2m-1-2l)}{2^k k! (2m-2k)!}, \\ S_2^{(m,n)} &= \sum_{k=0}^m \frac{t_2^{2m+1-2k} \prod_{l=k}^m (2n+2m+1-2l)}{2^k k! (2m+1-2k)!}, \\ S_1^{\prime(m,n)} &= \sum_{k=0}^{m-1} \frac{t_2^{2m-2k-1} \prod_{l=k}^{m-2} (2n+2m-1-2l)}{2^k k! (2m-1-2k)!}, \\ S_2^{\prime(m,n)} &= \sum_{k=0}^m \frac{t_2^{2m-2k} \prod_{l=k}^{m-1} (2n+2m+1-2l)}{2^k k! (2m-2k)!}. \end{aligned}$$

Using the relations (2.61), (2.62), (2.67), (2.68) and the expressions for the  $\phi^{(1)}$ 's in (2.39), it can be verified (see Appendix A4.2) that the multiple scales series matches the corresponding exact solution to  $O(St)$ , for velocity dependent corrections to the leading order solution.

It is seen that the multiple scales series for this initial condition is of the form

$$P(\mathbf{x}, \mathbf{v}, t_1, t_2; St, Pe) = P^{(0)}(\mathbf{x}, \mathbf{v}, t_1, t_2; St, Pe) + St P^{(1)}(\mathbf{x}, \mathbf{v}, t_1, t_2; St, Pe) + \dots \quad (2.69)$$

Since the  $P^{(i)}$ 's are themselves functions of  $St$ , the term  $St^i P^{(i)}$  will also include higher order contributions of  $O(St^{i+a})$  ( $a > 0$ ). For instance,  $b_{m,n}^{(0)} \bar{H}_m \bar{H}_n$  in the leading order solution ( $P^{(0)} = \sum b_{m,n}^{(0)} \bar{H}_m \bar{H}_n$ ) contains terms of the form  $b_{m,n}^{(0)} w_1^m w_2^n$  that are  $O(St^{\frac{m+n}{2}})$  when expressed in terms of  $(u, v)$ , and therefore  $o(St)$  for  $m+n > 2$ . Strictly speaking, they should not be considered when comparing the exact and multiple scales solutions to  $O(St)$ ; it is, however, possible in this case (as illustrated in the appendices) to cast the series in a form which can be identified with terms in the exact solution.

### 2.4.3 The athermal limit

In the absence of Brownian motion, a particle at rest at the origin of a simple shear flow remains so for all time. Therefore, to illustrate the relaxation of a non-Brownian particle from its initial state, we must choose an initial condition in position space different from that used above. Accordingly, we first derive the (finite  $Pe$ ) form of the multiple scales solutions when the particle at time  $t = 0$  is at  $(x, y) \equiv (0, y_0)$  with a Maxwellian distribution of velocities. The non-Brownian limit is obtained by letting  $Pe \rightarrow \infty$  in the final expression for the probability density. The initial condition is

$$P(\mathbf{x}, \mathbf{v}, 0) = \delta(x)\delta(y - y_0) \left( \frac{Pe St}{2\pi} \right) \exp \left[ -\frac{Pe St(u^2 + v^2)}{2} \right], \quad (2.70)$$

which can be written in the form

$$\begin{aligned}
P(\mathbf{x}, \mathbf{v}, 0) &= \delta(x)\delta(y - y_0) \left( \frac{Pe St}{2\pi} \right) \exp \left[ -\frac{(Pe St)v^2}{2} \right] \exp \left[ -\frac{Pe St(u - y + y)^2}{2} \right], \\
&= \delta(x)\delta(y - y_0) \left( \frac{Pe St}{2\pi} \right) \exp \left[ -\frac{(Pe St)v^2}{2} \right] \\
&\quad \sum_{m=0}^{\infty} \left( \frac{Pe St}{2} \right)^{\frac{m}{2}} \frac{y^m}{m!} \frac{d^m}{du^m} \left\{ \exp \left[ -Pe St \frac{(u - y)^2}{2} \right] \right\},
\end{aligned}$$

and in terms of the rescaled variables  $(\hat{\mathbf{x}}, \mathbf{w})$ , the renormalized probability density becomes

$$\bar{P}(\hat{\mathbf{x}}, \mathbf{w}, 0) = \frac{1}{2\pi} \sum_{m=0}^{\infty} \delta(\hat{x})\delta(\hat{y} - \hat{y}_0) \frac{(-1)^m \hat{y}_0^m}{m! 2^{\frac{m}{2}}} \bar{H}_m \left( \frac{w_1}{2^{\frac{1}{2}}} \right) \bar{H}_0 \left( \frac{w_2}{2^{\frac{1}{2}}} \right), \quad (2.71)$$

where the delta function allows us to replace  $\hat{y}$  by  $\hat{y}_0$ . The initial conditions for the coefficients

$b_{m,n}^{(0)}$  (see (2.21)) are

$$\begin{aligned}
b_{m,0}^{(0)}(\hat{x}, \hat{y}, 0) &= \delta(\hat{x})\delta(\hat{y} - \hat{y}_0) \frac{(-1)^m \hat{y}_0^m}{m! 2^{\frac{m}{2}}}, \\
b_{m,n}^{(0)}(\hat{x}, \hat{y}, 0) &= 0 \quad \forall \quad n \neq 0.
\end{aligned}$$

From (2.22), we observe that the system of equations for the  $b_{m,n}^{(0)}$ 's ( $n > 0$ ) is independent of the  $b_{m,0}^{(0)}$ 's, and the trivial initial conditions imply that these are zero for all times. With this simplification, the  $b_{m,0}^{(0)}$ 's satisfy

$$\frac{\partial b_{m,0}^{(0)}}{\partial t_2} + \hat{y} \frac{\partial b_{m,0}^{(0)}}{\partial \hat{x}} = 0, \quad (2.72)$$

which gives

$$b_{m,0}^{(0)}(\hat{x}, \hat{y}, t_2) = \frac{(-1)^m \delta(\hat{x} - \hat{y}t_2)\delta(\hat{y} - \hat{y}_0)\hat{y}_0^m}{m! 2^{\frac{m}{2}}}. \quad (2.73)$$

From (2.39), to leading order,

$$\begin{aligned}\bar{P}^{(0)}(\bar{\mathbf{x}}, \mathbf{w}, t_1, t_2; St, Pe) &= \sum_{m=0}^{\infty} b_{m,0}^{(0)} e^{-mt_1} \bar{H}_m\left(\frac{w_1}{2^{\frac{1}{2}}}\right) \bar{H}_0\left(\frac{w_2}{2^{\frac{1}{2}}}\right), \\ &= \sum_{m=0}^{\infty} \frac{(-1)^m \delta(\hat{x} - \hat{y}t_2) \delta(\hat{y} - \hat{y}_0) \hat{y}_0^m}{m! 2^{\frac{m}{2}}} \bar{H}_m\left(\frac{w_1}{2^{\frac{1}{2}}}\right) \bar{H}_0\left(\frac{w_2}{2^{\frac{1}{2}}}\right).\end{aligned}\quad (2.74)$$

To find the limiting form of the above expression as  $Pe \rightarrow \infty$ , we first consider the limiting forms of the Hermite functions.

$$\begin{aligned}\lim_{\substack{Pe \rightarrow \infty \\ St \text{ finite}}} \bar{H}_0\left(\frac{w_1}{2^{\frac{1}{2}}}\right) \bar{H}_0\left(\frac{w_2}{2^{\frac{1}{2}}}\right) &= \lim_{Pe St \rightarrow \infty} \left(\frac{Pe St}{2\pi}\right) \exp\left[-\frac{w_1^2 + w_2^2}{2}\right], \\ &= \lim_{Pe St \rightarrow \infty} \left(\frac{Pe St}{2\pi}\right) \exp\left[-Pe St \frac{(u-y)^2 + v^2}{2}\right], \\ &= \delta(u-y)\delta(v), \\ \lim_{\substack{Pe \rightarrow \infty \\ St \text{ finite}}} \bar{H}_m\left(\frac{w_1}{2^{\frac{1}{2}}}\right) \bar{H}_n\left(\frac{w_2}{2^{\frac{1}{2}}}\right) &= 2^{\frac{m+n}{2}} (-1)^{(m+n)} \lim_{Pe St \rightarrow \infty} \frac{d^{(m+n)}}{dw_1^m dw_2^n} \left\{ \bar{H}_0\left(\frac{w_1}{2^{\frac{1}{2}}}\right) \bar{H}_0\left(\frac{w_2}{2^{\frac{1}{2}}}\right) \right\}, \\ &= (-1)^{m+n} \left(\frac{2}{Pe St}\right)^{\frac{m+n}{2}} \delta^{(m)}(u-y)\delta^{(n)}(v), \\ \Rightarrow \lim_{Pe St \rightarrow \infty} (-1)^{m+n} \left(\frac{Pe St}{2}\right)^{\frac{m+n}{2}} \bar{H}_m\left(\frac{w_1}{2^{\frac{1}{2}}}\right) \bar{H}_n\left(\frac{w_2}{2^{\frac{1}{2}}}\right) &= \delta^{(m)}(u-y)\delta^{(n)}(v).\end{aligned}$$

Using the above limits, (2.74) takes the form

$$P^{(0)}(\mathbf{x}, \mathbf{v}, t_1, t_2; St) = \sum_{m=0}^{\infty} \delta(x - y_0 t_2) \delta(y - y_0) \frac{(y_0 e^{-t_1})^m}{m!} \delta^{(m)}(u - y_0) \delta(v), \quad (2.75)$$

where we have replaced  $y$  by  $y_0$ . Treating the summation (formally) as a Taylor series expansion, we get

$$P^{(0)}(\mathbf{x}, \mathbf{v}, t_1, t_2; St) = \delta(x - y_0 t_2) \delta(y - y_0) \delta(v) \delta(u - y_0 + y_0 e^{-t_1}), \quad (2.76)$$

where the term proportional to  $y_0$  in the argument of the last delta function captures, to leading order, the relaxation of the particle from a state of rest at  $t = 0$  to the steady state velocity of  $y_0 \mathbf{1}_x$  in a time of  $O(\tau_p)$ .

The exact solution for this case is readily obtained by solving the Langevin equations of motion, viz. equation (2.3) with  $\mathbf{F}^B = 0$ , for the same initial conditions. We get

$$x = y_0(t_2 - St) + St y_0 e^{-t_1},$$

$$y = y_0,$$

$$u = y_0(1 - e^{-t_1}),$$

$$v = 0,$$

so that the probability density corresponding to this deterministic trajectory can be written as

$$\delta\{x - y_0 t_2 + y_0 St(1 - e^{-t_1})\} \delta(y - y_0) \delta(v) \delta(u - y_0 + y_0 e^{-t_1}),$$

which, to leading order, is identical to (2.76).

## 2.5 Conclusions and discussion

A multiple scales analysis was carried out for a single Brownian particle in a simple shear flow for small  $St$  by expanding the exact probability density in a series of Hermite functions of the fluctuation velocity. It was shown that to  $O(St)$  the method reproduces the exact solutions for two sets of initial conditions in velocity space, a delta function and a Maxwellian. The structure of the multiple scales hierarchy differs from the usual case of a position dependent forcing (Wycoff & Balazs 1987a) in that arguments based on secularity are not sufficient to

obtain the consistency conditions that determine the dependence of the expansion coefficients on the slower time scales. The success of the multiple scales method clearly implies the existence of an equivalent Chapman-Enskog approach for the same problem (see next chapter).

The  $O(St)$  correction to the Smoluchowski equation was obtained that accounts for the first effects of particle inertia on the spatial probability density. The  $O(St)$  corrections to the spatial density depend on the original phase space initial condition for the Brownian particle, and are therefore different for the two initial conditions considered. For non-rectilinear flows, the inertial corrections remain finite in the limit of vanishing Brownian motion ( $Pe \rightarrow \infty$ ). For shear flow, however, inertia exerts an influence in the athermal limit only when hydrodynamic interactions between particles are taken into account.

For the more pertinent case of a suspension of interacting particles, the fundamental equation is again an  $N$ -body Fokker-Planck equation where both the drag on a particle and the diffusivity tensor are now position-space dependent owing to hydrodynamic interactions. In the dimensionless form the multiparticle Fokker-Planck equation is

$$\begin{aligned} \frac{\partial P_N}{\partial t} &+ St \sum_{i=1}^N \mathbf{v}_i \cdot \frac{\partial P_N}{\partial \mathbf{x}_i} + \sum_{i,j=1}^N (\mathbf{m}_{ij}^{-1} \cdot \mathbf{F}^o_j) \cdot \frac{\partial P_N}{\partial \mathbf{v}_i} \\ &= \sum_{i,j,k=1}^N \mathbf{m}_{ij}^{-1} \cdot \mathbf{R}_{jk}^{FU} : \frac{\partial}{\partial \mathbf{v}_i} (\mathbf{v}_k P_N) + \frac{1}{Pe St} \sum_{i,j,k,l=1}^N \mathbf{m}_{ij}^{-1} \cdot \mathbf{R}_{jk}^{FU} \cdot \mathbf{m}_{kl}^{-1} : \frac{\partial^2 P_N}{\partial \mathbf{v}_i \partial \mathbf{v}_l}, \end{aligned}$$

where the force  $\mathbf{F}^o$  is assumed to be due to an external flow and is scaled accordingly. The  $\mathbf{m}$ 's are (constant) inertia tensors and the  $\mathbf{R}^{FU}$ 's are the configuration dependent hydrodynamic resistance tensors. The velocity  $\mathbf{v}$  in this equation includes both translational and rotational degrees of freedom. The spatial dependence of the drift and diffusivity coefficients make it very difficult to obtain an analytic solution for arbitrary  $Pe$  and  $St$ . Despite the complex

configurational dependence, however, the neglect of fluid inertia still gives rise to a drag linear in the particle velocities, and the structure of the Fokker-Planck equation with respect to the velocity variables is therefore unaltered. Though the multiple scales method in the above form is no longer applicable in this case (see next chapter), one can still employ a Chapman-Enskog expansion for small  $St$  and again reduce the difficulty of the original problem to that of solving relatively tractable (Smoluchowski-type) equations in position space for the expansion coefficients, while capturing the inertial relaxations associated with the velocity distribution in a perturbative manner. The Chapman-Enskog procedure allows for a possible non-analytic parametric dependence of the expansion coefficients on  $St$  and  $Pe$ . This is particularly important for the case of interacting particles since the limit of weak Brownian motion ( $St = 0$ ,  $Pe \rightarrow \infty$ ) is known to be singular (Brady & Morris 1997) and is characterised by the concentration of the positional probability in  $O(aPe^{-1})$  boundary layers near particle-particle contact. These boundary-layer effects are, in part, the reason for persistent non-Newtonian effects even in large  $Pe$  suspensions.

## Bibliography

- [1] Blawdziewicz, J. & Szamel, G. 1993 Structure and rheology of semidilute suspensions under shear. *Physical Review E* **48(6)**, 4632-4636.
- [2] Brady, J.F. & Morris, J.F. 1997 Microstructure of strongly sheared suspensions and its impact on rheology and diffusion. *J. Fluid Mech.* **348**, 103-139.
- [3] Chandrasekhar, S. 1954 Stochastic problems in physics and astronomy, in *Selected papers on noise and stochastic processes* (ed. Nelson Wax), pp. 3-91. Dover.
- [4] Chapman, S. & Cowling, T.G. 1970 *The mathematical theory of non-uniform gases*. Cambridge University Press.
- [5] Elrick, D.E. 1962 Source functions for diffusion in uniform shear flow. *Aust. J. Phys.* **15**, 283-288.
- [6] Hinch, E.J. 1975 Application of the Langevin equation to fluid suspensions. *J. Fluid Mech.* **72**, 499-511.
- [7] Miguel, S.M. & Sancho, J.M. 1979 Brownian motion in shear flow. *Physica* **99A**, 357-364.
- [8] Risken, H. 1989 *The Fokker-Planck Equation*. Springer-Verlag, pp. 25.
- [9] Smoluchowski, M.V. 1915 Über brownsche Molekularbewegung unter Einwirkung äubere Kräfte und deren Zusammenhang mit der verallgemeinerte Diffusionsgleichung. *Ann. d. Physik* **48**, 1103-1112.

- [10] Subramanian, G. & Brady, J.F. Multiple scales analysis of the Fokker-Planck equation for simple shear flow. *Physica A*, to be submitted.
- [11] Subramanian, G. & Brady, J.F. Multiple scales analysis of the Fokker-Planck equation for a planar linear flow. *Physica A*, to be submitted.
- [12] Subramanian, G. & Brady, J.F. Multiple scales analysis of the Fokker-Planck equation for inertial suspensions. *Physica A*, to be submitted.
- [13] Subramanian, G. & Brady, J.F. Effect of particle inertia on suspension dynamics I: Relative inplane trajectories in shear flow. *J. Fluid. Mech.*, to be submitted.
- [14] Titulaer, U.M. 1978 A systematic solution procedure for the Fokker-Planck equation of a Brownian particle in the high-friction case. *Physica* **91A**, 321-344.
- [15] Uhlenbeck, G.E. & Ornstein, L.S. 1954 On the theory of Brownian motion, in *Selected papers on noise and stochastic processes* (ed. Nelson Wax), pp. 93-111. Dover.
- [16] Wycoff, D. & Balazs, N.L. 1987a Multiple time scales analysis for the Kramers-Chandrasekhar equation. *Physica* **146A**, 175-200.
- [17] Wycoff, D. & Balazs, N.L. 1987b Multiple time scales analysis for the Kramers-Chandrasekhar equation with a weak magnetic field. *Physica* **146A**, 201-218.

## Chapter 3

# Chapman-Enskog formulation for the Fokker-Planck equation

### 3.1 Introduction

The structure of the multiple scales formulation in the previous chapter bears resemblance to the Chapman-Enskog expansion, a method originally developed as a means to solve the Boltzmann equation. The Boltzmann equation governs the singlet distribution function  $P_1(\mathbf{x}, \mathbf{u}, t)$  in a molecular hard-sphere gas (Chapman & Cowling 1970), and is given by

$$\frac{\partial P_1}{\partial t} + \mathbf{u} \cdot \frac{\partial P_1}{\partial \mathbf{x}} + \frac{\partial}{\partial \mathbf{u}} \cdot \left( \frac{\mathbf{F}^o}{m} P_1 \right) = \frac{\partial_c P_1}{\partial t}, \quad (3.1)$$

where the term on the right hand side represents the change in  $P_1$  due to hard-sphere collisions. The Chapman-Enskog method resolves variations in  $P_1$  on time scales much longer than the collisional time (i.e., the time interval between two successive collisions) and on length scales much larger than the (molecular) mean free path. It is valid in the so-called hydrodynamic regime, where the probability density only depends implicitly on the space and time variables through functions that characterise the macroscopic state of the gas (e.g., density, velocity, pressure, etc.). The expansion is thus a singular one, accurate only after an initial temporal boundary layer; the dynamics during this initial period correspond to the so-called kinetic regime. The inability to resolve the shortest time scales in this case stems from the insolubility of the leading-order time dependent equation involving the non-linear (integral)

collision operator  $(\partial_c/\partial t)$ .

A Chapman-Enskog-like procedure can be carried out for the Fokker-Planck equation, and the resulting expansion then describes the evolution of the phase space probability density (for the Brownian particle) on time scales much greater than the inertial relaxation time ( $\tau_p$ ); this is done in Chapter 4. For the Fokker-Planck equation with a hydrodynamic drag linear in the velocity, however, one can make further progress, since the equation is linear and the leading-order time dependent equation reduces to an eigenvalue problem that is easily solved. As was found in Chapter 2, the eigenfunctions are the Hermite functions and form a complete orthogonal set. This implies that unlike the Boltzmann equation, one can formulate a Chapman-Enskog method for the Fokker-Planck equation that accounts for variations of the probability density on the shortest time scales of  $O(\tau_p)$ <sup>1</sup>. Indeed, this has already been done for a single Brownian particle in a conservative force-field by Titulaer (1978). In what follows, we outline a similar formulation for the non-equilibrium case when the forcing is due to a simple shear flow; the resulting expansion for the phase space probability density and the corrected Smoluchowski equation obtained are identical to that derived in the previous chapter using the multiple scales formalism. The Chapman-Enskog formulation is more general, however, and remains valid even in cases where the drift and diffusion coefficients in the Fokker-Planck equation are configuration dependent. As will be seen in section 3.3, the multiple scales formalism fails in these cases.

---

<sup>1</sup>Note that the spatial variations of the probability density are still neglected at leading order, and are thus assumed to be on a scale much larger than the Brownian mean free path  $(kT/m)^{\frac{1}{2}}\tau_p$ . Including the spatial dependence at leading order would, of course, imply solving the full problem!

### 3.2 Equivalence of the Chapman-Enskog and multiple scales formalisms for a single Brownian particle in shear flow

We again consider equation (2.15) in section 2.3.2 of Chapter 2:

$$\frac{\partial \bar{P}}{\partial t} + St \hat{y} \frac{\partial \bar{P}}{\partial \hat{x}} + St \left( w_1 \frac{\partial \bar{P}}{\partial \hat{x}} + w_2 \frac{\partial \bar{P}}{\partial \hat{y}} \right) = \frac{\partial}{\partial w_1} (w_1 \bar{P}) + \frac{\partial}{\partial w_2} (w_2 \bar{P}) + \left( \frac{\partial^2 \bar{P}}{\partial w_1^2} + \frac{\partial^2 \bar{P}}{\partial w_2^2} \right), \quad (3.2)$$

and expand the (rescaled) probability density in the form

$$\bar{P}(\hat{\mathbf{x}}, \mathbf{w}, t) = \sum_{m,n} P_{m,n}(\hat{\mathbf{x}}, \mathbf{w}, t) = \sum_{m,n} \left\{ c_{m,n}(\hat{\mathbf{x}}, t) \psi_{m,n}(\mathbf{w}) + \sum_{i=1}^{\infty} St^i P_{m,n}^{(i)}(\hat{\mathbf{x}}, \mathbf{w}, \mathbf{c}(\hat{\mathbf{x}}, t)) \right\}, \quad (3.3)$$

where  $\mathbf{c}(\hat{\mathbf{x}}, t) \equiv \{c_{m,n}(\hat{\mathbf{x}}, t)\}_{m,n=0}^{\infty}$  and  $\mathbf{w}$  is the scaled fluctuation velocity. The  $\psi_{m,n}$ 's are the eigenfunctions defined in section 2.2 of Chapter 1; thus

$$\psi_{m,n}(\mathbf{w}) = \bar{H}_m \left( \frac{w_1}{2^{1/2}} \right) \bar{H}_n \left( \frac{w_2}{2^{1/2}} \right).$$

The time derivative in the Chapman-Enskog formalism is expanded as

$$\frac{\partial}{\partial t} = - (m + n) + \sum_{i=1}^{\infty} St^i \partial_{m,n}^{(i-1)}, \quad (3.4)$$

when acting on the  $P_{m,n}$ 's; the leading order term in (3.4) is the eigenvalue associated with the eigenfunction  $\psi_{m,n}$ . We now elaborate the motivation behind the use of (3.3) and (3.4).

If one were to neglect the  $O(St)$  spatial derivatives in (3.2), then the reduced equation involves only the fluctuation velocity  $\mathbf{w}$  and has already been examined in Chapter

1 (see (2.7)). Its general solution is given by

$$\bar{P}^{red} = \sum_{m,n} P_{m,n}^{red}(\mathbf{w}, t) = \sum_{m,n} c_{m,n}(t) \psi_{m,n}(\mathbf{w}), \quad (3.5)$$

where the  $c_{m,n}$ 's ( $\propto e^{-(m+n)t}$ ) are functions of time only. Since each of the  $P_{m,n}^{red}$ 's in (3.5) is proportional to  $e^{-(m+n)t}$ , the action of the time derivative on  $P_{m,n}^{red}$  is equivalent to multiplying by the factor  $-(m+n)$ , that is to say, for the reduced problem  $\partial/\partial t = -(m+n)$  when acting on  $P_{m,n}^{red}$ . This defines the action of  $\partial/\partial t$  on  $\bar{P}^{red}$  since

$$\frac{\partial \bar{P}^{red}}{\partial t} = \frac{\partial}{\partial t} \left( \sum_{m,n} P_{m,n}^{red} \right) = \sum_{m,n} \frac{\partial P_{m,n}^{red}}{\partial t} = \sum_{m,n} -(m+n) P_{m,n}^{red}.$$

Now examining (3.2), we see that (3.5) is no longer an exact solution, and neither will  $\partial/\partial t$  acting on the  $P_{m,n}$ 's be necessarily equivalent to multiplying by  $-(m+n)$ . However, the Chapman-Enskog formalism recognizes that both of these still hold at leading order. Thus (3.5) with the  $c_{m,n}$ 's now regarded as functions of both space and time differs from the exact solution only at  $O(St)$ , the discrepancy being generated by the  $O(St)$  spatial derivatives in (3.2). This discrepancy is then accounted for by adding  $O(St)$  corrections to all the  $P_{m,n}^{red}$ 's (the  $P_{m,n}^{(1)}$ 's in (3.3)). The pattern repeats at successive orders in  $St$ , i.e., the addition of the  $O(St)$  corrections generates a discrepancy at  $O(St^2)$  that is accounted for by the  $P_{m,n}^{(2)}$ 's and so forth, which suggests the use of (3.3) as a solution of (3.2) for small  $St$ . A similar argument suggests the form (3.4) for the action of the time derivative, the higher-order corrections in this case being the operators  $\partial_{m,n}^{(i)}$ 's for  $i \geq 0$ . The subscripts  $m$  and  $n$  indicate that the action of the operator  $\partial_{m,n}^{(i)}$  (on the  $P_{m,n}$ 's) will in general be different for each  $m$  and  $n$ . This is, of course, true even at leading order since the multiplicative factors  $(m+n)$  are obviously functions of  $m$  and  $n$ . The  $\partial_{m,n}^{(i)}$ 's are treated as unknowns, and their action obtained from solvability

conditions imposed at each order in the perturbation procedure.

Using (3.4) and (3.3) in (3.2) yields that the time dependence of all  $P_{m,n}^{(i)}$ 's for  $i \geq 1$  is contained implicitly in the  $c_{m,n}$ 's and therefore the  $\partial_{m,n}^{(i)}$ 's, in effect, act on the  $c_{m,n}$ 's. If (say)  $P_{m,n}^{(l)} = L(c_{j,k})$ ,  $L$  being an arbitrary spatial operator, then the action of  $\partial_{m,n}^{(i)}$  on  $P_{m,n}^{(l)}$  is obtained by replacing  $c_{j,k}$  by  $\partial_{m,n}^{(i)}c_{j,k}$ , i.e.,  $\partial_{m,n}^{(i)}(Lc_{j,k}) = L(\partial_{m,n}^{(i)}c_{j,k})$ <sup>2</sup>. We emphasize that this is not an equality, but rather a requirement once we regard  $\partial_{m,n}^{(i)}$  as acting only on functions of time (the  $c_{m,n}$ 's in this case). Indeed, it will be seen below that the  $\partial_{m,n}^{(i)}$ 's are determined in terms of spatial operators and the latter do not necessarily commute with  $L$ .

For either  $m$  or  $n$  not equal to zero, the time derivative defined by (3.4) acting on the  $c_{m,n}$ 's predicts an exponential decay on the scale of  $\tau_p$  at leading order. Thus the  $c_{m,n}$ 's for  $m+n > 0$  represent the fast scales that characterise the momentum relaxations;  $c_{0,0}$  for which case  $\partial/\partial t$  is  $O(St)$ , characterizes the slower spatial relaxation processes. If one were only interested in dynamics of  $O(\dot{\gamma}^{-1})$  or longer, it suffices to consider  $c_{0,0}$  alone (see Chapter 4). This, however, would only be valid for large times and the connection with the initial distribution would be lost. Also note that  $\bar{P}$  has a diagonal structure at leading order, i.e.,  $P_{m,n}^{(0)} \propto \psi_{m,n}$ , which is no longer true for the higher order contributions; this is analogous to that found for the  $P^{(i)}$ 's in the multiple scales formalism (see section 2.2, Chapter 2).

Using (3.4) and (3.3) in (3.2) one obtains, by construction, an identity at leading order. After suitable simplification, to  $O(St)$ , one has

$$L_{m,n}P_{m,n}^{(1)} = \left[ \frac{\partial}{\partial w_1}w_1 + \frac{\partial}{\partial w_2}w_2 + \left( \frac{\partial^2}{\partial w_1^2} + \frac{\partial^2}{\partial w_2^2} \right) + (m+n) \right] P_{m,n}^{(1)}$$

---

<sup>2</sup>This requirement is met in a natural way in the multiple scales formalism since the terms in the expansion of the time derivative are of the form  $\partial/\partial t_i$ , where  $t_i$  is still treated as a time-like variable.

$$\begin{aligned}
&= \left( \partial_{m,n}^{(0)} + \hat{y} \frac{\partial}{\partial \hat{x}} \right) c_{m,n} \bar{H}_m \bar{H}_n + \left[ \frac{1}{2^{\frac{1}{2}}} \frac{\partial c_{m,n}}{\partial \hat{x}} \bar{H}_{m+1} \bar{H}_n + \frac{1}{2^{\frac{1}{2}}} \frac{\partial c_{m,n}}{\partial \hat{y}} \bar{H}_m \bar{H}_{n+1} \right. \\
&\quad + 2^{\frac{1}{2}} m \frac{\partial c_{m,n}}{\partial \hat{x}} \bar{H}_{m-1} \bar{H}_n + 2^{\frac{1}{2}} n \frac{\partial c_{m,n}}{\partial \hat{x}} \bar{H}_m \bar{H}_{n-1} + \frac{c_{m,n}}{2} \bar{H}_{m+1} \bar{H}_{n+1} \\
&\quad \left. + n c_{m,n} \bar{H}_{m+1} \bar{H}_{n-1} \right], \tag{3.6}
\end{aligned}$$

where  $\bar{H}_m \equiv \bar{H}_m(w_1/2^{\frac{1}{2}})$  and  $\bar{H}_n \equiv \bar{H}_n(w_2/2^{\frac{1}{2}})$ , respectively. The terms proportional to  $\bar{H}_m \bar{H}_n$  and  $\bar{H}_{m+1} \bar{H}_{n-1}$  on the right-hand side are both solutions of the homogeneous equation  $L_{m,n}(P_{m,n}^{(1)}) = 0$ , and must therefore be eliminated in order to render (3.6) solvable. Setting individual terms to zero will, however, lead to trivial results for the  $c_{m,n}$ . Instead, we observe that

$$\bar{P}^{(1)} = \sum_{m,n} P_{m,n}^{(1)} = \sum_{q=0}^{\infty} \sum_{m+n=q} P_{m,n}^{(1)},$$

and therefore

$$L_{m,n} \left( \sum_{m+n=q} P_{m,n}^{(1)} \right) = \sum_{m+n=q} \{\text{R.H.S. of (3.6)}\}, \tag{3.7}$$

where the operator

$$L_{m,n} = \left[ \frac{\partial}{\partial w_1} w_1 + \frac{\partial}{\partial w_2} w_2 + \left( \frac{\partial^2}{\partial w_1^2} + \frac{\partial^2}{\partial w_2^2} \right) + q \right],$$

remains the same for all  $P_{m,n}^{(1)}$  with  $m+n$  fixed, thereby enabling one to go from (3.6) to (3.7).

By a simple rearrangement, one finds that the sum on the right-hand side of (3.7) contains terms of the form

$$\left[ \left( \partial_{m,n}^{(0)} + (n+1) \hat{y} \frac{\partial}{\partial \hat{x}} \right) c_{m,n} + c_{m-1,n+1} \right] \bar{H}_m \bar{H}_n,$$

proportional to the homogenous solutions. Equating these terms to zero shows that  $\partial_{m,n}^{(0)}$  is identical to  $\partial/\partial t_2$  (see (2.22)). The above resummation is a natural consequence when the

analysis is formulated in terms of tensorial Hermite functions, as is necessary when considering hydrodynamic interactions (see section 3.4).

The expression for  $P^{(1)}$  may now be obtained by solving (3.6) with the remaining terms for each  $m$  and  $n$ . Without loss of generality, the coefficients of the homogeneous solutions in  $P^{(1)}$  may be set to zero. One can then verify that the  $O(St)$  contribution to  $\bar{P}$  in the Chapman-Enskog expansion, as given by the particular solution at this order, is identical to that obtained using the multiple scales method (see (2.10) and (2.24)). A similar calculation at  $O(St^2)$  yields  $\partial_{m,n}^{(1)}$ , and combining the expressions for  $\partial_{m,n}^{(0)}$  and  $\partial_{m,n}^{(1)}$  gives equation (2.34) for the  $c_{m,n}$ 's. This then shows that the Chapman-Enskog method is equivalent to the multiple scales formalism for a single Brownian particle in simple shear flow. This equivalence can, in fact, be shown to hold for an isolated Brownian particle (of constant mass) subject to a Stokes drag in an arbitrary position dependent force field (see Wycoff & Balazs 1987a). However, as will be seen below, the requirement of an explicit exponential form for the fast scales (the  $t_1$  scale in Chapter 2) in the multiple scales formalism restricts its applicability to precisely these cases.

### 3.3 Chapman-Enskog method for a configuration dependent drag force in one dimension

The multiple scales method formulated in Chapter 1 fails if the ‘mass’ of the Brownian particle is no longer constant, or if the drag it experiences is a function of spatial position. Such circumstances, as will be seen later, arise naturally in the context of multiphase systems. For instance, owing to hydrodynamic interactions, the drag on a given particle in a suspension is dependent on the relative positions (and possibly orientations) of other particles (Kim & Karrila 1991). The case of a position dependent mass is relevant for non-spherical parti-

cles in whose case the inertia matrix is a function of particle orientation, and in bubbly liquids (Yurkovetsky & Brady 1996) where the virtual mass matrix characterizing the inertial interactions of bubbles is configuration dependent, a feature characteristic of fluid inertia.

The reason for the failure of the multiple scales formalism is that the functions representing the dependence of the probability density on the fast time scales of  $O(\tau_p)$  are no longer superpositions of decaying exponentials as was assumed in (2.9). In order to see this, we examine the simplistic case of a Brownian particle in one dimension with a position dependent drag in the absence of an external force field<sup>3</sup>, the spatial domain still being infinite in extent. The (non-dimensional) Fokker-Planck equation for this problem is given by

$$\frac{\partial P}{\partial t} + \epsilon u \frac{\partial P}{\partial x} = f(x) \left[ \frac{\partial P}{\partial u} (uP) + \frac{\partial^2 P}{\partial u^2} \right], \quad (3.8)$$

where  $\epsilon = (\tau_p/\tau_D)^{\frac{1}{2}}$  (see Appendix A1) and  $f(x)$ , which denotes the spatial dependence of the drag coefficient, is an arbitrary non-zero function of position. The Chapman-Enskog expansion developed in the previous section is still valid for this problem since it does not assume any specific functional form for the fast time scales. This generality is, of course, at the expense of not knowing the explicit analytical forms of the momentum relaxation processes for arbitrary  $f(x)$ .

Following arguments in section 3.2, we expand  $P$  as

$$\begin{aligned} P(x, u, t; \epsilon) &= \sum_n P_n(x, u, t; \epsilon), \\ &= \sum_n \left( c_n(x, t; \epsilon) \bar{H}_n\left(\frac{u}{2^{\frac{1}{2}}}\right) + \epsilon P_n^{(1)}(x, u, c_n(x, t)) + \epsilon^2 P_n^{(2)}(x, u, c_n(x, t)) + \dots \right), \end{aligned} \quad (3.9)$$

---

<sup>3</sup>The case where both the mass and drag are position dependent is dealt with in section 3.4, in the context of inertial suspensions.

using

$$\frac{\partial}{\partial t} = -nf(x) + \epsilon \partial_n^{(0)} + \epsilon^2 \partial_n^{(0)} + \dots, \quad (3.10)$$

where the leading order term in the expansion for the time derivative is now a function of  $x$ , denoting the spatial dependence of the momentum relaxations.

We now use (3.9) and (3.10) in (3.8), and solve upto  $O(\epsilon^4)$  in a manner analogous to the previous section; the solvability conditions in one dimension are readily obtained without the need for resummation. The resulting equations for the expansion coefficients are

$$\frac{\partial c_n}{\partial t} = -nf(x)c_n + \epsilon^2 \frac{\partial}{\partial x} \left( \frac{1}{f(x)} \frac{\partial c_n}{\partial x} \right) - \epsilon^4 (2n+1) \frac{\partial}{\partial x} \left\{ \frac{f'(x)}{f^3(x)} \frac{\partial}{\partial x} \left( \frac{1}{f(x)} \frac{\partial c_n}{\partial x} \right) \right\} + O(\epsilon^6), \quad (3.11)$$

where the inertial corrections in (3.11) appear at successive orders in  $\epsilon^2$  (and therefore in integral powers of the particle mass  $m$ ). At  $O(\epsilon^4)$  we now have a non-fickian term proportional to  $f'(x)$  that was absent for the case of a constant drag, and is a consequence of the exact solution of (3.8) no longer being a Gaussian for non-zero  $\epsilon$ .

If  $f(x) = f$  were constant, the coefficients  $c_n$  for  $n \geq 1$  are related to  $c_0$  as

$$c_n = c_0 e^{-nft}, \quad (3.12)$$

and  $P^{(0)} = \sum_n c_n(x, t; \epsilon) \bar{H}_n(u/2^{1/2})$  is consistent with the form (2.9) assumed in the multiple scales procedure. Here  $c_0 \equiv c_0(x, \epsilon^2 t; \epsilon)$  is the solution of the corrected Smoluchowski equation ((3.11) for  $n = 0$ ) to all orders in  $\epsilon$ ,  $\epsilon^2 t$  being the slow time scale (denoted by  $t_2$  in

Chapter 2 and Appendix A1); thus

$$\frac{\partial c_0}{\partial(\epsilon^2 t)} = \frac{\partial}{\partial x} \left( \frac{1}{f(x)} \frac{\partial c_0}{\partial x} \right) - \epsilon^2 \frac{\partial}{\partial x} \left\{ \frac{f'(x)}{f^3(x)} \frac{\partial}{\partial x} \left( \frac{1}{f(x)} \frac{\partial c_0}{\partial x} \right) \right\} + O(\epsilon^4) = \mathcal{K}(x, \epsilon) c_0. \quad (3.13)$$

Assuming a leading order solution of the form  $P^{(0)} = \sum c_0 e^{-nf(x)t} \bar{H}_n(u/2^{\frac{1}{2}})$  in the general case, however, leads to inconsistencies at  $O(\epsilon)$  and higher, due to terms of the form  $t\{f'(x) \sum n c_n(x, t) e^{-nf(x)t} \bar{H}_n(u/2^{\frac{1}{2}})\}$ ; the (explicit) algebraic dependence on  $t$  invalidates the procedure used in Chapter 1 for deriving recurrence relations between the  $c_n$ 's. That the relationship between coefficients characterising the fast and slow time scales is not as simple may be seen by deriving the analog of (3.12) in the general case, valid for short times. Again considering (3.11), the solution for  $c_n$  for small  $\epsilon$  can be written as

$$c_n(x, t; \epsilon) = e^{-ntf(x)} \left[ c_0(x, \epsilon^2 t; \epsilon) + \epsilon^2 c_n^{(1)}(x, \epsilon^2 t, t) + O(\epsilon^4) \right], \quad (3.14)$$

whence,  $c_n^{(1)}$  satisfies

$$\frac{\partial c_n^{(1)}}{\partial t} = -\frac{2ntf'(x)}{f(x)} \frac{\partial c_0}{\partial x} - nt c_0 \frac{\partial}{\partial x} \left( \frac{f'(x)}{f(x)} \right) + n^2 t^2 c_0 \frac{\{f'(x)\}^2}{f(x)}.$$

For short times, this can be solved to yield

$$\begin{aligned} c_n^{(1)} = & -\frac{2nf'(x)}{f(x)} \left[ \frac{t^2}{2} \frac{\partial}{\partial x} c_0(x, 0; \epsilon) + \epsilon^2 \frac{t^3}{3} \frac{\partial}{\partial x} \mathcal{K}(x; \epsilon) c_0(x, 0; \epsilon) + \dots \right] - n \frac{\partial}{\partial x} \left( \frac{f'(x)}{f(x)} \right) \left[ \frac{t^2}{2} c(x, 0; \epsilon) \right. \\ & \left. + \epsilon^2 \frac{t^3}{3} \mathcal{K}(x; \epsilon) c_0(x, 0; \epsilon) + \dots \right] + n^2 \frac{f'(x)^2}{f(x)} \left[ \frac{t^3}{3} c_0(x, 0; \epsilon) + \epsilon^2 \frac{t^4}{4} \mathcal{K}(x; \epsilon) c_0(x, 0; \epsilon) \right], \quad (3.15) \end{aligned}$$

valid when  $t \ll O(\epsilon^{-\frac{2}{3}})$ . The involved relation between  $c_n$  and  $c_0$  in this case can now be contrasted with (3.12) and the form (2.9) assumed in the multiple scales formalism. Never-

theless, the coefficients  $c_n$  for  $n \geq 1$  still become asymptotically small for times greater than  $O(\tau_p)$ .

As would be expected, the inertial corrections to the Smoluchowski equation do not alter the equilibrium distribution in cases where it exists. The latter corresponds to a zero flux in the stationary state and is still given by the solution of the leading order Smoluchowski equation times a Maxwellian velocity distribution. In one dimension a vanishing flux at infinity, and thence at every point  $x$  in the domain, is a sufficient condition for the existence of an equilibrium distribution. For the above case in particular, it follows from (3.13) that the equilibrium spatial density satisfies

$$\frac{1}{f(x)} \frac{\partial c_0^{eq}}{\partial x} = 0,$$

and is therefore a constant. It is easily seen that the inertial term at  $O(\epsilon^2)$  in (3.13) vanishes for a constant number density. This remains true for a Brownian particle in any number of dimensions in the presence a potential force field described by  $\Psi(\mathbf{x})$  (consistent with a vanishing flux at infinity) since the associated Maxwell-Boltzmann distribution,  $e^{-\Psi(\mathbf{x})} e^{-\frac{u^2}{2}}$ , satisfies the governing Fokker-Planck equation.

In two or more dimensions, the force field need no longer be conservative as is the case for simple shear flow. The possibility of a stationary solution of the form  $e^{-\Psi(\mathbf{x})}$  is precluded in such cases. Even when a scalar potential function exists, the solution  $e^{-\Psi(\mathbf{x})}$  may be inconsistent with boundary conditions imposed at infinity and thus represent an aphysical distribution. An example is planar extensional flow where the velocity field (and the resulting hydrodynamic force field) is derivable from a potential  $\Psi(x, y) = K(x^2 - y^2)$ . A solution of the form  $e^{-K(x^2 - y^2)}$  would tend to infinity along the compressional axis. Planar extension, however, supports a constant spatial density in the inertialess approximation which would be

the physically relevant solution.

In the above non-equilibrium cases, the inertial corrections found using the Chapman-Enskog expansion may be important in determining the modified stationary state distributions. Indeed, again considering planar extension, the Smoluchowski equation, to  $O(St)$ , is found to be

$$\frac{\partial c_0}{\partial t} + Kx \frac{\partial c_0}{\partial x} - Ky \frac{\partial c_0}{\partial y} = \frac{1}{Pe} \left( \frac{\partial^2 c_0}{\partial x^2} + \frac{\partial^2 c_0}{\partial y^2} \right) + St \left[ K^2 \left( \frac{\partial}{\partial x} (xc_0) + \frac{\partial}{\partial y} (yc_0) \right) + \frac{K}{Pe} \left( \frac{\partial^2 c_0}{\partial y^2} - \frac{\partial^2 c_0}{\partial x^2} \right) \right],$$

which clearly does not support a constant number density as a steady solution in contrast to the zero-inertia limit. The Stokes number here is given by  $St = (\mathbf{\Gamma}:\mathbf{\Gamma})^{\frac{1}{2}}\tau_p$ ,  $\mathbf{\Gamma}$  being the velocity gradient tensor;  $Pe = 6\pi\eta a^3(\mathbf{\Gamma}:\mathbf{\Gamma})^{\frac{1}{2}}/kT$ . The physical reason, of course, is that the particles now migrate across the curvilinear streamlines on account of inertial forces, and this migration will eventually be balanced by Brownian diffusion arising from a gradient in the number density.

The aforementioned considerations become relevant for suspensions subjected to external flows, in which case the force field is almost always non-conservative on account of hydrodynamic interactions, and inertial corrections may therefore be crucial in determining the spatial microstructure. In the next section we outline a Chapman-Enskog formalism to determine the microstructure of Brownian suspensions for small but finite particle inertia.

## 3.4 Chapman-Enskog method for inertial suspensions

### 3.4.1 Introduction

In this section we employ the Chapman-Enskog method as a means to investigate the effects of particle inertia in a suspension of arbitrarily shaped Brownian particles subjected to

an external linear flow. The phase-space probability density again satisfies a Fokker-Planck equation with the force field and diffusivities being modified to include the effects of hydrodynamic interactions among particles. The Fokker-Planck equation contains additional terms to account for the configuration dependence of the particle inertia matrix which may be necessary for non-spherical particles. The ambient linear flow field  $\mathbf{u}^\infty = \mathbf{\Gamma} \cdot \mathbf{y}$ , where  $\mathbf{\Gamma}$ , the (traceless) velocity gradient tensor, gives rise to a non-conservative hydrodynamic force field except when it is symmetric. Even for a symmetric  $\mathbf{\Gamma}$ , however, the force field experienced by an individual particle is not conservative on account of hydrodynamic interactions; the particle surfaces act as sources of vorticity and render the resultant velocity (and force) field rotational.

The application of the Chapman-Enskog formalism involves initially expanding the non-equilibrium probability density in an infinite series of tensorial Hermite functions of the fluctuation velocity. The latter is no longer the difference between the particle velocity and that of the ambient linear flow at its location, but instead is the deviation of the actual particle velocity from that of an inertialess particle at the same location. As in Chapter 1, the analysis is restricted in its validity to cases where the inertial relaxation time of an individual particle is much smaller than the flow time scale ( $O(\mathbf{\Gamma}:\mathbf{\Gamma})^{-\frac{1}{2}}$ ). The analysis places no restriction on the volume fraction, however, and also allows for an arbitrary ratio of the configurational (diffusive) and flow time scales<sup>4</sup>. The leading order term in the Hermite function expansion is again a local Maxwellian in the fluctuation velocity as was for the case of a single Brownian particle, and therefore does not explicitly involve the hydrodynamic resistance/mobility functions; the effect of hydrodynamic interactions is, in part, to alter the

---

<sup>4</sup>In a statistically homogeneous concentrated suspension, one can distinguish two distinct regimes of linear behavior as regards the mean square displacement of a single particle, those characterised by the short-time ( $D_0^s$ ) and the long-time ( $D_\infty^s$ ) self-diffusivities. The appropriate generalization for a concentrated suspension of the diffusive time scale  $\tau_D = a^2/D$  of a single Brownian particle, is obtained by replacing  $D$  by  $D_0^s(\phi)$  (Brady & Morris 1997).

rate of approach to this local equilibrium. Each particle ‘feels’ the presence of the others and may be regarded as suspended in a medium with an increased effective viscosity, which changes the rate of momentum relaxation. In light of the arguments in section 3.3 for a spatially varying drag in one dimension, we expect that the momentum relaxations will no longer be expressible as simple superpositions of decaying exponentials owing to the configuration dependent inertia and resistance matrices, thereby rendering the original multiple scales formalism developed in Chapter 1 inapplicable.

With the inclusion of hydrodynamic interactions, the force field and diffusivity in the Fokker-Planck equation become complex functions of the particle configuration, making it extremely difficult to obtain an analytical solution. In the limit when the momentum and spatial relaxation processes occur on separate time scales, the Chapman-Enskog method reduces the difficulty of the problem from that of solving for the exact phase-space probability density to determining the series coefficients in the Hermite function expansion that depend on configuration coordinates alone and satisfy Smoluchowski-like equations. The procedure, in principle, yields inertial corrections to the Smoluchowski equation to any desired order. We will, however, restrict our attention to the first effects of particle inertia, i.e., the  $O(St)$  inertial modification, while commenting on the general form and the physical relevance of the higher order terms.

In section 3.4.2 we give the governing equations together with the assumptions made in the subsequent analysis. The Chapman-Enskog method is outlined in sections 3.4.3.1 and 3.4.3.2 for a configuration dependent and constant inertia tensor, respectively. The  $O(St)$  inertial correction to the Smoluchowski equation is derived for the latter case (see (3.53)). The range of validity of these and higher order corrections is analyzed in section 3.4.4. Section 3.5 summarizes the results and considers possible extensions of the method to cases where

the particles interact via direct hard-sphere like collisions.

### 3.4.2 Problem formulation

The phase-space density for a system of  $N$  interacting Brownian particles satisfies a Fokker-Planck equation (also see section 2.5 in Chapter 1) given by

$$\begin{aligned} \frac{\partial P_N}{\partial \bar{t}} + \sum_{i=1}^N \mathbf{u}_i \cdot \frac{\partial P_N}{\partial \mathbf{y}_i} + \sum_{i,j,k,l=1}^N \frac{\partial}{\partial \mathbf{u}_i} \cdot \left[ \left( \frac{1}{2} \mathbf{m}_{ij}^{-1} \cdot \frac{\partial \mathbf{m}_{kl}}{\partial \mathbf{x}_j} - \mathbf{m}_{ij}^{-1} \cdot \frac{\partial \mathbf{m}_{jk}}{\partial \mathbf{x}_l} \right) : \mathbf{u}_k \mathbf{u}_l P_N \right] + \sum_{i,j=1}^N (\mathbf{m}_{ij}^{-1} \cdot \mathbf{F}^{\circ j}) \cdot \frac{\partial P_N}{\partial \mathbf{u}_i} \\ = \sum_{i,j,k=1}^N \mathbf{m}_{ij}^{-1} \cdot \mathbf{R}_{jk}^{FU} : \frac{\partial}{\partial \mathbf{u}_i} (\mathbf{u}_k P_N) + kT \sum_{i,j,k,l=1}^N \mathbf{m}_{ij}^{-1} \cdot \mathbf{R}_{jk}^{FU} \cdot \mathbf{m}_{kl}^{-1} : \frac{\partial^2 P_N}{\partial \mathbf{u}_i \partial \mathbf{u}_l}, \end{aligned} \quad (3.16)$$

where  $P_N(\{\mathbf{y}_i\}, \{\mathbf{u}_i\}, \bar{t})$  is the probability density of finding the  $N$  particles in the  $2N$ -dimensional elemental phase space volume  $[\{(\mathbf{y}_1, \mathbf{y}_1 + d\mathbf{y}_1), (\mathbf{u}_1, \mathbf{u}_1 + d\mathbf{u}_1)\}, \dots, \{(\mathbf{y}_N, \mathbf{y}_N + d\mathbf{y}_N), (\mathbf{u}_N, \mathbf{u}_N + d\mathbf{u}_N)\}]$  at time  $\bar{t}$ ; the  $\mathbf{m}$ 's are the inertia tensors and the  $\mathbf{R}^{FU}$ 's are the hydrodynamic resistance tensors. Thus,  $-\sum_{j=1}^N \mathbf{R}_{ij}^{FU} \cdot \mathbf{u}_j$  represents the hydrodynamic drag force on particle  $i$  in a suspension of  $N$  particles with velocities  $\{\mathbf{u}_j\}$ , and  $\sum_{j,k=1}^N \mathbf{m}_{ij}^{-1} \cdot \mathbf{R}_{jk}^{FU} \cdot \mathbf{u}_k$  is the acceleration of the  $i^{\text{th}}$  particle in response to similar forces acting on the system. Because fluid inertia is neglected, the drag is linear in the particle velocities and the resistance tensors are only functions of the instantaneous particle configuration. This assumption is valid when the particles are much denser than the suspending fluid since the ratio of particle to fluid inertia scales with the density ratio of the two phases (see Chapter 1). The symbols  $\mathbf{y}$ ,  $\mathbf{u}$  and  $\mathbf{F}$  are used to denote  $(\mathbf{y}, \mathbf{p})$ ,  $(\mathbf{u}, \boldsymbol{\omega})$  and  $(\mathbf{F}, \mathbf{L})$  where  $\mathbf{p}$ ,  $\boldsymbol{\omega}$  and  $\mathbf{L}$  are the orientation vector, the angular velocity and the hydrodynamic torque, respectively. In a similar manner,  $\mathbf{m} \equiv (m\boldsymbol{\delta}, \mathbf{I})$ , where  $\mathbf{I}$  is the moment of inertia tensor, and  $\mathbf{R}^{FU} \equiv \begin{pmatrix} \mathbf{R}^{FU} & \mathbf{R}^{F\Omega} \\ \mathbf{R}^{LU} & \mathbf{R}^{L\Omega} \end{pmatrix}$ ; the elements of  $\mathbf{R}^{FU}$  denote the couplings between the components of  $\mathbf{F}$  and  $\mathbf{u}$ .

Thus, (3.16) includes both translational and rotational degrees of freedom cou-

pled by hydrodynamic interactions. In general, the external force field  $\mathbf{F}^o$  may include any configuration dependent interparticle forcing. Here we are concerned with the case when  $\mathbf{F}^o$  is the hydrodynamic force experienced by an individual particle due to the external (linear) flow  $\mathbf{u}^\infty$ , and therefore scales as  $(6\pi\eta a)|\mathbf{u}^\infty|$ . In the absence of hydrodynamic interactions,  $\mathbf{F}^o = 6\pi\eta a\mathbf{u}^\infty$ , and the net hydrodynamic force experienced by an individual particle is  $-(6\pi\eta a)(\mathbf{u} - \mathbf{u}^\infty)$ , ensuring that a force-free non-Brownian inertialess particle will follow the fluid streamlines. However, in presence of hydrodynamic interactions, particle pathlines deviate from the streamlines even in the limit of zero-inertia;  $\mathbf{F}^o$  now takes the form  $6\pi\eta a\bar{\mathbf{R}}(\mathbf{x}) \cdot \mathbf{u}^\infty + \mathbf{F}_{dev}^o$ , where  $\bar{\mathbf{R}}(\mathbf{x}) \rightarrow 1, \mathbf{F}_{dev}^o \rightarrow 0$  as the volume fraction goes to zero. One may define a drag coefficient  $\bar{R}(\phi)$  determined from an ensemble average of the drag force on any given particle, and  $\eta\bar{R}(\phi)$  can now be interpreted as an effective viscosity of the suspension. The expressions for  $\bar{\mathbf{R}}(\mathbf{x})$  and  $\mathbf{F}_{dev}^o$  for pair-wise interactions are given in Kim & Karrila (1991).

The terms proportional to  $(\nabla_{\mathbf{x}} \mathbf{m})$  on the left hand side of (3.16) arise for a configuration dependent inertia matrix and may be derived from a Lagrangian description using generalized coordinates (Grassia, Hinch & Nitsche 1995). The Langevin equations corresponding to (3.16) are given in terms of the Lagrangian  $\mathcal{L}$  as

$$\frac{d}{dt} \left( \frac{\partial \mathcal{L}}{\partial \mathbf{u}_i} \right) - \frac{\partial \mathcal{L}}{\partial \mathbf{x}_i} = \mathbf{F}^h + \mathbf{F}^B,$$

where  $\mathbf{F}^h$  is the hydrodynamic force due to the external flow field. In the absence of interparticle forces, i.e., when  $\mathbf{F}^h = -(6\pi\eta a)\mathbf{u} + \mathbf{F}^o$ , the Lagrangian is simply the total kinetic energy  $\mathcal{L} = (1/2) \sum_{ij} \mathbf{u}_i \cdot \mathbf{m}_{ij} \cdot \mathbf{u}_j$ . The drift and diffusion coefficients that appear in (3.16) can then be derived in the usual manner from the short time behavior of the first and second

moments of  $\mathbf{x}$  and  $\mathbf{u}$  (see Risken 1989)<sup>5</sup>.

The inertial relaxation time for a particle in a concentrated suspension depends on the volume fraction via the effective viscosity, and is given by  $\bar{\tau}_p = m/(6\pi\eta a\bar{R}(\phi))$ . Thus, the ratio of the inertial and flow time scales, which defines the appropriate Stokes number for a concentrated suspension, is  $\bar{St} = St/R(\phi)$ , where  $St = m(\mathbf{\Gamma}:\mathbf{\Gamma})^{\frac{1}{2}}/(6\pi\eta a)$  is the Stokes number of an isolated Brownian particle. Since  $\bar{R}(\phi)$  is a monotonic increasing function of  $\phi$  (Jeffrey & Acrivos 1976),  $\bar{St} < St$ , and the effective particle inertia decreases with increasing  $\phi$ . We will continue to use  $St$  as the dimensionless parameter to represent the magnitude of particle inertia remembering, however, that the condition for the convergence of the solution is now  $\bar{St} \ll 1$ . Using  $\bar{St}$  would in any case imply calculating  $\bar{R}(\phi)$ , which in turn would entail knowledge of the flow induced microstructure; the latter is, of course, yet to be determined. This then implies that the range of validity of the Chapman-Enskog solution increases with  $\phi$ , and for concentrated suspensions, one expects the perturbative solution to provide an accurate description even for  $St$  of  $O(1)$  or greater.

Using  $\mathbf{y}_i = a\mathbf{x}_i$ ,  $\mathbf{u}_i = \{(\mathbf{\Gamma}:\mathbf{\Gamma})^{\frac{1}{2}}a\}\mathbf{v}_i$ , and scaling the inertia and resistance tensors with  $m$  and  $(6\pi\eta a)$ , respectively<sup>6</sup>, we obtain the dimensionless form of (3.16) as

$$\begin{aligned} \frac{\partial P_N}{\partial t} + St \left\{ v_i \frac{\partial P_N}{\partial x_i} + \frac{\partial}{\partial v_i} \left[ \left( \frac{m_{ij}^{-1}}{2} \frac{\partial m_{kl}}{\partial x_j} - m_{ij}^{-1} \frac{\partial m_{jk}}{\partial x_l} \right) v_k v_l P_N \right] \right\} \\ = \frac{\partial}{\partial v_i} m_{ij}^{-1} R_{jk}^{FU} \{ (v_k - R_{kl}^{FU-1} F_l^o) P_N \} + \left( \frac{1}{Pe St} \right) m_{ij}^{-1} R_{jk}^{FU} m_{kl}^{-1} \frac{\partial^2 P_N}{\partial v_i \partial v_l}, \quad (3.17) \end{aligned}$$

where  $Pe = a^2(\mathbf{\Gamma}:\mathbf{\Gamma})^{\frac{1}{2}}/D$ . Summation over repeated indices is implied in (3.17) and all

<sup>5</sup>We assume that the Brownian force  $\mathbf{F}^B$  is a Gaussian white noise process, in which case the third and higher moments do not enter the statistical description.

<sup>6</sup>The scalings used above for the inertia and resistance tensors only apply to the translational degrees of freedom; the moment of inertia of a particle scales as  $ml^2$  and the element  $\mathbf{R}^{L\Omega}$  scales as  $\eta l^3$  for a particle with characteristic length  $l$ . This difference is, however, immaterial since the dimensionless parameters obtained remain unchanged.

subsequent tensorial relations; thus a given index  $i$  ranges from 1 to  $6N$  in 3 dimensions. We continue to use the same symbols for the dimensionless inertia and resistance tensors to avoid notational complexity. The Peclet number defined above represents the ratio of the configurational and flow time scales for an isolated Brownian particle. As was the case with the Stokes number, the appropriate Peclet number in a concentrated suspension is a function of the volume fraction, and is given by  $\bar{P}e = Pe(D/D_0^s(\phi))$ , where  $D_0^s(\phi)$  is the short-time self-diffusivity (defined as the instantaneous mobility). This, however, is not a concern since, as will be seen, the Chapman-Enskog scheme is valid for arbitrary  $Pe$  provided only that  $\bar{S}t \ll 1$ ; the Peclet number serves to set the scale for the velocity fluctuations through the combination  $Pe St$ . We will therefore retain  $Pe$  as the relevant measure of the relative importance of flow and Brownian effects.

Using the flow time scale for non-dimensionalization and scaling the resistance tensors as before, the Smoluchowski equation corresponding to (3.17) is:

$$\frac{\partial}{\partial t} \left( \frac{g_N}{\sqrt{\det m_{ab}}} \right) + \frac{1}{\sqrt{\det m_{ab}}} \frac{\partial}{\partial x_i} \left( R_{ij}^{FU-1} F_j^o g_N \right) = \frac{1}{Pe \sqrt{\det m_{ab}}} \frac{\partial}{\partial x_i} \left( \sqrt{\det m_{ab}} R_{ij}^{FU-1} \frac{\partial}{\partial x_j} \left( \frac{g_N}{\sqrt{\det m_{ab}}} \right) \right), \quad (3.18)$$

where  $g_N$  is the configurational probability density at time  $t$  (see Grassia, Hinch & Nitsche 1995). Equation (3.18) describes the configurational dynamics for zero inertia with a configuration dependent inertia tensor. In the presence of hydrodynamic interactions, one has a tensorial diffusivity ( $\equiv \mathbf{R}^{FU-1}$ ) and the hydrodynamic velocity field,  $(\mathbf{R}^{FU-1} \cdot \mathbf{F}^o)$ , is no longer solenoidal. When  $\mathbf{F}^o = 0$ , the equilibrium distribution is given by  $g_N^{eq} = \sqrt{\det \mathbf{m}}$ ; in one dimension, this would imply that regions with vigorous thermal activity are depleted in favor of regions of higher mass and feeble thermal velocities. When  $\mathbf{m}, \mathbf{R}^{FU} = \delta$  and

$\mathbf{F}^o = -\nabla V(\mathbf{x})$ ,  $V$  being a scalar potential,  $g_N^{eq} \propto \exp[-Pe V(\mathbf{x})]$ , the familiar Boltzmann distribution. In section 3.4.3.2, we will derive corrections to (3.18) that account for the effects of particle inertia in a suspension for the special case of a constant  $\mathbf{m}$ .

### 3.4.3 Multiple scales analysis

#### 3.4.3.1 Configuration dependent inertia tensor

In this section we examine the general form of the multiple scales solution to (3.17). Before considering the detailed structure of the solution, we look at a simplified form of (3.17) obtained by neglecting the  $O(St)$  term involving spatial gradients:

$$\frac{\partial P}{\partial t} = \frac{\partial}{\partial w_i} \left( m_{ij}^{-1} R_{jk}^{FU} w_k P \right) + m_{ij}^{-1} R_{jk}^{FU} m_{kl}^{-1} \frac{\partial^2 P}{\partial w_i \partial w_l}, \quad (3.19)$$

where  $w_i$  is the scaled fluctuation velocity defined by  $w_i = (Pe St)^{\frac{1}{2}} (v_i - R_{ij}^{FU-1} F_j^o)$ , and we have replaced  $P_N$  by  $P$ , the size ( $N$ ) of the system now being understood. Since the inertia tensor  $\mathbf{m}$  is symmetric and positive definite, one may write  $\mathbf{m} = \mathbf{m}^{\frac{1}{2}\dagger} \cdot \mathbf{m}^{\frac{1}{2}}$  (' $\dagger$ ' denotes the transpose), and thereby define the non-singular variable transformation  $\bar{w}_i = m_{ij}^{\frac{1}{2}} w_j$ . In the new variables (3.19) becomes

$$\frac{\partial \bar{P}}{\partial t} = (m^{\frac{1}{2}})^{-1}_{ji} R_{jk}^{FU} (m^{\frac{1}{2}})^{-1}_{kl} \left[ \frac{\partial}{\partial \bar{w}_i} (\bar{w}_l \bar{P}) + \frac{\partial^2 \bar{P}}{\partial \bar{w}_i \partial \bar{w}_l} \right] = \mathbf{L}_H(\bar{\mathbf{w}}), \quad (3.20)$$

where  $\bar{P} = (\sqrt{\det \mathbf{m}})^{-1} P$  is the rescaled (in order to satisfy the integral constraint) probability density. Since the resistance tensor  $\mathbf{R}^{FU}$  factors out, the steady state solution only depends on the  $\mathbf{R}^{FU}$ 's implicitly (through  $\bar{\mathbf{w}}$ ), and is given by  $e^{-\frac{\bar{\mathbf{w}} \cdot \bar{\mathbf{w}}}{2}}$ , with a suitable normalization constant. Thus the solution is a local Maxwellian in the fluctuation velocity  $\bar{\mathbf{w}}$ , a measure of the difference between the actual particle velocity at the given location and that corresponding

to the zero-inertia-pathline passing through the same location.

Since the inertia and resistance tensors only depend on configurational degrees of freedom, the general solution of (3.20) is given by

$$\bar{P}(\bar{\mathbf{w}}, t) = \sum_{M=0}^{\infty} a_{i_1 i_2 \dots i_M}^M(\mathbf{x}, t) \left\{ \bar{H}_M \left( \frac{\bar{\mathbf{w}}}{2^{\frac{1}{2}}} \right) \right\}_{i_1 i_2 \dots i_M}, \quad (3.21)$$

where

$$\{\bar{H}_M(\mathbf{z})\}_{i_1 i_2 \dots i_M} = (-1)^M \frac{\partial^M}{\partial z_{i_1} \partial z_{i_2} \dots \partial z_{i_M}} (e^{-\mathbf{z} \cdot \mathbf{z}}), \quad (3.22)$$

is the tensorial Hermite function of order  $M$ ; the coefficient  $\mathbf{a}^M$  is an  $M^{\text{th}}$  order tensor satisfying the relation

$$\begin{aligned} \frac{\partial}{\partial t} (a_{i_1 i_2 \dots i_M}^M) &= -R_{jk}^{FU} (m^{\frac{1}{2}})^{-1}_{ki} \left[ a_{i_1 i_2 \dots i_{M-1} i}^M (m^{\frac{1}{2}})^{-1}_{jM} + a_{i_1 i_2 \dots i_{M-2} i i_M}^M (m^{\frac{1}{2}})^{-1}_{j^{i_{M-1}}} + \dots \right. \\ &\quad \left. + \dots + a_{i_2 i_3 \dots i_M}^M (m^{\frac{1}{2}})^{-1}_{j^{i_1}} \right], \\ &= -M \mathcal{A}_{i_1 i_2 \dots i_M i'_1 i'_2 \dots i'_M}^{(M)} a_{i'_1 i'_2 \dots i'_M}^M. \end{aligned} \quad (3.23)$$

where  $\mathcal{A}^{(M)}$  is a tensor of order  $2M$  defined by

$$\begin{aligned} \mathcal{A}_{i_1 i_2 \dots i_M i'_1 i'_2 \dots i'_M}^{(M)} &= \frac{1}{M} \left[ \delta_{i_1 i'_1} \delta_{i_2 i'_2} \dots \delta_{i_{M-1} i'_{M-1}} R_{jk}^{FU} (m^{\frac{1}{2}})^{-1}_{ki'_M} (m^{\frac{1}{2}})^{-1}_{j^{i_M}} \right. \\ &\quad \left. + \delta_{i_1 i'_1} \dots \delta_{i_{M-2} i'_{M-2}} \delta_{i_M i'_M} R_{jk}^{FU} (m^{\frac{1}{2}})^{-1}_{ki'_{M-1}} (m^{\frac{1}{2}})^{-1}_{j^{i_{M-1}}} \right. \\ &\quad \left. + \dots + \delta_{i_2 i'_2} \delta_{i_3 i'_3} \dots \delta_{i_M i'_M} R_{jk}^{FU} (m^{\frac{1}{2}})^{-1}_{ki'_1} (m^{\frac{1}{2}})^{-1}_{j^{i_1}} \right], \end{aligned} \quad (3.24)$$

and has been used in the interests of notational brevity. Here we have used the fact that the  $\mathbf{a}^M$ 's can, without loss in generality, be chosen as invariant with respect to the interchange of any pair of their  $M$  indices. This implies that  $\mathcal{A}^{(M)}$  must be made symmetric with respect to

its first group of  $M$  indices  $(i_1, i_2, \dots, i_M)$ , and in addition, may be symmetrized with respect to its last group of  $M$  indices  $(i'_1, i'_2, \dots, i'_M)$ ; the symmetry of  $\mathbf{R}^{FU}$  makes  $\mathcal{A}^{(M)}$  invariant to the interchange  $i_1 \leftrightarrow i'_1, i_2 \leftrightarrow i'_2, \dots, i_M \leftrightarrow i'_M$ <sup>7</sup>. It must also be noticed that in the presence of hydrodynamic interactions, the different degrees of freedom in velocity space are coupled. Thus an isolated term of the form  $\prod_{i=1}^{6N} \bar{H}_{n_i}(\bar{w}_i/2^{\frac{1}{2}})$  is no longer an eigenfunction of the operator  $\mathbf{L}_H$  in (3.20); instead, one now interprets  $\bar{\mathbf{H}}_M(\bar{\mathbf{w}}/2^{\frac{1}{2}})$  as a tensorial eigenfunction with  $M\mathcal{A}^{(M)}$  as the associated matrix of eigenvalues. The orthogonality and completeness of the Hermite functions  $\bar{\mathbf{H}}_M$  enables one to determine the coefficients  $\mathbf{a}^M(\mathbf{x}, 0)$  corresponding to an arbitrary initial distribution (Grad 1949).

The form of (3.21) with the  $\mathbf{a}^M$ 's given by (3.23) motivates the use of a generalized Chapman-Enskog expansion for  $P$  in (3.17) of the form

$$\begin{aligned}
P(\mathbf{x}, \mathbf{v}, t) &= (\sqrt{\det \mathbf{m}}) \bar{P}(\mathbf{x}, \bar{\mathbf{w}}, t) = (\sqrt{\det \mathbf{m}}) \sum_{M=0}^{\infty} \bar{P}_M(\mathbf{x}, \bar{\mathbf{w}}, t), \\
&= (\sqrt{\det \mathbf{m}}) \sum_{M=0}^{\infty} \left\{ a_{i_1 i_2 \dots i_M}^M(\mathbf{x}, t) \left\{ \bar{H}_M \left( \frac{\bar{\mathbf{w}}}{2^{\frac{1}{2}}} \right) \right\}_{i_1 i_2 \dots i_M} + St \bar{P}_M^{(1)}(\mathbf{x}, \bar{\mathbf{w}}, \mathbf{a}^M(\mathbf{x}, t)) \right. \\
&\quad \left. + St^2 \bar{P}_M^{(2)}(\mathbf{x}, \bar{\mathbf{w}}, \mathbf{a}^M(\mathbf{x}, t)) + \dots \right\}, \tag{3.25}
\end{aligned}$$

for small  $St$ . As was seen earlier, the linearity of the Fokker-Planck equation allows one to treat the temporal evolution of each of the  $\bar{P}_M$ 's separately; the coupling between these various modes occurs at  $O(St)$  and higher via the initial conditions. In order to obtain non-trivial equations at each order in  $St$ , the time derivative is also expressed as an infinite

---

<sup>7</sup>With these symmetries in mind, the tensor  $\mathcal{A}^{(M)}$  is actually an average over  $M \cdot M!$  permutations of its  $2M$  indices, rather than the  $M$  permutations indicated in (3.24). It is this form of  $\mathcal{A}^{(M)}$  which should be used, for instance, in (3.27), when solving for the fast scales. The higher-order Chapman-Enskog solutions obtained with either definition of  $\mathcal{A}^{(M)}$  remain the same, however.

sequence of operators given by

$$\frac{\partial}{\partial t} \bar{P}_M^{(i)} = \left[ -M \underline{\mathcal{A}} + St \partial_M^{(0)} + St^2 \partial_M^{(1)} + \dots \right] \bar{P}_M^{(i)}, \quad (3.26)$$

where the operator at leading order is defined by

$$\underline{\mathcal{A}} b_{i_1 i_2 \dots i_{M_1}}^{M_1} = \mathcal{A}_{i_1 i_2 \dots i_{M_1} i'_1 i'_2 \dots i'_{M_1}}^{(M_1)} b_{i'_1 i'_2 \dots i'_{M_1}}^{M_1}.$$

Here,  $\mathbf{b}^{M_1}$  is a tensor of order  $M_1$  and an arbitrary function of  $\mathbf{x}$  and  $t$ ; this definition follows naturally from (3.21) and (3.23). As before, the operators  $\partial_M^{(i)}$  will be determined from solvability conditions at successive orders in  $St$ . We observe that (3.25) and (3.26) are tensorial analogues of (3.9) and (3.10) (see section 3.3). Similar to the one-dimensional case, we expect that the relaxations on the fast time scales of  $O(\bar{\tau}_p)$  ( $\equiv |\mathcal{A}^{(M)}|^{-1}$ ) will no longer be expressible as superpositions of exponentials. The relations between coefficients characterizing the fast ( $\mathbf{a}^M$ ,  $M \geq 1$ ) and slow ( $a^0$ ) scales will therefore be multi-dimensional analogs of (3.14) and (3.15), where the exponential  $e^{-nft}$  is now replaced by  $e^{-M \mathcal{A}^{(M)} t}$ , the latter being interpreted as the classical power series:

$$(e^{-\mathcal{A}^{(M)} t})_{i_1 i_2 \dots i_M i'_1 i'_2 \dots i'_M} = \sum_{n=0}^{\infty} \frac{(-1)^n t^n}{n!} \{ \mathcal{A}^{(M)} \odot \mathcal{A}^{(M)} \odot \mathcal{A}^{(M)} \dots n \text{ times} \}_{i_1 i_2 \dots i_M i'_1 i'_2 \dots i'_M}, \quad (3.27)$$

where

$$\mathcal{A}_{i_1 i_2 \dots i_M i''_1 i''_2 \dots i''_M}^{(M)} \odot \mathcal{A}_{i'''_1 i'''_2 \dots i'''_M i''''_1 i''''_2 \dots i''''_M}^{(M)} = \mathcal{A}_{i_1 i_2 \dots i_M i''_1 i''_2 \dots i''_M}^{(M)} \mathcal{A}_{i'''_1 i''''_1 \dots i''''_M i''''_1 i''''_2 \dots i''''_M}^{(M)}.$$

As was the case for a single Brownian particle in simple shear (see section 3.2), the solution to

(3.17) has a diagonal structure at leading order since  $\bar{P}_M^{(0)}$  is proportional to  $\bar{\mathbf{H}}_M$  (see (3.25)).

Again, the higher order contributions do not share this property, and will in general be given by

$$\bar{P}_M^{(i)} = \sum_{M_1=0}^{\infty} \{b_{M,M_1}^{(i)}\}_{i_1 i_2 \dots i_{M_1}} \{\bar{H}_{M_1}\}_{i_1 i_2 \dots i_{M_1}},$$

where  $\mathbf{b}_{M,M_1}^{(0)} = \delta_{M,M_1} \mathbf{a}^{M_1}$ , which reproduces the leading order solution. In what follows, we will use the above formalism to determine the Smoluchowski operator to  $O(St)$ . Again referring back to the one-dimensional case, this would be equivalent to determining the expression for  $\mathcal{K}(x, \epsilon)$  in (3.13) to  $O(\epsilon^2)$ .

Using  $P = (\sqrt{\det \mathbf{m}}) \bar{P}$  in (3.17), we obtain

$$\begin{aligned} \frac{\partial \bar{P}}{\partial t} + St \left\{ v_i \frac{\partial \bar{P}}{\partial x_i} + \frac{\partial}{\partial v_i} \left[ \left( \frac{m_{ij}^{-1}}{2} \frac{\partial m_{kl}}{\partial x_j} - m_{ij}^{-1} \frac{\partial m_{jk}}{\partial x_l} \right) v_k v_l \bar{P} \right] + \frac{v_i \bar{P}}{2} \frac{\partial}{\partial x_i} \ln(\det m_{ab}) \right\} \\ = \frac{\partial}{\partial v_i} m_{ij}^{-1} R_{jk}^{FU} \{ (v_k - R_{kl}^{FU-1} F_l^o) \bar{P} \} + \left( \frac{1}{Pe St} \right) m_{ij}^{-1} R_{jk}^{FU} m_{kl}^{-1} \frac{\partial^2 \bar{P}}{\partial v_i \partial v_l}, \end{aligned}$$

for the rescaled probability. Changing variables from  $(\mathbf{x}, \mathbf{v})$  to  $(\mathbf{x}, \bar{\mathbf{w}})$ , and substituting (3.25),

we finally obtain the following sequence of equations:

$$\begin{aligned}
\mathbf{L}_H^{(M)}(\bar{\mathbf{w}})\bar{P}_M^{(i)} &= \sum_{j=0}^{i-1} \partial_M^{(j)} \bar{P}_M^{(i-j-1)} \\
&+ \frac{1}{(PeSt)^{\frac{1}{2}}} \left[ \frac{1}{2} \{ (m^{\frac{1}{2}})_{ij}^{-1} \bar{w}_j - (PeSt)^{\frac{1}{2}} F_i^h \} \bar{P}_M^{(i-1)} \frac{\partial}{\partial x_i} \{ \ln(\det m_{ab}) \} + \bar{w}_j (m^{\frac{1}{2}})_{ij}^{-1} \frac{\partial \bar{P}_M^{(i-1)}}{\partial x_i} \right] \\
&- \frac{1}{(PeSt)^{\frac{1}{2}}} \{ (m^{\frac{1}{2}})_{lk}^{-1} (m^{\frac{1}{2}})_{mj}^{-1} + (m^{\frac{1}{2}})_{lj}^{-1} (m^{\frac{1}{2}})_{mk}^{-1} \} \frac{\partial m_{km}^{\frac{1}{2}}}{\partial x_l} \bar{w}_j \bar{P}_M^{(i-1)} \\
&+ \frac{1}{(PeSt)^{\frac{1}{2}}} (m^{\frac{1}{2}})_{kj}^{-1} (m^{\frac{1}{2}})_{lb}^{-1} \left( \frac{\partial m_{al}^{\frac{1}{2}}}{\partial x_k} - \frac{\partial m_{ak}^{\frac{1}{2}}}{\partial x_l} \right) \frac{\partial}{\partial w_j} (\bar{w}_a \bar{w}_b \bar{P}_M^{(i-1)}) \\
&+ (PeSt)^{\frac{1}{2}} \left[ (m^{\frac{1}{2}})_{jn}^{-1} (m^{\frac{1}{2}})_{pk}^{-1} \left( \frac{\partial m_{pl}^{\frac{1}{2}}}{\partial x_j} - \frac{\partial m_{pj}^{\frac{1}{2}}}{\partial x_l} \right) - \frac{\partial m_{nk}^{\frac{1}{2}}}{\partial x_l} \right] F_k^h F_l^h \frac{\partial \bar{P}_M^{(i-1)}}{\partial \bar{w}_n} \\
&+ \left[ (m^{\frac{1}{2}})_{jn}^{-1} (m^{\frac{1}{2}})_{lm}^{-1} m_{pk}^{\frac{1}{2}} \left( \frac{\partial m_{pl}^{\frac{1}{2}}}{\partial x_j} - \frac{\partial m_{pj}^{\frac{1}{2}}}{\partial x_l} \right) - (m^{\frac{1}{2}})_{lm}^{-1} \left( \frac{\partial m_{nk}^{\frac{1}{2}}}{\partial x_l} + \frac{\partial m_{nl}^{\frac{1}{2}}}{\partial x_k} \right) \right. \\
&- \left. (m^{\frac{1}{2}})_{jn}^{-1} \left( \frac{\partial m_{mk}^{\frac{1}{2}}}{\partial x_j} - \frac{\partial m_{mj}^{\frac{1}{2}}}{\partial x_k} \right) \right] F_k^h \bar{w}_m \frac{\partial \bar{P}_M^{(i-1)}}{\partial \bar{w}_n} + F_k^h \frac{\partial \bar{P}_M^{(i-1)}}{\partial x_k} + F_i^h (m^{\frac{1}{2}})_{kl}^{-1} \frac{\partial m_{jk}^{\frac{1}{2}}}{\partial x_i} \bar{w}_l \frac{\partial \bar{P}_M^{(i-1)}}{\partial \bar{w}_j} \\
&- (m^{\frac{1}{2}})_{ij}^{-1} m_{nl}^{\frac{1}{2}} \frac{\partial F_l^h}{\partial x_i} \bar{w}_j \frac{\partial \bar{P}_M^{(i-1)}}{\partial \bar{w}_n} - (PeSt)^{\frac{1}{2}} F_i^h \frac{\partial F_l^h}{\partial x_i} m_{nl}^{\frac{1}{2}} \frac{\partial \bar{P}_M^{(i-1)}}{\partial \bar{w}_n}, \tag{3.28}
\end{aligned}$$

where the operator

$$\mathbf{L}_H^{(M)}(\bar{\mathbf{w}}) \equiv \left[ (m^{\frac{1}{2}})_{ji}^{-1} R_{jk}^{FU} (m^{\frac{1}{2}})_{kl}^{-1} \left( \frac{\partial}{\partial \bar{w}_i} (\bar{w}_l + \frac{\partial^2}{\partial \bar{w}_i \partial \bar{w}_l}) \right) + M \underline{\mathcal{A}} \right],$$

and we have used  $\mathbf{F}^h$  to denote the hydrodynamic force field ( $\mathbf{R}^{FU-1} \cdot \mathbf{F}^o$ ).

By construction, we have an identity at leading order ( $i = 0$ ). For  $i = 1$ , we get

$$\mathbf{L}_H^{(M)}(\bar{\mathbf{w}})\bar{P}_M^{(1)} = (\partial_M^{(0)} a_{i_1 i_2 \dots i_M}^M) \{ \bar{H}_M \}_{i_1 i_2 \dots i_M} + (\text{residual}) \text{ R.H.S. of (3.28) for } i = 1, \tag{3.29}$$

where  $\partial_M^{(0)}$  will be determined by removing the homogenous solutions, viz. terms proportional

to  $\bar{\mathbf{H}}_M$  on the right hand side of (3.29). These terms will only arise from the ‘flow’ terms,

i.e., those containing  $\mathbf{F}^h$ . While this may be seen from (3.28) after suitable manipulations, it should even otherwise be evident, since as seen in section 3.3, the corrections to the Smoluchowski equation in the absence of an external flow field, proceed in powers of  $\epsilon^2$ , where  $\epsilon = \tau_p/\tau_D$ . Thus, we expect the ‘non-flow’ terms to appear in the solvability conditions only at alternate orders in  $St$ ; however, the resulting contributions to the Smoluchowski equation will not necessarily be of the same order owing to the associated factor of  $(Pe St)$ . The first non-trivial contribution from the non-flow terms will then be at  $O(St^2)$  ( $i = 2$ ), and this gives rise to the familiar Brownian diffusion term in (3.18) (see below).

For now, again looking at the flow terms in (3.28), we note that the terms in the solvability condition at this order will be linear in  $\mathbf{F}^h$ . This restricts consideration to the following five terms:

$$\begin{aligned} & \left[ (m^{\frac{1}{2}})_{jn}^{-1} (m^{\frac{1}{2}})_{lm}^{-1} m_{pk}^{\frac{1}{2}} \left( \frac{\partial m_{pl}^{\frac{1}{2}}}{\partial x_j} - \frac{\partial m_{pj}^{\frac{1}{2}}}{\partial x_l} \right) - (m^{\frac{1}{2}})_{lm}^{-1} \left( \frac{\partial m_{nk}^{\frac{1}{2}}}{\partial x_l} + \frac{\partial m_{nl}^{\frac{1}{2}}}{\partial x_k} \right) - (m^{\frac{1}{2}})_{jn}^{-1} \left( \frac{\partial m_{mk}^{\frac{1}{2}}}{\partial x_j} - \frac{\partial m_{mj}^{\frac{1}{2}}}{\partial x_k} \right) \right] \\ & F_k^h \bar{w}_m \frac{\partial \bar{P}_M^{(0)}}{\partial \bar{w}_n}, \quad F_k^h \frac{\partial \bar{P}_M^{(0)}}{\partial x_k}, \quad F_i^h (m^{\frac{1}{2}})_{kl}^{-1} \frac{\partial m_{jk}^{\frac{1}{2}}}{\partial x_i} \bar{w}_l \frac{\partial \bar{P}_M^{(0)}}{\partial \bar{w}_j}, \quad - (m^{\frac{1}{2}})_{ij}^{-1} m_{nl}^{\frac{1}{2}} \frac{\partial F_l^h}{\partial x_i} \bar{w}_j \frac{\partial \bar{P}_M^{(0)}}{\partial \bar{w}_n}, \\ & - \frac{1}{2} F_k^h \bar{P}_M^{(0)} \frac{\partial}{\partial x_k} \{ \ln (\det m_{ab}) \}. \end{aligned}$$

Using the recurrence relation for the  $\bar{\mathbf{H}}_M$ 's, the solvability condition is found to be

$$\begin{aligned} & \partial_M^{(0)} a_{i_1 i_2 \dots i_M}^M + \frac{\partial}{\partial x_k} (a_{i_1 i_2 \dots i_M}^M F_k^h) - M F_i^h (m^{\frac{1}{2}})_{kl}^{-1} \left\{ \frac{\partial m_{i_M k}^{\frac{1}{2}}}{\partial x_i} a_{i_1 i_2 \dots i_{M-1} l}^M \right\} \\ & + M (m^{\frac{1}{2}})_{ij}^{-1} \frac{\partial F_l^h}{\partial x_i} \left\{ m_{i_M l}^{\frac{1}{2}} a_{i_1 i_2 \dots i_{M-1} j}^M \right\}_s - M F_k^h \left\{ \left[ (m^{\frac{1}{2}})_{j i_M}^{-1} (m^{\frac{1}{2}})_{pk}^{-1} m_{lm}^{\frac{1}{2}} \left( \frac{\partial m_{pl}^{\frac{1}{2}}}{\partial x_j} - \frac{\partial m_{pj}^{\frac{1}{2}}}{\partial x_l} \right) \right. \right. \\ & \left. \left. - (m^{\frac{1}{2}})_{lm}^{-1} \left( \frac{\partial m_{i_M k}^{\frac{1}{2}}}{\partial x_l} + \frac{\partial m_{i_M l}^{\frac{1}{2}}}{\partial x_k} \right) + (m^{\frac{1}{2}})_{j i_M}^{-1} \left( \frac{\partial m_{mk}^{\frac{1}{2}}}{\partial x_j} - \frac{\partial m_{mj}^{\frac{1}{2}}}{\partial x_k} \right) \right] a_{i_1 i_2 \dots i_{M-1} m}^M \right\}_s = 0, \quad (3.30) \end{aligned}$$

where  $\{\cdot\}_s$  is a symmetrizing operator and serves to define the totally symmetric tensor

$$\{\mathbf{C}_{i_1 i_2 \dots i_l}\}_s = \frac{1}{l!} \sum \mathbf{C}_{i_{p_1} i_{p_2} \dots i_{p_l}},$$

the sum being over all permutations of the numbers  $1, 2, 3, \dots, l$  (Wycoff and Balazs 1987b).

The series coefficient  $a^0$ , neglecting exponentially small corrections, is equal to the spatial probability density  $g_N$  for all times greater than  $O(\bar{\tau}_p)$ . The equation for  $a^0$  is obtained from (3.30) by setting  $M = 0$ ; thus

$$\partial_0^{(0)} a^0 + \frac{\partial}{\partial x_k} (a^0 F_k^h) = 0, \quad (3.31)$$

which is seen to be the limiting form of (3.18) for  $Pe \rightarrow \infty$ . As in Chapter 1, the diffusive term at the next order will come out to be  $O(1/Pe St)$  from the solvability condition at  $O(St^2)$ , and serves, in part, to determine  $\partial^{(1)}$ ; the resulting contribution to the Smoluchowski equation is, of course,  $O(1/Pe)$ .

While one could proceed for the general case, in the absence of a specific problem to examine and in light of the algebraic complexity of (3.28), we will restrict ourselves to obtaining the  $O(St)$  correction to the Smoluchowski equation when the inertia tensor  $\mathbf{m}$  is configuration independent (see next section). For the variable inertia case, we will focus on extracting the leading order diffusive term alone, so the resulting Smoluchowski equation obtained from combining the solvability conditions at  $O(St)$  and  $O(St^2)$  can be compared to (3.18), thereby ensuring the consistency of the formalism at leading order.

The derivation of the diffusive term requires considering the non-flow terms alone in (3.28) for  $i = 1$ , and one need only examine the solution  $\bar{P}_M^{(1)}$  for  $M = 0$ . The solution for general  $M$ , albeit algebraically more involved, is no more difficult; an expression for  $\bar{P}_M^{(1)}$  is

derived in Appendix B1, and serves to illustrate the general solution procedure at successive orders in  $St$ . We now look at (3.28) for  $i = 1$  and  $M = 0$ ,

$$\begin{aligned} \mathbf{L}_H(\bar{\mathbf{w}})(\bar{P}_0^{(1)})^{diff} &= \frac{1}{(PeSt)^{\frac{1}{2}}} \left[ \frac{1}{2} (m^{\frac{1}{2}})_{ij}^{-1} \bar{w}_j \bar{P}_0^{(0)} \frac{\partial}{\partial x_i} \{ \ln(\det m_{ab}) \} + \bar{w}_j (m^{\frac{1}{2}})_{ij}^{-1} \frac{\partial \bar{P}_0^{(0)}}{\partial x_i} \right] \\ &\quad - \frac{1}{(PeSt)^{\frac{1}{2}}} \{ (m^{\frac{1}{2}})_{lk}^{-1} (m^{\frac{1}{2}})_{mj}^{-1} + (m^{\frac{1}{2}})_{lj}^{-1} (m^{\frac{1}{2}})_{mk}^{-1} \} \frac{\partial m_{km}^{\frac{1}{2}}}{\partial x_l} \bar{w}_j \bar{P}_0^{(0)} \\ &\quad + \frac{1}{(PeSt)^{\frac{1}{2}}} (m^{\frac{1}{2}})_{kj}^{-1} (m^{\frac{1}{2}})_{lb}^{-1} \left( \frac{\partial m_{al}^{\frac{1}{2}}}{\partial x_k} - \frac{\partial m_{ak}^{\frac{1}{2}}}{\partial x_l} \right) \frac{\partial}{\partial w_j} (\bar{w}_a \bar{w}_b \bar{P}_0^{(0)}), \end{aligned} \quad (3.32)$$

with the associated solvability condition determined from (3.28) for  $i = 2$  as

$$\begin{aligned} \{ \partial_0^{(1)} \}^{diff} \bar{P}_0^{(0)} + \frac{1}{(PeSt)^{\frac{1}{2}}} \left( (m^{\frac{1}{2}})_{ij}^{-1} \left[ \bar{w}_j \frac{\partial}{\partial x_i} (\bar{P}_0^{(1)})^{diff} \right]_{\bar{H}_0} + \left\{ \frac{1}{2} (m^{\frac{1}{2}})_{ij}^{-1} \frac{\partial}{\partial x_i} \{ \ln(\det m_{ab}) \} - \right. \right. \\ \left. \left. \{ (m^{\frac{1}{2}})_{lk}^{-1} (m^{\frac{1}{2}})_{mj}^{-1} + (m^{\frac{1}{2}})_{lj}^{-1} (m^{\frac{1}{2}})_{mk}^{-1} \} \frac{\partial m_{km}^{\frac{1}{2}}}{\partial x_l} \right\} [\bar{w}_j \{ \bar{P}_0^{(1)} \}^{diff}]_{\bar{H}_0} \right) = 0, \end{aligned} \quad (3.33)$$

the superscript ‘*diff*’ being used for obvious reasons. From (B.6) in Appendix B1, the solution of (3.32) is given by

$$(\bar{P}_0^{(1)})^{diff} = \{ b_{0,1}^{(1)} \}_{i_1}^{diff} \{ \bar{H}_1 \}_{i_1} + \{ b_{0,3}^{(1)} \}_{i_1 i_2 i_3}^{diff} \{ \bar{H}_3 \}_{i_1 i_2 i_3},$$

whence the solvability condition reduces to

$$\begin{aligned} \{ \partial_0^{(1)} \}^{diff} \bar{P}_0^{(0)} + \frac{2^{\frac{1}{2}}}{(PeSt)^{\frac{1}{2}}} \left[ (m^{\frac{1}{2}})_{ij}^{-1} \frac{\partial}{\partial x_i} \{ b_{0,1}^{(1)} \}_j^{diff} + \left\{ \frac{1}{2} (m^{\frac{1}{2}})_{ij}^{-1} \frac{\partial}{\partial x_i} \{ \ln(\det m_{ab}) \} - \right. \right. \\ \left. \left. \{ (m^{\frac{1}{2}})_{lk}^{-1} (m^{\frac{1}{2}})_{mj}^{-1} + (m^{\frac{1}{2}})_{lj}^{-1} (m^{\frac{1}{2}})_{mk}^{-1} \} \frac{\partial m_{km}^{\frac{1}{2}}}{\partial x_l} \right\} \{ b_{0,1}^{(1)} \}_j^{diff} \right] = 0. \end{aligned} \quad (3.34)$$

From (B.3) and (B.7) with  $M = 0$ ,  $\mathbf{b}_{0,1}^{(1)diff}$  is given as

$$\{b_{0,1}^{(1)}\}_j^{diff} = \frac{1}{2^{\frac{1}{2}}(Pe\ St)^{\frac{1}{2}}} m_{jq}^{\frac{1}{2}} R_{qp}^{FU-1} \left[ -\frac{\partial a^0}{\partial x_p} + \frac{\partial}{\partial x_p} (\sqrt{\ln \det m_{ab}}) \right]. \quad (3.35)$$

Using (3.35) in (3.34), we find  $\{\partial_0^{(1)}\}^{diff}$  to be

$$\{\partial_0^{(1)}\}^{diff} = \frac{\partial}{\partial x_i} R_{ij}^{FU-1} (\sqrt{\det m_{ab}}) \frac{\partial}{\partial x_j} \left( \frac{a^0}{\sqrt{\det m_{ab}}} \right). \quad (3.36)$$

Combining (3.36) and (3.31) and using  $\partial/\partial t = \partial_0^{(0)} + St \{\partial_0^{(1)}\}^{diff}$  (see (3.26)),  $t$  now being on the flow time scale, it is easily seen that we recover the correct leading order Smoluchowski equation.

### 3.4.3.2 Configuration independent inertia tensor

It is evident from equation (3.11), valid for a position dependent drag force, that the appearance of non-Fickian terms in the Smoluchowski equation is independent of the configuration dependence of the inertia tensor. In this section therefore, we derive the form of the  $O(St)$  correction to the Smoluchowski equation for a constant  $\mathbf{m}$ . As will be seen below, it is necessary to derive expressions for the operators  $\partial_0^{(i)}$  in (3.26) upto  $i = 3$  in order to obtain the complete  $O(St)$  correction to equation (3.18).

With the above simplifications, the sequence of equations given by (3.28) reduces to

$$\begin{aligned} \mathbf{L}_H(\bar{\mathbf{w}}) \bar{P}_0^{(i)} &= \sum_{j=0}^{i-1} \partial_0^{(j)} \bar{P}_0^{(i-j-1)} + \frac{1}{(Pe\ St)^{\frac{1}{2}}} \bar{w}_j (m^{\frac{1}{2}})_{ij}^{-1} \frac{\partial \bar{P}_0^{(i-1)}}{\partial x_i} + F_k^h \frac{\partial \bar{P}_0^{(i-1)}}{\partial x_k} \\ &\quad - (m^{\frac{1}{2}})_{ij}^{-1} m_{nl}^{\frac{1}{2}} \frac{\partial F_l^h}{\partial x_i} \bar{w}_j \frac{\partial \bar{P}_0^{(i-1)}}{\partial \bar{w}_n} - (Pe\ St)^{\frac{1}{2}} F_i^h \frac{\partial F_l^h}{\partial x_i} m_{nl}^{\frac{1}{2}} \frac{\partial \bar{P}_0^{(i-1)}}{\partial \bar{w}_n}, \end{aligned} \quad (3.37)$$

For  $i = 1$ , eliminating terms proportional to the homogeneous solution  $\bar{H}_0$  gives us the same definition for  $\partial_0^{(0)}$  as (3.31), this being independent of  $\mathbf{m}$ . Having removed the secular terms, we examine (3.37) for  $i = 1$ , including both flow and non-flow terms:

$$\begin{aligned} \mathbf{L}_H(\bar{\mathbf{w}})\bar{P}_0^{(1)} = & \left\{ \frac{1}{(2PeSt)^{\frac{1}{2}}} (m^{\frac{1}{2}})_{ii_1}^{-1} \frac{\partial a^0}{\partial x_i} + \frac{(PeSt)^{\frac{1}{2}} a^0}{2^{\frac{1}{2}}} F_i^h \frac{\partial F_l^h}{\partial x_i} m_{i_1 l}^{\frac{1}{2}} \right\} \{\bar{H}_1\}_{i_1} \\ & + \frac{a^0}{2} (m^{\frac{1}{2}})_{ii_1}^{-1} m_{i_2 l}^{\frac{1}{2}} \frac{\partial F_l^h}{\partial x_i} \{\bar{H}_2\}_{i_1 i_2}. \end{aligned}$$

Thus,  $\bar{P}_0^{(1)}$  is found to be<sup>8</sup>

$$\bar{P}_0^{(1)} = \{b_{0,1}^{(1)}\}_{i_1} \{\bar{H}_1\}_{i_1} + \{b_{0,2}^{(1)}\}_{i_1 i_2} \{\bar{H}_2\}_{i_1 i_2}, \quad (3.38)$$

where

$$\begin{aligned} R_{jk}^{FU} (m^{\frac{1}{2}})_{ki}^{-1} (m^{\frac{1}{2}})_{j_1 i_1}^{-1} \{b_{0,1}^{(1)}\}_i &= - \left[ \frac{1}{(2PeSt)^{\frac{1}{2}}} (m^{\frac{1}{2}})_{ii_1}^{-1} \frac{\partial a^0}{\partial x_i} + \frac{(PeSt)^{\frac{1}{2}} a^0}{2^{\frac{1}{2}}} F_i^h \frac{\partial F_l^h}{\partial x_i} m_{i_1 l}^{\frac{1}{2}} \right], \\ R_{jk}^{FU} (m^{\frac{1}{2}})_{ki}^{-1} \{ \{b_{0,2}^{(1)}\}_{i_1 i} (m^{\frac{1}{2}})_{j_2 i_2}^{-1} + \{b_{0,2}^{(1)}\}_{i_2 i} (m^{\frac{1}{2}})_{j_1 i_1}^{-1} \} &= - \frac{a^0}{4} \frac{\partial F_l^h}{\partial x_i} \{ (m^{\frac{1}{2}})_{ii_1}^{-1} m_{i_2 l}^{\frac{1}{2}} + (m^{\frac{1}{2}})_{ii_2}^{-1} m_{i_1 l}^{\frac{1}{2}} \}. \end{aligned} \quad (3.39)$$

Here we have explicitly shown the action of the symmetrizing operator for the case of two indices  $i_1$  and  $i_2$ . The term independent of  $F^h$  in (3.38) could also have been obtained directly from (3.35) for  $\{\mathbf{b}_{0,1}^{(1)}\}^{diff}$ .

We now use (3.38) for  $\bar{P}_0^{(1)}$  at the next order ( $i = 2$ ) to obtain  $\partial_0^{(1)}$ , and then  $\bar{P}_0^{(2)}$ .

Unlike  $\partial_0^{(0)}$ , the operator  $\partial_0^{(1)}$  will involve both flow and non-flow contributions. The former are non-linear in the external forcing  $\mathbf{F}^h$ , and represent the first effect of particle inertia in the limit  $Pe \rightarrow \infty$ , while the latter correspond to Brownian diffusion for a constant  $\mathbf{m}$ . For

---

<sup>8</sup>As in section 3.2, the homogeneous solutions ( $\propto \bar{H}_0$ ) at this and higher orders may, without loss of generality be taken as zero by allowing the coefficients  $\alpha^M$  to satisfy  $St$  dependent initial conditions.

$i = 2$ , we have

$$\begin{aligned} \mathbf{L}_H(\bar{\mathbf{w}})\bar{P}_0^{(2)} &= \partial_0^{(0)}\bar{P}_0^{(1)} + \partial_0^{(1)}\bar{P}_0^{(0)} + \frac{1}{(Pe\,St)^{\frac{1}{2}}}\bar{w}_j(m^{\frac{1}{2}})_{ij}^{-1}\frac{\partial\bar{P}_0^{(1)}}{\partial x_i} \\ &\quad + F_k^h\frac{\partial\bar{P}_0^{(1)}}{\partial x_k} - (m^{\frac{1}{2}})_{ij}^{-1}m_{nl}^{\frac{1}{2}}\frac{\partial F_l^h}{\partial x_i}\bar{w}_j\frac{\partial\bar{P}_0^{(1)}}{\partial\bar{w}_n} - (Pe\,St)^{\frac{1}{2}}F_i^h\frac{\partial F_l^h}{\partial x_i}m_{nl}^{\frac{1}{2}}\frac{\partial\bar{P}_0^{(1)}}{\partial\bar{w}_n}, \end{aligned} \quad (3.40)$$

and the solvability condition is given by (3.33) for a constant  $\mathbf{m}$ :

$$\partial_0^{(1)}\bar{P}_0^{(0)} + \frac{1}{(Pe\,St)^{\frac{1}{2}}}(m^{\frac{1}{2}})_{ij}^{-1}\left[\bar{w}_j\frac{\partial\bar{P}_0^{(1)}}{\partial x_i}\right]_{\bar{H}_0} = 0,$$

where  $[\cdot]_{\bar{H}_0}$  denotes the term proportional to  $\bar{H}_0$ , which arises from the term proportional to  $\bar{\mathbf{H}}_1$  in  $\bar{P}_0^{(1)}$ . Using the expression for  $\mathbf{b}_{0,1}^{(1)}$  from (3.39), we finally obtain

$$\partial_0^{(1)}a^0 = \frac{1}{(Pe\,St)}\frac{\partial}{\partial x_i}\left[R^{FU-1}_{ij}\frac{\partial a^0}{\partial x_j}\right] + \frac{\partial}{\partial x_i}\left[R^{FU-1}_{ij}F_l^h\frac{\partial F_n^h}{\partial x_l}m_{nj}a^0\right]. \quad (3.41)$$

Combining (3.31) and (3.41) gives us the familiar convection-diffusion equation at leading order with the  $O(St)$  flow induced inertial correction for non-Brownian particles,

$$\frac{\partial a^0}{\partial t} + \frac{\partial}{\partial x_k}(a^0 F_k^h) = \frac{1}{Pe}\frac{\partial}{\partial x_i}\left[R^{FU-1}_{ij}\frac{\partial a^0}{\partial x_j}\right] + St\frac{\partial}{\partial x_i}\left[R^{FU-1}_{ij}F_l^h\frac{\partial F_n^h}{\partial x_l}m_{nj}a^0\right], \quad (3.42)$$

where we have used (3.26) to  $O(St)$  for  $M = 0$ , i.e.,  $\partial/\partial t = (\partial_0^{(0)} + St\partial_0^{(1)})$ ; the Brownian term is now  $O(1/Pe)$ . Though correct to leading order, (3.42) does not yet contain the complete  $O(St)$  correction. It is necessary go to higher orders in  $St$  in order to derive the missing terms.

We have thus far obtained exact expressions for  $\partial_0^{(0)}$  and  $\partial_0^{(1)}$ . The higher order operators will, however, also contain terms that contribute only at  $o(St)$ , and these will be

neglected in the subsequent analysis. Therefore, we only derive ‘partial’ expressions for  $\partial_0^{(2)}$  and  $\partial_0^{(3)}$  via the corresponding solvability conditions, including terms relevant to the  $O(St)$  correction. It is seen from (3.37) that each additional spatial derivative adds a scale factor of  $(PeSt)^{-\frac{1}{2}}$ , and each  $\mathbf{F}^h$  a factor of  $(PeSt)^{\frac{1}{2}}$  in the definition of the Smoluchowski operators  $\partial_0^{(i)}$ . The Brownian term in  $\partial_0^{(1)}$  above, for instance, contains second-order derivatives and is  $O(1/PeSt)$ . Unlike chapter 1 (see Appendix A3), however, derivatives of fourth and higher orders of  $O(1/PeSt)^n$  ( $n \geq 2$ ) do not cancel out in general, and give rise to the non-Fickian terms starting at  $O(St)$ .

Since none of the  $\bar{P}_0^{(i)}$ 's for  $i \geq 1$  contain  $\bar{H}_0$  (see earlier footnote), the general form of the solvability condition for  $i \geq 1$  can be written as

$$\partial_0^{(i)} \bar{P}_0^{(0)} + \frac{1}{(PeSt)^{\frac{1}{2}}} (m^{\frac{1}{2}})_{ij}^{-1} \left[ \bar{w}_j \frac{\partial \bar{P}_0^{(i)}}{\partial x_i} \right]_{\bar{H}_0} = 0, \quad (3.43)$$

where the subscript  $[\cdot]_{\bar{H}_0}$  is used to denote the term proportional to  $\bar{H}_0$ . Using the recurrence relations for the Hermite functions, this simplifies to

$$\partial_0^{(i)} a^0 = -\frac{2^{\frac{1}{2}}}{(PeSt)^{\frac{1}{2}}} (m^{\frac{1}{2}})_{i1}^{-1} \frac{\partial}{\partial x_i} \left( \{b_{0,1}^{(i)}\}_{i_1} \right), \quad (3.44)$$

where  $\mathbf{b}_{0,1}^{(i)}$  is the coefficient of the term proportional to  $\bar{\mathbf{H}}_1$  in  $\bar{P}_0^{(i)}$ . Thus, deriving the expressions for  $\partial_0^{(2)}$  and  $\partial_0^{(3)}$  will entail knowledge of  $\mathbf{b}_{0,1}^{(2)}$  and  $\mathbf{b}_{0,1}^{(3)}$ , respectively. Moreover, since we intend to look at the  $O(St)$  correction, we only need consider terms of  $O(1/PeSt)$  in  $\partial_0^{(2)}$  and those of  $O(1/PeSt)^2$  in  $\partial_0^{(3)}$  (see (3.26)).

In order to obtain  $\partial_0^{(2)}$ , we first use (3.41) to eliminate the secular terms in (3.40),

so that

$$\begin{aligned} \mathbf{L}_H(\bar{\mathbf{w}})[\bar{P}_0^{(2)}]_{\bar{\mathbf{H}}_1} &= \left[ \partial_0^{(0)} [\{b_{0,1}^{(1)}\}_{i_1} \nabla_{\mathbf{x}} a^0] + \frac{\partial}{\partial x_k} \left( F_k^h \{b_{0,1}^{(1)}\}_{i_1} \nabla_{\mathbf{x}} a^0 \right) + \frac{2(2^{\frac{1}{2}})}{(Pe\ St)^{\frac{1}{2}}} (m^{\frac{1}{2}})_{ij}^{-1} \frac{\partial}{\partial x_i} \left( \{b_{0,2}^{(1)}\}_{j i_1} \right) \right. \\ &\quad \left. + (m^{\frac{1}{2}})_{ij}^{-1} m_{i_1 l}^{\frac{1}{2}} \frac{\partial F_l^h}{\partial x_i} \{b_{0,1}^{(1)}\}_j \nabla_{\mathbf{x}} a^0 \right] \{\bar{H}_1\}_{i_1}, \end{aligned} \quad (3.45)$$

where we only consider the part of  $\mathbf{b}_{0,1}^{(1)}$  (defined by (3.39)) that depends on  $\nabla_{\mathbf{x}} a^0$ , the other term involving  $\mathbf{F}^h$  being  $O(St)$  smaller. The solution of (3.45) is easily found, and is given by

$$\begin{aligned} [\bar{P}_0^{(2)}]_{\bar{\mathbf{H}}_1} &= - (m^{\frac{1}{2}})_{i_1 m} R_{ml}^{FU^{-1}} (m^{\frac{1}{2}})_{kl} \left[ \partial_0^{(0)} [\{b_{0,1}^{(1)}\}_k \nabla_{\mathbf{x}} a^0] + \frac{\partial}{\partial x_j} \left( F_j^h \{b_{0,1}^{(1)}\}_k \nabla_{\mathbf{x}} a^0 \right) \right. \\ &\quad \left. + \frac{2(2^{\frac{1}{2}})}{(Pe\ St)^{\frac{1}{2}}} (m^{\frac{1}{2}})_{ij}^{-1} \frac{\partial}{\partial x_i} \left( \{b_{0,2}^{(1)}\}_{jk} \right) + (m^{\frac{1}{2}})_{ij}^{-1} m_{kl}^{\frac{1}{2}} \frac{\partial F_l^h}{\partial x_i} \{b_{0,1}^{(1)}\}_j \nabla_{\mathbf{x}} a^0 \right] \{\bar{H}_1\}_{i_1}. \end{aligned} \quad (3.46)$$

From (3.46) we obtain  $[\mathbf{b}_{0,1}^{(2)}]_{(Pe\ St)^{-\frac{1}{2}}}$ , and using this in (3.44) for  $i = 2$ , we get

$$\begin{aligned} [\partial_0^{(2)} a^0]_{(Pe\ St)^{-1}} &= \frac{2^{\frac{1}{2}}}{(Pe\ St)^{\frac{1}{2}}} \frac{\partial}{\partial x_m} \left\{ R_{ml}^{FU^{-1}} (m^{\frac{1}{2}})_{kl} \left[ \partial_0^{(0)} [\{b_{0,1}^{(1)}\}_k \nabla_{\mathbf{x}} a^0] + \frac{\partial}{\partial x_j} \left( F_j^h \{b_{0,1}^{(1)}\}_k \nabla_{\mathbf{x}} a^0 \right) \right. \right. \\ &\quad \left. \left. + \frac{2(2^{\frac{1}{2}})}{(Pe\ St)^{\frac{1}{2}}} (m^{\frac{1}{2}})_{ij}^{-1} \frac{\partial}{\partial x_i} \left( \{b_{0,2}^{(1)}\}_{jk} \right) + (m^{\frac{1}{2}})_{ij}^{-1} m_{kn}^{\frac{1}{2}} \frac{\partial F_n^h}{\partial x_i} \{b_{0,1}^{(1)}\}_j \nabla_{\mathbf{x}} a^0 \right] \right\}. \end{aligned} \quad (3.47)$$

The term in (3.47) involving the gradient of  $\mathbf{b}_{0,1}^{(1)}$ , and thence, second-order derivatives of  $a^0$ , will cancel out on using the definition of  $\partial_0^{(0)}$  viz. (3.31). Those that remain are proportional to  $\mathbf{b}_{0,1}^{(1)}$  and  $\nabla_{\mathbf{x}} \mathbf{b}_{0,2}^{(1)}$ , both of which are linear functionals of  $\nabla_{\mathbf{x}} a^0$  as is evident from (3.39). This implies that  $\partial_0^{(2)}$  will involve second-order derivatives of  $a^0$  with coefficients that depend linearly on  $(\nabla_{\mathbf{x}} \mathbf{F}^h)$ . The resulting contributions to the Smoluchowski equation are  $O(St/Pe)$ , and include both the  $O(St)$  corrections to the Brownian diffusivity and the  $O(St/Pe)$  Brow-

nian drift velocity. The analysis therefore predicts that, at  $O(St)$ , the diffusive behavior of an inertial suspension is flow dependent. In Chapter 1 this correction took the form of an  $O(St)$   $xy$  diffusivity for an isolated Brownian particle in a simple shear flow (see (2.40)).

From (3.44), we see that the  $O(1/PeSt)^2$  term in  $\partial_0^{(3)}$  is related to the  $O(1/PeSt)^{\frac{3}{2}}$  term in  $\mathbf{b}_{0,1}^{(3)}$ . In order to obtain the latter, we consider (3.37) for  $i = 3$ :

$$\begin{aligned} \mathbf{L}_H(\bar{\mathbf{w}})\bar{P}_0^{(3)} &= \partial_0^{(0)}\bar{P}_0^{(2)} + \partial_0^{(1)}\bar{P}_0^{(1)} + \partial_0^{(2)}\bar{P}_0^{(0)} + \frac{1}{(PeSt)^{\frac{1}{2}}}\bar{w}_j(m^{\frac{1}{2}})_{ij}^{-1}\frac{\partial\bar{P}_0^{(2)}}{\partial x_i} \\ &\quad + F_k^h\frac{\partial\bar{P}_0^{(2)}}{\partial x_k} - (m^{\frac{1}{2}})_{ij}^{-1}m_{nl}^{\frac{1}{2}}\frac{\partial F_l^h}{\partial x_i}\bar{w}_j\frac{\partial\bar{P}_0^{(2)}}{\partial\bar{w}_n} - (PeSt)^{\frac{1}{2}}F_i^h\frac{\partial F_l^h}{\partial x_i}m_{nl}^{\frac{1}{2}}\frac{\partial\bar{P}_0^{(2)}}{\partial\bar{w}_n}, \end{aligned} \quad (3.48)$$

where the solution for  $\bar{P}_0^{(3)}$  will be found after having used  $\partial_0^{(2)}$  from (3.47) to eliminate the secular terms on the right-hand side. The terms in  $[\bar{P}_0^{(2)}]_{\bar{\mathbf{H}}_1}$  are all  $O(1/PeSt)^{\frac{1}{2}}$  (see (3.46)), and therefore contribute terms of  $O(1/PeSt)$  in  $\mathbf{b}_{0,1}^{(3)}$ ; these lead to corrections to the Smoluchowski equation at  $O(St^2)$  and are not considered here. The  $O(1/PeSt)^{\frac{3}{2}}$  contributions come from  $[\bar{P}_0^{(2)}]_{\bar{\mathbf{H}}_2}^*$  and  $[\partial_0^{(1)}\bar{P}_0^{(1)*}]$ , where the action of  $\partial_0^{(1)}$  is defined in (3.41); the superscript ‘\*’ indicates that we only need the  $O(1/PeSt)$  contributions in the respective terms. Again considering (3.40), we find

$$[\bar{P}_0^{(2)}]_{\bar{\mathbf{H}}_2}^* = \{b_{0,2}^{(2)}\}_{i_1i_2}^* \{\bar{H}_2\}_{i_1i_2},$$

where

$$R_{jk}^{FU}(m^{\frac{1}{2}})_{ki}^{-1} \left\{ (m^{\frac{1}{2}})_{ji_1}^{-1} \{b_{0,2}^{(2)}\}_{ii_2}^* \right\}_s = \frac{-1}{2(2^{\frac{1}{2}})(PeSt)^{\frac{1}{2}}} \left\{ (m^{\frac{1}{2}})_{ii_2}^{-1} \frac{\partial}{\partial x_i} \{b_{0,1}^{(1)}\}_{i_1}^{\nabla \times a^0} \right\}_s. \quad (3.49)$$

Having found  $[\bar{P}_0^{(2)}]_{\bar{\mathbf{H}}_2}^*$ , we only include terms relevant to the  $O(St)$  correction in

(3.48) to obtain

$$\begin{aligned} \mathbf{L}_H(\bar{\mathbf{w}})\bar{P}_0^{(3)} &= \left(\partial_0^{(1)}\{b_{0,1}^{(1)}\}_{i_1}^{\nabla_{\mathbf{x}}a^0}\right)\{\bar{H}_1\}_{i_1} + \frac{1}{(PeSt)^{\frac{1}{2}}}(m^{\frac{1}{2}})_{ij}^{-1}\left[\bar{w}_j\frac{\partial}{\partial x_i}[\bar{P}_0^{(2)}]_{\bar{\mathbf{H}}_2}^*\right]_{\bar{\mathbf{H}}_1}, \\ &= \left[\left(\partial_0^{(1)}\{b_{0,1}^{(1)}\}_{i_1}^{\nabla_{\mathbf{x}}a^0}\right) + \frac{2(2^{\frac{1}{2}})}{(PeSt)^{\frac{1}{2}}}(m^{\frac{1}{2}})_{ij}^{-1}\frac{\partial}{\partial x_i}\left(\{b_{0,2}^{(2)}\}_{j i_1}^*\right)\right]\{\bar{H}_1\}_{i_1}. \end{aligned} \quad (3.50)$$

Solving (3.50), the  $O(1/PeSt)^{\frac{3}{2}}$  term in  $\mathbf{b}_{0,1}^{(3)}$  is given by

$$\left[\{b_{0,1}^{(3)}\}_{i_1}\right]_{(PeSt)^{-\frac{3}{2}}} = -(m^{\frac{1}{2}})_{i_1 m}R_{ml}^{FU-1}(m^{\frac{1}{2}})_{kl}\left[\left(\partial_0^{(1)}\{b_{0,1}^{(1)}\}_k^{\nabla_{\mathbf{x}}a^0}\right) + \frac{2(2^{\frac{1}{2}})}{(PeSt)^{\frac{1}{2}}}(m^{\frac{1}{2}})_{ij}^{-1}\frac{\partial}{\partial x_i}\left(\{b_{0,2}^{(2)}\}_{jk}^*\right)\right], \quad (3.51)$$

and using (3.51) in (3.44) with  $i = 3$ , one finally obtains

$$\left[\partial_0^{(3)}a^0\right]_{(PeSt)^{-2}} = \frac{2^{\frac{1}{2}}}{(PeSt)^{\frac{1}{2}}}\frac{\partial}{\partial x_m}\left\{R_{ml}^{FU-1}(m^{\frac{1}{2}})_{kl}\left[\left(\{b_{0,1}^{(1)}\}_k^{\nabla_{\mathbf{x}}(\partial_0^{(1)}a^0)}\right) + \frac{2(2^{\frac{1}{2}})}{(PeSt)^{\frac{1}{2}}}(m^{\frac{1}{2}})_{ij}^{-1}\frac{\partial}{\partial x_i}\left(\{b_{0,2}^{(2)}\}_{jk}^*\right)\right]\right\}, \quad (3.52)$$

where the change in the superscript associated with the first term indicates that the action of  $\partial_0^{(1)}$  is obtained by replacing  $a_0$  by  $\partial_0^{(1)}a^0$  (see section 3.2). The operator  $\partial_0^{(3)}a^0$  involves fourth order derivatives of  $a^0$  and is independent of  $\mathbf{F}^\circ$ . While it can be shown using the expressions for  $\{b_{0,1}^{(1)}\}_{i_1}^{\nabla_{\mathbf{x}}a^0}$  and  $\mathbf{b}_{0,2}^{(2)}$  that the two contributions in (3.52) have opposing signs, they do not cancel out in general. This is seen from the fact that, while an explicit expression for the first term in terms of the tensors  $(\nabla_{\mathbf{x}}^n a^0)$ ,  $\mathbf{m}^{\frac{1}{2}}$  and  $\mathbf{R}^{FU}$  is easily derived using (3.39) for  $\mathbf{b}_{0,1}^{(1)}$  and (3.41) for  $\partial_0^{(1)}$ , this is not the case for the second term since  $\mathbf{b}_{0,2}^{(2)*}$  is only defined through the action of the symmetrizing operator in (3.49)<sup>9</sup>. For one dimension, (3.52) reduces to the non-Fickian term in (3.13) with  $\mathbf{R}^{FU}(\mathbf{x}) \equiv f(x)$  (see section 3.3). To see this, we need

<sup>9</sup>This does not, of course, imply that one cannot solve for the elements of  $\mathbf{b}_{0,2}^{(2)*}$ ; (3.49) is a regular system of linear equations, and one can always obtain the individual elements of  $\mathbf{b}_{0,2}^{(2)*}$  in terms of the elements of the other known tensors.

to scale  $t$  with  $\tau_p$  as in (3.13), which adds a factor of  $St$ , and the term  $\partial_0^{(3)}a^0$  in the rescaled equation becomes  $O(\epsilon^4)$  with  $\epsilon^2 = St/Pe = \tau_p/\tau_D$ .

It will be seen in the next section that the operators  $\partial_0^{(i)}$  for  $i > 3$  are only relevant at  $O(St^2)$  and higher. Considering the expressions for  $\partial_0^{(0)}$ ,  $\partial_0^{(1)}$ ,  $\partial_0^{(2)}$  and  $\partial_0^{(3)}$  as given by (3.31), (3.41), (3.47) and (3.52), respectively, the Smoluchowski equation, to  $O(St)$ , can now be written as

$$\frac{\partial g_N}{\partial t} + \frac{\partial}{\partial x_i} \left[ (V_i^{(0)} + St \{ V_i^{(1)conv} + \frac{1}{Pe} V_i^{(1)Brow} \}) g_N \right] = \frac{1}{Pe} \frac{\partial}{\partial x_i} (D_{ij}^{(0)} + St D_{ij}^{(1)}) \frac{\partial g_N}{\partial x_j} + \frac{St}{Pe^2} [\mathcal{L}_{\mathbf{x}}]^4 g_N, \quad (3.53)$$

where the  $\mathbf{V}^{(i)}$ 's and the  $\mathbf{D}^{(i)}$ 's are, respectively, the drift velocities and the diffusion coefficients at successive orders in  $St$ ; they are given by

$$\begin{aligned} V_i^{(0)} &= F_k^h, \\ V_i^{(1)conv} &= R^{FU-1}_{ij} F_l^h \frac{\partial F_n^h}{\partial x_l} m_{nj}, \\ V_i^{(1)Brow} &= -R^{FU-1}_{ij} m_{jk} R^{FU-1}_{kl} \frac{\partial F_n^h}{\partial x_l \partial x_n} - 4R^{FU-1}_{im} \frac{\partial}{\partial x_j} \left\{ \frac{(m^{\frac{1}{2}})_{jk}^{-1} \{b_{0,2}^{(1)}\}_{kl} m_{lm}^{\frac{1}{2}}}{g_N} \right\}, \\ D_{ij}^{(1)} &= -R^{FU-1}_{ik} R^{FU-1}_{jl} \frac{\partial F_n^h}{\partial x_l} m_{nk} + R^{FU-1}_{ik} m_{kl} R^{FU-1}_{lm} \frac{\partial F_j^h}{\partial x_m} \\ &\quad - R^{FU-1}_{ik} m_{kn} F_l^h \frac{\partial}{\partial x_l} R^{FU-1}_{nj} + \frac{4}{g_N} R^{FU-1}_{ik} (m^{\frac{1}{2}})_{kl}^{-1} \{b_{0,2}^{(1)}\}_{lm} m_{mj}^{\frac{1}{2}}, \end{aligned}$$

and  $\mathbf{D}^{(0)}$  here represents the Stokes-Einstein diffusion coefficient. The  $\{b_{0,2}^{(1)}\}_{ij}$ 's are as defined in (3.39). The fourth-order derivative contributions,  $[\mathcal{L}_{\mathbf{x}}]^4 a^0$ , come from  $\partial_0^{(3)}$ ; here,  $\mathcal{L}_{\mathbf{x}}$  denotes a spatial gradient with associated configuration dependent factors, i.e.,

$$[\mathcal{L}_{\mathbf{x}}]^k g_N = \left[ \frac{\partial}{\partial x_{i_1}} h_{i_1 i_2}^1(\mathbf{x}) \frac{\partial}{\partial x_{i_2}} h_{i_2 i_3}^2(\mathbf{x}) \dots h_{i_{k-1} i_k}^{k-1}(\mathbf{x}) \frac{\partial}{\partial x_{i_k}} \right] g_N.$$

It must be noticed that  $\mathbf{b}_{0,2}^{(1)} \propto g_N$ , and therefore both  $\mathbf{V}^{(1)}$  and  $\mathbf{D}^{(1)}$  are independent of  $g_N$  as they must be.

### 3.4.4 Higher order inertial corrections

Having determined the operators  $\partial_0^{(i)}$  for  $i \leq 3$ , we observe that the orders of the highest derivative in  $\partial_0^{(0)}$ ,  $\partial_0^{(1)}$ ,  $\partial_0^{(2)}$  and  $\partial_0^{(3)}$  are 1, 2, 2 and 4 respectively. This pattern repeats at higher orders, that is,  $\partial_0^{(4)}$  again has fourth order derivatives, the operators  $\partial_0^{(5)}$  and  $\partial_0^{(6)}$  will contain sixth order derivatives, and so forth. Thus, the highest order of derivatives in both  $\partial_0^{(2k-1)}$  and  $\partial_0^{(2k)}$  is  $2k$ . This pattern ensures that the familiar convection-diffusion equation (3.18) for a constant  $\mathbf{m}$  is indeed the correct leading order equation and that the  $O(St)$  correction terminates with derivatives of the fourth order. More generally, the Chapman-Enskog formalism for an inertial suspension leads to a corrected Smoluchowski equation of the following form:

$$\begin{aligned} \frac{\partial g_N}{\partial t} + \frac{\partial}{\partial \mathbf{x}_i} [(\mathbf{R}^{FU-1} \cdot \mathbf{F}^{\circ})_i g_N] &= \frac{1}{Pe} \left( \frac{\partial}{\partial \mathbf{x}_i} \mathbf{R}^{FU-1}_{ij} \frac{\partial g_N}{\partial \mathbf{x}_j} \right) + St \left( \mathcal{L}_x^{(1)} + \frac{1}{Pe} [\mathcal{L}_x^{(1)}]^2 + \frac{1}{Pe^2} [\mathcal{L}_x^{(1)}]^4 \right) g_N \\ &+ \dots + St^k \sum_{i=0}^{k+1} \frac{1}{Pe^i} [\mathcal{L}_x^{(k)}]^{2i} g_N + \dots, \end{aligned} \quad (3.54)$$

where we have used  $\mathcal{L}_x^{(k)}$  to denote an operator of the form  $\mathcal{L}_x$  at  $O(St^k)$  (see previous section). The highest derivative contribution at any order in  $St$  is independent of the flow  $\mathbf{F}^{\circ}$ ; at  $O(St)$  this is the term containing fourth order derivatives (see (3.53)). The explicit form of the  $Pe$  independent terms,  $\mathcal{L}_x^{(k)} g_N$ , at any order in  $St$ , can always be given in terms of the tensors  $\mathbf{m}$  and  $\mathbf{R}^{FU}$ . While this may be shown from the structure of the formalism in previous sections by proving the redundancy of the symmetrizing operator for these cases, it is more easily demonstrated from an explicit solution of the deterministic equations of

motion in this limit (see Chapter 3, section 4.2). These terms represent inertial corrections to the probability density of a non-Brownian suspension. We recall that in Chapter 1 such corrections were absent for an isolated Brownian particle in a simple shear flow owing to the rectilinear ambient streamlines.

The general form (3.54) will remain valid even when the inertia tensor  $\mathbf{m}$  is configuration dependent. The latter is expected to only affect the forms of the factors  $\mathbf{h}^i(\mathbf{x})$  in the operators  $\mathcal{L}_{\mathbf{x}}^{(k)}$ . Finally, the order of the highest derivative in the  $O(St^k)$  contribution will remain unchanged even for  $M \geq 1$  (the fast scales), i.e., the equation for the  $\mathbf{a}^M$ 's is of the same form as (3.54); this is seen, in part, from comparing the consistency conditions for the operators  $\partial_M^{(0)}$  ( $M \geq 1$ ), and  $\partial_0^{(0)}$  given by (3.30) and (3.31) respectively.

For a statistically homogeneous suspension, the spatial probability density  $g_N$  is translationally invariant, i.e.,  $g_N(\mathbf{x}_1, \mathbf{x}_2, \dots, \mathbf{x}_N, t) \equiv g_N(\mathbf{r}_2, \mathbf{r}_3, \dots, \mathbf{r}_N, t)$ , where  $\mathbf{r}_i = \mathbf{x}_i - \mathbf{x}_{i-1}$ . Thus changing to relative coordinates, (3.53) becomes

$$\frac{\partial g_N}{\partial t} + \frac{\partial}{\partial r_i} \left[ (\hat{V}_i^{(0)} + St \{ \hat{V}_i^{(1)conv} + \frac{1}{Pe} \hat{V}_i^{(1)Brow} \}) g_N \right] = \frac{1}{Pe} \frac{\partial}{\partial r_i} (\hat{D}_{ij}^{(0)} + St \hat{D}_{ij}^{(1)}) \frac{\partial g_N}{\partial r_j} + \frac{St}{Pe^2} \mathcal{L}'_{\mathbf{x}}{}^4 a_0, \quad (3.55)$$

where  $\hat{V}^{(k)}$  and  $\hat{D}^{(k)}$  are suitable linear combinations of  $V^{(k)}$  and  $D^{(k)}$ , and  $\mathcal{L}'_{\mathbf{x}}{}^4$  denotes the modified form of the fourth order derivative correction in relative coordinates; the indices  $i$  and  $j$  now span the configurational degrees of freedom of  $(N-1)$  particles. We observe that the inertial corrections are not relevant in the limit  $Pe \ll 1$ , since the Stokes number in this case would be extremely small and the effects of particle inertia negligible<sup>10</sup>. The high  $Pe$  limit for the leading order problem, viz. (3.55) for  $St = 0$ , is singular; strong convection effects

<sup>10</sup>The ratio  $St/Pe$  is independent of the flow time scale, and is of the same order as the ratio of the mean free path (defined in the context of Brownian motion as the product of the thermal velocity  $(kT/m)^{\frac{1}{2}}$  and the correlation time, the latter being of  $O(\tau_p)$ ) to the size of the particle; thus,  $St/Pe \ll 1$ .

are balanced by Brownian diffusion in asymptotically thin boundary layers near particle-particle contact. At these small relative separations, the interactions between the particles are dominated by lubrication forces; for spherical particles this leads to the radial component of the leading order relative velocity ( $\hat{V}_r^{(0)}$ ) and the corresponding diffusion coefficient ( $\hat{D}_{rr}^{(0)}$ ) vanishing linearly with decreasing separation; the dominant balance yields the thickness of the boundary layer  $|\mathbf{r}_i - \mathbf{r}_j - 2| \sim O(Pe^{-1})$  (Brady & Morris 1997). It may be shown that the  $O(St)$  corrections to the velocity field ( $\mathbf{V}_{conv}^{(1)}$  and  $\mathbf{V}_{Brow}^{(1)}$ ) and the diffusivity ( $\mathbf{D}^{(1)}$ ) again have linearly decaying radial components close to contact, and therefore remain uniformly small for all relative positions of particles. Moreover, since the non-Fickian term is  $O(1/Pe)$  smaller than the other  $O(St)$  corrections, the leading order balance and the resulting scaling for the boundary layer is expected to remain unaltered for  $Pe \gg 1$ .

It is possible that the near-field linear decay of the ‘diffusion coefficients’  $\mathbf{h}^i(\mathbf{x})$  may be violated in the higher-order derivatives appearing at  $O(St^2)$  and higher, implying that they become comparable to the leading order terms for sufficiently small interparticle separations. Even so, the ‘inner’ layer in such cases will most likely be  $O(St/Pe)$  or smaller, and resorting to matched asymptotic expansions in order to obtain a uniformly valid solution will amount to resolving length scales smaller than the Brownian mean free path; in this sense the higher-order derivative corrections are similar to the Burnett and super-Burnett corrections encountered in the kinetic theory of gases (Cercignani 1975). Therefore in the limit  $Pe \gg 1$ , notwithstanding possibly aphysical boundary layers, the finite  $St$  Smoluchowski equation (3.54) again involves a second-order differential operator at leading order, and the no-flux boundary conditions suffice to make the problem determinate.

### 3.5 Conclusions

A generalized Chapman-Enskog expansion was used to determine the phase-space probability density for an inertial suspension. The probability density was expanded in an infinite series of Hermite functions involving the fluctuation velocity, and Smoluchowski-like configuration space equations satisfied by the expansion coefficients were obtained. The method is restricted in its validity to the case where  $\bar{S}t = St/|\bar{R}(\phi)| \ll 1$ , or equivalently, when the inertial relaxation time of an individual particle is much smaller than the flow time scale. The analysis yielded inertial corrections to the Smoluchowski equation that characterise the effect of particulate phase inertia on suspension microstructure and rheology. The  $O(St)$  correction was found to consist of three terms: the first term is an  $O(St)$  modification of the inertialess velocity field ( $\mathbf{R}^{FU} \cdot \mathbf{F}^o$ ) and includes an  $O(St/Pe)$  Brownian drift velocity; the second is a Fickian term that leads to a flow dependent  $O(St)$  correction to the diffusivity tensor; and the third term is an  $O(St/Pe^2)$  non-Fickian term comprising fourth order derivatives. The non-Fickian contributions are expected to be unimportant in the limit  $Pe \gg 1$ ; the residual inertial corrections can then be treated in a regular manner, and do not in any essential way increase the difficulty of solving for the spatial probability density for finite Stokes numbers.

The solution derived using the Chapman-Enskog formulation above remains uniformly valid provided the nature of the near-field interactions between particles for small but finite inertia are assumed to have the same character as that for inertialess particles (see Chapter 3, section 4.3). For these cases, lubrication forces between particles are strong enough to prevent interparticle contact. In the absence of hydrodynamic interactions, collisions between particles will fundamentally alter the probability density in regions of configuration space where particle surfaces are in close contact<sup>11</sup>. In the limit of small  $St$ , the memory

---

<sup>11</sup>Weak hydrodynamic interactions are characteristic of highly charged particles in solutions of low ionic strength, in which case the electrostatic repulsion acts at length scales much greater than the actual size of

of a collision lasts only for a short distance (the distance travelled by the particle in a time interval of  $O(\bar{\tau}_p)$ ), however, and one would still expect the multiple scales solution to be valid over most of the domain except in configurational boundary layers, wherein the collisional distribution dominates; the inertial term  $St(\mathbf{u} \cdot \partial P / \partial \mathbf{x})$  has to be retained at leading order in these regions). A uniformly valid solution in this limit would, in principle, be obtained via matched asymptotic expansions.

## Bibliography

- [1] Batchelor, G.K. & Green, J.T. 1972 The determination of the bulk stress in a suspension of spherical particles to  $O(c^2)$ . *J. Fluid Mech.* **56**, 401-427.
- [2] Brady, J.F. & Morris, J.F. 1997 Microstructure of strongly sheared suspensions and its impact on rheology and diffusion. *J. Fluid Mech.* **348**, 103-139.
- [3] Cercignani, C. 1975 *Theory and application of the Boltzmann equation*. Elsevier.
- [4] Chapman, S. & Cowling, T.G. 1970 *The mathematical theory of non-uniform gases*. Cambridge University Press.
- [5] Grad, H. 1949 A note on  $N$ -dimensional Hermite polynomials. *Communs. in Pure and Appl Math.* **2**, 331.
- [6] Grassia, P.S., Hinch, E.J. & Nitsche, L.C. 1995 Computer simulations of Brownian motion of complex systems. *J. Fluid Mech.* **282**, 373-403.
- [7] Hinch, E.J. 1975 Application of the Langevin equation to fluid suspensions. *J. Fluid Mech.* **72**, 499-511.
- [8] Jeffrey, D.J. & Acrivos, A. 1976 Rheological properties of suspensions of rigid particles. *AIChE J.* **22**(3), 417-436.
- [9] Kevorkian, J. & Cole, J.D. 1995 *Multiple Scale and Singular Perturbation Methods*. Springer-Verlag.

- [10] Kim, S. & Karrila, S.J. 1991 *Microhydrodynamics: principles and applications*. Butterworth-Heinemann.
- [11] Risken, H. 1989 *The Fokker-Planck Equation*. Springer-Verlag pp. 25.
- [12] Miguel, S.M. & Sancho, J.M. 1979 Brownian motion in shear flow. *Physica* **99A**, 357-364.
- [13] Smoluchowski, M.V. 1915 Über brownsche Molekularbewegung unter Einwirkung äubere Kräfte und deren Zusammenhang mit der verallgemeinerte Diffusionsgleichung. *Ann. d. Physik* **48**, 1103-1112.
- [14] Titulaer, U.M. 1978 A systematic solution procedure for the Fokker-Planck equation of a Brownian particle in the high-friction case. *Physica* **91A**, 321-344.
- [15] Wycoff, D. & Balazs, N.L. 1987a Multiple time scales analysis for the Kramers-Chandrasekhar equation. *Physica* **146A**, 175-200.
- [16] Wycoff, D. & Balazs, N.L. 1987b Multiple time scales analysis for the Kramers-Chandrasekhar equation with a weak magnetic field. *Physica* **146A**, 201-218.
- [17] Yurkovetsky, Y. & Brady, J.F. 1996 Statistical mechanics of bubbly liquids. *Phys. Fluids* **8**(4), 881-895.

## Chapter 4

# Trajectory analysis for inertial, non-Brownian suspensions: in-plane trajectories

### 4.1 Introduction

Understanding the role of inertia in fluid-particle flows is critical both to the successful design and scale-up of industrial processes and to the modelling of naturally occurring phenomena. In addition, from a fundamental viewpoint, it is of interest to investigate the separate roles of particle and fluid inertia in flows, the magnitudes of these being determined by the Stokes ( $St$ ) and Reynolds numbers ( $Re$ ), respectively. We examine suspensions of heavy particles,  $\rho_p/\rho_f \gg 1$ , for which the Stokes number is finite, but the Reynolds number of the flow is small enough for inertial forces in the fluid to be neglected. In the limit of zero  $Re$ , if one also neglects the unsteady term in the Navier-Stokes equations, the motion of the fluid satisfies the quasi-steady Stokes equations and is therefore uniquely determined by the current velocities and configuration of the particles (and positions and velocities of the boundaries if any). The interactions between particles are then completely characterized by configuration-dependent resistance tensors whose expressions for the case of pair-wise interactions are well-known and have been tabulated in detail (see Kim & Karrila 1991). For finite  $St$ , however, the particles do not instantaneously relax to the local fluid velocity, and the momentum of the particle enters as an independent variable. Gas-solid suspensions fall in this parameter regime. In contrast, for particles suspended in a liquid,  $St \approx Re$ , and at small  $Re$ , particle inertia is negligible.

Inertialess flows of suspensions have been extensively studied and are fairly well understood. In contrast, there has been relatively limited work for cases where inertial effects exert a significant influence on flow behaviour. One such investigation has been carried out by Koch and coworkers (Koch 1990, Kumaran & Koch 1993ab, Tsao & Koch 1995, Sangani et al 1996) who, in a series of papers, have studied non-Brownian suspensions in the limit  $Re = 0$ ,  $St > O(1)$ . Fluid inertia is again negligible and the statistics of the particles are governed by the Boltzmann equation that accounts for momentum transfer via solid-body collisions. The macroscopic behaviour of dilute suspensions in this limit is found to depend on the relative magnitudes of the inertial relaxation time  $\tau_p$  and the collision time  $\tau_c = af(\phi)/T_p^{1/2}$ , where  $\phi$  is the volume fraction ( $f(\phi) \rightarrow \phi^{-1}$  as  $\phi \rightarrow 0$ ) and  $T_p = \langle \mathbf{u}' \cdot \mathbf{u}' \rangle$  is a measure of the magnitude of particle velocity fluctuations. A pronounced non-Newtonian rheology results at  $O(1)$  Stokes numbers, characterized by the presence of normal stress differences.

In this chapter, we consider simple shear flow of dilute suspensions in the limit  $Re = 0$ ,  $St \ll 1$ , and in the absence of Brownian motion ( $Pe \rightarrow \infty$ ). This serves to complement the above efforts and helps characterize suspension properties as a function of  $St$  for zero  $Re$ . The limit  $Re = St = 0$ , in the absence of non-hydrodynamic forces, generates a symmetric microstructure with a Newtonian rheology (Batchelor & Green 1972b); we investigate, in depth, the deviation from this limit for small but finite particle inertia. In the analysis below we consider only pair-particle interactions, and the results will therefore be quantitatively accurate only for dilute suspensions ( $\phi \rightarrow 0$ ). Some of the qualitative implications, however, are expected to remain valid even for higher volume fractions. For small  $St$ , lubrication forces between particles are strong enough to prevent solid-body contacts (see section 4.3) and particles never come close enough for their separation to become comparable

to molecular length scales (for instance, the mean free path  $\lambda$  for a gas-solid suspension). We will therefore assume that the continuum approximation for the suspending fluid remains valid for all possible particle configurations and solid-body collisions are not considered as a source of momentum transfer. In this limit, the structure of the equation governing the pair-probability  $P_2$  is identical to that for  $P_N$  derived in Chapter 3 (see section 4.2). A central result of our analysis is that the rheology of a finite  $St$  suspension for pair-wise interactions in the absence of non-hydrodynamic forces is indeterminate. This indeterminacy is due to the existence of a singular curve in configuration space where particles accumulate, thus precluding the possibility of a steady distribution. Therefore particle inertia, though a possible mechanism for microstructural asymmetry, does not lead to a well-posed rheological problem with pairwise interactions alone. We also show that the asymmetry of the finite  $St$  hydrodynamic interactions leads to a finite (anisotropic) shear-induced self-diffusivity. This then provides a mechanism for diffusive suspension behavior even in the absence of short-range interparticle forces or surface roughness (Davis 1996, daCunha & Hinch 1996, Leighton & Acrivos 1987ab).

## 4.2 Equations for particle trajectories

Before specializing to the non-Brownian limit, we briefly reconsider the derivation of the Smoluchowski equation from the Fokker-Planck equation. If one were not concerned with the effects of inertia on shorter time scales, i.e., with relating the initial conditions in position space for the Smoluchowski equation to that of the full Fokker-Planck equation (in phase space), one can employ a much simpler form of the formalism given in previous chapters, involving only the slower time scales. Of course, this so-called Bogliubov solution could also have been obtained from the general solution of the Fokker-Planck equation derived in

Chapter 3; it is, in fact, equivalent to considering the evolution of the  $P_0^{(i)}$ 's alone in (3.25), and thence obtaining the equation (3.54) for  $a^0$ . However, the relative simplicity of the evolving slow scales may have been obscured in the generality of the formalism. Therefore, at the possible expense of repetition, we delineate the method of obtaining this long-time solution directly from the governing equation.

The Fokker-Planck equation governing the pair-probability  $P_2(\mathbf{U}, \mathbf{x}, t; St)$  is given as

$$\frac{\partial P_2}{\partial t} + St \mathbf{U} \cdot \nabla_{\mathbf{x}} P_2 = \nabla_{\mathbf{U}} \cdot [\mathbf{m}^{-1} \cdot \mathbf{R}_{FU} \cdot (\mathbf{U} - \mathbf{R}_{FU}^{-1} \cdot \mathbf{F}^o) P_2] + \frac{1}{(Pe St)} (\mathbf{m}^{-1} \cdot \mathbf{R}_{FU} \cdot \mathbf{m}^{-1}) : \nabla_{\mathbf{U}} \nabla_{\mathbf{U}} P_2, \quad (4.1)$$

where, for the sake of simplicity, we have restricted attention to cases involving a constant inertia tensor. Upon integrating (4.1) with respect to velocity coordinates, and assuming  $P_2$  and its derivatives to decay sufficiently rapidly as  $|\mathbf{U}| \rightarrow \infty$ , we obtain

$$\frac{\partial}{\partial t} \left( \int P_2 d\mathbf{U} \right) + St \int (\mathbf{U} \cdot \nabla_{\mathbf{x}} P_2) d\mathbf{U} = 0.$$

Writing  $P_2(\mathbf{x}, \mathbf{U}, t)$  as  $g(\mathbf{x}, t; St) P_2'(\mathbf{U} | \mathbf{x}, t; St)$  with  $P_2'$  being the conditional velocity distribution for the configuration  $\mathbf{x}$ , and using the fact that  $\int P_2' d\mathbf{U} = 1$ , we have

$$\frac{\partial g}{\partial t} + St \nabla_{\mathbf{x}} \cdot \left[ \left( \int \mathbf{U} P_2' d\mathbf{U} \right) g \right] = 0, \quad (4.2)$$

where  $g$  now represents the probability density in configuration space. No approximations have been made at this stage, and (4.2) for  $g$  is exact. As was seen in Chapter 3,  $P_2'$  at leading order can be written in the form  $\sum_{M=0}^{\infty} \mathbf{a}^M(\mathbf{x}, t; St) \odot \bar{\mathbf{H}}_M((Pe St/2)^{\frac{1}{2}} \mathbf{V})$ , where  $\mathbf{V} = \mathbf{U} - \mathbf{R}_{FU}^{-1} \cdot \mathbf{F}^o$  is the fluctuation velocity, and the slow modes are contained in  $a^0(\mathbf{x}, t; St)$ .

Since we are not concerned with terms that become exponentially small on the flow time scale, the equation for  $g$ , to any order in  $St$ , can be obtained without the need to calculate the  $\mathbf{a}^M$ 's for  $M \geq 1$ .

For small  $St$  one can approximate  $P'_2$  as

$$P'_2(\mathbf{U}|\mathbf{x}, t; St) = P_2'^{(0)} + St P_2'^{(1)} + \dots \quad (4.3)$$

Using this expansion in (4.2), it is evident that we must similarly expand either  $g$  or the time operator in order to avoid trivial solutions. The essence of the Chapman-Enskog method, of course, lies in expanding the latter, which allows for  $g$  to be a non-analytic function of  $St$ ; thus

$$\frac{\partial}{\partial t} = St \left( \partial^{(0)} + St \partial^{(1)} + \dots \right), \quad (4.4)$$

where the leading order term is now taken to be  $O(St)$  in order to capture the slower scales alone. Using (4.3) and (4.4) in (4.1),  $P_2'^{(0)}$  is found to be a steady state Maxwellian in the fluctuation velocity, and the higher order terms in the series for  $P'_2$  depend on time only in an implicit manner via  $g$ . The expansion (4.3) for  $P'_2$  can now be written as

$$P'_2(\mathbf{U}|\mathbf{x}, t; St) = \mathcal{C} \exp \left[ -\frac{(Pe St)}{2} \mathbf{V} \cdot \mathbf{V} \right] + St P_2'^{(1)}(\mathbf{U}|\mathbf{x}; g(\mathbf{x}, t; St)) + \dots, \quad (4.5)$$

with  $\mathcal{C}$  being a suitable normalization constant. On substituting  $P_2'^{(0)}$  in the flux term of (4.2), one obtains the convective Smoluchowski equation for  $g$  in the absence of inertia (see (3.31)).

The higher order solutions represent the corrections for finite  $St$  and  $Pe$ . The equation for  $g$

for finite  $St$  then takes the form

$$\frac{\partial g}{\partial t} + \nabla_{\mathbf{x}} \cdot \left[ \left( \langle \mathbf{U}^{(0)} \rangle + St \langle \mathbf{U}^{(1)} \rangle + \dots \right) g \right] = 0, \quad (4.6)$$

where

$$\langle \mathbf{U}^{(i)} \rangle = \int \mathbf{U} P_2^{(i)} d\mathbf{U} \quad (i \geq 0).$$

Equation (4.6) should be identical to (3.54) for  $a^0$  in Chapter 3, and the  $\langle \mathbf{U}^{(i)} \rangle$ 's are therefore generalized velocities; for finite  $Pe$ , they contain terms that involve gradients of  $g$ . For instance, a velocity of the form  $-(\mathbf{D} \cdot \nabla_{\mathbf{x}} \log g)$  accounts for Brownian diffusion at leading order.

We now investigate the non-Brownian limit of the two-particle Smoluchowski equation for the case of spherical particles in a linear flow. This is obtained in the limit  $Pe \rightarrow \infty$  from equation (3.54); to  $O(St)$ , it takes the form

$$\frac{\partial g}{\partial t} + \nabla_{\mathbf{x}} \cdot (\mathbf{R}_{FU}^{-1} \cdot \mathbf{F}^o g) - St \nabla_{\mathbf{x}} \cdot [\mathbf{R}_{FU}^{-1} \cdot \{ (\mathbf{R}_{FU}^{-1} \cdot \mathbf{F}^o) \cdot \nabla_{\mathbf{x}} (\mathbf{R}_{FU}^{-1} \cdot \mathbf{F}^o) \cdot \mathbf{m} \} g] = 0, \quad (4.7)$$

where  $\mathbf{x}$  now denotes the configurational variables corresponding to a pair of particles. The force  $\mathbf{F}^o$  for a linear flow field is given by

$$\mathbf{F}^o = \mathbf{R}_{FU} \cdot \mathbf{U}^\infty + \mathbf{R}_{FE} : \mathbf{E}^\infty, \quad (4.8)$$

where  $\mathbf{U}^\infty$  is the ambient velocity and  $\mathbf{E}^\infty$  is the rate of strain tensor (Brady and Bossis 1988). For a statistically homogeneous suspension of spherical particles, only the relative positions of the centers of mass are relevant. Thus,  $g \equiv g(\mathbf{r}, t)$  where  $\mathbf{r}$  is the relative separation of the

two spheres, and in relative coordinates one obtains (see Appendix C1)

$$\frac{\partial g}{\partial t} + \nabla_{\mathbf{r}} \cdot (\mathbf{V}^{(0)} g) + St \nabla_{\mathbf{r}} \cdot (\mathbf{V}^{(1)} g) = 0, \quad (4.9)$$

where

$$\begin{aligned} \mathbf{V}^{(0)} = & (\mathbf{U}_2^\infty - \mathbf{U}_1^\infty) - 2(\mathbf{M}_{UF}^{11} - \mathbf{M}_{UF}^{12}) \cdot (\mathbf{R}_{FE}^{11} + \mathbf{R}_{FE}^{12}) : \mathbf{E}^\infty \\ & - 2(\mathbf{M}_{UL}^{11} + \mathbf{M}_{UL}^{12}) \cdot (\mathbf{R}_{LE}^{11} + \mathbf{R}_{LE}^{12}) : \mathbf{E}^\infty, \end{aligned} \quad (4.10)$$

$$\begin{aligned} \mathbf{V}^{(1)} = & -(\mathbf{M}_{UF}^{11} - \mathbf{M}_{UF}^{12}) \cdot \{\mathbf{V}^{(0)} \cdot \nabla_{\mathbf{r}} \mathbf{V}^{(0)}\} + \frac{2}{5}(\mathbf{M}_{UL}^{11} + \mathbf{M}_{UL}^{12}) \cdot \{\mathbf{V}^{(0)} \cdot \nabla_{\mathbf{r}} [(2(\mathbf{M}_{\Omega F}^{11} - \mathbf{M}_{\Omega F}^{12}) \cdot \\ & (\mathbf{R}_{FE}^{11} + \mathbf{R}_{FE}^{12}) : \mathbf{E}^\infty + 2(\mathbf{M}_{\Omega L}^{11} + \mathbf{M}_{\Omega L}^{12}) \cdot (\mathbf{R}_{LE}^{11} + \mathbf{R}_{LE}^{12}) : \mathbf{E}^\infty]\}. \end{aligned} \quad (4.11)$$

The  $O(St)$  inertial correction  $\mathbf{V}^{(1)}$  contains the familiar  $\mathbf{V} \cdot \nabla_{\mathbf{x}} \mathbf{V}$  term symptomatic of translational inertia. The second term in  $\mathbf{V}^{(1)}$  of the form  $\mathbf{V} \cdot \nabla_{\mathbf{x}} \boldsymbol{\Omega}$  arises due to the coupling of the translational and rotational degrees of freedom in presence of hydrodynamic interactions.

From (4.9) the equations for the relative particle trajectories, to  $O(St)$ , are given by

$$\frac{d\mathbf{r}}{dt} = \mathbf{V}^{(0)}(\mathbf{r}) + St \mathbf{V}^{(1)}(\mathbf{r}). \quad (4.12)$$

The velocity field on the right hand side of (4.12) is a known function of  $\mathbf{r}$ , and a particle at  $\mathbf{r}$  can only move with this velocity. Therefore the particle momenta are no longer allowed to vary in an independent manner. One may imagine endowing the system of non-Brownian particles with an arbitrary set of initial velocities. Upon allowing the system to evolve, the particles rapidly relax in a time of  $O(\bar{\tau}_p)$  ( $\bar{\tau}_p$  is the inertial relaxation time of an individual particle in the suspension; see Chapter 3) to the value given by the field  $\mathbf{V}^{(0)} + St \mathbf{V}^{(1)}$  at their current locations; for all later times, the trajectories for pair-interactions are accurately described to

$O(St)$  by (4.12). The above argument is, however, not restricted to dilute suspensions. The Smoluchowski equation given by (4.7) is valid for a suspension of arbitrary concentration provided the hydrodynamic resistance tensors are modified accordingly, and the variable  $\mathbf{x}$  is extended to include all configurational degrees of freedom. In this case, the inertial velocity field,  $(\mathbf{R}_{FU}^{-1} \cdot \mathbf{F}^o) - St(\mathbf{R}_{FU}^{-1} \cdot \mathbf{F}^o) \cdot \nabla_{\mathbf{x}}(\mathbf{R}_{FU}^{-1} \cdot \mathbf{F}^o) \cdot \mathbf{m}$ , will again describe the configurational dynamics after a time of  $O(\bar{\tau}_p)$ . As was seen in Chapter 3,  $\bar{\tau}_p$  is a decreasing function of the volume fraction. The lack of validity during an initial interval of  $O(\bar{\tau}_p)$  is not a limitation, since one is interested in configurational changes on the time scale of  $O(\dot{\gamma}^{-1}) (\gg \bar{\tau}_p)$ .

For the case of non-Brownian particles, the asymptotic equations for the relative particle trajectories (4.12) can also be obtained starting from the equations of relative motion, which from the linearity of the Stokes equations, can be written in the following form:

$$St \mathbf{m} \cdot \frac{d\mathbf{V}}{dt} = -\mathbf{R}_{FU} \cdot (\mathbf{V} - \mathbf{V}^\infty) + \mathbf{R}_{FE} : \mathbf{E}^\infty, \quad (4.13)$$

where  $\mathbf{V} = (\mathbf{U}_2 - \mathbf{U}_1, \boldsymbol{\Omega}_1 + \boldsymbol{\Omega}_2)$  and  $\mathbf{m} = \begin{pmatrix} \mathbf{I} & 0 \\ 0 & \frac{2}{5}\mathbf{I} \end{pmatrix}$  for solid spheres;  $\mathbf{R}_{FU}$  and  $\mathbf{R}_{FE}$  now denote appropriate combinations of resistance elements that influence relative motion. One recognizes that the acceleration on the left hand side involves the Lagrangian derivative of the particle velocity; since  $\mathbf{V}(t) \equiv \mathbf{V}(\mathbf{r}(t))$ , one can rewrite (4.13) as

$$\begin{aligned} St \mathbf{m} \cdot [\mathbf{V} \cdot \nabla_{\mathbf{r}} \mathbf{V}] &= -\mathbf{R}_{FU} \cdot [\mathbf{V} - (\mathbf{V}^\infty + \mathbf{R}_{FU}^{-1} \cdot \mathbf{R}_{FE} : \mathbf{E}^\infty)], \\ \Rightarrow St \mathbf{m} \cdot [\mathbf{V} \cdot \nabla_{\mathbf{r}} \mathbf{V}] &= -\mathbf{R}_{FU} \cdot (\mathbf{V} - \mathbf{R}_{FU}^{-1} \cdot \mathbf{F}^o). \end{aligned} \quad (4.14)$$

Equation (4.14) is still the exact equation of relative motion. However, in expanding the relative velocity  $\mathbf{V}$  as  $\mathbf{V}_0 + St \mathbf{V}_1 + \dots$  for small  $St$ , one eliminates the need for an initial condition, thereby restricting the validity of the resulting solution to times much greater than

$O(\bar{\tau}_p)$ ; one obtains

$$O(1) : \quad -\mathbf{R}_{FU} \cdot (\mathbf{V}^{(0)} - \mathbf{R}_{FU}^{-1} \cdot \mathbf{F}^o) = 0, \quad (4.15)$$

$$O(St^i) : \quad \mathbf{m} \cdot \sum_{k=0}^{i-1} \mathbf{V}^{(k)} \cdot \nabla_{\mathbf{r}} \mathbf{V}^{(i-k-1)} = -\mathbf{R}_{FU} \cdot \mathbf{V}^{(i)} \quad (i \geq 1). \quad (4.16)$$

Solving successively,

$$\mathbf{V}^{(0)} = \mathbf{R}_{FU}^{-1} \cdot \mathbf{F}^o,$$

$$\mathbf{V}^{(1)} = (\mathbf{R}_{FU}^{-1} \cdot \mathbf{F}^o) \cdot \nabla_{\mathbf{r}} (\mathbf{R}_{FU}^{-1} \cdot \mathbf{F}^o) \cdot \mathbf{m},$$

$$\begin{aligned} \mathbf{V}^{(2)} = & (\mathbf{R}_{FU}^{-1} \cdot \mathbf{F}^o) \cdot \nabla_{\mathbf{r}} [(\mathbf{R}_{FU}^{-1} \cdot \mathbf{F}^o) \cdot \nabla_{\mathbf{r}} (\mathbf{R}_{FU}^{-1} \cdot \mathbf{F}^o) \cdot \mathbf{m}] \\ & + [(\mathbf{R}_{FU}^{-1} \cdot \mathbf{F}^o) \cdot \nabla_{\mathbf{r}} (\mathbf{R}_{FU}^{-1} \cdot \mathbf{F}^o) \cdot \mathbf{m}] \cdot \nabla_{\mathbf{r}} (\mathbf{R}_{FU}^{-1} \cdot \mathbf{F}^o), \end{aligned}$$

and so forth. The velocity fields  $\mathbf{V}^{(0)}$  and  $\mathbf{V}^{(1)}$  can be verified as being identical to (4.10) and (4.11).

### 4.3 Nature of inertial velocity corrections for small Stokes numbers

In this section we compare the relative magnitudes of the velocities  $\mathbf{V}^{(0)}$  and  $St \mathbf{V}^{(1)}$  as functions of  $\mathbf{r}$  in order to ascertain if there exist regions of non-uniformity where the perturbation may be singular, knowledge of which would then help solve (4.12) for the particle trajectories.

Using explicit expressions for the resistance and mobility tensors (Kim & Karrila 1991) in (4.10),  $\mathbf{V}^{(0)}$  is found to be

$$V_i^{(0)} = \Gamma_{ij}^\infty r_j - \left[ A \frac{r_i r_j}{r^2} + B \left( \delta_{ij} - \frac{r_i r_j}{r^2} \right) \right] E_{jk}^\infty r_k, \quad (4.17)$$

where  $A$  and  $B$  are functions of the scalar separation  $r$ . For  $St \ll 1$ , the inertial velocity  $St \mathbf{V}^{(1)}$  remains asymptotically small for large  $r$  because  $\mathbf{V}_{(r \gg 1)}^{(1)} \approx \mathbf{V}^{(0)} \cdot \nabla_{\mathbf{r}} \mathbf{V}^{(0)} \approx (\mathbf{\Gamma}^\infty \cdot \mathbf{\Gamma}^\infty) \mathbf{r}$ , and therefore grows in the same manner as the leading order velocity. In fact, the inertial corrections at all higher orders are at most of  $O(r)$  for  $r \gg 1$  (in particular,  $\mathbf{V}^{(i)} \propto (\mathbf{\Gamma}^\infty)^i \cdot \mathbf{r}$ ). For shear flow,  $(\mathbf{\Gamma}^\infty)^i = 0$  ( $i \geq 2$ ), and the inertial corrections therefore decay for large  $r$ <sup>1</sup>.

For very small separations, the radial component of  $\mathbf{V}^{(0)}$  behaves as

$$\begin{aligned} \lim_{r \rightarrow 2} V_r^{(0)} &= \lim_{r \rightarrow 2} (1 - A) E_{ij}^\infty \frac{r_i r_j}{r}, \\ &= 4.077(r - 2)(2E_{ij}^\infty n_i n_j), \end{aligned}$$

where we have used the near-field behavior of  $A$ , and  $\mathbf{n}$  is the unit normal directed along the line of centers. Thus, the radial component of  $\mathbf{V}^{(0)}$  goes to zero linearly with decreasing inter-particle separation, and the no-flux boundary condition at particle-particle contact,  $g(\mathbf{V} \cdot \mathbf{n}) = 0$ , is automatically satisfied to leading order. The tangential components of  $\mathbf{V}^{(0)}$ , however, remain finite at contact.

The radial component of  $\mathbf{V}^{(1)}$ , similar to that of  $\mathbf{V}^{(0)}$ , vanishes in a linear manner for small separations. Although not readily apparent, the radial components of the inertial corrections at all higher orders also exhibit the same near-field behavior (see below). This precludes the possibility of a radial boundary layer at contact or at infinity. However, there are points of symmetry in the leading order flow where  $V_r^{(0)}$  is identically zero, which give rise to angular boundary layers since the  $O(St)$  correction has a non-zero radial component at these locations. For instance, the fore-aft symmetric trajectory space for shear flow gives rise to singular points at 90 and 270 deg (the flow direction corresponds to 0 deg) in a plane perpendicular to the vorticity direction. In planar extension the singular layers are along a

<sup>1</sup>Here,  $(\mathbf{\Gamma}^\infty)^i = \mathbf{\Gamma}^\infty \cdot \mathbf{\Gamma}^\infty \dots \mathbf{\Gamma}^\infty$   $i$  times.

pair of orthogonal axes rotated 45 deg. with respect to the extensional and compressional axes. The perturbation analyses for finite  $St$  shear flow trajectories in sections 4.4 and 5.3 (Chapter 5) take this into account.

We now consider a simplified form of the equation for the relative motion of a pair of particles in a linear flow field in order to examine the near-field behavior of the relative velocity for arbitrary  $St$ , and thereby verify the aforementioned near-field form of the inertial corrections. The equation for the relative translational velocity is given by

$$St \frac{d\mathbf{V}}{dt} = -(\mathbf{R}_{FU}^{11} - \mathbf{R}_{FU}^{12}) \cdot (\mathbf{V} - \mathbf{U}^\infty) + (\mathbf{R}_{F\Omega}^{11} + \mathbf{R}_{F\Omega}^{12}) \cdot (\boldsymbol{\Omega}_1 + \boldsymbol{\Omega}_2 - 2\boldsymbol{\Omega}^\infty) - 2(\mathbf{R}_{FE}^{11} + \mathbf{R}_{FE}^{12}) : \mathbf{E}^\infty, \quad (4.18)$$

where  $\mathbf{V} = (\mathbf{U}_2 - \mathbf{U}_1)$ , and we have written the translational and rotational contributions on the right-hand side separately. Taking the radial component of the above equation (which eliminates the rotational part), and using the expressions for the resistance tensors (Kim & Karrila 1991), we obtain

$$St \frac{dV_i}{dt} n_i = -X^A V_r + \left( rX^A - \frac{4}{3}X^G \right) E_{rr}, \quad (4.19)$$

where  $X^A = X_{11}^A - X_{12}^A$  and  $X^G = X_{11}^G - X_{12}^G$ . For small separations, the above equation takes the form

$$St \frac{dV_i}{dt} n_i = -\frac{V_r}{r-2} + \lim_{r \rightarrow 2} \left( 2X^A - \frac{4}{3}X^G \right) E_{rr}. \quad (4.20)$$

The singular terms in  $X^A$  and  $X^G$  cancel out and therefore  $(2X^A - \frac{4}{3}X^G)$  remains  $O(1)$  near contact. The solution of the above equation is impeded by the fact that  $d/dt(V_i n_i) \neq (dV_i/dt)n_i$ ; the curvature of the particle pathlines results in inertial forces proportional to  $dn_i/dt$ . However, one can retain the essential character of the above problem by considering

a simplified form of (4.20) in one dimension, thereby eliminating the effects of curvature. The simplified equation contains the balance of a constant force  $((2X^A - \frac{4}{3}X^G)_{r=2}E_{rr})$  and a singular drag term  $(X_{r \rightarrow 2}^A V_r)$ . Thus,

$$St_1 \frac{du}{dt} = 1 - \frac{u}{L-x},$$

$$u = u_0 \text{ at } t = 0,$$

$$x = 0 \text{ at } t = 0,$$

where the constant force is scaled to unity,  $L$  is chosen as the location of the singularity, and we have used  $St_1$  to denote the magnitude of the acceleration term and to differentiate it from the Stokes number ( $St$ ) defined elsewhere. Rewriting  $(du/dt)$  as  $(u du/dx)$  and using  $y = L - x$ ,  $\hat{u} = dy/dt$ , one obtains

$$\begin{aligned} St_1 \hat{u} \frac{d\hat{u}}{dy} &= -1 - \frac{\hat{u}}{y}, \\ \Rightarrow St_1 \frac{d\hat{u}}{dy} &= -\left(\frac{1}{y} + \frac{1}{\hat{u}}\right), \end{aligned} \tag{4.21}$$

with the initial condition  $\hat{u} = -u_0$  at  $y = L$ . We note that the solution for  $St_1 = 0$  is simply  $u = y$ . Insight can be gained into the solution for arbitrary  $St_1$  by considering the following two limiting cases:

Case 1: If  $u_0 \gg y_0$ , which corresponds to an initially highly energetic particle, then the leading order balance for short times is

$$St_1 \frac{d\hat{u}}{dy} = -\frac{1}{y},$$

giving

$$\hat{u} = -u_0 + \frac{1}{St_1} \ln\left(\frac{y_0}{y}\right). \quad (4.22)$$

Case 2: If  $u_0 \ll y_0$ , which corresponds to an initially slowly moving particle, then the leading order balance for short times is

$$St_1 \frac{d\hat{u}}{dy} = -\frac{1}{\hat{u}},$$

and the corresponding short time behavior is

$$\hat{u} = u_0^2 + \frac{2}{St_1}(y_0 - y). \quad (4.23)$$

Figs 4.1 and 4.2 show plots of  $|\hat{u}|$  versus  $y$  for the two limiting initial conditions considered above for various values of  $St_1$ . In Fig 4.1, where  $u_0 \gg y_0$ , the velocity for small times decreases logarithmically and is well described by equation (4.22). This solution is, however, not valid for all separations since it predicts a finite separation at which the relative velocity goes to zero. At smaller separations, there is a rapid transition from the steep logarithmic decline to a gradual linear variation, corresponding to the rapidly diminishing magnitude of the acceleration term. This transition becomes increasingly abrupt for large  $St_1$ , and shifts to smaller separations with increasing  $St_1$ . For the case where  $u_0 \ll y_0$ , Fig 4.2 shows that the velocity increases for small times in accordance with equation (4.23), and does so till a point where  $|\hat{u}| \gg y$ ; the dynamics thereafter follow the previous case.

We therefore see that for small enough separations, the approach velocity always decreases linearly with separation. The point of transition to this asymptotic regime is a

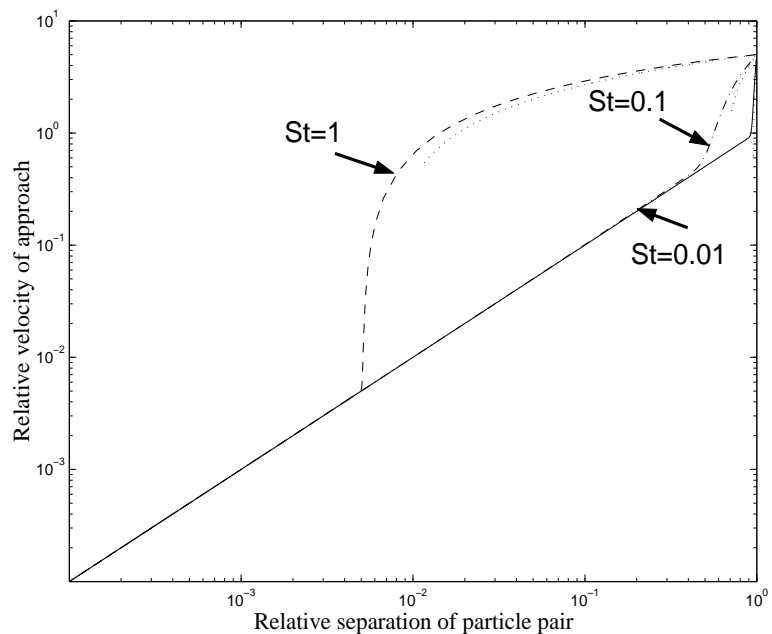


Figure 4.1: Comparison of the theoretical approximation (4.22) (represented by dotted lines in all three cases) and the exact numerical solution for the initial condition  $u_0 = 5, y_0 = 1$ , for three different Stokes numbers. The dashed line denotes the numerical solution for  $St_1 = 1$ , the dash-dot line for  $St_1 = 0.1$ , and the solid line for  $St_1 = 0.01$ .

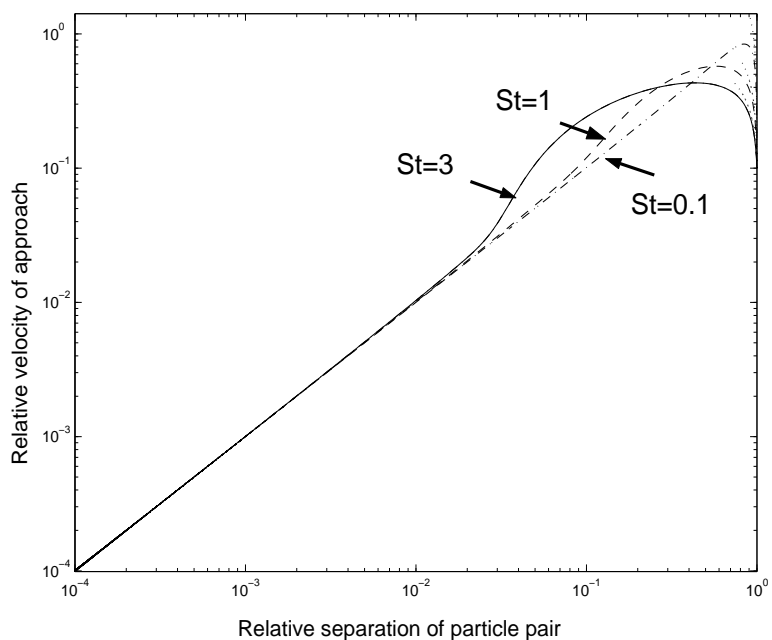


Figure 4.2: Comparison of the theoretical approximation (4.23) (represented by dotted lines in all three cases) and the exact numerical solution for the initial condition  $u_0 = 0.1, y_0 = 1$ , for three different Stokes numbers. The solid line denotes the numerical solution for  $St_1 = 3$ , the dashed line for  $St_1 = 1$ , and the dash-dot line for  $St_1 = 0.1$ .

strong function of Stokes number, however<sup>2</sup>. This explains the identical near-field behavior of the inertial corrections  $\mathbf{V}^{(i)}$  ( $i \geq 1$ ) at all orders. The asymptotic linear variation also implies that two particles do not come into contact in a finite time. Indeed, it has already been pointed out by Sundararajakumar & Koch (1996) that interparticle contact, and hence solid-body collisions, need to be taken into account only for  $St > O(1)$  when the gap thickness reduces to levels where the continuum approximation breaks down. For  $St \ll 1$ , lubrication forces still dominate the near-field behavior and the situation is identical to that for inertialess particles.

#### 4.4 Relative in-plane trajectories of two spheres in simple shear flow

Batchelor & Green (1972a) derived equations for the zero-Stokes particle pathlines in simple shear flow; each relative trajectory was described by the functions  $\phi(r)$  and  $\theta(r)$ , where  $(r, \theta, \phi)$  are the spherical polar coordinates with the origin at the centre of one sphere. Here,  $\theta = 0$  ( $x$  axis) corresponds to the direction of the ambient vorticity, and therefore  $\theta = \pi/2$  represents the plane of shear. We formulate equations (4.12) for the  $O(St)$  corrected particle trajectories in spherical coordinates thereby exploiting the availability of an explicit leading order solution. The velocity gradient tensor for shear flow is

$$\dot{\mathbf{\Gamma}} = \begin{bmatrix} 0 & 0 & 0 \\ 0 & 0 & 1 \\ 0 & 0 & 0 \end{bmatrix}, \quad (4.24)$$

---

<sup>2</sup>This can be seen from equation (4.22) by looking at the fictitious separation corresponding to a zero approach velocity, which has an exponential dependence on  $St_1$ .

so that the  $yz$  plane is the plane of shear with  $y$  being the direction of flow (see Fig 4.3). In the spherical coordinate system, we have

$$\begin{aligned}\dot{\Gamma}_{rr} &= \sin^2 \theta \sin \phi \cos \phi, & \dot{\Gamma}_{\theta\theta} &= \cos^2 \theta \sin \phi \cos \phi, \\ \dot{\Gamma}_{\phi\phi} &= -\sin \phi \cos \phi, & \dot{\Gamma}_{r\theta} &= \dot{\Gamma}_{\theta r} = \sin \theta \cos \theta \sin \phi \cos \phi, \\ \dot{\Gamma}_{r\phi} &= \sin \theta \cos^2 \phi, & \dot{\Gamma}_{\phi r} &= -\sin \theta \sin^2 \phi, \\ \dot{\Gamma}_{\theta\phi} &= \cos \theta \cos^2 \phi, & \dot{\Gamma}_{\phi\theta} &= -\cos \theta \sin^2 \phi.\end{aligned}$$

Taking the ratio of the in-plane radial ( $V_r = \frac{dr}{dt}$ ) and tangential velocities ( $V_\phi = r \frac{d\phi}{dt}$ ), we obtain the equation, correct to  $O(St)$ , governing the relative trajectories of the two spheres in the shearing plane (from here on termed as the in-plane trajectories):

$$\frac{d\phi}{dr} = \frac{-\{\sin^2 \phi + (B/2)(\cos^2 \phi - \sin^2 \phi)\} + St f_1(r, \phi)}{r(1-A) \sin \phi \cos \phi + St f_2(r, \phi)}, \quad (4.25)$$

where

$$\begin{aligned}f_1(r, \phi) &= -H \sin \phi \cos \phi \left[ \left\{ 2B(A-B) - r(1-A) \frac{dB}{dr} \right\} \frac{(\cos^2 \phi - \sin^2 \phi)}{2} + 2(A-B) \sin^2 \phi \right] \\ &\quad - \frac{6E}{5r} \sin \phi \cos \phi \left[ \frac{(\cos^2 \phi - \sin^2 \phi)}{2} \left\{ r(1-A) \frac{dC}{dr} + 2C(B-1) \right\} + C \right],\end{aligned}$$

and

$$f_2(r, \phi) = -rG \left[ \sin^2 \phi \cos^2 \phi \left\{ (A-B)^2 - r(1-A) \frac{dA}{dr} \right\} + \frac{(B-2A)}{2} \sin^2 \phi - \frac{B}{2} \cos^2 \phi - \frac{B(B-2A)}{4} \right].$$

Here,  $(r f_1)$  and  $f_2$  respectively denote the  $O(St)$  inertial corrections to the in-plane tangential and radial velocities. The functions  $A$  and  $B$ , as seen before, characterize the relative trans-

lational velocity of the spheres, while  $C$  denotes the angular velocity correction on account of hydrodynamic interactions; the function  $E$  represents the translation-rotation coupling. Explicit expressions for  $A$ ,  $B$ ,  $C$ ,  $G$ ,  $H$  and  $E$  can be obtained from Kim and Karrila (1991).

Although we have retained the  $O(St)$  denominator term on the right hand side in (4.25), the resulting solution is meaningful only to  $O(St)$ . We first note that (4.25) with only the leading order terms remains unchanged on replacing  $\phi$  by  $\pi \pm \phi$ , which is indicative of the fore-aft symmetry of the zero-Stokes trajectory space. With the  $O(St)$  terms included, (4.25) remains unchanged only on replacing  $\phi$  by  $\pi + \phi$ , which follows from the antisymmetry of simple shear flow. It was seen in section 4.3 that there is no non-uniformity in the small  $St$  expansion with respect to  $r$ , but that there is a non-uniformity in  $\phi$ . At  $\phi = \pi/2$  the  $O(1)$  term in the denominator equals zero since the zero-Stokes trajectory is purely tangential at this point<sup>3</sup>. On the other hand,  $f_2(r, \pi/2) \neq 0$  due to the radial velocity induced at  $O(St)$  which destroys the fore-aft symmetry. This can also be understood by noting that with  $f_1$  and  $f_2$  included, (4.25) is no longer invariant to reflection across the gradient( $z$ ) axis ( $\phi \leftrightarrow \pi - \phi$ ). Therefore, the perturbation is singular in nature necessitating care in the analysis when  $\phi$  is close to  $\pi/2$ .

The analysis in the following sections will yield a picture of the entire ( $r$ - $\phi$ ) phase plane. In what follows it will be necessary to treat  $\phi$  as the dependent variable and not  $r$ , since the solution of the trajectory equation at the zeroth order yields  $\phi$  as an explicit function of  $r$  and not the other way around (Batchelor & Green 1972a). Also, since (4.25) is a first order differential equation, we need only one boundary condition. The zero-Stokes trajectories may be characterised by prescribing their offset ( $z^{-\infty}$ ) far upstream or downstream (the ‘outer’ layers), or their offset at  $\phi = \pi/2$  (the ‘inner’ layer). Depending on where this boundary

---

<sup>3</sup>The same happens at  $\phi = 3\pi/2$ . However, owing to the antisymmetry of simple shear, it suffices to consider only the upper half of the phase plane ( $0 \leq \phi \leq \pi$ ).

condition is imposed, the solutions in the particular layer are determined to all orders in  $St$ . These solutions will then determine the solutions in the other layers by matching. We shall impose the boundary condition at  $\phi = \pi, r \rightarrow \infty$ , so that both the actual and zero-Stokes trajectories start from the same upstream offset. Therefore, the solution in the outer layer denoted O1 below (see section 4.4.1) is determined to all orders independent of the other layers (see Fig 4.3).

Before going into the details of the analysis, we give a physical motivation of the results to come. At zero Stokes number, the shearing plane comprises two classes of relative trajectories:

1. ‘Open’ trajectories which start from a finite upstream offset and tend to an identical downstream offset as  $t \rightarrow \infty$ , consistent with the fore-aft symmetry.
2. ‘Closed’ trajectories which represent bound orbits of the two spheres.

The limiting zero-Stokes open trajectory, or the separatrix, separates these two classes and tends to a zero offset both upstream and downstream, i.e.,  $z^{\pm\infty} \rightarrow 0$  as  $y \rightarrow \pm\infty$  (see Fig 4.17).

The effect of inertia in the particle equation of motion (4.14) is represented by  $St(\mathbf{V} \cdot \nabla_{\mathbf{r}} \mathbf{V})$ . Inertial modifications of the zero-Stokes phase plane may be understood by considering this term with  $\mathbf{V}$  now taken to be the velocity along a zero-Stokes trajectory<sup>4</sup>. The term  $\mathbf{V} \cdot \nabla_{\mathbf{r}} \mathbf{V}$  is related to the change in the velocity vector along the zero-Stokes path-line, and therefore to its curvature. From Fig 4.3, it is evident that any open zero-Stokes trajectory in the plane of shear has a pair of inflection points that serve to separate regions of positive curvature (concave upward with respect to the  $y$  axis) lying outside from the re-

---

<sup>4</sup>There is also an inertial term of the form  $(\mathbf{V} \cdot \nabla_{\mathbf{r}} \boldsymbol{\Omega})$  associated with the translation-rotation coupling that arises in presence of hydrodynamic interactions. This effect is relatively small, however, and is restricted to a quantitative modification of the phase plane (see section 4.4.2).

gion of negative curvature (concave downward) in between. Starting from far upstream, a particle with finite inertia is unable to faithfully follow the (upwardly) concave portion of the zero-Stokes trajectory, and thus comes in closer than a similar inertialess particle. The intermediate region of negative curvature then pushes the particle outward causing it to cross the  $z$ -axis ( $\phi = \pi/2$ ) with a positive radial velocity ( $= St f_2(c, \frac{\pi}{2})$ ); the region of positive curvature in the downstream portion of the trajectory again pushes the particle down leading to a net displacement in the velocity gradient direction that is negative (for  $z$  positive). The magnitude of this displacement evidently depends on the inertia of the particle, and is found to be  $O(St)$  for open trajectories with  $O(1)$  initial offsets (see (4.45)). Decreasing the upstream offset, one expects the gradient displacement to become increasingly negative. For small enough offsets, the finite  $St$  trajectory passes very close to the reference sphere in the region where it is concave downward, and lubrication forces reduce the effective inertia of the particle, in turn suppressing its outward radial motion in this region. At the same time, the regions of positive curvature are enhanced since the trajectory has to now pass around the surface of the reference sphere excluded volume. As will be seen in section 4.4.3, this leads to a continuous increase in the gradient displacement from being  $O(St)$  for far-field open trajectories to becoming  $O(St^{\frac{1}{2}})$  for open trajectories with  $O(St^{\frac{1}{2}})$  initial offsets (see (4.54)). Thus, the effect of inertia is to destroy the fore-aft symmetry of the zero-Stokes open trajectories in the shearing plane by inducing a non-zero gradient displacement.

In contrast to the fore-aft symmetry of the zero-Stokes separatrix, the limiting finite  $St$  trajectory (for  $z$  positive) starts from an offset of  $O(St^{\frac{1}{2}})$  at  $y = -\infty$ , and tends to a zero offset as  $y \rightarrow \infty$ . Trajectories with initial offsets less than this critical value spiral onto a stable limit cycle, the location of which is predicted to be independent of  $St$ . Trajectories starting from points asymptotically close to the surface of the reference sphere spiral out onto

this limit cycle. The limit cycle is responsible for the indeterminacy of the finite  $St$  rheological problem for pair-wise interactions, and necessitates the inclusion of other non-hydrodynamic mechanisms or three-particle interactions to obtain a definite pair-distribution function.

The asymmetry of the open trajectories leads to a shear-induced diffusivity whose gradient component scales as  $St^2 \ln St$  (see (4.62)). The enhancement by a factor of  $\ln St$  over what one would naively expect from an  $O(St)$  asymmetry is related to the increased magnitude of the gradient displacement for open trajectories with  $O(St^{\frac{1}{2}})$  offsets. It would be very difficult to detect this region of  $O(St^{\frac{1}{2}})$  and the resulting enhancement of the diffusivity from a numerical integration of the trajectory equations alone, especially taking into account the latter's logarithmic character. Thus, our analysis provides a reliable and necessary guide for trajectory calculations.

In section 4.4.1 we formulate the perturbation scheme and apply it to open trajectories with offsets greater than  $O(St^{\frac{1}{2}})$  in order to determine the in-plane gradient displacements, which then serve to characterize the finite  $St$  asymmetry of the trajectory plane. Section 4.4.2 contains a qualitative explanation of the effect that the translation-rotation coupling has on the in-plane gradient displacement. In section 4.4.3 an expression for the critical offset of the limiting trajectory is derived and compared with numerical results. Sections 4.4.4 and 4.4.5 are devoted to the evaluation of the far-field in-plane gradient displacement and the in-plane value of the gradient diffusivity, respectively. Finally in section 4.4.6, we consider the location of the stable limit cycle and its domain of attraction in the shearing plane.

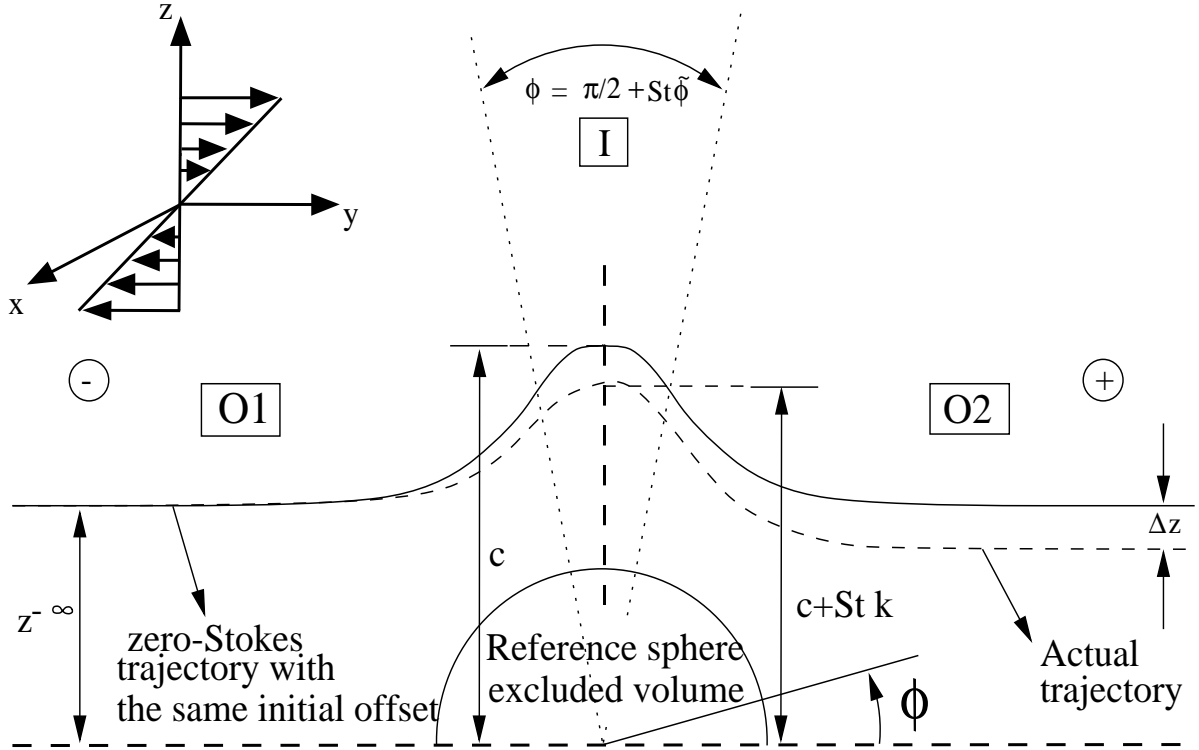


Figure 4.3: Finite  $St$  open trajectory with  $O(1)$  initial offset.

#### 4.4.1 Open trajectories with initial offsets much greater than $O(St^{\frac{1}{2}})$

In this section we develop a perturbation method for finite  $St$  open trajectories with  $O(1)$  offsets (see Fig 4.3). It will be seen later that the method remains valid for trajectories with initial offsets greater than  $O(St^{\frac{1}{2}})$ .

##### 4.4.1.1 Outer layer O1

In this layer we perform a regular perturbation expansion in the form of a power series in  $St$  as

$$\phi = \phi_0 + St \phi_1 + \dots \quad (4.26)$$

Substituting this in equation (4.25), we obtain

$$O(1) : \frac{d\phi_0}{dr} = - \frac{\sin^2 \phi_0 + \frac{B}{2} (\cos^2 \phi_0 - \sin^2 \phi_0)}{r(1-A) \sin \phi_0 \cos \phi_0}, \quad (4.27)$$

$$O(St) : \frac{d\phi_1}{dr} = \frac{\frac{B}{2} - \sin^2 \phi_0}{r \sin^2 \phi_0 \cos^2 \phi_0 (1-A)} \phi_1 + \frac{f_1(r, \phi_0)}{r(1-A) \sin \phi_0 \cos \phi_0} + \frac{\{(1-B) \sin^2 \phi_0 + \frac{B}{2}\} f_2(r, \phi_0)}{r^2(1-A)^2 \sin^2 \phi_0 \cos^2 \phi_0}. \quad (4.28)$$

The boundary condition can be written as

$$r \sin \phi \rightarrow z^{-\infty} \quad \text{as } y \rightarrow -\infty,$$

which ensures that the zero and finite  $St$  trajectories start from the same upstream offset.

At successive orders in  $St$ , one obtains

$$O(1) : r \sin \phi_0 \rightarrow z^{-\infty} \quad \text{as } r \rightarrow \infty,$$

$$O(St) : r \phi_1^- \rightarrow 0 \quad \text{as } \phi_0 \rightarrow \pi (r \rightarrow \infty),$$

where the branch of  $\phi_1$  in the interval  $\phi_0 \in (\pi/2, \pi)$  is denoted by the superscript ‘-’; the corresponding branch in  $\phi_0 \in (0, \pi/2)$  will be denoted by ‘+’. As alluded to in the introduction, the asymmetry of the finite  $St$  open trajectories will be characterised by their net displacements in the gradient and vorticity directions. Symmetry requirements clearly imply that finite  $St$  trajectories starting in the shearing plane remain in it for all time. Thus the vorticity displacement for these cases is evidently zero, and the lateral displacement  $(\Delta z)_{inplane}$  in the

velocity gradient direction is given as

$$\begin{aligned}
(\Delta z)_{inplane} &= r \sin \phi \Big|_{y=-\infty}^{y=+\infty}, \\
&= r \sin(\phi_0 + St \phi_1) \Big|_{y=-\infty}^{y=+\infty}, \\
&= St \{ (r \phi_1 \cos \phi_0)_{\phi_0 \rightarrow 0, r \rightarrow \infty} - (r \phi_1 \cos \phi_0)_{\phi_0 \rightarrow \pi, r \rightarrow \infty} \}, \\
&= St \lim_{r \rightarrow \infty} r \phi_1^+.
\end{aligned} \tag{4.29}$$

Using the boundary condition at  $O(1)$ , the zeroeth order solution is written as (Batchelor and Green 1972a)

$$r^2 \sin^2 \phi_0 = (z^{-\infty})^2 \exp \left[ - \int_r^\infty q(r') dr' \right] + \int_r^\infty \exp \left[ - \int_{r'}^r q(r'') dr'' \right] \frac{B'r'}{(1-A')} dr', \tag{4.30}$$

where

$$q(r) = \frac{2(A-B)}{(1-A)r},$$

and the ‘ $'$ ’ in  $A, B$ , etc. implies evaluation at  $r'$ .

In accordance with (4.29) for the lateral displacement, we formulate the  $O(St)$  equation in terms of  $r\phi_1$  as the dependent variable to obtain

$$\begin{aligned}
O(St) : \frac{d}{dr}(r\phi_1) + \left\{ \frac{\sin^2 \phi_0 - \frac{B}{2}}{r \sin^2 \phi_0 \cos^2 \phi_0 (1-A)} - \frac{1}{r} \right\} r\phi_1 &= \frac{f_1(r, \phi_0)}{(1-A) \sin \phi_0 \cos \phi_0} \\
&+ \frac{\{(1-B) \sin^2 \phi_0 + \frac{B}{2}\} f_2(r, \phi_0)}{r(1-A)^2 \sin^2 \phi_0 \cos^2 \phi_0},
\end{aligned} \tag{4.31}$$

whose general solution is given by

$$\begin{aligned}
r\phi_1 = & I'_{\phi_1} \exp \left[ - \int^r \left\{ \frac{\sin^2 \phi'_0 - \frac{B'}{2}}{r' \sin^2 \phi'_0 \cos^2 \phi'_0 (1 - A')} - \frac{1}{r'} \right\} dr' \right] \\
& + \int^r \exp \left[ - \int_{r'}^r \left\{ \frac{\sin^2 \phi''_0 - \frac{B''}{2}}{r'' \sin^2 \phi''_0 \cos^2 \phi''_0 (1 - A'')} - \frac{1}{r''} \right\} dr'' \right] \left\{ \frac{f_1(r', \phi'_0)}{(1 - A') \sin \phi'_0 \cos \phi'_0} \right. \\
& \left. + \frac{\{(1 - B') \sin^2 \phi'_0 + \frac{B'}{2}\} f_2(r', \phi'_0)}{r'(1 - A')^2 \sin^2 \phi'_0 \cos^2 \phi'_0} \right\} dr',
\end{aligned}$$

where  $I'_{\phi_1}$  is an integration constant. Using the boundary condition at  $O(St)$ , the solution upstream reduces to

$$\begin{aligned}
r\phi_1^- = & - \int_r^\infty \exp \left[ - \int_{r'}^r \left\{ \frac{\sin^2 \phi''_0 - \frac{B''}{2}}{r'' \sin^2 \phi''_0 \cos^2 \phi''_0 (1 - A'')} - \frac{1}{r''} \right\} dr'' \right] \left\{ \frac{f_1(r', \phi'_0)}{(1 - A') \sin \phi'_0 \cos \phi'_0} \right. \\
& \left. + \frac{\{(1 - B') \sin^2 \phi'_0 + \frac{B'}{2}\} f_2(r', \phi'_0)}{r'(1 - A')^2 \sin^2 \phi'_0 \cos^2 \phi'_0} \right\} dr'. \quad (4.32)
\end{aligned}$$

Note that the term involving  $f_2$  contains  $\cos^2 \phi_0$  in the denominator, and is singular as  $\phi_0 \rightarrow \pi/2$  ( $\cos^2 \phi_0 \sim (r - c)$ ). Here,  $c$  is the distance of nearest approach for the zero-Stokes trajectory, i.e., the value of  $r$  at  $\phi_0 = \pi/2$ , and is therefore given by

$$c^2 = (z^{-\infty})^2 \exp \left[ - \int_c^\infty q(r') dr' \right] + \int_c^\infty \exp \left[ - \int_{r'}^c q(r'') dr'' \right] \frac{B'r'}{(1 - A')} dr'. \quad (4.33)$$

This singularity in the integral term is made explicit by first noting that there exists a similar (negative) logarithmic singularity in the integral inside the exponential (which also contains  $\cos^2 \phi_0$  in the denominator of its integrand). This then allows us to simplify (4.32) to yield (see

Appendix C3)

$$r\phi_1^- = -\frac{1}{r \cos \phi_0 \sin \phi_0} \int_r^\infty \exp\left[-\int_{r'}^r q(r'') dr''\right] \left\{ \frac{r' f_1(r', \phi'_0)}{(1-A')} + \frac{\{(1-B') \sin^2 \phi'_0 + \frac{B'}{2}\} f_2(r', \phi'_0)}{(1-A')^2 \sin \phi'_0 \cos \phi'_0} \right\} dr', \quad (4.34)$$

where the singularity in the exponential has now been transferred to the prefactor; the  $\cos \phi_0$  in the denominator of the  $f_2$  term only goes to zero as  $(r-c)^{\frac{1}{2}}$  (as  $r \rightarrow c$ ), and is therefore integrable.

#### 4.4.1.2 Inner layer I

In the inner layer, the radial component of the  $O(St)$  inertial velocity is important at leading order, and we have to accordingly rescale the dependent and independent variables to take this into account. Since  $\phi$  is close to  $\pi/2$ , and hence  $r$  close to  $c$ , we assume rescaled coordinates  $\tilde{\phi}$  and  $\tilde{r}$  of the form

$$\begin{aligned} \phi^I &= \frac{\pi}{2} + St\tilde{\phi}, \\ r &= c + St^2\tilde{r}, \end{aligned}$$

as can be verified for the required leading order balance. In terms of the rescaled coordinates, (4.25), at leading order, becomes

$$\frac{d\tilde{\phi}}{d\tilde{r}} = \frac{(1 - \frac{B_0}{2})}{c(1 - A_0)\tilde{\phi} - f_2(c, \frac{\pi}{2})}, \quad (4.35)$$

where the subscript, '0', used for the hydrodynamic functions here and in all subsequent expressions, denotes the value of the function at  $r = c$  unless stated otherwise. The above

scaling suggests that the radial coordinate of the inertial trajectory differs from that of the zero-Stokes trajectory by  $O(St^2)$  in the inner layer. Since the zero-Stokes trajectory space is fore-aft symmetric, one could equally well have perturbed the given inertial trajectory about a zero-Stokes trajectory with the same downstream offset, and obtained similarly an  $O(St^2)$  difference between their radial coordinates at  $\phi = \pi/2$ . This in turn would imply that the radial coordinates of the two zero-Stokes trajectories differ by  $O(St^2)$ . On the other hand, the limiting offsets of these two trajectories differ by an amount equal to the net lateral displacement of the inertial trajectory which from (4.29) is  $O(St)$ , assuming  $r\phi_1^+$  to be an  $O(1)$  quantity (this being consistent with the domain of validity of the outer expansion). From (4.33), an  $O(St)$  difference in the offsets would lead to an  $O(St)$  difference in the radial coordinates at  $\pi/2$ , which is clearly inconsistent with the scaling found above for the inner layer. The resolution lies in recognizing that though the variation of the radial distance in the inner layer is indeed  $O(St^2)$ , this variation is about a base value which differs from  $c$  by  $O(St)$  (see Fig 4.3). The  $O(St)$  coefficient being a constant, only affects the matching procedure, and the leading order inner equation remains unaltered. Thus, the correct coordinates for the inner layer are

$$\begin{aligned}\phi^I &= \frac{\pi}{2} + St\tilde{\phi}, \\ r &= c + Stk + St^2\tilde{r},\end{aligned}$$

where  $\tilde{\phi}$  still satisfies (4.35).

In deriving (4.35) using the coordinates above, the only assumption that needs to be made is  $Stk, St^2\tilde{r} \ll c$ ; no restriction is placed on the relative magnitudes of  $Stk$  and  $St^2\tilde{r}$ . The constant  $k$  will be found from matching the inner and outer expansions in their

domain of overlap, and will turn out to be negative as it should be since the in-plane inertial trajectory, starting from the same upstream offset, ends up closer to the reference particle at  $\phi = \pi/2$  than the corresponding zero-Stokes trajectory (see Fig 4.3).

Though the above argument does give us *a priori* the correct inner coordinates, even in the absence of this knowledge, one could have gone on with the original rescaled coordinates to find an inconsistency when matching, that would then point to the same resolution. The solution to (4.35) is given by

$$\tilde{\phi}^{\mp} = \frac{G_0(2-B_0)(2A_0-B_0)}{4(1-A_0)} \left[ 1 \pm \left\{ 1 + \frac{16(\tilde{r}-I_i)(1-A_0)}{cG_0^2(2-B_0)(2A_0-B_0)^2} \right\}^{\frac{1}{2}} \right], \quad (4.36)$$

where  $I_i$  is an integration constant, and we have used

$$f_2(c, \frac{\pi}{2}) = \frac{cG_0(2-B_0)(2A_0-B_0)}{4}.$$

The two values of  $\tilde{\phi}$  for each value of  $\tilde{r}$  not being equal in magnitude indicates the  $O(St)$  asymmetry of the inertial trajectory. A qualitative picture of the inner solution can be obtained by setting  $I_i = 0$  in (4.36). It is then seen that the minimum value of  $\tilde{r}$  possible is  $\tilde{r}_{min} = -\frac{cG_0^2(2-B_0)(2A_0-B_0)^2}{16(1-A_0)}$ , where the two branches  $\tilde{\phi}^+$  and  $\tilde{\phi}^-$  coincide, i.e.  $\tilde{\phi}^+ = \tilde{\phi}^- = \tilde{\phi}_{min} = \frac{G_0(2-B_0)(2A_0-B_0)}{4(1-A_0)}$ . The value of  $\tilde{\phi}_{min}$  being positive,  $\phi_0 \in (\pi/2, \pi)$ , and the smallest radial separation occurs in the upstream quadrant. As will be seen,  $I_i$  does not affect the matching to  $O(St)$ .

#### 4.4.1.3 Layer O2

Since the zero-Stokes trajectory is fore-aft symmetric, the leading order solution remains the same. The (simplified) form of the  $O(St)$  solution in this layer is given by

$$r\phi_1^+ = I_{\phi_1}^+ \frac{z^{-\infty}}{r \sin \phi_0 \cos \phi_0} \exp \left[ \int_r^\infty q(r') dr' \right] - \frac{1}{r \cos \phi_0 \sin \phi_0} \int_r^\infty \exp \left[ - \int_{r'}^r q(r'') dr'' \right] \left\{ \frac{r' f_1(r', \phi'_0)}{(1-A')} + \frac{\{(1-B') \sin^2 \phi'_0 + \frac{B'}{2}\} f_2(r', \phi'_0)}{(1-A')^2 \sin \phi'_0 \cos \phi'_0} \right\} dr', \quad (4.37)$$

where  $I_{\phi_1}^+$  is an integration constant which will be determined from matching considerations.

Here, we have used the identity (C.10) with  $r' = \infty$ , i.e.,

$$\exp \left[ \int_r^\infty \left\{ \frac{(1-B'') \sin^2 \phi''_0 - \frac{B''}{2}}{r'' \sin^2 \phi''_0 (1-A'')} - \frac{1}{r''} \right\} dr'' \right] = \frac{z^\infty}{r \sin \phi_0} \exp \left[ \int_r^\infty q(r'') dr'' \right],$$

since  $\lim_{r' \rightarrow \infty} r' \sin \phi'_0 = z^\infty$ .

#### 4.4.1.4 Asymptotic Matching

We can formally carry out the matching by taking the inner limit of the outer expansion and vice versa. In this case, however, it is more instructive to perform the matching via the ‘intermediate matching principle’ (Kevorkian & Cole 1996, Van Dyke 1975) which then indicates the domain of overlap between the outer and inner expansions. Taking the intermediate dependent variable to be of the general form  $\phi = \pi/2 + St^\alpha \hat{\phi}$ , the corresponding form for the independent variable is obtained from (4.25) as  $r = c + St^{2\alpha} \hat{r}$ . To begin with,  $\alpha$  is assumed to be greater than zero; this estimate will be refined during the course of matching. We now rewrite the outer and inner solutions, to  $O(St)$ , in terms of the intermediate variables. For

the solutions in layer O1,

$$\begin{aligned}
\lim_{r \rightarrow c+St^{2\alpha}\hat{r}} \phi_0 &= \frac{\pi}{2} + (St)^\alpha \left\{ \frac{(2-B_0)\hat{r}}{(1-A_0)c} \right\}^{\frac{1}{2}} + O(St^{3\alpha}), \\
\lim_{r \rightarrow c+St^{2\alpha}\hat{r}} St \phi_1^- &= \frac{-St^{1-\alpha}}{c^2 \left\{ \frac{(2-B_0)\hat{r}}{(1-A_0)c} \right\}^{\frac{1}{2}}} \int_{c+St^{2\alpha}\hat{r}}^{\infty} \exp \left[ -\int_{r'}^c q(r'') dr'' \right] \left\{ \frac{r' f_1(r', \phi'_0)}{(1-A')} \right. \\
&\quad \left. + \frac{\{(1-B') \sin^2 \phi'_0 + \frac{B'}{2}\} f_2(r', \phi'_0)}{(1-A')^2 \sin \phi'_0 \cos \phi'_0} \right\} dr', \\
&= \frac{-St^{1-\alpha}}{c (c\hat{r})^{\frac{1}{2}} \left\{ \frac{(2-B_0)}{(1-A_0)} \right\}^{\frac{1}{2}}} \int_c^{\infty} \exp \left[ -\int_{r'}^c q(r'') dr'' \right] \left\{ \frac{r' f_1(r', \phi'_0)}{(1-A')} \right. \\
&\quad \left. + \frac{\{(1-B') \sin^2 \phi'_0 + \frac{B'}{2}\} f_2(r', \phi'_0)}{(1-A')^2 \sin \phi'_0 \cos \phi'_0} \right\} dr' \\
&\quad + \frac{St^{1-\alpha}}{c (c\hat{r})^{\frac{1}{2}} \left\{ \frac{(2-B_0)}{(1-A_0)} \right\}^{\frac{1}{2}}} \int_c^{c+St^{2\alpha}\hat{r}} \exp \left[ -\int_{r'}^c q(r'') dr'' \right] \\
&\quad \left\{ O(1) + \frac{(1 - \frac{B_0}{2}) f_2(c, \frac{\pi}{2})}{(1-A_0)^2 (1)(St)^\alpha \left\{ \frac{(2-B_0)\hat{r}}{(1-A_0)c} \right\}^{\frac{1}{2}}} \right\} dr', \\
&= \frac{-St^{1-\alpha}}{c (c\hat{r})^{\frac{1}{2}} \left\{ \frac{(2-B_0)}{(1-A_0)} \right\}^{\frac{1}{2}}} \int_c^{\infty} \exp \left[ -\int_{r'}^c q(r'') dr'' \right] \left\{ \frac{r' f_1(r', \phi'_0)}{(1-A')} \right. \\
&\quad \left. + \frac{\{(1-B') \sin^2 \phi'_0 + \frac{B'}{2}\} f_2(r', \phi'_0)}{(1-A')^2 \sin \phi'_0 \cos \phi'_0} \right\} dr' + St \frac{G_0(2-B_0)(2A_0-B_0)}{4(1-A_0)} \\
&\quad + o(St).
\end{aligned}$$

When taking the intermediate limit of  $\phi_1^-$ , the  $O(St)^{2\alpha}$  correction to  $c$ , and the first non-linear term of  $O(St^{3\alpha})$  in the expansions of  $\cos \phi_0$  and  $\sin \phi_0$ , both of which appear in the prefactor multiplying the integrals, contribute errors of only  $O(St^{1+\alpha})$  which is  $o(St)$  for  $\alpha > 0$ . Also,  $\phi_1^-$  is an even function of  $\cos \phi_0$ , and therefore yields the same value for both  $\phi_0$  and  $\pi - \phi_0$ . When writing the limiting form of  $\phi_1^-$  above, we have used the asymptotic expression for  $\cos \phi_0$  in  $(0, \pi/2)$  in the prefactor, which then restricts  $\phi_0$  in the integral to the same interval.

Therefore

$$\begin{aligned}
\lim_{r \rightarrow c+St^{2\alpha\hat{r}}} \phi^{O1} &= \lim_{r \rightarrow c+St^{2\alpha\hat{r}}} (\phi_0 + St\phi_1^-), \\
&= \frac{\pi}{2} + (St)^\alpha \left\{ \frac{(2-B_0)\hat{r}}{(1-A_0)c} \right\}^{\frac{1}{2}} - \frac{St^{1-\alpha}}{c(c\hat{r})^{\frac{1}{2}} \left\{ \frac{(2-B_0)}{(1-A_0)} \right\}^{\frac{1}{2}}} \int_c^\infty \exp\left[-\int_{r'}^c q(r'')dr''\right] \left\{ \frac{r'f_1(r',\phi'_0)}{(1-A')} \right. \\
&+ \left. \frac{\{(1-B')\sin^2\phi'_0 + \frac{B'}{2}\}f_2(r',\phi'_0)}{(1-A')^2\sin\phi'_0\cos\phi'_0} \right\} dr' + St \left\{ \frac{G_0(2-B_0)(2A_0-B_0)}{4(1-A_0)} \right\} + O(St^{3\alpha}) + o(St). \quad (4.38)
\end{aligned}$$

For the inner layer we obtain from (4.36),

$$\lim_{r \rightarrow c+St^{2\alpha\hat{r}}} St\tilde{\phi}^- = \lim_{St \rightarrow 0} St \frac{G_0(2-B_0)(2A_0-B_0)}{4(1-A_0)} \left[ 1 + \left\{ 1 + \frac{16(St^{2\alpha-2}\hat{r} - St^{-1}k - I_i)(1-A_0)}{cG_0^2(2-B_0)(2A_0-B_0)^2} \right\}^{\frac{1}{2}} \right],$$

where we have used the ‘-’ branch of  $\tilde{\phi}$ , since this is the one relevant in the interval  $(\pi/2, \pi)$ .

If  $\alpha > 1/2$ , then  $St^{2\alpha-2} \ll St^{-1}$  and the term containing  $k$  is dominant. It can be readily verified that the resulting expansion does not match with (4.38). The same holds true even for  $\alpha = 1/2$  when the two terms are of the same order. Therefore taking  $\alpha < 1/2$ , and neglecting terms of  $o(St)$ , one obtains

$$\begin{aligned}
\lim_{r \rightarrow c+St^{2\alpha\hat{r}}} St\tilde{\phi}^- &= \frac{G_0(2-B_0)(2A_0-B_0)}{4(1-A_0)} \left[ St + 4St^\alpha \left\{ \frac{(\hat{r} - St^{1-2\alpha}k)(1-A_0)}{cG_0^2(2-B_0)(2A_0-B_0)^2} \right\}^{\frac{1}{2}} \right], \\
\Rightarrow \lim_{r \rightarrow c+St^{2\alpha\hat{r}}} \phi^{I-} &= \frac{\pi}{2} + (St)^\alpha \left\{ \frac{(2-B_0)\hat{r}}{(1-A_0)c} \right\}^{\frac{1}{2}} + St \frac{G_0(2-B_0)(2A_0-B_0)}{4(1-A_0)} \\
&\quad - St^{1-\alpha} \left\{ \frac{(2-B_0)}{c(1-A_0)} \right\}^{\frac{1}{2}} \left( \frac{k}{2\hat{r}^{\frac{1}{2}}} \right) + o(St). \quad (4.39)
\end{aligned}$$

Comparing the two limiting forms viz. (4.38) and (4.39), we see that for matching to hold to  $O(St)$  we require  $St^{3\alpha} \ll St$  which implies  $\alpha > 1/3$ . This is essentially the requirement that the non-linear terms (not included in the inner layer at this order) in the expansion of the sines and cosines in the leading order outer equation be subdominant as compared to the

$O(St)$  inertial correction. Thus the domain of overlap, to  $O(St)$ , is given by  $1/3 < \alpha < 1/2$ .

Matching the other terms gives

$$\begin{aligned}
-\left(\frac{2-B_0}{1-A_0}\right)^{\frac{1}{2}} \frac{k}{2} &= -\frac{1}{c} \left(\frac{1-A_0}{2-B_0}\right)^{\frac{1}{2}} \int_c^\infty \exp\left[-\int_{r'}^c q(r'') dr''\right] \\
&\quad \left\{ \frac{r' f_1(r', \phi'_0)}{(1-A')} + \frac{\{(1-B') \sin^2 \phi'_0 + \frac{B'}{2}\} f_2(r', \phi'_0)}{(1-A')^2 \sin \phi'_0 \cos \phi'_0} \right\} dr', \\
\Rightarrow k &= \frac{2}{c} \left(\frac{1-A_0}{2-B_0}\right) \int_c^\infty \exp\left[-\int_{r'}^c q(r'') dr''\right] \left\{ \frac{r' f_1(r', \phi'_0)}{(1-A')} \right. \\
&\quad \left. + \frac{\{(1-B') \sin^2 \phi'_0 + \frac{B'}{2}\} f_2(r', \phi'_0)}{(1-A')^2 \sin \phi'_0 \cos \phi'_0} \right\} dr'. \quad (4.40)
\end{aligned}$$

In the above integral,  $\phi'_0 \in (0, \pi/2)$ . Although not evident from (4.40),  $k$  will turn out to be less than zero, so the inertial trajectory is closer to the reference sphere (by  $O(St)$ ) at  $\phi = \pi/2$  than the corresponding zero-Stokes trajectory.

We now consider the other branch of the inner solution relevant to the interval  $(0, \pi/2)$ , whose limiting form for the purposes of matching with the solutions in layer O2, is similarly given as

$$\begin{aligned}
\lim_{r \rightarrow c+St^{2\alpha}\tilde{r}} \phi^{I+} &= \frac{\pi}{2} - (St)^\alpha \left\{ \frac{(2-B_0)\tilde{r}}{(1-A_0)c} \right\}^{\frac{1}{2}} + St^{1-\alpha} \left\{ \frac{(2-B_0)}{c(1-A_0)} \right\}^{\frac{1}{2}} \left( \frac{k}{2\hat{r}^{\frac{1}{2}}} \right) \\
&\quad + St \frac{G_0(2-B_0)(2A_0-B_0)}{4(1-A_0)} + o(St). \quad (4.41)
\end{aligned}$$

The limiting form<sup>5</sup> of expression (4.37) as  $r \rightarrow c + St^{2\alpha}\hat{r}$  is given as

$$\begin{aligned} \lim_{r \rightarrow c + St^{2\alpha}\hat{r}} St\phi_1^+ &= \frac{St^{1-\alpha}I_{\phi_1}^+ z^{-\infty}}{c(c\hat{r})^{\frac{1}{2}} \left\{ \frac{(2-B_0)}{(1-A_0)} \right\}^{\frac{1}{2}}} \exp \left[ \int_c^\infty q(r') dr' \right] \\ &\quad - \frac{St^{1-\alpha}}{c(c\hat{r})^{\frac{1}{2}} \left\{ \frac{(2-B_0)}{(1-A_0)} \right\}^{\frac{1}{2}}} \int_c^\infty \exp \left[ - \int_{r'}^c q(r'') dr'' \right] \left\{ \frac{r' f_1(r', \phi'_0)}{(1-A')} \right. \\ &\quad \left. + \frac{\{(1-B') \sin^2 \phi'_0 + \frac{B'}{2}\} f_2(r', \phi'_0)}{(1-A')^2 \sin \phi'_0 \cos \phi'_0} \right\} dr' + St \frac{G_0(2-B_0)(2A_0-B_0)}{4(1-A_0)} + o(St), \end{aligned}$$

and therefore,

$$\begin{aligned} \lim_{r \rightarrow c + St^{2\alpha}\hat{r}} \phi^{O2} &= \lim_{r \rightarrow c + St^{2\alpha}\hat{r}} (\phi_0 + St\phi_1^+), \\ &= \frac{\pi}{2} - (St)^\alpha \left\{ \frac{(2-B_0)\hat{r}}{(1-A_0)c} \right\}^{\frac{1}{2}} + \lim_{r \rightarrow c + St^{2\alpha}\hat{r}} \phi_1^+ + o(St), \end{aligned} \quad (4.42)$$

where the limiting form of  $\phi_1^+$  is given above, and  $\alpha$  is assumed to be in the overlap domain.

Again, matching terms in the limiting forms (4.42) and (4.41), and using the definition of  $k$  as given by (4.40), we obtain

$$(St)^{1-\alpha} \left\{ \frac{(2-B_0)}{c(1-A_0)} \right\}^{\frac{1}{2}} \left( \frac{k}{2\hat{r}^{\frac{1}{2}}} \right) = \frac{St^{1-\alpha}I_{\phi_1}^+ z^{-\infty}}{c(c\hat{r})^{\frac{1}{2}} \left\{ \frac{(2-B_0)}{(1-A_0)} \right\}^{\frac{1}{2}}} \exp \left[ \int_c^\infty q(r') dr' \right] - (St)^{1-\alpha} \left\{ \frac{(2-B_0)}{c(1-A_0)} \right\}^{\frac{1}{2}} \left( \frac{k}{2\hat{r}^{\frac{1}{2}}} \right).$$

The expression for  $I_{\phi_1}^+$  is given by

$$I_{\phi_1}^+ = k \frac{c}{z^{-\infty}} \frac{(2-B_0)}{(1-A_0)} \exp \left[ - \int_c^\infty q(r') dr' \right]. \quad (4.43)$$

<sup>5</sup>Note that the sign of the term in  $r\phi_1^+$  involving the integration constant depends on the branch of  $\cos \phi_0$  used. In this case, we have to use the positive branch since  $\phi_0 \in (0, \pi/2)$ .

From (4.29), (4.40) and (4.43), we obtain the following expression for the lateral displacement.

$$(\Delta z)_{inplane} = St I_{\phi_1}^+, \quad (4.44)$$

$$= 2 \frac{St}{z^{-\infty}} \int_c^\infty \exp \left[ - \int_{r'}^\infty q(r') dr' \right] \left\{ \frac{r' f_1(r', \phi'_0)}{(1 - A')} + \frac{\{(1 - B') \sin^2 \phi'_0 + \frac{B'}{2}\} f_2(r', \phi'_0)}{(1 - A')^2 \sin \phi'_0 \cos \phi'_0} \right\} dr'. \quad (4.45)$$

The above integral yields negative values which shows that a given finite-Stokes trajectory in the shearing plane suffers a net downward displacement in the gradient direction (see section 4.4.4). It must be noted that the domain of existence of the solutions in the outer layers O1 and O2 is  $r \geq c$ , since  $\sin \phi_0$  no longer takes real values when  $r < c$ . This value of  $r$  is attained on the inertial trajectory when  $\phi \sim \pi/2 \pm O(St^{\frac{1}{2}})$ , where the inner solution remains valid ( $\tilde{r} = -St^{-1}k$ ). As seen above, the matching occurs in the region  $\phi \sim \pi/2 + O(St^\alpha)$  where  $1/3 < \alpha < 1/2$ , so the outer solution is real valued in the domain of overlap.

#### 4.4.2 The effect of hydrodynamic coupling on the in-plane gradient displacement

In presence of hydrodynamic interactions, the translational and rotational degrees of freedom of different particles are coupled; a change in the translational velocity of one will induce corresponding changes in all angular velocities, and vice versa. This implies that the resistance of a given particle to rotation on account of a finite moment of inertia will lead to an altered translational velocity, and thence a modified trajectory. These inertial effects, represented by  $\mathbf{V} \cdot \nabla_{\mathbf{r}} \boldsymbol{\Omega}$ , are weaker than the translational inertial term  $\mathbf{V} \cdot \nabla_{\mathbf{r}} \mathbf{V}$ , and their omission does not lead to a qualitative alteration of the finite  $St$  trajectories. Nevertheless, they are important from a conceptual viewpoint and therefore elaborated below.

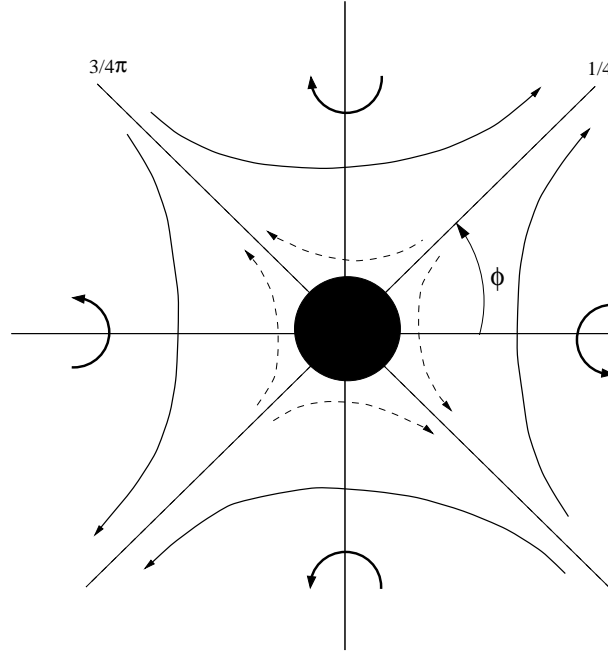


Figure 4.4: Stresslet velocity field induced by a sphere in shear flow. The solid arrows denote the extensional portion of the ambient shear flow and the dotted arrows the disturbance velocity field. The thick black arrows indicate the sign of the disturbance vorticity in the corresponding regions.

We first observe that this term is of significance only in the near-field regions since the resistance tensor,  $\mathbf{M}_{LU}$ , characterising the translation-rotation coupling is only  $O(1/r^2)$  for large  $r$ . A qualitative understanding of this effect can, however, still be obtained by looking at widely separated particles. Restricting our attention to  $\phi \in (0, \pi)$ , we see that the induced stresslet velocity field (see Fig 4.4) due to the reference sphere acts to retard the angular velocity of the second sphere (due to the ambient shear flow) in the regions  $\phi < \pi/4$  and  $\phi > 3\pi/4$ , and enhance it in  $\pi/4 < \phi < 3\pi/4$ . At any given value of  $r$ , the corrected angular velocity therefore goes from a minimum at  $\pi$  through a maximum at  $\pi/2$ , and back to the same value at  $\phi = 0$ . While an inertialess particle would instantaneously respond to this changing angular velocity, at finite  $St$ , the rotational inertia of an actual particle resists the changing angular velocity field by inducing an  $O(St)$  torque in the opposite sense. The resulting (perturbative) rotational velocity field displaces the second particle, or what is equivalent in the relative frame, displaces the given particle in the opposite direction.

$z^{-\infty}$	$(\Delta z)_{inplane}$	$(\Delta z)_{inplane}$ (w/o rotation)
3	-0.00684	-0.00670
1	-0.0384	-0.0351
0.5	-0.0481	-0.0418
0.2	-0.0713	-0.0935
0.16	spirals in	-0.0993

Table 4.1:  $(\Delta z)_{inplane}$  values with and without the  $\mathbf{U} \cdot \nabla_{\mathbf{x}} \boldsymbol{\Omega}$  contribution:  $St = 0.1$ .

Upstream of the reference sphere, the angular velocity along a zero-Stokes pathline decreases on one hand due to the increasing magnitude of the retarding correction, but increases on the other since the motion is directed towards decreasing  $\phi$  (and therefore from a retarding to an enhancing correction). In the downstream quadrant  $(0, \pi/2)$ , the angular velocity correction goes from enhancing to opposing, but at the same time decreases in magnitude as one moves further downstream. The effect of changing radial distance (represented by the term proportional to  $E dC/dr$  in the expression for  $f_1$ ; see (4.25)) dominates far enough upstream and downstream, leading to a positive contribution to the gradient displacement. However, the angular effect, which induces a right-handed inertial torque upstream and one of the opposite sense downstream, is found to be larger owing to which the net contribution of  $\mathbf{U} \cdot \nabla_{\mathbf{r}} \boldsymbol{\Omega}$  to the gradient displacement is negative.

Since the term proportional to  $E$  in  $f_1$  (see (4.25)) represents the translation-rotation coupling, its effect can be isolated by calculating the gradient displacement for a given finite  $St$  trajectory with and without this term. In table 4.1, we tabulate values of  $(\Delta z)_{inplane}$  calculated from numerical integration of (4.25) (see section 4.4.4) with and without the coupling term for a Stokes number of 0.1, and it is seen that the in-plane gradient displacement is smaller in magnitude in the latter case.

### 4.4.3 In-plane Limiting trajectory

It is evident from (4.45) that when the offset  $z^{-\infty}$  is  $O(St^\beta)$  ( $\beta > 0$ ), then the lateral displacement is no longer  $O(St)$ , but increases to  $O(St^{1-\beta})$ <sup>6</sup>, till at  $\beta = \frac{1}{2}$ , both  $(\Delta z)_{inplane}$  and  $z^{-\infty}$  become  $O(St^{\frac{1}{2}})$ . In this latter case, the above expression will cease to be valid since  $(\Delta z)_{inplane}$  becoming comparable in magnitude to  $z^{-\infty}$  would imply that  $\phi_0$  and  $St\phi_1$  become comparable in magnitude. This is clearly outside the realm of the perturbative scheme in the previous section and must be treated in an alternate manner. This can also be seen from the asymptotic expressions for  $\phi_0^+$  and  $\phi_1^+$  for  $r \gg 1$ . We have

$$\begin{aligned} \lim_{r \gg 1} \phi_0^+ &\approx \left[ \frac{(z^{-\infty})^2}{r^2} + \frac{16}{9r^5} \right]^{\frac{1}{2}}, \\ \lim_{r \gg 1} St\phi_1^+ &\approx St \frac{I_{\phi_1}^+}{r}. \end{aligned}$$

Provided  $r \gg St^{-\frac{1}{3}}$ ,  $(z^{-\infty})^2/r^2$  dominates, and  $\phi_0^+ \sim O(z^{-\infty}/r)$ . Since the integration constant  $St I_{\phi_1}^+$  is of the same order as  $(\Delta z)_{inplane}$  viz.  $O(St^{\frac{1}{2}})$  (see (4.44)), both  $\phi_0^+$  and  $St\phi_1^+$  become  $O(St^{\frac{1}{2}})/r$  when  $z^{-\infty} \sim O(St^{\frac{1}{2}})$ . The non-uniformity in this case is on account of integrated effects and could not have been anticipated based on the order of magnitude of terms in the governing equations. Indeed, the  $O(St)$  terms in (4.25) decay more rapidly than the leading order terms in the limit  $r \gg 1$ , and therefore remain uniformly small.

The limiting trajectory for finite  $St$  is the critical trajectory which separates the open trajectories that originate upstream and lie outside it, from the spiralling trajectories inside (this spiralling effect will be shown later; see section 4.4.6). This limiting trajectory starts from a finite offset of  $O(St^{\frac{1}{2}})$  at  $y = -\infty$ , and tends to  $z = 0$  at  $y = +\infty$ . All trajectories starting at  $y = -\infty$  from an offset less than this limiting value will cross the

---

<sup>6</sup>See appendix C4 for an alternate analysis leading to the same result.

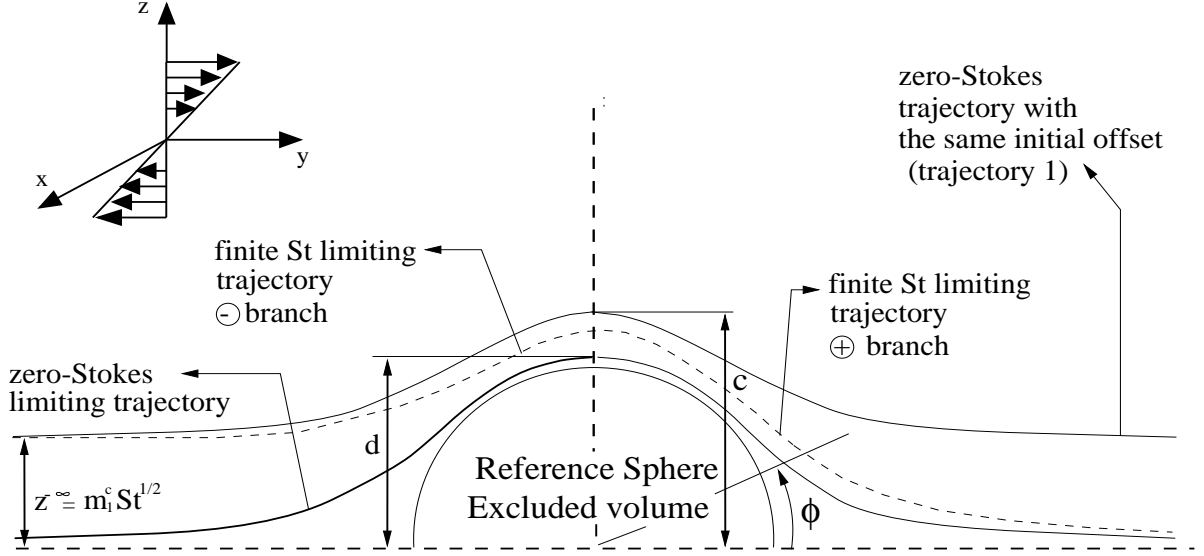


Figure 4.5: Finite  $St$  limiting trajectory in the plane of shear.

horizontal axis with a finite tangential velocity and at a finite distance downstream, as can easily be verified by calculating  $V_\phi$  at  $\phi = 0$ ; they then spiral in towards the reference sphere.

We calculate the two branches corresponding to the intervals  $\phi \in (0, \pi/2)$  and  $\phi \in (\pi/2, \pi)$  of the limiting trajectory separately, and piece them together at  $\phi = \pi/2$ , which then determines the magnitude of the initial offset. As shown in Fig 4.5, the ‘-’ branch of the limiting trajectory ( $\phi \in (\pi/2, \pi)$ ) will be perturbed about a zero Stokes trajectory with the same (unknown) initial offset (trajectory 1), and the ‘+’ ( $\phi \in (0, \pi/2)$ ) branch about the zero-Stokes limiting trajectory that also tends to  $z = 0$  as  $y \rightarrow +\infty$ . Let  $z^{-\infty} = St^\beta m_1^c$  ( $\beta > 0$ ) correspond to the initial offset of both the finite  $St$  limiting trajectory and trajectory 1 about which it is perturbed. Using (4.33) for trajectory 1 and expanding for small  $St$ , we have

$$c = \left\{ \int_c^\infty \exp \left[ - \int_{r'}^c q(r'') dr'' \right] \frac{B' r'}{(1 - A')} dr' \right\}^{\frac{1}{2}} \left[ 1 + \frac{m_1^{c2} St^{2\beta}}{2} \frac{\exp \left\{ \int_c^\infty q(r') dr' \right\}}{\int_c^\infty \exp \left[ - \int_{r'}^c q(r'') dr'' \right] \frac{B' r'}{(1 - A')} dr'} \right]. \quad (4.46)$$

Thus, an  $O(St^\beta)$  change in the initial offset produces, at leading order, only an  $O(St^{2\beta})$  alteration of the radial distance at  $\phi = \pi/2$ , which illustrates the ‘squeezing effect’ for trajectories with small offsets. As before, matching the outer and inner solutions in  $(\pi/2, \pi)$  yields (4.40) for the integration constant  $k(c)$ . The radial distance of the actual trajectory at  $\phi = \pi/2$  is, to  $O(St)$ , given by

$$r_{\pi/2}^- = c + St k(c) \quad (4.47)$$

where the argument of  $k$  is used to denote evaluation at  $c$ .

Exactly the same procedure is applied to the ‘+’ branch of the finite  $St$  limiting trajectory, the only difference being that it is perturbed about the zero-Stokes limiting trajectory so that

$$r^2 \sin^2 \phi_0^+ = \int_r^\infty \exp \left[ - \int_{r'}^r q(r'') dr'' \right] \frac{B' r'}{(1 - A')} dr'. \quad (4.48)$$

The distance of nearest approach for the zero-Stokes limiting trajectory is denoted by  $d$  and satisfies equation (4.46) with  $m_1^c = 0$ , i.e.,

$$d = \left\{ \int_d^\infty \exp \left[ - \int_{r'}^d q(r'') dr'' \right] \frac{B' r'}{(1 - A')} dr' \right\}^{\frac{1}{2}}. \quad (4.49)$$

Thus, the radial distance of the actual trajectory at  $\phi = \pi/2$  for the ‘+’ branch is given by

$$r_{\pi/2}^+ = d - St k(d). \quad (4.50)$$

The difference in sign in this case compared to (4.47) is because we go from the choice of the negative to the positive square root for the inner solution  $\tilde{\phi}$ , but the corresponding matching contributions in  $\phi_1^-$  and  $\phi_1^+$  remain the same. Since the two branches considered belong to

the same trajectory, we have

$$\begin{aligned}
r_{\pi/2}^- &= r_{\pi/2}^+, \\
\Rightarrow c + St k(c) &= d - St k(d), \\
\Rightarrow c &= d - 2St k(d)
\end{aligned} \tag{4.51}$$

to  $O(St)$ . Therefore  $c$  differs from  $d$  by  $O(St)^7$ , and from equations (4.46) and (4.49), this implies that

$$O(St^{2\beta}) \sim O(St) \Rightarrow \beta = \frac{1}{2}.$$

This shows that the initial offset of the limiting finite  $St$  trajectory is  $O(St^{\frac{1}{2}})$ . As mentioned earlier, the non-trivial exponent of  $1/2$  rather than  $1$  arises on account of the squeezing effect of trajectories close to the reference sphere. Using  $c = d + St p$ , an expression for  $p$  in terms of the initial offset can be found using (4.46) for  $\beta = 1/2$ ; one obtains

$$\begin{aligned}
d + St p &= \left\{ \int_{d+St p}^{\infty} \exp \left[ - \int_{r'}^{d+St p} q(r'') dr'' \right] \frac{B' r'}{(1-A')} dr' \right\}^{\frac{1}{2}} \left[ 1 \right. \\
&\quad \left. + \frac{m_1^{c_2} St}{2} \frac{\exp \left[ \int_d^{\infty} q(r') dr' \right]}{\int_d^{\infty} \exp \left[ - \int_{r'}^d q(r'') dr'' \right] \frac{B' r'}{(1-A')} dr'} \right], \\
\Rightarrow d + St p &= \left[ \left( \int_d^{\infty} \exp \left[ - \int_{r'}^d q(r'') dr'' \right] \frac{B' r'}{(1-A')} dr' \right) \exp \left[ - \int_d^{d+St p} q(r') dr' \right] \right. \\
&\quad \left. - \int_d^{d+St p} \exp \left[ - \int_{r'}^{d+St p} q(r'') dr'' \right] \frac{B' r'}{(1-A')} dr' \right]^{\frac{1}{2}} \\
&\quad \left[ 1 + \frac{m_1^{c_2} St}{2} \frac{\exp \left[ \int_d^{\infty} q(r') dr' \right]}{\int_d^{\infty} \exp \left[ - \int_{r'}^d q(r'') dr'' \right] \frac{B' r'}{(1-A')} dr'} \right].
\end{aligned}$$

---

<sup>7</sup>It must be remembered that  $k < 0$  so that as expected,  $c > d$ .

Using the definition of  $d$  from (4.49) and with some manipulation, one obtains

$$d + St p = d \left( 1 - \frac{St}{2d^2} \left( \frac{2p(A_0 - B_0)}{(1 - A_0)d} d^2 + \frac{B_0 p d}{(1 - A_0)} \right) + \frac{m_1^{c^2} St}{2d^2} \exp \left[ \int_d^\infty \frac{2(A' - B')}{(1 - A')r'} dr' \right] \right),$$

where the subscript ‘0’ now indicates evaluation of the relevant hydrodynamic function at  $r = d$ . Equating orders we observe that  $O(1)$  is an identity, while at  $O(St)$ ,

$$p = \frac{m_1^{c^2} (1 - A_0)}{d (2 - B_0)} \exp \left[ \int_d^\infty q(r') dr' \right]. \quad (4.52)$$

With  $p$  given by (4.52), we use  $c = d + St p$  in (4.51) to obtain

$$\frac{m_1^{c^2} (1 - A_0)}{d (2 - B_0)} \exp \left[ \int_d^\infty q(r') dr' \right] = -2k(d).$$

Therefore, the offset of the limiting finite  $St$  trajectory is  $m_1^c (St)^{\frac{1}{2}}$ , where  $m_1^c$  is given by

$$\begin{aligned} m_1^c &= \left\{ -2k(d) d \frac{(2 - B_0)}{(1 - A_0)} \right\}^{\frac{1}{2}} \exp \left[ - \int_d^\infty q(r') dr' \right], \quad (4.53) \\ &= \left( -4 \int_d^\infty \exp \left[ - \int_{r'}^\infty q(r'') dr'' \right] \left\{ \frac{r' f_1(r', \phi'_0)}{(1 - A')} + \frac{\{(1 - B') \sin^2 \phi'_0 + \frac{B'}{2}\} f_2(r', \phi'_0)}{(1 - A')^2 \sin \phi'_0 \cos \phi'_0} \right\} dr' \right)^{\frac{1}{2}}. \quad (4.54) \end{aligned}$$

Since  $k(d) < 0$ , the argument of the square root in the above expression is positive and  $m_1^c$  is real valued. Note that there are open trajectories with  $O(St^{\frac{1}{2}})$  initial offsets that lie outside the limiting trajectory. The expression for the gradient displacement for these cases is derived in Appendix C4, and will be used for the evaluation of the in-plane self-diffusivity in section 4.4.5.

$St$	$m_1^c St^{\frac{1}{2}}$ (numer.)	$m_1^c St^{\frac{1}{2}}$ (theor.)
0.01	0.05	0.051
0.1	0.165	0.162
0.5	0.409	0.362
1	0.657	0.512

Table 4.2: Comparison of theoretical and numerical values of the critical offset in the shearing plane.

From (4.52) we see that the  $O(St)$  correction  $p$  is proportional to  $(1 - A_0)$ ; since the value of  $d$  is very close to the contact value of the inter-particle distance, one can approximate  $(1 - A_0)$  as  $4.077(d - 2)$  ( $d - 2 \ll 1$ ). Thus for near-field approach, the effective inertia of the particle with regard to radial motion is characterized by a modified Stokes number  $\hat{St} \propto St(r - 2)$  which decreases linearly with decreasing separation. Therefore as seen in section 4.3, even for  $St \sim O(1)$ , there is always a separation at which  $\hat{St} \ll 1$ , and inertia of the particle is no longer important at these separations. This can also be understood from the fact that the radial component of the drag has a  $1/(r - 2)$  singularity at contact which implies that the near-field motion of the particles is equivalent to that in a fluid with an effective viscosity of order  $\mu/(r - 2)$ . This immediately suggests  $\hat{St}$  as the appropriate measure of particle inertia. This argument is not necessarily true, however, for arbitrary  $St$ , since for  $St$  large enough the separation corresponding to  $\hat{St} \ll 1$  might be small enough for the continuum approximation to be invalid (Sundararajakumar & Koch 1996).

In table 4.2 and Fig 4.6, we compare the theoretical expression for  $m_1^c$ , (4.53), with that obtained from numerical integration of (4.25) using an adaptive Runge-Kutta fourth order method, for different Stokes numbers. In the latter case, the gradient displacement was obtained by carrying out the integration from 200 units upstream to the same distance downstream. There was no significant change in this value on further increasing this distance.

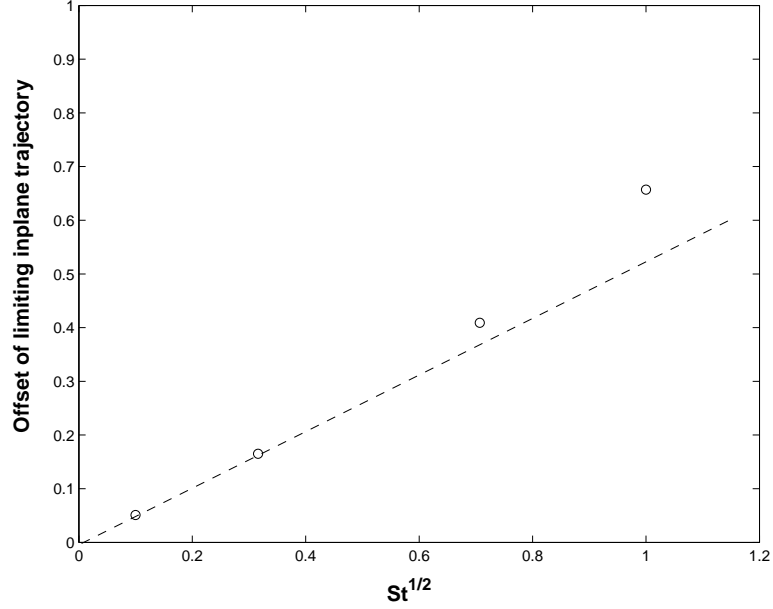


Figure 4.6: The critical offset ( $m_1^c St^{\frac{1}{2}}$ ) values obtained from numerical integration of the in-plane trajectory equation (4.25) are plotted as a function of  $St^{\frac{1}{2}}$ ; the dashed line represents the theoretical approximation (4.53).

The theoretical and numerical values agree well upto a Stokes number of about 0.5, which confirms the  $St^{\frac{1}{2}}$  scaling of the critical offset. Even for a Stokes number of 1, the theoretical value is not too far off; this is because for  $St = 1$ , the limiting finite  $St$  trajectory still passes very close to the sphere ( $r_{min} \sim 2.0001$ ), and as seen earlier, the inertia of the particle is suppressed by lubrication forces at these separations, which translates to an effective Stokes number for motion close to the sphere that is much less than 1.

#### 4.4.4 Far-field analytical expression for in-plane gradient displacement

The expression for  $(\Delta z)_{inplane}$  is given by (4.45),

$$(\Delta z)_{inplane} = \frac{2St}{z^{-\infty}} \int_c^{\infty} \exp \left[ -\int_{r'}^{\infty} q(r') dr' \right] \left\{ \frac{r' f_1(r', \phi'_0)}{(1-A')} + \frac{\{(1-B') \sin^2 \phi'_0 + \frac{B'}{2}\} f_2(r', \phi'_0)}{(1-A')^2 \sin \phi'_0 \cos \phi'_0} \right\} dr'.$$

To find the far-field expression for  $(\Delta z)_{inplane}$  (i.e., in the limit  $c$  (or  $z^{-\infty}$ )  $\gg 1$ )<sup>8</sup>, we use the following far-field approximations for the hydrodynamic functions,

$$\begin{aligned} A &= \frac{5}{r^3} - \frac{8}{r^5} + O\left(\frac{1}{r^7}\right), & B &= \frac{16}{3r^5} + O\left(\frac{1}{r^7}\right), \\ C &= \frac{5}{2r^3} + O\left(\frac{1}{r^6}\right), & E &= \frac{1}{2r^2} + O\left(\frac{1}{r^7}\right), \\ G &= 1 - \frac{3}{2r} + O\left(\frac{1}{r^3}\right), & H &= 1 - \frac{3}{4r} + O\left(\frac{1}{r^3}\right), \\ \sin^2 \phi_0 &= \frac{c^2}{r^2} + O\left(\frac{1}{c^3}\right), & \cos^2 \phi_0 &= \left(1 - \frac{c^2}{r^2}\right) + O\left(\frac{1}{c^3}\right). \end{aligned}$$

A term of  $O(1/r^k)$  will, upon integration, yield a term of  $O(1/c^{k-1})$  for  $(\Delta z)_{inplane}$ , and for  $c \gg 1$ ,  $(\Delta z)_{inplane}$  will therefore be in the form of a power series in  $1/c$ . We will calculate  $(\Delta z)_{inplane}$  to  $O(1/c^4)$ ; to this order, the exponential factor in the integral expression can be approximated by 1. Also, in the expressions above and those to follow, a neglected term of the general form  $O(1/r^{n-s}c^s)$  is denoted by  $O(1/r^n)$ , since both will contribute terms of  $O(1/c^{n-1})$  in the final expression for  $(\Delta z)_{inplane}$ . We now find the asymptotic approximations for the other two terms in the integrand involving  $f_1$  and  $f_2$ .

$$\begin{aligned} f_1 &: \frac{r' f_1(r', \phi'_0)}{(1 - A')} \\ &\approx \frac{-r' \sin \phi'_0 \cos \phi'_0}{(1 - A')} \left[ H' \left[ -r' \frac{dB'}{dr'} \frac{(\cos^2 \phi'_0 - \sin^2 \phi'_0)}{2} + 2(A' - B') \sin^2 \phi'_0 \right] + O\left(\frac{1}{r'^6}\right) \right], \\ &= \frac{10}{r'^2} \cos \phi'_0 \sin^3 \phi'_0 + \frac{3}{4r'} \left( \frac{10}{r'^2} \right) \cos \phi'_0 \sin^3 \phi'_0 \\ &\quad - \sin \phi'_0 \cos \phi'_0 \left[ \frac{40}{3r'^4} - \sin^2 \phi'_0 \left( \frac{80}{3r'^4} + \frac{16}{r'^4} + \frac{32}{r'^4} \right) \right] + O\left(\frac{1}{r'^5}\right), \\ &= \left( -\frac{10}{r'^2} + \frac{15}{2r'^3} \right) \left( 1 - \frac{c^2}{r'^2} \right)^{\frac{1}{2}} \frac{c^3}{r'^3} - \frac{c}{r'} \left( 1 - \frac{c^2}{r'^2} \right)^{\frac{1}{2}} \left[ \frac{40}{3r'^4} - \frac{c^2}{r'^2} \left( \frac{160}{3r'^4} \right) \right] + O\left(\frac{1}{r'^5}\right). \end{aligned}$$

<sup>8</sup>The difference between  $c$  and  $z^{-\infty}$  in this limit is only  $O(1/(z^{-\infty})^3)$ , as can be verified from the zero-Stokes trajectory equation; we can therefore use them interchangeably at the order of approximation considered in this section.

$$\begin{aligned}
f_2 &: \frac{\{(1-B') \sin^2 \phi'_0 + \frac{B'}{2}\} f_2(r', \phi'_0)}{(1-A')^2 \sin \phi'_0 \cos \phi'_0}, \\
&\approx \frac{-r' G' \sin \phi_0}{\cos \phi'_0} \left[ \sin^2 \phi'_0 \cos^2 \phi'_0 \left( -r' \frac{dA'}{dr'} \right) + \frac{(B'-2A')}{2} \sin^2 \phi'_0 - \frac{B'}{2} \cos^2 \phi'_0 + O\left(\frac{1}{r'^6}\right) \right], \\
&= \left( -1 + \frac{3}{2r'} \right) \left[ \left( \frac{15}{r'^2} \right) \sin^3 \phi'_0 \cos \phi'_0 - \left( \frac{5}{r'^2} \right) \frac{\sin^3 \phi'_0}{\cos \phi'_0} \right] - \frac{1}{\cos \phi'_0} \left[ \frac{32}{3r'^4} \sin^3 \phi'_0 \right. \\
&\quad \left. - \frac{40}{r'^4} \sin^3 \phi'_0 \cos^2 \phi'_0 - \frac{16}{6r'^4} \sin \phi'_0 \cos^2 \phi'_0 \right] + O\left(\frac{1}{r'^5}\right), \\
&= - \left[ \left( \frac{15}{r'^2} \right) \frac{c^3}{r'^3} \left( 1 - \frac{c^2}{r'^2} \right)^{\frac{1}{2}} - \left( \frac{5}{r'^2} \right) \frac{c^3}{r'^3} \left( 1 - \frac{c^2}{r'^2} \right)^{-\frac{1}{2}} \right] + \left[ \left( \frac{45}{2r'^3} \right) \frac{c^3}{r'^3} \left( 1 - \frac{c^2}{r'^2} \right)^{\frac{1}{2}} \right. \\
&\quad \left. - \left( \frac{15}{2r'^3} \right) \frac{c^3}{r'^3} \left( 1 - \frac{c^2}{r'^2} \right)^{-\frac{1}{2}} \right] - \left[ \left( \frac{32}{3r'^4} \right) \frac{c^3}{r'^3} \left( 1 - \frac{c^2}{r'^2} \right)^{-\frac{1}{2}} - \left( \frac{40}{r'^4} \right) \frac{c^3}{r'^3} \left( 1 - \frac{c^2}{r'^2} \right)^{\frac{1}{2}} \right. \\
&\quad \left. - \frac{16}{6r'^4} \frac{c}{r'} \left( 1 - \frac{c^2}{r'^2} \right)^{\frac{1}{2}} \right] + O\left(\frac{1}{r'^5}\right).
\end{aligned}$$

Having found the requisite asymptotic expressions, we proceed to evaluate  $(\Delta z)_{inplane}$  by considering terms at successive orders in  $1/c$ .

$$\begin{aligned}
O\left(\frac{1}{c^2}\right) &: \frac{2}{z^{-\infty} c} \int_c^\infty (1) \left[ \left( -\frac{10}{r'^2} \right) \left( 1 - \frac{c^2}{r'^2} \right)^{\frac{1}{2}} \frac{c^3}{r'^3} - \left( \frac{15}{r'^2} \right) \frac{c^3}{r'^3} \left( 1 - \frac{c^2}{r'^2} \right)^{\frac{1}{2}} + \left( \frac{5}{r'^2} \right) \frac{c^3}{r'^3} \left( 1 - \frac{c^2}{r'^2} \right)^{-\frac{1}{2}} \right] dr', \\
&= \frac{2}{z^{-\infty} c} \int_c^\infty \left[ \left( \frac{5}{r'^2} \right) \frac{c^3}{r'^3} \left( 1 - \frac{c^2}{r'^2} \right)^{-\frac{1}{2}} - \left( \frac{25}{r'^2} \right) \left( 1 - \frac{c^2}{r'^2} \right)^{\frac{1}{2}} \frac{c^3}{r'^3} \right] dr'.
\end{aligned}$$

Changing variables  $a' = c^2/r'^2$ , we get

$$\begin{aligned}
&- \frac{1}{z^{-\infty} c} \int_0^2 \left[ 5a'(1-a')^{-\frac{1}{2}} - 25a'(1-a')^{\frac{1}{2}} \right] da', \\
&= - \frac{1}{z^{-\infty} c} \left[ 5Be\left(2, \frac{1}{2}\right) - 25Be\left(2, \frac{3}{2}\right) \right], \\
&= 0,
\end{aligned}$$

where  $Be(r, s)$  is the Beta function (Abramowitz and Stegun 1972). At the next order,

$$\begin{aligned} O\left(\frac{1}{c^3}\right) &: \frac{2}{z^{-\infty}} \int_c^\infty (1) \left[ \left(\frac{15}{2r'^3}\right) \left(1 - \frac{c^3}{r'^3}\right)^{\frac{1}{2}} \frac{c^3}{r'^3} + \left(\frac{45}{2r'^3}\right) \frac{c^3}{r'^3} \left(1 - \frac{c^2}{r'^2}\right)^{\frac{1}{2}} - \left(\frac{15}{2r'^3}\right) \frac{c^3}{r'^3} \left(1 - \frac{c^2}{r'^2}\right)^{-\frac{1}{2}} \right] dr', \\ &= \frac{1}{z^{-\infty} c^2} \left[ 30Be\left(\frac{5}{2}, \frac{3}{2}\right) - \frac{15}{2}Be\left(\frac{5}{2}, \frac{1}{2}\right) \right], \\ &= -\frac{15\pi}{16(z^{-\infty})^3}, \end{aligned}$$

where we gave replaced  $c$  by  $z^{-\infty}$  (see earlier footnote). At the next order,

$$\begin{aligned} O\left(\frac{1}{c^4}\right) &: \frac{2}{z^{-\infty}} \int_c^\infty (1) \left[ -\frac{c}{r'} \left(1 - \frac{c^2}{r'^2}\right)^{\frac{1}{2}} \left[ \frac{40}{3r'^4} - \frac{c^2}{r'^2} \left(\frac{160}{3r'^4}\right) \right] - \left(\frac{32}{3r'^4}\right) \frac{c^3}{r'^3} \left(1 - \frac{c^2}{r'^2}\right)^{-\frac{1}{2}} \right. \\ &\quad \left. + \left(\frac{40}{r'^4}\right) \frac{c^3}{r'^3} \left(1 - \frac{c^2}{r'^2}\right)^{\frac{1}{2}} + \frac{16}{6r'^4} \frac{c}{r'} \left(1 - \frac{c^2}{r'^2}\right)^{\frac{1}{2}} \right] dr', \\ &= \frac{1}{z^{-\infty} c^3} \left[ \frac{280}{3}Be\left(3, \frac{3}{2}\right) - \frac{32}{3}Be\left(2, \frac{3}{2}\right) - \frac{32}{3}Be\left(3, \frac{1}{2}\right) \right], \\ &= 0. \end{aligned}$$

Therefore, the far-field expression for  $(\Delta z)_{inplane}$  is given by

$$\lim_{c \gg 1} (\Delta z)_{inplane} = -(St) \frac{15\pi}{16(z^{-\infty})^3} + O\left(\frac{1}{z^{-\infty}}\right)^5. \quad (4.55)$$

The reason for the  $O(1/c^2)$  terms cancelling out identically, in turn leading to the  $O(1/z^{-\infty})^3$  decay is because the deviation of the particle pathline from the corresponding streamline of the ambient simple shear is  $O(1/z^{-\infty})^3$  for  $z^{-\infty} \gg 1$ , as can be seen from (4.30) using the far-field approximations for the hydrodynamic functions. In the absence of interactions, the relative trajectories are coincident with the streamlines, which for the case of simple shear flow are just straight lines. Motion of the particle along such a rectilinear path will not lead to an orthogonal displacement for any value of  $St$ . Therefore  $(\Delta z)_{inplane}$ , for  $z^{-\infty} \gg 1$ , should

$c$	$(\Delta z)_{inplane/numer}$	$(\Delta z)_{inplane/far-field}$	$(\Delta z)_{inplane/theor}$
5	-0.001941	-0.002356	-0.001976
10	-0.000282	-0.000295	-0.000291
15	-0.0000864	-0.0000873	
20	-0.000037	-0.0000368	

Table 4.3: Comparison of numerical and analytical values, and the far-field approximation (4.55) for  $(\Delta z)_{inplane}$  for  $St = 0.1$ .

be of the same order as the leading order hydrodynamic interactions, which then leads to the above scaling.

In table 4.3, we compare the far-field approximation for  $(\Delta z)_{inplane}$  above with that obtained from the numerical integration of (4.25). Also listed is the exact numerical value of the integral expression (4.45) for  $(\Delta z)_{inplane}$  (denoted below and in the table by  $(\Delta z)_{inplane/theor}$ ), valid for trajectories with offsets  $z^{-\infty} \gg O(St^{\frac{1}{2}})$ . This is calculated using Gauss-Legendre quadrature; the upper limit in the integral was taken to be 80 units, and further increase in this value did not change the value of  $(\Delta z)_{inplane/theor}$  for the cases shown. We have calculated  $(\Delta z)_{inplane/theor}$  for the first two cases only, since for  $z^{-\infty} \geq 15$  the absolute value of  $(\Delta z)_{inplane}$  becomes very small and convergence with increasing number of Gauss-Legendre points is slow. However, the values for  $z^{-\infty} = 5$  and 10 suffice to show the accuracy of the far-field expression in approximating (4.45).

#### 4.4.5 Calculation of in-plane self-diffusivity in the velocity gradient direction ( $D_{zz}^{ip}$ )

A particle moving along a finite  $St$  open trajectory in the shearing plane suffers a net displacement in the gradient direction after a single interaction. A sequence of such uncorrelated displacements will lead to the particle executing a random walk characterised in general by a tensorial diffusivity (see Fig 4.7). The transverse components (i.e., the  $zz$  and  $xx$  components)

of the self-diffusivity tensor in the dimensionless form are given by (Zarraga & Leighton 2001)

$$\hat{D}_{zz} = \frac{3}{8\pi} \int_{-\infty}^{\infty} \int_{-\infty}^{\infty} dx^{-\infty} dz^{-\infty} |z^{-\infty}| (\Delta z)^2,$$

$$\hat{D}_{xx} = \frac{3}{8\pi} \int_{-\infty}^{\infty} \int_{-\infty}^{\infty} dx^{-\infty} dz^{-\infty} |z^{-\infty}| (\Delta x)^2,$$

where  $\hat{D}_{ii} = D_{ii}/\dot{\gamma}a^2\phi$ .

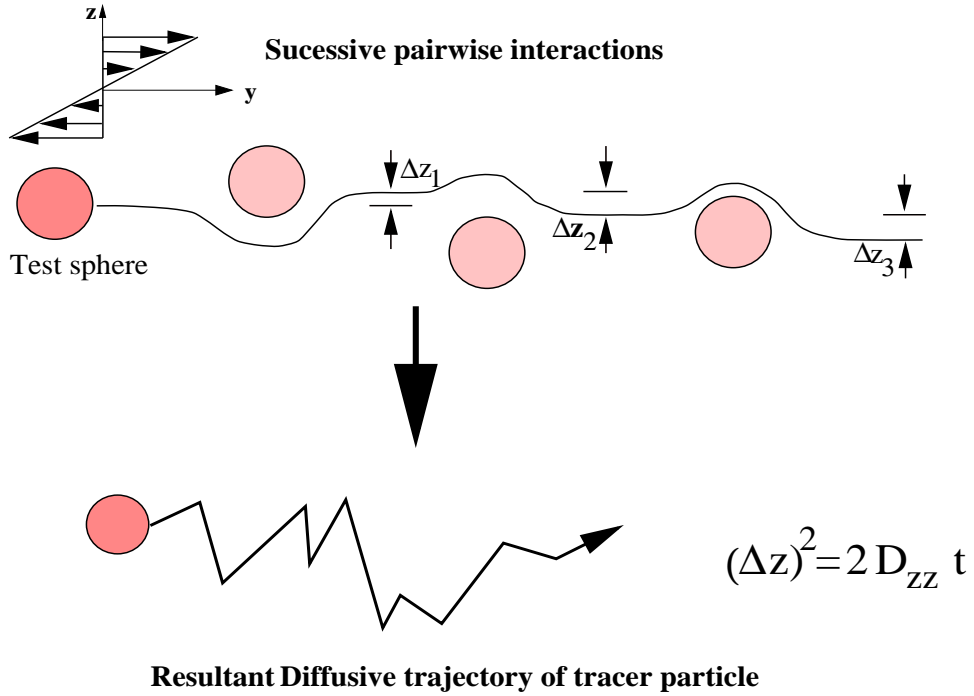


Figure 4.7: Tracer particle (darker shade) undergoing a random walk due to successive uncorrelated pair-interactions.

For the  $xx$  component, one needs to calculate the vorticity displacement  $(\Delta x)$  for any open trajectory, which in turn necessitates consideration of off-plane trajectories. Here we only evaluate the in-plane value of  $\hat{D}_{zz}$  from the expressions for  $(\Delta z)_{inplane}$  derived in previous sections and in Appendix C4. This would entail integrating only with respect to the  $z$  coordinate. Even so, as will be seen later in section 5.3.4, the scaling with  $St$  given

by the analysis in this section remains unaltered on subsequent integration with respect to  $x^{-\infty}$ . The projected in-plane value,  $\hat{D}_{zz}^{ip}$ , is given as

$$\frac{8\pi}{3}\hat{D}_{zz}^{ip} = 2 \int_0^\infty |z^{-\infty}| (\Delta z)_{inplane}^2 dz^{-\infty} = 2 \int_{m_1^c(St)^{\frac{1}{2}}}^\infty |z^{-\infty}| (\Delta z)_{inplane}^2 dz^{-\infty}, \quad (4.56)$$

where  $m_1^c$  is the offset of the limiting finite  $St$  open trajectory, and is given by (4.53). Owing to the antisymmetry of simple shear, it suffices to consider encounters in only one half of the shearing plane. The change in the lower limit from 0 to the limiting offset is because a sensible diffusivity can only be evaluated over the open trajectories. The rapid far-field decay of the in-plane gradient displacement (see (4.55)) ensures that the diffusivity integral is convergent with respect to the upper limit. Since  $(\Delta z)_{inplane} \sim O(St)$  for all trajectories with  $O(1)$  initial offsets, a naive estimate would suggest that  $\hat{D}_{zz}^{ip} \sim O(St^2)$ . However, for small initial offsets  $(\Delta z)_{inplane} \propto 1/z^{-\infty}$ , and the diffusivity integral has a logarithmic divergence that is cut off at an offset of  $O(St^{\frac{1}{2}})$ . This enhances the magnitude of  $\hat{D}_{zz}^{ip}$  by a factor of  $\ln St$ ; thus  $\hat{D}_{zz}^{ip} \sim (St)^2(\ln St + K)$ , where  $K$  is an  $O(1)$  constant.

For the purposes of this calculation, the ensemble of open in-plane trajectories can be divided into two regions based on the scaling of the gradient displacement:

Region 1: open trajectories with initial offsets greater than  $O(St^{\frac{1}{2}})$ , for which  $(\Delta z)_{inplane} < O(St^{\frac{1}{2}})$ .

Region 2: open trajectories with  $O(St^{\frac{1}{2}})$  initial offset for which  $\Delta z \sim O(St^{\frac{1}{2}})$  (this includes the limiting in-plane trajectory).

Accordingly, we divide the interval of integration as below:

$$\begin{aligned} \frac{4\pi \hat{D}_{zz}^{ip}}{3} &= \int_{m_1^c(S)t^{\frac{1}{2}}}^{bSt^{\frac{1}{2}-\epsilon}} |z^{-\infty}| (\Delta z)_{inplane}^2 dz^{-\infty} + \int_{bSt^{\frac{1}{2}-\epsilon}}^{\infty} |z^{-\infty}| (\Delta z)_{inplane}^2 dz^{-\infty} \\ &= I_1 + I_2, \end{aligned} \quad (4.57)$$

where  $0 < \epsilon < \frac{1}{2}$ . In the limit  $St \ll 1$ , we can have  $bSt^{-\epsilon} \gg 1$ , and at the same time  $bSt^{\frac{1}{2}-\epsilon} \ll 1$ , so there is a region of overlap between the two families of trajectories; while  $bSt^{-\epsilon}$  in  $I_1$  can be interpreted as a large offset on the scale of  $St^{\frac{1}{2}}$ ,  $bSt^{\frac{1}{2}-\epsilon}$  appears as a small  $O(1)$  offset in  $I_2$ . The objective is to obtain the leading order term in (4.57) independent of  $b$  and  $\epsilon$ , which will then be the first term in a small  $St$  asymptotic series for  $\hat{D}_{zz}^{ip}$ .

Region 1:  $z^{-\infty} > O(St^{\frac{1}{2}})$ :

$$I_1 = \int_{m_1^c(S)t^{\frac{1}{2}}}^{bSt^{\frac{1}{2}-\epsilon}} |z^{-\infty}| (\Delta z)_{inplane}^2 dz^{-\infty},$$

which may be rewritten as

$$I_1 = \int_{m_1^c(S)t^{\frac{1}{2}}}^{(bSt^{-\epsilon})St^{\frac{1}{2}}} |z^{-\infty}| (\Delta z)_{inplane}^2 dz^{-\infty}.$$

Regarding both the upper and lower limits as  $O(St^{\frac{1}{2}})$ , and changing variables to  $z^{-\infty} = (St)^{\frac{1}{2}} \hat{z}^{-\infty}$ , we get

$$I_1 = St \int_{m_1^c}^{bSt^{-\epsilon}} |\hat{z}^{-\infty}| (\Delta z)_{inplane}^2 d\hat{z}^{-\infty}. \quad (4.58)$$

We now use  $\Delta z = m_1'(St^{\frac{1}{2}})$ , where  $m_1'$  is given by equation (C.23) with  $m_1$  replaced by  $\hat{z}^{-\infty}$ .

We obtain

$$|\Delta z|_{inplane} = St^{\frac{1}{2}} \left\{ \hat{z}^{-\infty} - \left[ (\hat{z}^{-\infty})^2 + 2k(d) d \frac{(2-B_0)}{(1-A_0)} \exp\left(-\int_d^{\infty} q(r') dr'\right) \right]^{\frac{1}{2}} \right\},$$

$$\begin{aligned}
&= St^{\frac{1}{2}} \left\{ \hat{z}^{-\infty} - \left[ (\hat{z}^{-\infty})^2 - 2 |k(d)| d \frac{(2-B_0)}{(1-A_0)} \exp \left( -\int_d^\infty q(r') dr' \right) \right]^{\frac{1}{2}} \right\}, \\
\Rightarrow (\Delta z)_{inplane}^2 &= St \left\{ \hat{z}^{-\infty} - [(\hat{z}^{-\infty})^2 - (m_1^c)^2]^{\frac{1}{2}} \right\}^2, \tag{4.59}
\end{aligned}$$

where we have used (4.53) for  $m_1^c$  (see section 4.4.3). Using (4.59) in (4.58),

$$I_1 = (St)^2 \int_{m_1^c}^{bSt^{-\epsilon}} \hat{z}^{-\infty} \left\{ \hat{z}^{-\infty} - [(\hat{z}^{-\infty})^2 - (m_1^c)^2]^{\frac{1}{2}} \right\}^2 d\hat{z}^{-\infty}.$$

Using the substitution  $\hat{z}^{-\infty} = m_1^c \sec \psi$ , we get

$$\begin{aligned}
I_1 &= (St)^2 \int_{m_1^c}^{bSt^{-\epsilon}} m_1^c \sec \psi \{m_1^c (\sec \psi - \tan \psi)\}^2 m_1^c \sec \psi \tan \psi d\psi, \\
&= (St)^2 (m_1^c)^4 \int_{m_1^c}^{bSt^{-\epsilon}} \sec^2 \psi \tan \psi (\sec \psi - \tan \psi)^2 d\psi, \\
\Rightarrow I_1 &= (St)^2 (m_1^c)^4 \left[ \frac{1}{2 \cos^4 \psi} - \frac{1}{2 \cos^2 \psi} + \frac{\sin \psi}{4 \cos^2 \psi} - \frac{\sin \psi}{2 \cos^4 \psi} + \frac{1}{4} \ln \left\{ \tan \left( \frac{\pi}{4} + \frac{\psi}{2} \right) \right\} \right]_{\hat{z}^{-\infty}=m_1^c}^{\hat{z}^{-\infty}=bSt^{-\epsilon}}.
\end{aligned}$$

Rewriting in terms of  $\hat{z}^{-\infty}$ , we obtain

$$\begin{aligned}
I_1 &= (St)^2 (m_1^c)^4 \left[ \frac{(\hat{z}^{-\infty})^4}{2(m_1^c)^4} - \frac{(\hat{z}^{-\infty})^2}{2(m_1^c)^2} + \frac{1}{4} \left( \frac{(\hat{z}^{-\infty})^2}{(m_1^c)^2} - \frac{2(\hat{z}^{-\infty})^4}{(m_1^c)^4} \right) \left( 1 - \frac{(m_1^c)^2}{(\hat{z}^{-\infty})^2} \right)^{\frac{1}{2}} \right. \\
&\quad \left. + \frac{1}{4} \ln \left\{ \cot \left( \frac{1}{2} \sin^{-1} \left( \frac{m_1^c}{\hat{z}^{-\infty}} \right) \right) \right\} \right]_{\hat{z}^{-\infty}=m_1^c}^{\hat{z}^{-\infty}=bSt^{-\epsilon}},
\end{aligned}$$

where we have used  $\cos \psi = m_1^c / \hat{z}^{-\infty}$  and  $\sin \psi = \{1 - (m_1^c / \hat{z}^{-\infty})^2\}^{\frac{1}{2}}$ . The quantity within

brackets equals zero at the lower limit, and therefore

$$\begin{aligned}
I_1 &= (St)^2 (m_1^c)^2 \left[ \frac{(\hat{z}^{-\infty})^4}{2(m_1^c)^2} - \frac{(\hat{z}^{-\infty})^2}{2(m_1^c)^2} + \frac{1}{4} \left( \frac{(\hat{z}^{-\infty})^2}{(m_1^c)^2} - 2 \frac{(\hat{z}^{-\infty})^4}{(m_1^c)^4} \right) \left( 1 - \frac{(m_1^c)^2}{(\hat{z}^{-\infty})^2} \right)^{\frac{1}{2}} \right. \\
&\quad \left. + \frac{1}{4} \ln \left\{ \cot \left( \frac{1}{2} \sin^{-1} \left( \frac{m_1^c}{\hat{z}^{-\infty}} \right) \right) \right\} \right]_{\hat{z}^{-\infty}=bSt^{-\epsilon}}.
\end{aligned}$$

Since  $\hat{z}^{-\infty} = bSt^{-\epsilon} \gg 1$ , we find the asymptotic form of the first term for large  $\hat{z}^{-\infty}$ , giving

$$\begin{aligned} \left(1 - \frac{(m_1^c)^2}{(\hat{z}^{-\infty})^2}\right)^{\frac{1}{2}} &= 1 - \frac{(m_1^c)^2}{2(\hat{z}^{-\infty})^2} - \frac{(m_1^c)^4}{8(\hat{z}^{-\infty})^4} + O\left(\frac{1}{(\hat{z}^{-\infty})^6}\right), \\ \ln \left\{ \cot\left(\frac{1}{2} \sin^{-1}\left(\frac{m_1^c}{\hat{z}^{-\infty}}\right)\right) \right\} &= \ln \left( \frac{2\hat{z}^{-\infty}}{m_1^c} \right) + O\left(\frac{1}{(\hat{z}^{-\infty})^2}\right). \end{aligned}$$

Using these in the expression for  $I_1$ , we obtain

$$I_1 = (St)^2 (m_1^c)^4 \left\{ -\frac{1}{16} + \frac{1}{4} \ln \left( \frac{2\hat{z}^{-\infty}}{m_1^c} \right) + O\left(\frac{1}{(\hat{z}^{-\infty})^2}\right) \right\}_{\hat{z}^{-\infty} = bSt^{-\epsilon}}.$$

Retaining only through the logarithmic term

$$\begin{aligned} I_1 &= (St)^2 (m_1^c)^4 \left[ -\frac{1}{16} + \frac{1}{4} \ln\left(\frac{2}{m_1^c}\right) + \frac{1}{4} \ln(bSt^{-\epsilon}) \right], \\ &= (St)^2 \left[ \frac{(m_1^c)^4}{4} (\ln b - \epsilon \ln St) + K' \right], \end{aligned} \quad (4.60)$$

where

$$K' = -\frac{(m_1^c)^4}{16} \left\{ 1 + 4 \ln\left(\frac{m_1^c}{2}\right) \right\}. \quad (4.61)$$

Region 2:  $z^{-\infty} \sim O(St^{\frac{1}{2}})$ :

$$I_2 = \int_{bSt^{\frac{1}{2}-\epsilon}}^{\infty} |z^{-\infty}| (\Delta z)_{inplane}^2 dz^{-\infty},$$

in which we now use the gradient displacement as given by equation (4.45) in section 4.4.1,

i.e.,

$$(\Delta z)_{inplane}^2 = \frac{4(St)^2}{(z^{-\infty})^2} \left[ \int_c^{\infty} \exp \left[ -\int_{r'}^{\infty} q(r') dr' \right] \left\{ \frac{r' f_1(r', \phi'_0)}{(1-A')} + \frac{\{(1-B') \sin^2 \phi'_0 + \frac{B'}{2}\} f_2(r', \phi'_0)}{(1-A')^2 \sin \phi'_0 \cos \phi'_0} \right\} dr' \right]^2.$$

It must be noted that in the above integral,  $\Delta z$  contains functions of  $c$  which in turn are functions of  $z^{-\infty}$  via (4.33). Therefore,

$$I_2 = (St)^2 \int_{bSt^{\frac{1}{2}-\epsilon} z^{-\infty}}^{\infty} \frac{4dz^{-\infty}}{z^{-\infty}} \left( \int_c^{\infty} \exp \left[ - \int_{r'}^{\infty} q(r') dr' \right] \left\{ \frac{r' f_1(r', \phi'_0)}{(1-A')} + \frac{\{(1-B') \sin^2 \phi'_0 + \frac{B'}{2}\} f_2(r', \phi'_0)}{(1-A')^2 \sin \phi'_0 \cos \phi'_0} \right\} dr' \right)^2.$$

The above integral is logarithmically divergent at its lower limit, but the divergence is precisely cancelled off by an analogous term in  $I_1$ , and the leading order approximation to the diffusivity is independent of the  $b$  and  $\epsilon$ , as it should be. This can be seen by rewriting  $I_2$  as

$$I_2 = (St)^2 \left( \int_{bSt^{\frac{1}{2}-\epsilon} z^{-\infty}}^{\infty} \frac{4}{z^{-\infty}} \left[ \int_c^{\infty} \exp \left[ - \int_{r'}^{\infty} q(r') dr' \right] \left\{ \frac{r' f_1(r', \phi'_0)}{(1-A')} + \frac{\{(1-B') \sin^2 \phi'_0 + \frac{B'}{2}\} f_2(r', \phi'_0)}{(1-A')^2 \sin \phi'_0 \cos \phi'_0} \right\} dr' \right]^2 - \int_{bSt^{\frac{1}{2}-\epsilon} z^{-\infty}}^1 \frac{(m_1^c)^4}{4} \frac{dz^{-\infty}}{z^{-\infty}} \right) + (St)^2 \int_{bSt^{\frac{1}{2}-\epsilon} z^{-\infty}}^1 \frac{(m_1^c)^4}{4} \frac{dz^{-\infty}}{z^{-\infty}}.$$

The first term enclosed in parentheses is no longer divergent since the added integral exactly cancels off the logarithmic divergence. One can therefore extend the lower limit in the integrals to 0 incurring only an error of  $o(St)$ . The  $b$  and  $\epsilon$  dependent terms in the second integral are identically cancelled by the first term in (4.60).

Adding the expressions for  $I_1$  and  $I_2$ , one obtains

$$\frac{4\pi \hat{D}_{zz}^{ip}}{3} = 2(St)^2 \left\{ - \frac{(m_1^c)^4}{8} \ln St + K \right\}, \quad (4.62)$$

where  $K = K' + K''$ , and

$$K'' = \int_0^{\infty} dz^{-\infty} \left\{ \frac{4}{z^{-\infty}} \left[ \int_c^{\infty} \exp \left[ - \int_{r'}^{\infty} q(r'') dr'' \right] \left\{ \frac{r' f_1(r', \phi'_0)}{(1-A')} + \frac{\{(1-B') \sin^2 \phi'_0 + \frac{B'}{2}\} f_2(r', \phi'_0)}{(1-A')^2 \sin \phi'_0 \cos \phi'_0} \right\} dr' \right]^2 - \frac{(m_1^c)^4}{4z^{-\infty}} \mathbf{H}(1 - \hat{z}^{\infty}) \right\}.$$

$St$	$\hat{D}_{zz}^{ip} (numer.)$	$\hat{D}_{zz}^{ip} (anal.)$
0.1	$2.546 \times 10^{-3}$	$2.643 \times 10^{-3}$
0.01	$2.72 \times 10^{-5}$	$2.841 \times 10^{-5}$
0.001	$2.914 \times 10^{-7}$	$3.039 \times 10^{-7}$

Table 4.4: Comparison of analytical and numerical values of the in-plane diffusivity for different Stokes numbers.

$K'$  is defined by (4.61), and  $\mathbf{H}(x)$  is the heavyside function. The above expression clearly shows the non-analytic dependence of  $\hat{D}_{zz}^{ip}$  on  $St$ .

In table 4.4 we compare the values of  $\hat{D}_{zz}^{ip}$  given by (4.62) to those evaluated numerically for different Stokes numbers. The latter were obtained by (numerically) evaluating the diffusivity integral, (4.56); the in-plane gradient displacement for each open trajectory is obtained from the numerical integration of the trajectory equation (4.25).

#### 4.4.6 Behavior within the limiting trajectory

For  $St = 0$  the limiting open trajectory is fore-aft symmetric and asymptotes to the  $y$ -axis as  $y \rightarrow \pm\infty$ ; trajectories lying within form closed orbits. One may regard the plane of shear from a dynamical systems perspective. In order to carry forth this analogy, we introduce the change of variables  $r_1 = (r-2)$ ,  $\phi_1 = \phi$ , which maps the surface of the reference sphere ( $r = 2$ ) to the origin ( $r_1 = 0$ ), and is a one-to-one transformation at every other point in the plane. Thus for  $St = 0$ , the trajectory equations (4.25) constitute a two dimensional dynamical system of the form

$$\frac{d\mathbf{y}_1}{dt} = \mathbf{F}_0(\mathbf{y}_1), \quad (4.63)$$

where  $\mathbf{y}_1 = (y_1, z_1)$ ; the origin is a (local) ‘center’, a non-hyperbolic fixed point. In the  $(y_1, z_1)$  coordinates, the phase plane looks similar to that of a simple pendulum (see Fig

4.17). However, the crucial difference is that, while in the latter case one has a linear approximation (with pure imaginary eigenvalues) close to the origin, implying that the near-field closed orbits are approximately circular, the former affords no such simplification. That the system of equations (4.63) is not linearizable about the origin can be seen by writing down the equations in their explicit cartesian form for  $r_1 \rightarrow 0$ :

$$\begin{aligned}\frac{dy_1}{dt} &= \frac{z_1}{(y_1^2 + z_1^2)} \left[ 2(4.077)y_1^2 + z_1^2 + \frac{\hat{B}(0)}{2}(y_1^2 - z_1^2) \right], \\ \frac{dz_1}{dt} &= \frac{y_1}{(y_1^2 + z_1^2)} \left[ 2(4.077)z_1^2 - y_1^2 + \frac{\hat{B}(0)}{2}(z_1^2 - y_1^2) \right],\end{aligned}\tag{4.64}$$

where  $B(r) = \hat{B}(r_1)$ , and we have used that  $\lim_{r_1 \rightarrow 0} \hat{A}(r_1) = 1 - 4.077r_1$ . Since all terms in  $dy_1/dz_1$  are of  $O(r_1^3)$  for small  $r_1$ , there does not exist a non-trivial linear approximation in the vicinity of the fixed point. It must also be noted that the hydrodynamic function  $B$  approaches its contact value only in a logarithmic fashion, thereby precluding a Taylor series expansion about the singular point  $r_1 = 0$ .

The dynamical system for finite  $St$  can be written as

$$\frac{d\mathbf{y}_1}{dt} = \mathbf{F}_0(\mathbf{y}_1) + St \mathbf{F}_1(\mathbf{y}_1).\tag{4.65}$$

For small but finite  $St$  the limiting trajectory, as seen earlier, starts from an offset of  $O(St^{\frac{1}{2}})$  at  $y = -\infty (+\infty)$  for positive  $z$  (negative  $z$ ), and goes to zero as  $y \rightarrow \infty (-\infty)$ . It will be shown below that inertial effects lead to a bifurcation in the phase plane. For  $St > 0$ , the origin loses its (neutral) stability, and there appears a new stable limit cycle in the phase plane with its (in-plane) domain of attraction being the region of the plane included between

the pair of limiting trajectories for  $z$  positive and negative. Trajectories lying outside the limit cycle but within the limiting trajectories spiral into it, while those lying within the limit cycle spiral out onto it as  $t \rightarrow \infty$ . It must be emphasised that this bifurcation at  $St = 0$  is not a Hopf bifurcation, since the linear approximation yields a trivial Jacobian matrix and the smoothness conditions for the vector field  $\mathbf{F}_0 + St\mathbf{F}_1$  are not satisfied owing to the singular behavior of  $B$  close to contact; the derivation of the normal form for the Hopf bifurcation requires a vector field, which is  $C^r$ ,  $r \geq 5$  (Wiggins 1990). Indeed, unlike a supercritical Hopf bifurcation where the amplitude of the stable limit cycle grows as  $O(St^\alpha)$  with  $\alpha > 0$  (i.e., the limit cycle emerges in a smooth manner from the fixed point with variation in the parameter away from its critical value), the location of the limit cycle in this case is, to leading order, independent of  $St$  for small  $St$ . Since the finite  $St$  phase plane consists of a hyperbolic (stable) limit cycle and a hyperbolic (unstable) fixed point, it is structurally stable, i.e., a further small change in  $St$  will only lead to quantitative alterations of the trajectory topology (Guckenheimer & Holmes 1983).

#### 4.4.6.1 Analysis of stable limit cycle by perturbation

We first present a physical argument supporting the existence of a stable limit cycle for finite  $St$ , and then go on to locate it in the shearing plane by applying the perturbation analysis developed in previous sections.

From the zero-Stokes phase plane (see Fig 4.17) we see that while closed trajectories very near the reference sphere are almost circular (and hence, convex), those close to the separatrix resemble the open trajectories just above in that they have extensive regions with a concave curvature. Thus in the latter case, one would expect the analog of a negative gradient displacement for finite  $St$ ; this translates to a spiralling in behavior, i.e., a trajectory

starting from  $(-R_2, 0)$  intersects the  $y$  axis again at  $(R'_2, 0)$  with  $R'_2 < R_2$ . On the other hand, as one approaches the reference sphere, the curvature becomes uniformly convex, and inertia now tends to push the second sphere in a radially outward direction, which leads to a finite  $St$  trajectory that spirals outwards. This then implies the existence of a stable limit cycle in between. Since the inward and outward spiralling are due to the same underlying physical mechanism of particle inertia, it is plausible that a decrease (increase) in  $St$  would reduce (enhance) the rate of spiralling in both cases equally, suggesting that the location of the stable limit cycle may be independent of  $St$ .

Owing to the antisymmetry of simple shear, the points of intersection of the limit cycle with the  $y$  and  $z$  axes must be symmetrically located with respect to the origin. Utilizing this symmetry, one can, in a manner exactly similar to the analysis of the limiting finite  $St$  open trajectory (see section 4.4.3), perturb the portions of the limit cycle in  $(0, \pi/2)$  and  $(\pi/2, \pi)$  about the same zero-Stokes closed orbit (intersecting the  $y$  and  $z$  axes in  $(\pm R_2^{lim}, 0)$  and  $(0, \pm R_1^{lim})$  respectively), and then piece the two portions together. Perturbing the  $(\pi/2, \pi)$  branch gives us  $r_{\frac{\pi}{2}}^- = R_1^{lim} + St k_{lim}$  for its radial distance at  $\phi = \pi/2$ , and perturbing the  $(0, \pi/2)$  branch gives  $r_{\frac{\pi}{2}}^+ = R_1^{lim} - St k_{lim}$ . The condition  $r_{\frac{\pi}{2}}^+ = r_{\frac{\pi}{2}}^-$  then reduces to

$$k_{lim} = 0, \tag{4.66}$$

where  $k_{lim} \equiv k(R_1^{lim}, R_2^{lim})$ .

We now find the general expression for  $k$  for a finite  $St$  spiralling trajectory. The spiralling trajectory is perturbed about a zero-Stokes closed orbit that has the same radial distance ( $r = R_2$ ) at  $\phi = 0$ . It must be emphasised that an analogous perturbative scheme fails for the case where the inertial and zero-Stokes (closed) trajectories start from

the same point at  $\phi = \pi/2$ , since the solutions at  $O(1)$  and  $(St)$  become comparable in magnitude sufficiently far downstream (see Appendix C4); this is, of course, similar to the non-uniformity encountered for open trajectories with  $O(St^{\frac{1}{2}})$  offsets (see section 4.4.3). The boundary condition  $\phi_1 = 0$  at  $r = R_2$  is imposed in the inner layer around  $\phi = 0$ <sup>9</sup>. The  $O(1)$  and  $O(St)$  solutions are

$$r^2 \sin^2 \phi_0 = \int_r^{R_2} \exp \left[ - \int_{r'}^r q(r'') dr'' \right] \frac{B'r'}{(1-A')} dr',$$

$$r\phi_1 = \frac{1}{r \cos \phi_0 \sin \phi_0} \int_{R_2}^r \exp \left[ - \int_{r'}^r q(r'') dr'' \right] \left\{ \frac{r' f_1(r', \phi'_0)}{(1-A')} \right. \\ \left. + \frac{\{(1-B') \sin^2 \phi'_0 + \frac{B'}{2}\} f_2(r', \phi'_0)}{(1-A')^2 \sin \phi'_0 \cos \phi'_0} \right\} dr'.$$

It can easily be verified that the  $O(St)$  correction remains uniformly small for all  $r$ . In fact, this conclusion can be arrived at from a comparison of the  $O(1)$  and  $O(St)$  terms in the governing equation (4.25). On matching the solutions in the outer layer and in the inner layer around  $\phi = \pi/2$ , one obtains the radial distance of the finite  $St$  trajectory at  $\phi = \pi/2$  as  $R_1 + St k$ , where  $k$  is defined in terms of  $R_1$  and  $R_2$  as

$$k(R_1, R_2) = - \frac{2(1-A_0)}{c(2-B_0)} \int_{R_1}^{R_2} \exp \left[ - \int_{r'}^{R_1} q(r'') dr'' \right] \left\{ \frac{r' f_1(r', \phi'_0)}{(1-A')} \right. \\ \left. + \frac{\{(1-B') \sin^2 \phi'_0 + \frac{B'}{2}\} f_2(r', \phi'_0)}{(1-A')^2 \sin \phi'_0 \cos \phi'_0} \right\} dr'. \quad (4.67)$$

Here the subscript ‘0’ indicates evaluation of the particular hydrodynamic function at  $r = R_1$ , where  $R_1$  is the radial coordinate of the zero-Stokes orbit at  $\phi = \pi/2$ . The above expression can be compared to the analogous expression obtained for open trajectories viz. (4.40) in section 4.4.1.4. For the closed trajectory,  $R_1$  plays the role of  $c$  while  $R_2$  replaces the infinity.

<sup>9</sup>The zero-Stokes closed orbits become purely tangential at the points  $\phi = 0, \pi/2, 3\pi/2$  and  $\pi$ . Thus, besides those present for open trajectories, one has to also account for angular boundary layers around  $\phi = 0$  and  $\pi$  in the perturbation analysis.

The change in sign is because the  $k$  above refers to the quadrant  $(0, \pi/2)$  as opposed to  $(\pi/2, \pi)$  in (4.40).

When  $k > 0$ , the finite  $St$  trajectory starts from outside the zero-Stokes closed orbit at  $\phi = \pi/2$ , and intersects it at  $\phi = 0$ ; a positive value of  $k$  would thus correspond to a trajectory that spirals in. Likewise, a negative value of  $k$  would imply a trajectory that spirals out. Using (4.66) and (4.67), one obtains

$$\int_{R_1^{lim}}^{R_2^{lim}} \exp\left[-\int_{r'}^{R_1^{lim}} q(r'') dr''\right] \left\{ \frac{r' f_1(r', \phi'_0)}{(1-A')} + \frac{\{(1-B') \sin^2 \phi'_0 + \frac{B'}{2}\} f_2(r', \phi'_0)}{(1-A')^2 \sin \phi'_0 \cos \phi'_0} \right\} dr' = 0, \quad (4.68)$$

where  $R_1^{lim}$  and  $R_2^{lim}$  are related by the zero-Stokes trajectory equation. Equation (4.68) serves as an algebraic equation for the unknown  $R_1^{lim}$  (or  $R_2^{lim}$ ) and determines, to  $O(St)$  the coordinates of the limit cycle. Clearly, the solution of (4.68) is independent of  $St$ .

Below, we evaluate the integral on the left hand side of (4.68) numerically in order to isolate the region in which it changes sign.

$R_2$	$k_{lim}$
2.3	0.075
2.1	0.018
2.05	-0.0068

The perturbation theory therefore predicts the limit cycle to intersect the  $y$  axis at approximately  $(\pm 2.05, 0)$ .

In order to verify that this value is independent of  $St$ , we numerically integrate (4.25) for three different values of  $St$  ranging over an order of magnitude (from 0.2 to 0.02), with the initial points being  $(-2.5, 0)$ ,  $(-2.1, 0)$  and  $(-2.05, 0)$ . The sequence of figures from Fig 4.8 to 4.16 depicts the trajectories for these cases; the figures show a magnified view of the finite  $St$  spiralling trajectory in the region of its intersection with the negative  $y$  axis. One

observes that while the spirals become progressively tighter with decreasing  $St$ , the location of the limit cycle remains virtually independent of  $St$  in the range considered.

Finally, Figs 4.17 and 4.18 show the phase plane of trajectories for zero and finite Stokes number respectively. The figures have not been drawn to scale; the near-field portions of the trajectory plane, for instance, are intentionally magnified in order to clearly depict the finite  $St$  modifications. It can be seen that the inertial alteration of the phase plane is still consistent with the antisymmetry of the ambient simple shear flow. The qualitative effect of the  $(\mathbf{V} \cdot \nabla_{\mathbf{x}} \boldsymbol{\Omega})$  term remains the same as for the case of open trajectories and therefore makes the trajectories outside the limit cycle spiral in more rapidly; neglecting this coupling term would push the limit cycle further away from contact.

The nearest distances of approach for the zero-Stokes closed orbits are  $O(10^{-5}a)$ , and therefore, closed orbits may only be observed for extremely smooth inertialess spheres. The near-field inertial modifications described above will, in practice, be obscured by surface roughness of the spheres or the presence of short-ranged interparticle forces. This does not, however, undermine the fundamental role that these effects play in determining the interaction of two finite  $St$  particles. From the practical point of view, the inertial modifications remain important since effects similar to the above are observed for the case of off-plane trajectories (see Chapter 4), where the distances of approach are larger than the in-plane values. Even when the near-field interaction of the spheres is dominated by non-hydrodynamic mechanisms such as Van der Waals forces (leading to aggregation), the resulting rate of aggregation would depend on the fraction of trajectories that come closer to the reference sphere than a certain distance set by the interparticle force, which would be related to the distances of nearest approach of the finite  $St$  trajectories in Fig 4.18.

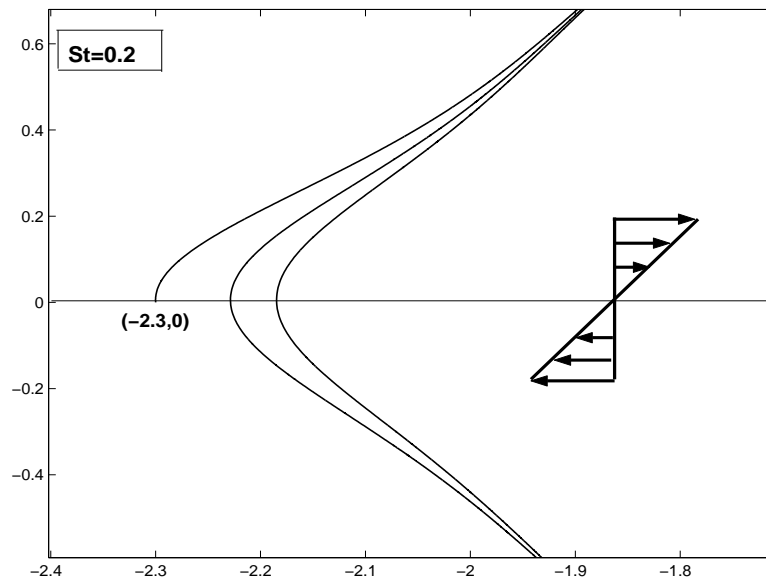


Figure 4.8: Trajectory spiralling into the limit cycle from  $(-2.3, 0)$  for  $St = 0.2$ .

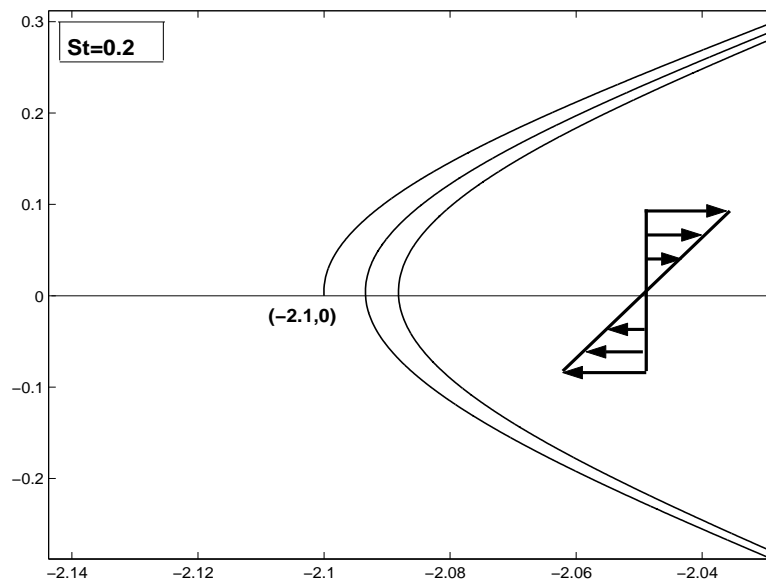


Figure 4.9: Trajectory spiralling into the limit cycle from  $(-2.1, 0)$  for  $St = 0.2$ .

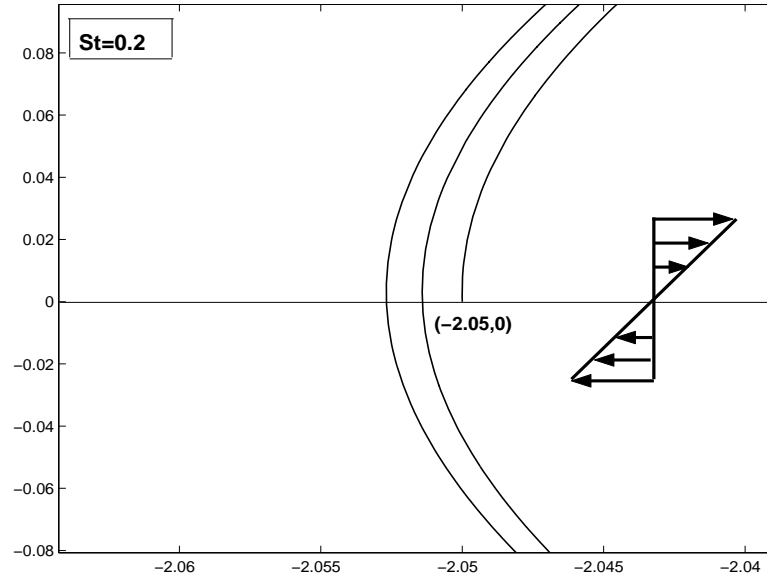


Figure 4.10: Trajectory spiralling out onto the limit cycle from  $(-2.05, 0)$  for  $St = 0.2$ .

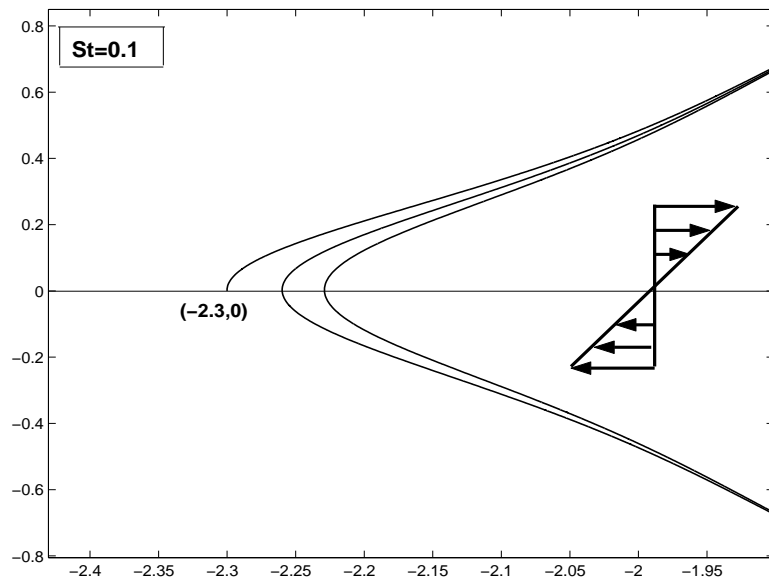


Figure 4.11: Trajectory spiralling into the limit cycle from  $(-2.3, 0)$  for  $St = 0.1$ .

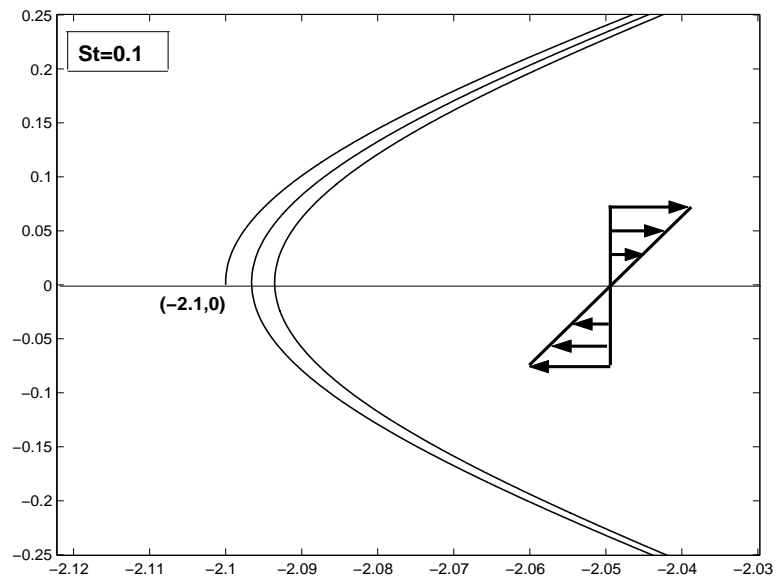


Figure 4.12: Trajectory spiralling into the limit cycle from  $(-2.1, 0)$  for  $St = 0.1$ .

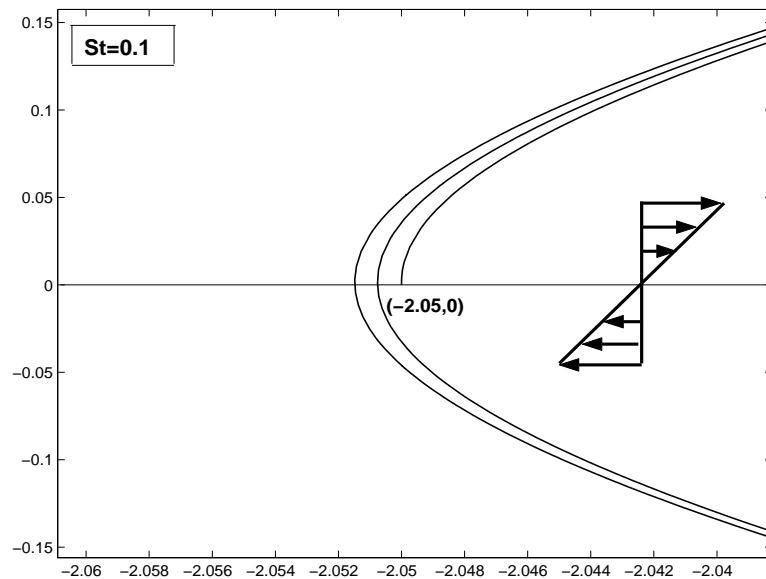


Figure 4.13: Trajectory spiralling out onto the limit cycle from  $(-2.05, 0)$  for  $St = 0.1$ .

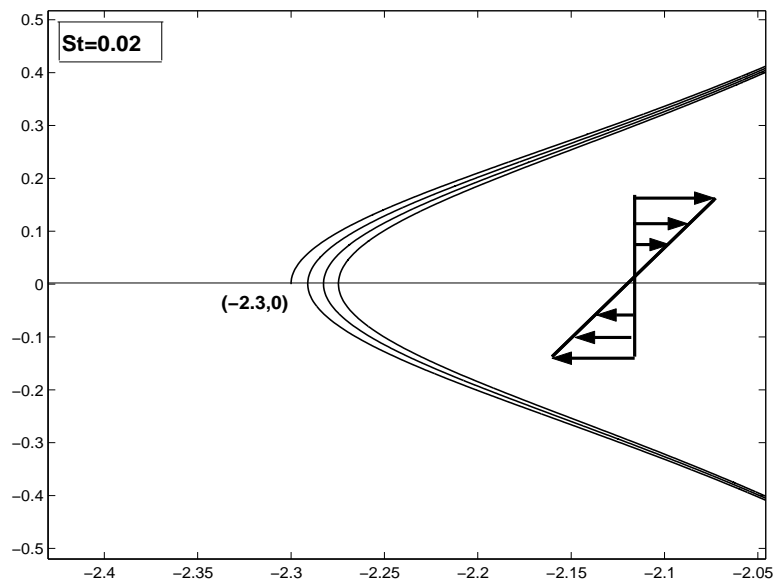


Figure 4.14: Trajectory spiralling into the limit cycle from  $(-2.3, 0)$  for  $St = 0.02$ .

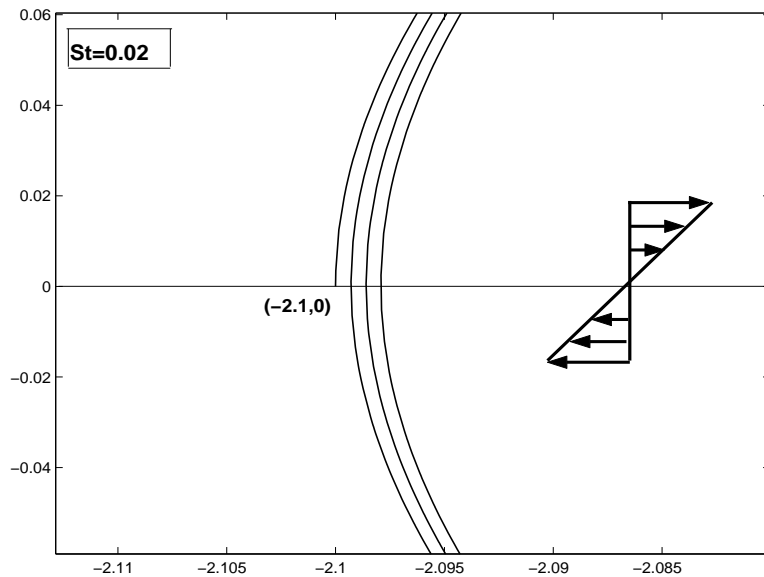


Figure 4.15: Trajectory spiralling into the limit cycle from  $(-2.1, 0)$  for  $St = 0.02$ .

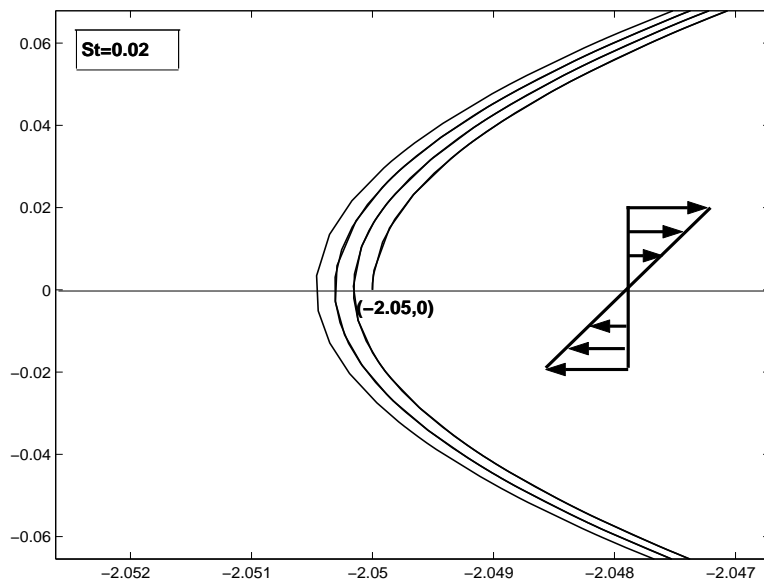


Figure 4.16: Trajectory spiralling out onto the limit cycle from  $(-2.05, 0)$  for  $St = 0.02$ .

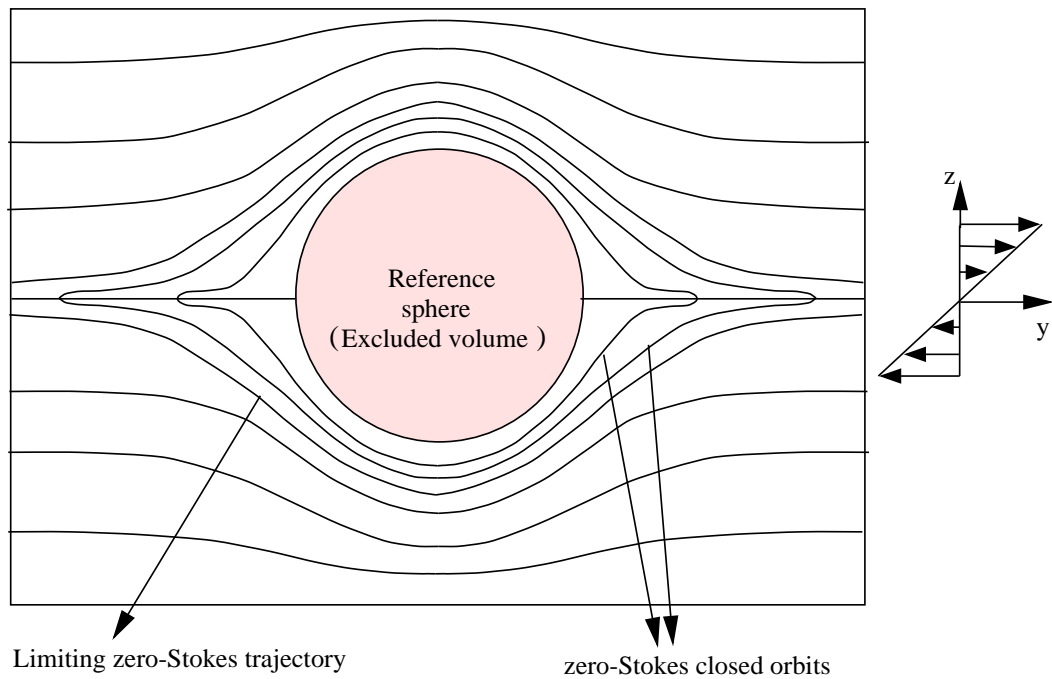


Figure 4.17: Phase plane of trajectories for  $St = 0$  in simple shear flow.

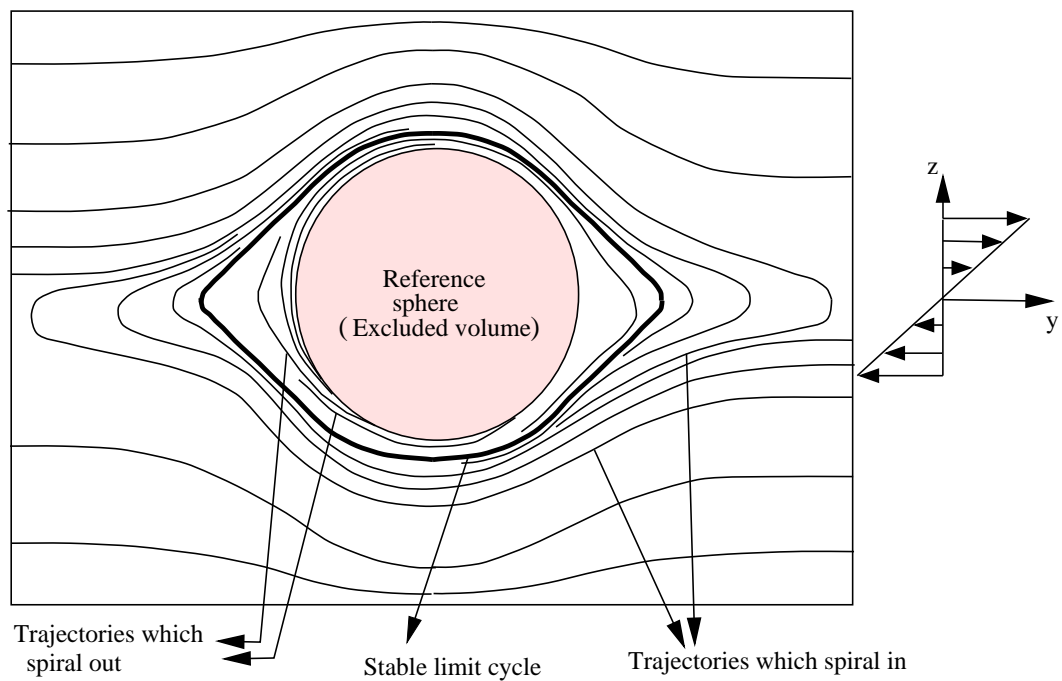


Figure 4.18: Phase plane of trajectories for finite  $St$  in simple shear flow.

## Bibliography

- [1] Abramowitz, M. & Stegun, I.A. 1972 *Handbook of Mathematical Functions*. Dover.
- [2] Batchelor, G.K. & Green, J.T. 1972a The hydrodynamic interaction of two small freely-moving spheres in a linear flow field. *J. Fluid Mech.* **56**, 375-400.
- [3] Batchelor, G.K. & Green, J.T. 1972b The determination of the bulk stress in a suspension of spherical particles to  $O(c^2)$ . *J. Fluid Mech.* **56**, 401-427.
- [4] Brady, J.F. & Bossis, G. 1988 Stokesian dynamics. *Ann. Rev. Fluid Mech.* **20**, 111-157.
- [5] daCunha, F.R. & Hinch, E.J. 1996 Shear-induced dispersion in a dilute suspension of rough spheres. *J. Fluid Mech.* **309**, 211-223.
- [6] Davis, R.H. 1996 Hydrodynamic diffusion of suspended particles: A symposium. *J. Fluid Mech.* **310**, 325-335.
- [7] Gradshteyn, I.S. & Ryzhik, I.M. 2000 *Table of Integrals, Series and Products*. Academic Press.
- [8] Guckenheimer, J. & Holmes, P. 1983 *Nonlinear oscillations, dynamical systems, and bifurcations of vector fields*. Springer-Verlag.
- [9] Kevorkian, J. & Cole, J.D. 1995 *Multiple Scale and Singular Perturbation Methods*. Springer-Verlag.
- [10] Kim, S. & Karrila, S.J. 1991 *Microhydrodynamics: Principles and Selected Applications*. Butterworth-Heinemann.

- [11] Koch, D.L. 1990 Kinetic theory for a monodisperse gas-solid suspension. *Phys. Fluids* **A2**(10), 1711-1723.
- [12] Kumaran, V. & Koch, D.L. 1993a Properties of a bidisperse particle-gas suspension. 1. collision time small compared with viscous relaxation time. *J. Fluid Mech.* **247**, 623-641.
- [13] Kumaran, V. & Koch, D.L. 1993b Properties of a bidisperse particle-gas suspension. 2. viscous relaxation time small compared with collision time. *J. Fluid Mech.* **247**, 643-660.
- [14] Lagerstrom, P.A. & Casten, R.G. 1972 Basic concepts underlying singular perturbation techniques. *SIAM Rev.* **14**, 63-120.
- [15] Leighton, D. & Acrivos, A. 1987a Measurement of shear-induced self-diffusion in concentrated suspensions. *J. Fluid Mech.* **177**, 109-131.
- [16] Leighton, D. & Acrivos, A. 1987b The shear-induced migration of particles in concentrated suspensions. *J. Fluid Mech.* **181**, 415-439.
- [17] Sangani, A.S., Mo, G., Tsao, H.K. & Koch, D.L. 1996 Simple shear flow of dense gas-solid suspensions at finite Stokes numbers. *J. Fluid Mech.* **313**, 309-341.
- [18] Sundararajakumar, R.R. & Koch, D.L. 1996 Non-continuum lubrication flows between particles colliding in a gas. *J. Fluid Mech.* **313**, 283-308.
- [19] Tsao, H.K. & Koch D.L. 1995 Simple shear flows of dilute gas-solid suspensions. *J. Fluid Mech.* **296**, 211-245.
- [20] Van Dyke, M. 1975 *Perturbation Methods in Fluid Mechanics*. Academic Press.
- [21] Wiggins, S. 1990 *Introduction to applied nonlinear dynamical systems and chaos*. Springer-Verlag.

- [22] Zarraga, I.E. & Leighton, D.T. 2001 Shear-induced diffusivity in a dilute bidisperse suspension of hard spheres. *J. Colloid Interf. Sci.* **243**, 503-514.

## Chapter 5

# Trajectory analysis for inertial non-Brownian suspensions: off-plane trajectories

### 5.1 Introduction

In the previous chapter we studied the finite  $St$  modification of trajectories in the shearing ( $yz$ ) plane. Here we examine the effects of particle inertia on off-plane trajectories. As for the in-plane case, the finite  $St$  off-plane open trajectories are no longer fore-aft symmetric, suffering net transverse displacements in both the gradient ( $z$ ) and vorticity ( $x$ ) directions. This is shown in Figs 5.1 and 5.2, where we have plotted the  $xz$  and  $yz$  projections of a trajectory for  $St = 0$  and  $St = 0.1$  in order to show both transverse displacements at finite  $St$ ; the trajectory originates from the same upstream point in the two cases.

The more dramatic effects of inertia occur via destruction of the off-plane closed orbits that exist for zero Stokes number. In contrast to the in-plane case (see Fig 4.18), the topology of the resulting spiralling trajectories is much more complex owing to the additional degree of freedom orthogonal to the shearing plane. A glimpse of this complex behavior is shown in Figs 5.3 and 5.4. Fig 5.3 shows a zero-Stokes closed orbit that passes through  $(x, y, z) \equiv (0.1, -3, 0)$ , while Fig 5.4 depicts a finite  $St$  spiralling trajectory passing through the same point. The spiralling trajectory approaches the shearing plane as  $t \rightarrow \infty$ .

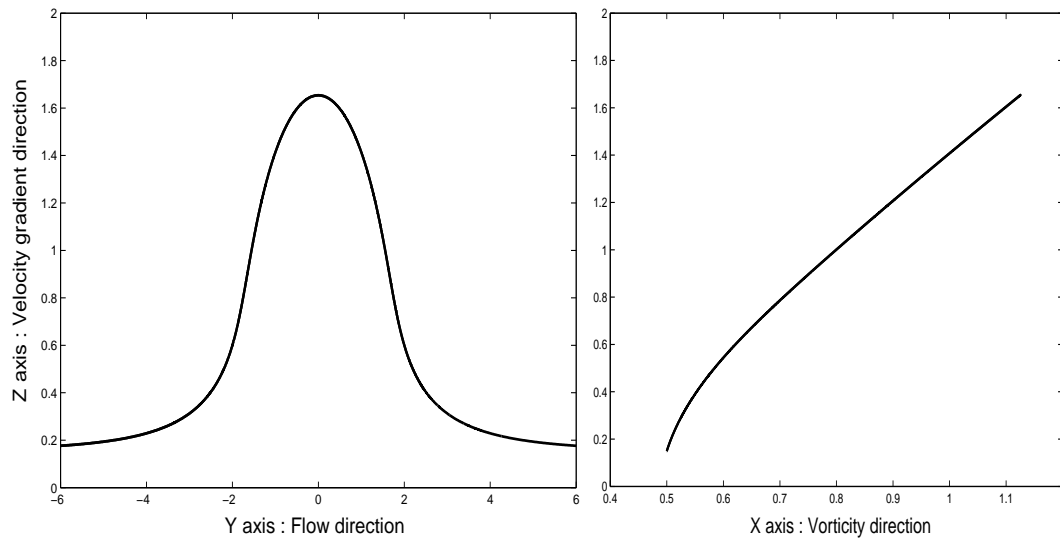


Figure 5.1: Zero  $St$  off-plane open trajectory for  $x^{-\infty} = 0.5$  with  $z^{-\infty} = 0.15$ :  $yz$  and  $xz$  projections;  $x^{-\infty}$  and  $z^{-\infty}$  are the upstream vorticity and gradient coordinates respectively.

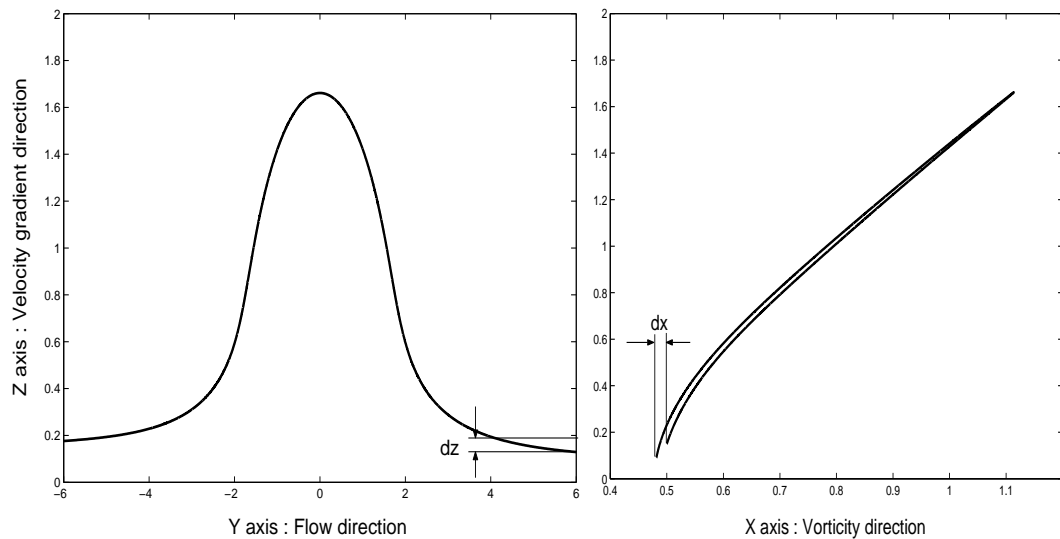


Figure 5.2: Finite  $St$  off-plane open trajectory for  $x^{-\infty} = 0.5$ ,  $z^{-\infty} = 0.15$  and  $St = 0.1$ :  $yz$  and  $xz$  projections;  $x^{-\infty}$  and  $z^{-\infty}$  are the upstream vorticity and gradient coordinates respectively.

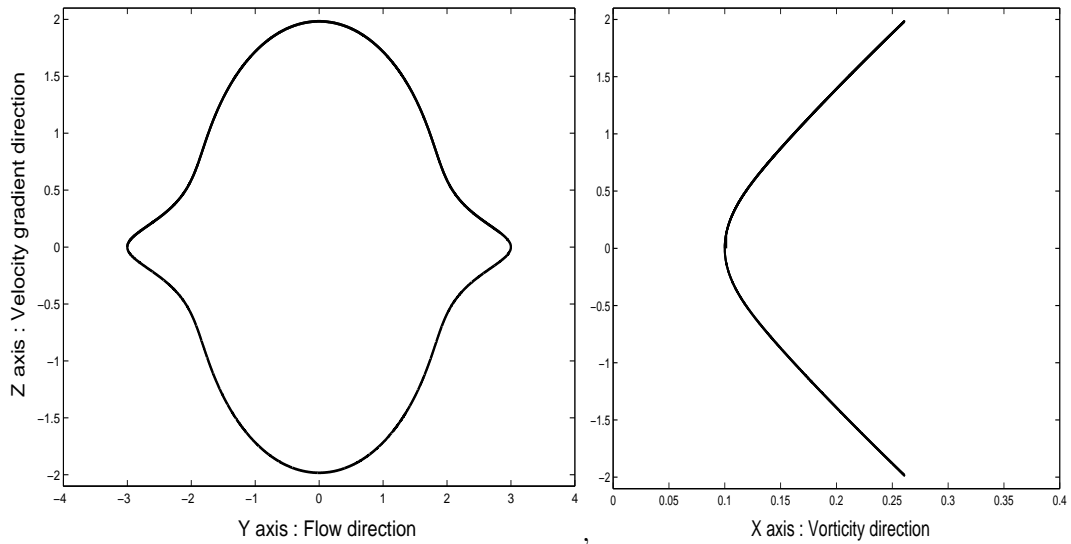


Figure 5.3: Zero  $St$  off-plane closed orbit through  $(x, y, z) \equiv (0.1, -3, 0)$ :  $yz$  and  $xz$  projections.

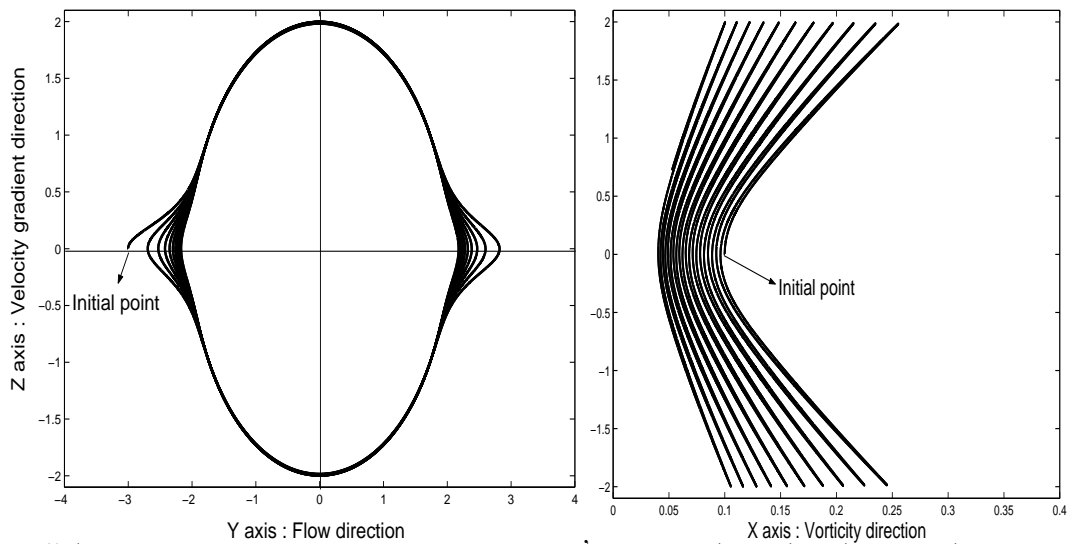


Figure 5.4: Inward spiralling off-plane trajectory starting from  $(x, y, z) \equiv (0.1, -3, 0)$  for  $St = 0.1$ :  $yz$  and  $xz$  projections.

It will be seen in section 5.3 that a perturbation scheme for the off-plane trajectories similar in structure to that formulated in Chapter 4 for in-plane trajectories explains the general features of the finite  $St$  trajectory space. Before proceeding to the detailed analysis, however, we discuss the physical mechanisms that lead to the behavior observed in Figs 5.2 and 5.4. Owing to the antisymmetry of simple shear flow and the symmetry across the shearing plane, it suffices to examine only a quadrant of the entire trajectory space. In what follows we restrict our attention to the quadrant  $x, z \geq 0$ .

## 5.2 Relative off-plane trajectories

### 5.2.1 Off-Plane open trajectories

We begin by looking at zero-Stokes open trajectories outside the shearing plane and the effect of inertia on their fore-aft symmetry when viewed in the flow-vorticity ( $xy$ ) plane. Off-Plane zero-Stokes trajectories, unlike those in the shearing plane, are not confined to the velocity-velocity gradient ( $yz$ ) plane. As shown by dotted lines in Fig 5.5, their projections onto the  $xy$  plane are not straight lines and qualitatively resemble the in-plane open trajectories in that they include two inflection points. Retracing the argument put forth for the case of in-plane trajectories (see section 4.1), one again considers the direction of the inertial force over regions of positive and negative curvature in the  $xy$  projection and thereby concludes that the net vorticity displacement ( $\Delta x$ ), similar to the in-plane gradient displacement  $(\Delta z)_{inplane}$ , will be  $O(St)$  and negative for finite  $St$  off-plane trajectories with  $x^{-\infty} \geq O(1)$ <sup>1</sup>; here,  $x^{-\infty}$  is the upstream off-plane coordinate. For  $x^{-\infty} \rightarrow 0$  the off-plane trajectories become increasingly planar since they approach their counterparts in the plane of shear, and their  $xy$  projections

---

<sup>1</sup>A negative  $\Delta x$  would mean that the open trajectory ends up downstream at a smaller value of the off-plane coordinate ( $x^{+\infty} < x^{-\infty}$ ) for  $z > 0$ .

do not have to pass around the reference sphere projected onto the  $xy$  plane. In fact, in contrast to the in-plane trajectories, the regions of positive and negative curvature in the  $xy$  projections rather than becoming more pronounced approach straight lines as  $x^{-\infty} \rightarrow 0$ . Therefore, notwithstanding their flattening out into straight lines, the  $xy$  projections are expected to remain qualitatively similar for all values of  $x^{-\infty}$ , implying that  $\Delta x$  is always negative and goes to zero as we approach the shearing plane. This also indicates that one should not expect an analog of the singular  $O(St^{\frac{1}{2}})$  region found for the in-plane gradient displacement for small  $x^{-\infty}$  (see section 4.4.3). That this is indeed the case will be seen in section 5.3.1 where we derive an expression for  $\Delta x$  which shows the uniform  $O(St)$  scaling for the vorticity displacement (see (5.20)).

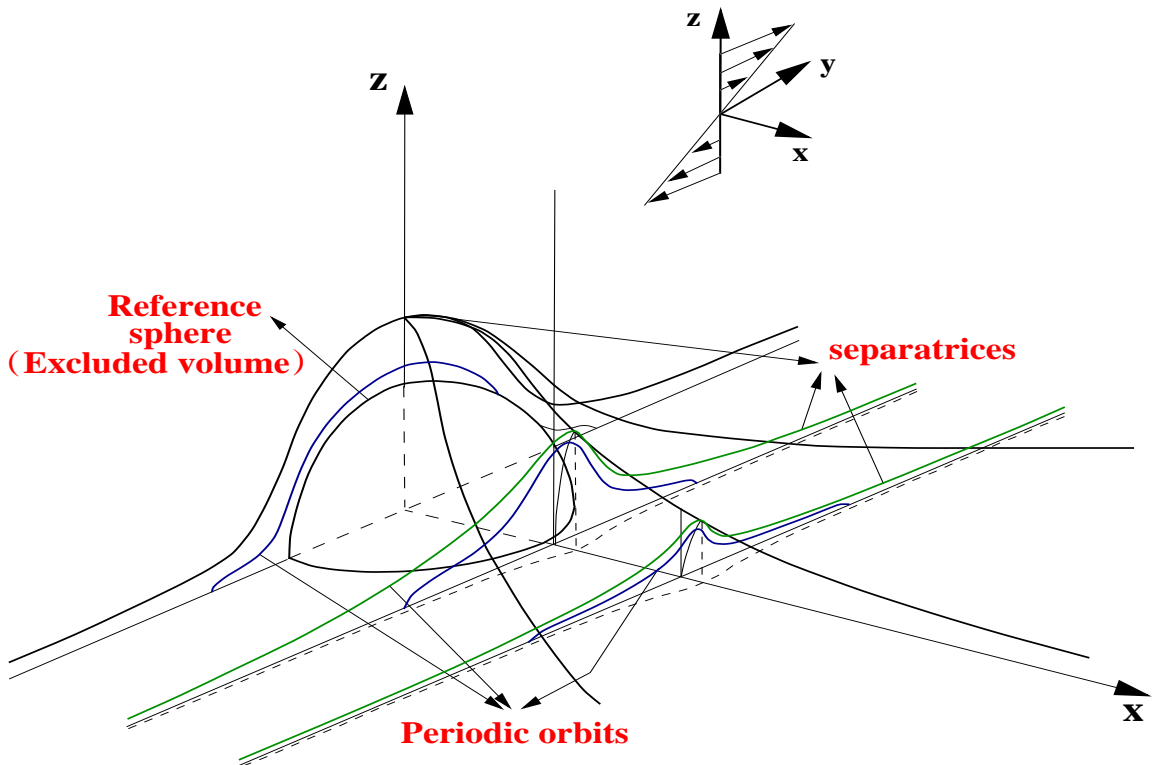


Figure 5.5: Axisymmetric separatrix envelope enclosing closed orbits at  $St = 0$

We next examine the gradient displacement ( $\Delta z$ ) of finite  $St$  off-plane open trajectories, again basing our arguments on the curvature of the corresponding zero-Stokes

trajectories. Since the  $yz$  projection of the zero-Stokes trajectory in Fig 5.1 has two inflection points, the argument used above (and in section 4.1 for the in-plane trajectories) implies that  $\Delta z$  will be  $O(St)$  and negative for an upstream offset  $z^{-\infty} \sim O(1)$ . For small values of  $x^{-\infty}$  the off-plane trajectories still resemble those in the plane of shear in that they pass very close to the surface of the reference sphere for small  $z^{-\infty}$ . Lubrication interactions therefore dominate in the near-field portions (with negative curvature as seen in the  $yz$  plane) of these trajectories leading to an increasingly negative  $\Delta z$  as  $z^{-\infty} \rightarrow 0$ . Albeit smaller in magnitude than the in-plane gradient displacement for the same  $z^{-\infty}$ ,  $\Delta z$  should still exhibit the same qualitative behavior for small  $x^{-\infty}$ . Thus, there must exist a singular region (in  $z^{-\infty}$ ) of  $O(St^{\frac{1}{2}})$ , where  $(\Delta z)$  becomes  $O(St^{\frac{1}{2}})$ , and thence the same order of magnitude as  $z^{-\infty}$ . Accordingly, for small  $x^{-\infty}$  one has an off-plane limiting trajectory that starts from a finite gradient offset of  $O(St^{\frac{1}{2}})$  upstream and goes to zero far downstream (i.e.,  $z^{+\infty} = 0$  as  $y \rightarrow \infty$ ), still suffering only an  $O(St)$  vorticity displacement. As for the in-plane case, trajectories starting from smaller gradient offsets for these values of  $x^{-\infty}$  will cross the  $y$  axis at a finite distance downstream, resulting in a spiralling behavior that is discussed in the next section. These conclusions are borne out in sections 5.3.1 and 5.3.2, where we derive expressions for  $\Delta z$  for trajectories with  $O(1)$  and  $O(St^{\frac{1}{2}})$  offsets, respectively (see (5.21) and (5.39)).

The above arguments with regard to  $\Delta z$ , however, remain valid only for off-plane trajectories with a negative gradient displacement. For fixed  $z^{-\infty}$  and for  $x^{-\infty}$  increasing, the trajectories move further away from the reference sphere, thereby diminishing the importance of the near-field lubrication interactions. For large enough  $x^{-\infty}$ , the magnitude of inertial forces (acting between the two inflection points of the in-plane projection) is sufficient to reverse the sign of the gradient displacement for small  $z^{-\infty}$ . This then implies the existence

of an intermediate finite  $St$  limiting trajectory corresponding to a critical value of the off-plane coordinate (say)  $x_c^{-\infty} (\approx 0.9)$ , for which  $z^{\pm\infty} \rightarrow 0$ , i.e.,  $\Delta z = 0$  (see Fig 5.6). The limiting trajectories for smaller values of  $x^{-\infty}$  are as described above. For  $x^{-\infty} \geq x_c^{-\infty}$ , the limiting trajectories start from  $z^{-\infty} = 0$  and suffer a positive gradient displacement; these trajectories are still referred to as ‘limiting’ since they serve to separate the open and spiralling trajectories for  $x^{-\infty} > x_c^{-\infty}$ . Despite the absence of a gradient displacement, this ‘neutral’ trajectory is not fore-aft symmetric since it still suffers an  $O(St)$  displacement in the vorticity direction; even its in-plane projection would be antisymmetric. Note that, while for smaller  $St$  the magnitude of the negative in-plane gradient displacement (to be overcome) is smaller, the inertial forces effecting this sign reversal are also correspondingly smaller, thereby suggesting that the location of the neutral trajectory  $x_c^{-\infty}$  may be independent of  $St$ . It is shown later in section 5.3.2 that this is indeed true to leading order.

Now considering a fixed  $x^{-\infty} (> x_c^{-\infty})$  and varying  $z^{-\infty}$ , the above arguments indicate that open trajectories with  $z^{-\infty} \sim O(1)$  or greater have a negative  $\Delta z$ , while those with  $z^{-\infty}$  sufficiently small have a positive  $\Delta z$ . Thus,  $\Delta z$  must change sign across  $z^{-\infty} = z_c^{-\infty}$  (say). As mentioned earlier, this occurs because for trajectories sufficiently far away from the reference sphere there is no lubrication mechanism to suppress the effects of inertial forces acting along the regions of negative curvature. Since both regions of positive and negative curvature become more pronounced for small  $z^{-\infty}$ , as manifested in a bigger hump in the  $yz$  projection<sup>2</sup>, it is plausible that the two contributions to the gradient displacement will balance out at a certain critical value of the gradient offset denoted above by  $z_c^{-\infty}$ . Again, since the underlying physical mechanism for both positive and negative gradient displacements remains the same, one expects that, similar to  $x_c^{-\infty}$ , the value of  $z_c^{-\infty}$  for fixed

---

<sup>2</sup>This occurs for off-plane zero-Stokes trajectories because, for  $z^{-\infty}$  small enough, they have to conform to the excluded volume of the axisymmetric separatrix envelope (see Fig 5.5).

$x^{-\infty}$  will be independent of  $St$ . This is shown to be the case in section 5.3.2.

We therefore see that, while open off-plane trajectories with gradient offsets  $O(1)$  or greater are altered for finite  $St$  in a manner consistent with our intuition based on investigations of in-plane trajectories (see Chapter 4), those with smaller values of  $z^{-\infty}$  behave quite differently. The neutral off-plane trajectory at  $x_c^{-\infty}$  acts to compartmentalize the finite  $St$  trajectory space, which in turn dictates the nature of the spiralling trajectories discussed next. As will be seen below and in section 5.5, this compartmentalization is independent of  $St$  for  $St \ll 1$  and has profound consequences with regard to suspension microstructure and rheology.

### 5.2.2 Off-plane spiralling trajectories

We now consider the inertial modifications of the zero-Stokes closed orbits, i.e., of the ensemble of trajectories lying inside the axisymmetric zero-Stokes separatrix envelope (see Fig 5.5). For any fixed off-plane coordinate, the zero-Stokes closed trajectories are similar in shape to open trajectories lying just outside the separatrix surface, except in regions asymptotically close to their points of intersection with the  $xy$  plane where the curvature (of the  $yz$  projection) changes sign as the trajectory crosses the  $y$  axis. Therefore one expects the qualitative effects of inertial forces, at least with regard to the vorticity displacement  $\Delta x$ , to remain the same even when acting on these closed orbits. Thus, the equivalent of a non-zero  $\Delta x$  for a zero-Stokes closed trajectory would be an  $O(St)$  difference between the  $x$  coordinates of the points of intersection with the flow-vorticity ( $xy$ ) plane. The resulting finite  $St$  trajectory is no longer closed; if we begin at  $x = x_1$  and  $\phi = \pi$ , the next point of intersection at  $\phi = 0$  (moving in a clockwise manner when viewed down the positive  $x$  axis) will correspond to  $x_2 = x_1 - St|(\Delta x)_1|$  with  $x_2 < x_1$  since  $\Delta x$  is negative. From the antisymmetry

of the simple shear flow, it immediately follows that this pattern repeats itself, i.e., the inertial trajectory will again intersect the  $xy$  plane at a third point ( $\phi = \pi$ ) corresponding to  $x_3 = x_2 - St|(\Delta x)_2|$ , and so on. The inertial trajectory in effect spirals towards the plane of shear, advancing by a distance of  $O(St)$  in each cycle (see Fig 5.6).

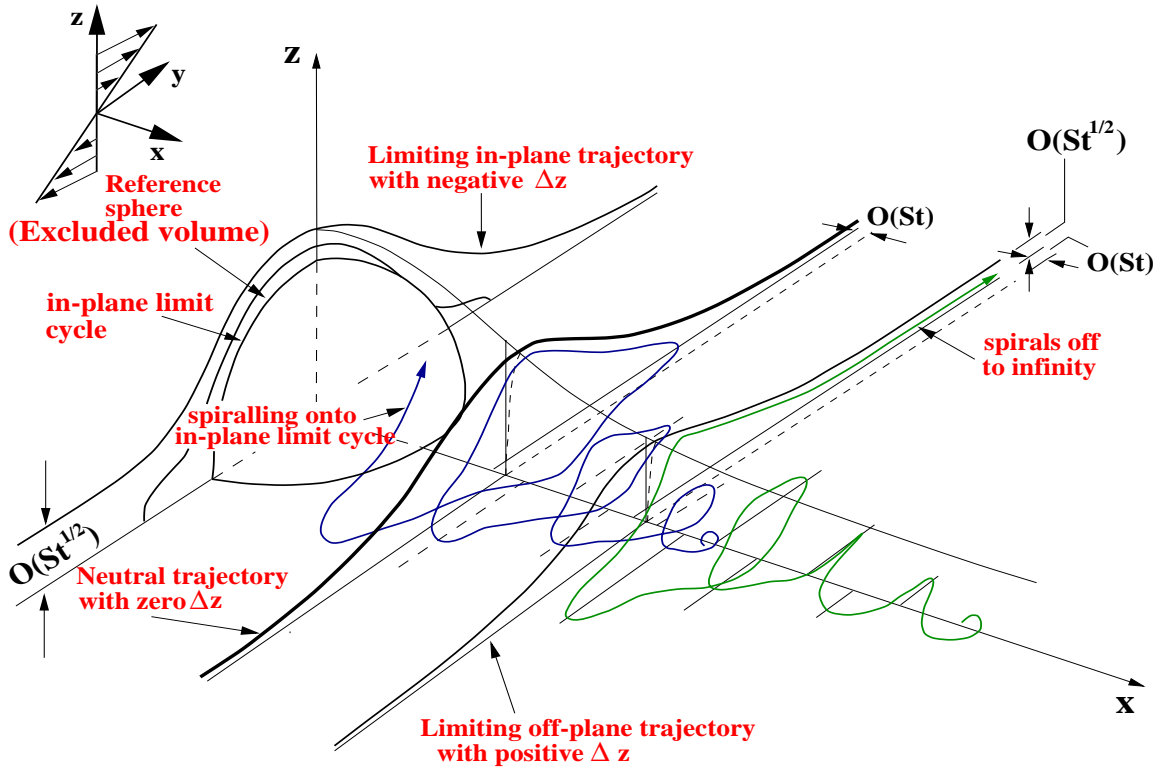


Figure 5.6: Finite  $St$  spiralling trajectories within the modified separatrix envelope.

In describing the above spiralling behavior further, the terms spiralling ‘inward’ and ‘outward’ will be used with reference to the  $y$  coordinates of the points of intersection (with the  $xy$  plane) of the spiralling trajectory, i.e., if two successive points of intersection have  $y$  coordinates  $y_1, y_2$ , such that  $y_2 > y_1$ , then the trajectory is said to spiral outwards, and vice versa. Thus, a trajectory spiralling outward in  $z$  (applying the above definition to points of intersection of the trajectory with the  $xz$  plane) and inward in  $y$  is still regarded as spiralling inward. This will be the case for virtually all off-plane spiralling trajectories since

the  $z$  extent (i.e, at  $\phi = \pi/2$ ) of the finite  $St$  separatrix envelope diminishes as one moves away from the plane of shear. It must also be remembered that the spiralling trajectories always lie within the envelope formed by the limiting finite  $St$  trajectories (see previous section). Thus, the phrase ‘spiralling off to infinity’ used below will refer to a spiralling trajectory that goes off to infinity while remaining within this envelope.

With the above terminology in mind, the nature of the spiralling trajectories, as seen in the  $yz$  plane, can be deduced from sign of  $\Delta z$ . The equivalent of a non-zero  $\Delta z$  for a zero-Stokes closed trajectory is an asymmetry with respect to the  $y$  coordinates of the points of intersection with the  $xy$  plane of the resulting finite  $St$  trajectory. Unlike the  $x$  coordinates, however, the difference between successive  $y$  coordinates need not be  $O(St)$ . This is owing to the non-uniformity arising from squeezing the entire family of zero-Stokes closed orbits covering the negative  $y$ -axis into an interval of  $O(d)$  or smaller on the  $z$ -axis, where  $d$  is the ordinate of the separatrix envelope at  $\phi = \pi/2$  for the particular off-plane coordinate. This squeezing occurs regardless of the proximity to the reference sphere; the latter only decides the relative magnitudes of the lubrication and inertial forces. The squeezing effect will, for instance, magnify an  $O(St)$  perturbation between a zero-Stokes closed orbit and the (spiralling) inertial trajectory at  $\phi = \pi/2$ , leading to an  $O(1)$  or larger difference between their points of intersection with the  $xy$  plane further downstream (see Appendix C3). One nevertheless expects that one of the following will occur:

1. Finite  $St$  trajectories just below the separatrix envelope (i.e., whose points of intersection with the  $xy$  plane are at large distances from the vorticity axis) in the region  $x < x_c^{-\infty}$  will spiral inward owing to the negative  $\Delta z$  for open trajectories immediately above; they eventually spiral onto the limit cycle in the plane of shear. Their behavior resembles, and indeed asymptotes to that of in-plane trajectories outside the limit cycle

but below the limiting in-plane trajectory (for which  $z^{+\infty} = 0$ ; see Fig 4.5). An example of such a trajectory was shown in Fig 5.4 in the introduction.

2. Finite  $St$  trajectories will spiral outward for  $x > x_c^{-\infty}$  owing to the reversal in the sign of  $\Delta z$  across  $x = x_c^{-\infty}$ . We can also have a spiralling out behavior when  $x < x_c^{-\infty}$  for trajectories that lie sufficiently away from the finite  $St$  separatrix envelope (i.e., whose points of intersection with the  $xy$  plane lie close to the vorticity axis), in which case the trajectories have to conform to the excluded volume of the reference sphere as they approach the plane of shear. These trajectories are still consistent with the negative  $\Delta z$  (for open trajectories) in  $x < x_c^{-\infty}$ , however, since though the points of intersection with the  $xy$  plane move away from the vorticity axis, the trajectory still moves closer to the surface of the sphere.
3. A subset of the finite  $St$  trajectories that spiral out will approach the limit cycle in the shearing plane from ‘within’. The long-time behavior of these trajectories asymptotes to that of the in-plane trajectories spiralling out onto the limit cycle (see Fig 4.18).

It must be emphasised that the above regimes need not necessarily correspond to distinct finite  $St$  trajectories. Indeed, the first two cases may describe different portions of the same finite  $St$  trajectory as it approaches the plane of shear. We do not consider the third case further, since in any event trajectories belonging to this class form a vanishingly small portion of the whole trajectory space.

The precise transition for a given finite  $St$  trajectory from a diverging to a converging spiral can be seen as follows. At zero Stokes number the trajectory space contains (at least) two invariant manifolds, the shearing plane that is locally a center manifold, and the vorticity axis. The latter is trivially so since all points on this axis have zero velocity.

For finite  $St$  the two manifolds remain invariant, and the modification of trajectories in the shearing plane was described in section 4.4.6. A spiralling finite  $St$  trajectory originates from (say) some point very near the vorticity axis ( $t \rightarrow -\infty$ ), and to begin with, spirals outwards from it. During its motion towards the plane of shear (in  $O(St)$  increments), the trajectory if it comes closer than  $x_c^{-\infty}$ , will eventually begin spiralling inward and approach the in-plane limit cycle as  $t \rightarrow \infty$ . On the other hand, if the outward spiralling is fast enough relative to the rate of approach, the trajectory will spiral off to infinity before crossing the neutral plane at  $x_c^{-\infty}$ . The possibility of escape doesn't exist for  $x < x_c^{-\infty}$  since the outlet to infinity is now cut off by the envelope of limiting trajectories that tends to zero to 0 as  $y \rightarrow \infty$  for  $x < x_c^{-\infty}$ <sup>3</sup>. Even having considered all open trajectories in the previous section, there were still regions of space, infinite in extent, left unaccounted for; for example, the quadrant  $x, z > 0$ , the region  $y > 0, x > x_c^{-\infty}$ , with  $z$  (of  $O(St^{\frac{1}{2}})$ ), bounded by the family of limiting finite  $St$  open trajectories, and similar symmetrically placed regions in other quadrants. It is precisely these regions that will be filled by trajectories spiralling off to infinity.

The correspondence between the nature of spiralling (close to the separatrix envelope) and the sign of  $\Delta z$  for the corresponding limiting open trajectory will not be exact due to 'end effects', that is to say, the transition from outward to inward spiralling for such trajectories will not occur exactly at  $x = x_c^{-\infty}$  (where  $\Delta z$  for the limiting off-plane trajectories changes sign). This discrepancy should be expected not only because of the small but finite distance of the spiralling trajectories from the separatrix envelope, but more importantly on account of inertial forces acting to push the spiralling trajectories further outwards (the equivalent of a positive  $\Delta z$ ) in the regions close to  $\phi = 0, \pi$  where the curvature changes sign.

<sup>3</sup>To be precise, the neutral plane should correspond to the downstream off-plane coordinate of the neutral trajectory viz.  $x_c^{-\infty} - St(\Delta x)_c$ , since it is beyond this value that the finite  $St$  limiting envelope cuts off the escape to  $y = \infty$ .

The above finite  $St$  modification of the closed orbits is still consistent with the antisymmetry of the ambient simple shear flow, since the same arguments could be carried out for the quadrant  $x > 0, z < 0$  with the only sign of  $y$  being reversed. Every finite  $St$  spiralling trajectory for  $x > 0$  therefore has a mirror image (obtained by reflection across the vorticity axis), and this pair of trajectories can, simplistically speaking, be likened to a pair of helices separated by half a pitch, and winding around a cylindrical surface. This topology will then be invariant to a rotation through  $\pi$  as required by the antisymmetry of simple shear.

From the above discussion, it is evident that the neutral off-plane trajectory at  $x_c^{-\infty}$  acts to separate finite  $St$  trajectories that spiral off to infinity from those that spiral onto the in-plane limit cycle. Since the location of this neutral trajectory is, to leading order, independent of  $St$ , so is its associated ‘filtering’ action. The region of spiralling trajectories has an infinite volume, and the effects described above should therefore be observable even for the case of rough spheres. Indeed, even if the neutral trajectory is destroyed on account of surface roughness, the far-field spiralling trajectories will persist. Although the time scale required to observe these inertial modifications increases as  $St \rightarrow 0$ , for any non-zero  $St$  the nature of pair-wise interactions between spherical particles is dramatically altered. This fundamentally changes the pair-distribution function for long-times, because regions of space that would have given rise to a finite time-periodic pair-distribution function for  $St = 0$  on account of particles rotating in stable closed orbits, will now either be depleted for long times on account of particles spiralling off to infinity, or serve as sites of accumulation (the in-plane limit cycle). Our analysis therefore shows that a trajectory calculation (e.g., Zarraga & Leighton 2001b) to characterise the microstructure and rheology of a finite  $St$  suspension via pair-wise interactions is a futile exercise unless one incorporates other mechanisms,

for example, three-particle effects or Brownian motion to render the distribution function determinate.

The above alteration of the zero-Stokes trajectory space is also consistent with the dynamical systems viewpoint introduced in section 4.4.6. The region enclosed by the axisymmetric zero-Stokes separatrix envelope may now be regarded as a center manifold embedded in three dimensions; the vorticity axis lying within this envelope consists of a continuum of elliptic fixed points (or ‘centers’). It is known that even the smallest amount of hyperbolicity can qualitatively alter such a trajectory configuration. In our case particle inertia is the source of this hyperbolicity.

In the next section we formulate a perturbation scheme to analyze finite  $St$  off-plane open trajectories and derive expressions for the transverse displacements in the gradient ( $\Delta z$ ) and vorticity ( $\Delta x$ ) directions. Having compared the analysis and numerics in detail for the in-plane case (see Chapter 4), here we mainly focus on the qualitative implications of the analysis and verify these by numerical integration of the trajectory equations (see (5.1) and (5.2)). We do, however, present far-field analytical expressions for  $\Delta z$  and  $\Delta x$  that will then be compared to their numerical counterparts; these also serve to delineate the domain of validity of the perturbation approach employed.

### 5.3 Perturbation analysis for off-plane trajectories

The relative off-plane trajectories are characterised by two equations describing the variation of  $\phi$  and  $\theta$  with  $r$ , that, to  $O(St)$ , are given as:

$$\frac{d\phi}{dr} = \frac{-\{\sin^2 \phi + (B/2)(\cos^2 \phi - \sin^2 \phi)\} + St f_1(r, \theta, \phi) / \sin \theta}{r(1-A) \sin^2 \theta \sin \phi \cos \phi + St f_2(r, \theta, \phi)}, \quad (5.1)$$

$$\frac{d\theta}{dr} = \frac{(1-B) \sin \theta \cos \theta \sin \phi \cos \phi + St f_3(r, \theta, \phi)}{r(1-A) \sin^2 \theta \sin \phi \cos \phi + St f_2(r, \theta, \phi)}, \quad (5.2)$$

where

$$f_1(r, \theta, \phi) = -H \sin^2 \theta \sin \phi \cos \phi \left[ \left\{ 2B(A-B) - r(1-A) \frac{dB}{dr} \right\} \sin \theta \frac{(\cos^2 \phi - \sin^2 \phi)}{2} \right. \\ \left. + 2(A-B) \sin \theta \sin^2 \phi \right] - \frac{6E}{5r} \sin \theta \sin \phi \cos \phi \left[ \sin^2 \theta \frac{(\cos^2 \phi - \sin^2 \phi)}{2} \left\{ r(1-A) \frac{dC}{dr} \right. \right. \\ \left. \left. + 2C(B-1) \right\} + \frac{C}{2}(1 + \sin^2 \theta) \right],$$

$$f_2(r, \theta, \phi) = -rG \left[ \sin^4 \theta \sin^2 \phi \cos^2 \phi \left\{ (A-B)^2 - r(1-A) \frac{dA}{dr} \right\} + \frac{(B-2A)}{2} \sin^2 \phi \sin^2 \theta \right. \\ \left. - \frac{B}{2} \cos^2 \phi \sin^2 \theta - \frac{B(B-2A)}{4} \sin^2 \theta \right],$$

and

$$f_3(r, \theta, \phi) = -H \sin \theta \cos \theta \left[ \frac{B(B-2)}{4} + \sin^2 \theta \sin^2 \phi \cos^2 \phi \left\{ 2(B-1)(A-B) - r(1-A) \frac{dB}{dr} \right\} \right] \\ - \frac{6E}{5r} \sin \theta \cos \theta \left[ \sin^2 \theta \sin^2 \phi \cos^2 \phi \left\{ r(1-A) \frac{dC}{dr} + 2C(B-1) \right\} + \frac{C}{4}(2 \sin^2 \phi - B) \right].$$

We continue to use the same symbols as before for the  $r$  and  $\phi$  components of the inertial correction. Thus  $r \sin \theta f_1$ ,  $f_2$  and  $r f_3$ , respectively, denote the  $\phi$ ,  $r$  and  $\theta$  components of the  $O(St)$  inertial velocity. The functions  $f_1$  and  $f_2$  reduce to their in-plane values for  $\theta = \pi/2$  (see section 4.4.1). It may easily be verified that the system is invariant to a rotation through  $\pi$ , and in addition is fore-aft symmetric for  $St = 0$ . On account of these symmetries, it suffices to consider the quadrant  $0 \leq \theta \leq \pi/2$ ,  $0 \leq \phi \leq \pi$  of the entire trajectory space

Considering the rhs's of the trajectory equations, we note that at  $\phi = \pi/2$  the  $O(1)$  terms in the denominator of (5.1) and in both the numerator and denominator of (5.2) are zero. On the other hand,  $f_2(r, \theta_t, \pi/2)$ ,  $f_3(r, \theta_t, \pi/2) \neq 0$  (where  $\theta_t$  is the value of  $\theta$  at  $\phi = \pi/2$ ), and therefore the perturbation is singular. Though the  $O(St)$  terms in the trajectory equations remain uniformly small as  $\theta \rightarrow 0$ , suggesting that the non-uniformity is

in  $\phi$  alone, it will be seen that the regular perturbation analysis is not valid for  $\theta_t \leq O(St^{\frac{5}{3}})$ . This lack of validity, however, does not affect the values of the diffusivities at leading order (see section 5.3.4).

The analysis for the most part resembles the in-plane case (see section 4.4) and we only tabulate the main steps in the procedure. Section 5.3.1 considers off-plane open trajectories with initial gradient offsets ( $z^{-\infty}$ ) greater than  $O(St^{\frac{1}{2}})$ , and the corresponding expressions for  $\Delta x$  and  $\Delta z$  are derived. In section 5.3.2 we examine off-plane trajectories with  $O(St^{\frac{1}{2}})$  initial gradient offsets, and study the nature of the envelope formed by the family of finite  $St$  limiting trajectories that serve to separate the open and the spiralling trajectories. Section 5.3.3 contains the analytical evaluation of the gradient and vorticity displacements in the various limiting cases, while in section 5.3.4 we use the results of sections 5.3.1, 5.3.2 and 5.3.3 to derive scalings for the  $xx$  and  $zz$  components of the diffusivity tensor. In each of the sections except 5.3.4, we present numerical results supporting the conclusions of the analysis.

### 5.3.1 Open trajectories with initial gradient offsets much greater than $O(St^{\frac{1}{2}})$ .

We perturb the inertial trajectory about a zero-Stokes trajectory which starts from the same initial point upstream ( $y \rightarrow -\infty$ ). Similar to the in-plane case, there are three regions:

$$\text{Outer layer O1} : \phi \in \left(\frac{\pi}{2} + O(1), \pi\right), \theta \in (\theta_t + O(1), \frac{\pi}{2}), r > \frac{c}{\sin \theta_t} + O(1),$$

$$\text{Inner layer I} : \phi = \frac{\pi}{2} + St\tilde{\phi}, \theta = \theta_t + St\hat{\theta}_f + St^2\tilde{\theta}, r = \frac{c}{\sin \theta_t} + Stk + St^2\tilde{r},$$

$$\text{Outer layer O2} : \phi \in (0, \frac{\pi}{2} - O(1)), \theta \in (\theta_t + O(1), \frac{\pi}{2}), r > \frac{c}{\sin \theta_t} + O(1).$$

### 5.3.1.1 Outer layer O1

In this layer using the regular expansions

$$\theta = \theta_0(r) + St \theta_1(r) + \dots, \quad (5.3)$$

$$\phi = \phi_0(r) + St \phi_1(r) + \dots, \quad (5.4)$$

in equations (5.1) and (5.2), we obtain

$$O(1): \frac{d\theta_0}{dr} = \frac{(1-B) \cos \theta_0}{r(1-A) \sin \theta_0}, \quad (5.5)$$

$$O(St): \frac{d\theta_1}{dr} = -\frac{(1-B)}{r(1-A)} \frac{1}{\sin^2 \theta_0} \theta_1 + \left\{ \frac{f_3(r, \theta_0, \phi_0)}{r(1-A) \sin^2 \theta_0 \cos \phi_0 \sin \phi_0} - \frac{(1-B)f_2(r, \theta_0, \phi_0) \cos \theta_0}{r^2(1-A)^2 \sin^3 \theta_0 \cos \phi_0 \sin \phi_0} \right\}, \quad (5.6)$$

and

$$O(1): \frac{d\phi_0}{dr} = -\frac{\sin^2 \phi_0 + (B/2)(\cos^2 \phi_0 - \sin^2 \phi_0)}{r(1-A) \sin^2 \theta_0 \sin \phi_0 \cos \phi_0}, \quad (5.7)$$

$$O(St): \frac{d\phi_1}{dr} = \left\{ \frac{(B/2) - \sin^2 \phi_0}{r(1-A) \sin^2 \theta_0 \sin^2 \theta_0 \cos^2 \phi_0} \right\} \phi_1 + \left\{ \frac{2 \cos \theta_0 \{\sin^2 \phi_0(1-B) + (B/2)\}}{r(1-A) \sin^3 \theta_0 \cos \phi_0 \sin \phi_0} \right\} \theta_1 + \left\{ \frac{f_1(r, \theta, \phi)}{r(1-A) \sin^3 \theta_0 \sin \phi_0 \cos \phi_0} + \frac{\{\sin^2 \phi_0(1-B) + (B/2)\} f_2(r, \theta, \phi)}{r^2(1-A)^2 \sin^4 \theta_0 \cos^2 \phi_0 \sin^2 \phi_0} \right\}. \quad (5.8)$$

The  $O(1)$  equation for  $\theta_0$  does not depend on  $\phi_0$ , and similarly, the  $O(St)$  equation for  $\theta_1$  does not depend on  $\phi_1$ . Thus in the outer layer, the  $\phi$  solutions are forced by the  $\theta$  solutions at the same order.

Since both the inertial and zero-Stokes trajectories originate from the same up-

stream point, the required boundary conditions are

$$\begin{aligned} r \cos \theta &\rightarrow x^{-\infty}, \\ r \sin \theta \sin \phi &\rightarrow z^{-\infty} \quad \text{as } y \rightarrow -\infty, \end{aligned}$$

which can be written at successive orders in  $St$  as

$$\begin{aligned} O(1) : \quad r \cos \theta_0 &\rightarrow x^{-\infty} \quad \text{as } r \rightarrow \infty, \\ O(St) : \quad r \theta_1^- &\rightarrow 0 \quad \text{as } r \rightarrow \infty (\phi_0 \rightarrow \pi), \\ \\ O(1) : \quad r \sin \theta_0 \sin \phi_0 &\rightarrow z^{-\infty} \quad \text{as } r \rightarrow \infty, \\ O(St) : \quad r \phi_1^- &\rightarrow 0 \quad \text{as } r \rightarrow \infty (\phi_0 \rightarrow \pi). \end{aligned}$$

The expressions for the lateral displacements in the vorticity and gradient directions are:

$$\Delta x = r \cos \theta \Big|_{\phi \rightarrow \pi}^{\phi \rightarrow 0} = -St \lim_{r \rightarrow \infty} r \theta_1^+, \quad (5.9)$$

$$\Delta y = r \sin \theta \sin \phi \Big|_{\phi \rightarrow \pi}^{\phi \rightarrow 0} = St \lim_{r \rightarrow \infty} r \phi_1^+. \quad (5.10)$$

Solving the  $O(1)$  equations, we obtain the Batchelor-Green expressions for  $\theta_0$  and  $\phi_0$ :

$$\cos \theta_0 = \frac{x^{-\infty}}{r} \exp \left[ \int_r^\infty \frac{q(r')}{2} dr' \right], \quad (5.11)$$

$$r^2 \sin^2 \phi_0 = \frac{(z^{-\infty})^2}{\sin^2 \theta_0} \exp \left[ \int_r^\infty q(r') dr' \right] + \frac{1}{\sin^2 \theta_0} \int_r^\infty \exp \left[ -\int_{r'}^r q(r'') dr'' \right] \frac{B' r'}{(1 - A')} dr'. \quad (5.12)$$

The upstream solutions at  $O(St)$ , after suitable simplification, are given as

$$r\theta_1^- = -\frac{1}{\sin\theta_0} \int_r^\infty \exp\left[-\int_{r'}^r \frac{q(r'')}{2} dr''\right] \left\{ \frac{f_3(r', \theta'_0, \phi'_0)}{(1-A') \sin\theta'_0 \cos\phi'_0 \sin\phi'_0} - \frac{(1-B')f_2(r', \theta'_0, \phi'_0) \cos\theta'_0}{r'(1-A')^2 \sin^2\theta'_0 \cos\phi'_0 \sin\phi'_0} \right\} dr', \quad (5.13)$$

$$r\phi_1^- = -\frac{1}{r \cos\phi_0 \sin\phi_0 \sin^2\theta_0} \int_r^\infty \exp\left[-\int_{r'}^r q(r'') dr''\right] \left\{ \frac{2r' \cos\theta'_0 \{(1-B') \sin^2\phi'_0 + \frac{B'}{2}\}}{(1-A') \sin\theta'_0} \theta_1^- + \frac{r' f_1(r', \theta'_0, \phi'_0)}{(1-A') \sin\theta'_0} + \frac{\{(1-B') \sin^2\phi'_0 + \frac{B'}{2}\} f_2(r', \theta'_0, \phi'_0)}{(1-A')^2 \sin^2\theta'_0 \sin\phi'_0 \cos\phi'_0} \right\} dr'. \quad (5.14)$$

We note that  $\theta_1^-$  and  $\phi_1^-$  are odd and even functions of  $\cos\phi_0$ , respectively; in (5.13)

$\phi'_0 \in (\pi/2, \pi)$ .

Since  $\theta_0$ , unlike  $\phi_0$ , remains real valued even for values of  $r$  less than the zero-Stokes minimum ( $c/\sin\theta_t$ ), we can obtain the vorticity displacement  $\Delta x$  without needing to solve the inner layer equation for  $\theta$ , i.e., by directly matching the limiting expressions in layers O1 and O2. We will therefore restrict ourselves to solving the inner equation for  $\phi$  alone.

### 5.3.1.2 Layer I

In the inner layer we have the expansions

$$\begin{aligned} \phi &= \frac{\pi}{2} + St \tilde{\phi}, \\ \theta &= \theta_t + St \theta_f + St^2 \tilde{\theta}, \\ r &= \frac{c}{\sin\theta_t} + St k + St^2 \tilde{r}, \end{aligned}$$

where the scalings of the dependent and independent variables are determined from the requirement of retaining inertial corrections to  $\mathbf{V}_r$  and  $\mathbf{V}_\theta$  at leading order (see (5.1) and

(5.2)). The variations in both  $r$  and  $\theta$  are  $O(St^2)$  about base values that contain  $O(St)$  constants; the arguments leading to these forms remain identical to the in-plane case. Again, the  $O(St)$  constants do not alter the leading order equations. The equation for  $\tilde{\phi}$ , at leading order, is given as

$$\frac{d\tilde{\phi}}{d\tilde{r}} = \frac{1 - \frac{B_0}{2}}{c \sin \theta_t (1 - A_0) \tilde{\phi} - f_2\left(\frac{c}{\sin \theta_t}, \theta_t, \frac{\pi}{2}\right)}, \quad (5.15)$$

whence

$$\tilde{\phi}^{\pm} = \frac{G_0(2 - B_0)(2A_0 - B_0)}{4(1 - A_0)} \left[ 1 \mp \left\{ 1 + \frac{16(\tilde{r} - I_i^{off})(1 - A_0)}{c G_0^2(2 - B_0)(2A_0 - B_0)^2 \sin \theta_t} \right\}^{\frac{1}{2}} \right], \quad (5.16)$$

and  $I_i^{off}$  is an integration constant whose value does not affect the  $O(St)$  matching. The subscript ‘0’ indicates evaluation at  $r = c/\sin \theta_t$ . The solution  $\tilde{\phi}$ , similar to the in-plane case, has two unequal branches indicative of the asymmetry at  $O(St)$ . It may similarly be verified that  $\tilde{\theta}$  has two (asymmetric) branches, each determined by the corresponding branch of  $\tilde{\phi}$ ; however, since these are  $O(St^2)$ , they are not considered here.

### 5.3.1.3 Layer O2

The leading order solutions in this layer remain the same, while the  $O(St)$  solutions are given by

$$r\theta_1^+ = \frac{I_{\theta_1^+}}{\sin \theta_0} \exp \left[ \int_r^\infty \frac{q(r')}{2} dr' \right] - \frac{1}{\sin \theta_0} \int_r^\infty \exp \left[ - \int_{r'}^r \frac{q(r'')}{2} dr'' \right] \left\{ \frac{f_3(r', \theta'_0, \phi'_0)}{(1 - A') \sin \theta'_0 \cos \phi'_0 \sin \phi'_0} - \frac{(1 - B') f_2(r', \theta'_0, \phi'_0) \cos \theta'_0}{r' (1 - A')^2 \sin^2 \theta'_0 \cos \phi'_0 \sin \phi'_0} \right\} dr', \quad (5.17)$$

$$\begin{aligned}
r\phi_1^+ = & \frac{z^{-\infty} I_{\phi_1^+}}{r \cos \phi_0 \sin \phi_0 \sin^2 \theta_0} \exp \left[ \int_r^\infty q(r') dr' \right] \\
& - \frac{1}{r \cos \phi_0 \sin \phi_0 \sin^2 \theta_0} \int_r^\infty \exp \left[ - \int_{r'}^r q(r'') dr'' \right] \left\{ \frac{2r' \cos \theta'_0 \{ (1 - B') \sin^2 \phi'_0 + \frac{B'}{2} \}}{(1 - A') \sin \theta'_0} \theta_1^+ \right. \\
& \left. + \frac{r' f_1(r', \theta'_0, \phi'_0)}{(1 - A') \sin \theta'_0} + \frac{\{ (1 - B') \sin^2 \phi'_0 + \frac{B'}{2} \} f_2(r', \theta'_0, \phi'_0)}{(1 - A')^2 \sin^2 \theta'_0 \sin \phi'_0 \cos \phi'_0} \right\} dr'. \quad (5.18)
\end{aligned}$$

Using the expression for  $\theta_1^+$ ,  $\phi_1^+$  becomes

$$\begin{aligned}
r\phi_1^+ = & \frac{z^{-\infty} I_{\phi_1^+}}{r \cos \phi_0 \sin \phi_0 \sin^2 \theta_0} \exp \left[ \int_r^\infty q(r') dr' \right] \\
& - \frac{1}{r \cos \phi_0 \sin \phi_0 \sin^2 \theta_0} \int_r^\infty \exp \left[ - \int_{r'}^r q(r'') dr'' \right] \left\{ \frac{2r' \cos \theta'_0 \{ (1 - B') \sin^2 \phi'_0 + \frac{B'}{2} \}}{(1 - A') \sin \theta'_0} \theta_{1m}^- \right. \\
& \left. + \frac{r' f_1(r', \theta'_0, \phi'_0)}{(1 - A') \sin \theta'_0} + \frac{\{ (1 - B') \sin^2 \phi'_0 + \frac{B'}{2} \} f_2(r', \theta'_0, \phi'_0)}{(1 - A')^2 \sin^2 \theta'_0 \sin \phi'_0 \cos \phi'_0} \right\} dr' \\
& - \frac{I_{\theta_1^+} x^{-\infty} \sin \phi_0}{r \sin^2 \theta_0 \cos \phi_0} \exp \left[ \int_r^\infty q(r') dr' \right]. \quad (5.19)
\end{aligned}$$

where the expression for  $\theta_{1m}^-$  is given by (5.13) with  $\phi'_0 \in (0, \pi/2)$ . Thus,  $\phi_0 \in (0, \pi/2)$  in (5.19).

#### 5.3.1.4 Vorticity and Gradient displacements

Just as for the in-plane case (see section 4.4.1.4), the inner and outer solutions tabulated above can be matched by rewriting them in intermediate variables; the domain of overlap remains unchanged. The resulting expressions for the vorticity and gradient displacements

$z^{-\infty}$	$(\Delta x)_{traj}(St = 0.1)$	$(\Delta x)_{traj}(St = 0.01)$
5	$-7.716 \times 10^{-5}$	$-7.718 \times 10^{-6}$
2	$-1.557 \times 10^{-3}$	$-1.552 \times 10^{-4}$
1	$-6.295 \times 10^{-3}$	$-6.302 \times 10^{-4}$
0.5	$-8.784 \times 10^{-3}$	$-8.921 \times 10^{-4}$
0.2	$-9.424 \times 10^{-3}$	$-9.593 \times 10^{-4}$

Table 5.1:  $\Delta x$  values for  $x^{-\infty} = 0.2$  and  $z^{-\infty}$  ranging from 5 to 0.1;  $St = 0.1, 0.01$ .

$z^{-\infty}$	$(\Delta x)_{traj}(St = 0.1)$	$(\Delta x)_{traj}(St = 0.01)$
5	$-3.536 \times 10^{-4}$	$-3.537 \times 10^{-5}$
2	$-5.146 \times 10^{-3}$	$-5.137 \times 10^{-4}$
1	$-1.427 \times 10^{-2}$	$-1.421 \times 10^{-3}$
0.5	$-1.719 \times 10^{-2}$	$-1.711 \times 10^{-3}$
0.2	$-1.697 \times 10^{-2}$	$-1.684 \times 10^{-3}$

Table 5.2:  $\Delta x$  values for  $x^{-\infty} = 1$  and  $z^{-\infty}$  ranging from 5 to 0.1;  $St = 0.1, 0.01$ .

are

$$\Delta x = -2St \int_{\frac{c}{\sin \theta_t}}^{\infty} \exp \left[ -\int_{r'}^{\infty} \frac{q(r'')}{2} dr'' \right] \left\{ \frac{f_3(r', \theta'_0, \phi'_0)}{(1-A') \sin \theta'_0 \cos \phi'_0 \sin \phi'_0} - \frac{(1-B') f_2(r', \theta'_0, \phi'_0) \cos \theta'_0}{r' (1-A')^2 \sin^2 \theta'_0 \cos \phi'_0 \sin \phi'_0} \right\} dr', \quad (5.20)$$

$$\Delta z = \frac{St}{z^{-\infty}} \left( 2 \int_{\frac{c}{\sin \theta_t}}^{\infty} \exp \left[ -\int_{r'}^{\infty} q(r'') dr'' \right] \left\{ \frac{2r' \cos \theta'_0 \left\{ (1-B') \sin^2 \phi'_0 + \frac{B'}{2} \right\}}{(1-A') \sin \theta'_0} \theta_{1m}^- + \frac{r' f_1(r', \theta'_0, \phi'_0)}{(1-A') \sin \theta'_0} + \frac{\left\{ (1-B') \sin^2 \phi'_0 + \frac{B'}{2} \right\} f_2(r', \theta'_0, \phi'_0)}{(1-A')^2 \sin^2 \theta'_0 \sin \phi'_0 \cos \phi'_0} \right\} dr' \right) - (\Delta x) \frac{x^{-\infty}}{z^{-\infty}}. \quad (5.21)$$

We first observe that (5.20) for  $\Delta x$  remains  $O(St)$  for all finite  $St$  open trajectories with  $\theta_t \sim O(1)$ , and tends to zero as  $\theta_t \rightarrow \pi/2$  ( $x^{-\infty} \rightarrow 0$ ) regardless of the gradient offset  $z^{-\infty}$ . This is consistent with physical arguments presented in section 5.1. In tables 5.1 and 5.2 we tabulate values of the vorticity displacement for open trajectories for two Stokes numbers ( $St = 0.1$  and  $0.01$ ). These values were obtained from a numerical integration of the trajectory equations (5.1) and (5.2) using an adaptive Runge-Kutta fourth order method and confirm the  $O(St)$  scaling.

The expression for  $\Delta z$  contains two terms. The first term is recognized as being the off-plane analogue of (4.45) in section 4.4, while the second term is proportional to  $\Delta x$ . We briefly dwell on the geometric significance of the latter. The vorticity displacement  $\Delta x = -St \lim_{r \rightarrow \infty} r \theta_1^+$  is of the form  $r d\theta$ , an  $O(St)$  arc element. For any finite  $r$ , such a displacement along an arc of a sphere gives rise to displacements in both the gradient and vorticity directions related by  $|(\Delta z)_r| = |(\Delta x)_r| x^{-\infty}/z^{-\infty}$  as shown in Fig 5.7; here  $(\Delta z)_r$ , for instance, is the difference between the  $z$  coordinates of points on the zero-Stokes trajectory and a fictitious inertial trajectory (for which the only gradient displacement is a concomitant consequence of motion along the arc element) at a radial distance  $r$  downstream. In the limit  $r \rightarrow \infty$ ,  $(\Delta z)_r \rightarrow (\Delta z)$ ,  $(\Delta x)_r \rightarrow (\Delta x)$ , and the vorticity displacement  $\Delta x$  is accompanied by  $|\Delta z| = |\Delta x| x^{-\infty}/z^{-\infty}$  in the gradient direction, the latter being identical to the second term in (5.21); as is evident from Fig 5.7, this contribution to the gradient displacement is always positive when  $\Delta x < 0$ .

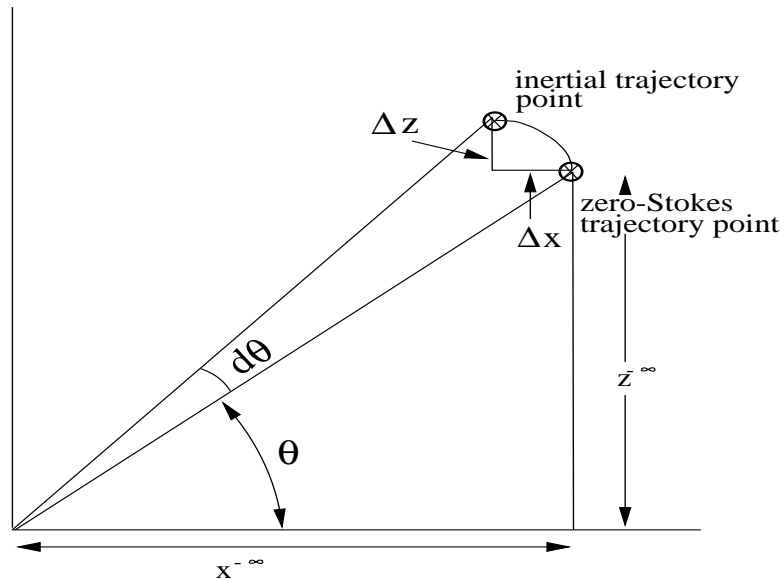


Figure 5.7: Geometric relation between gradient and vorticity displacements

The expression (5.21) for  $\Delta z$  is singular as  $z^{-\infty} \rightarrow 0$  provided the factor multiplying  $1/z^{-\infty}$  in (5.21) remains  $O(1)$ . When  $z^{-\infty} \sim O(St^{\frac{1}{2}})$ , the predicted gradient displacement is of the same order of magnitude as  $z^{-\infty}$ , and the  $O(St)$  solution  $\phi_1$  becomes comparable to  $\phi_0$  far enough downstream (as for the in-plane case); the expansion (5.4) is no longer valid for trajectories with these and smaller offsets. The alternate expression for  $\Delta z$  for trajectories with  $O(St^{\frac{1}{2}})$  gradient offsets, and its dependence on  $x^{-\infty}$  is detailed in the next section.

### 5.3.2 Open trajectories with initial gradient offsets of $O(St^{\frac{1}{2}})$

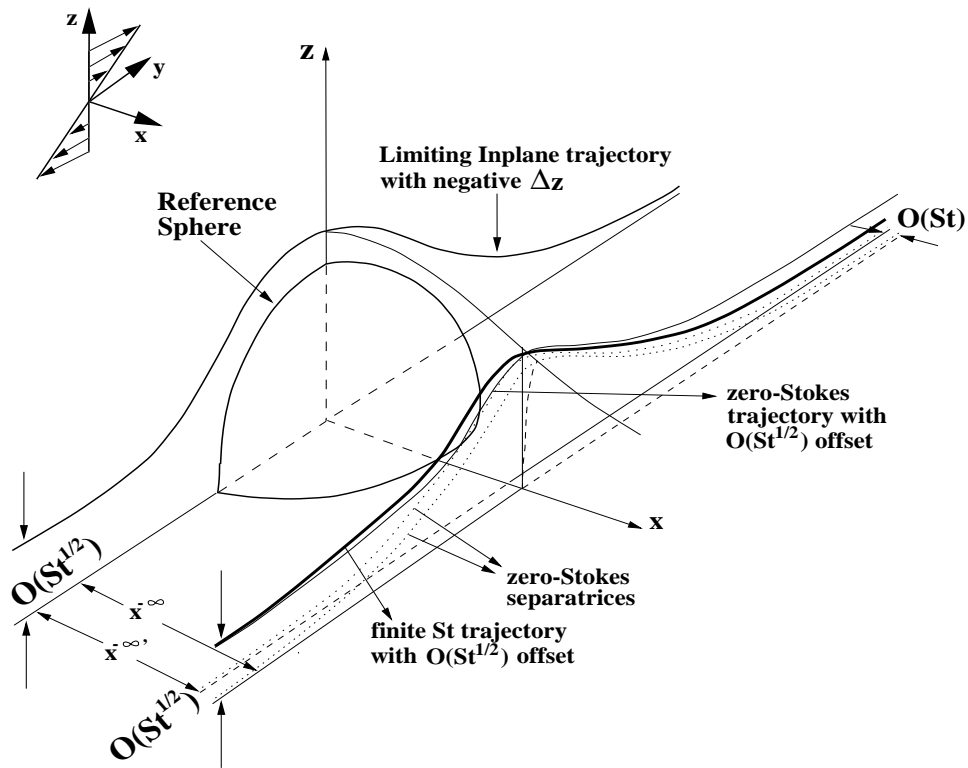


Figure 5.8: Off-Plane inertial trajectory with  $O(St^{\frac{1}{2}})$  initial gradient offset.

For trajectories with  $O(St^{\frac{1}{2}})$  (or smaller) gradient offsets ( $z^{-\infty}$ ), we piece together the  $(\pi/2, \pi)$  and  $(0, \pi/2)$  branches of the inertial trajectory at  $\phi = \pi/2$  (this is, of course, similar to the in-plane case; see Appendix C4). From Fig 5.8 we see that the inertial trajectory (heavy black

line) starts from a zero-Stokes trajectory (solid line) with a gradient offset of  $O(St^{\frac{1}{2}})$  and characterised by the parameters  $(c, \theta_t^c)$ ; since its gradient offset is only  $O(St^{\frac{1}{2}})$ , the zero-Stokes trajectory is asymptotically close to the zero-Stokes separatrix corresponding to the same value of the upstream off-plane coordinate ( $x^{-\infty}$ ) and characterised by  $(d, \theta_t^d)$  (dotted line). The inertial trajectory ends on a different zero-Stokes trajectory,  $(c', \theta_t^{c'})$  (not shown), close to a second zero-Stokes separatrix,  $(d', \theta_t^{d'})$  (dotted line) that corresponds to the same value of the downstream off-plane coordinate ( $x^{\infty'}$ ). Note that the parameters characterising the zero-Stokes separatrices are not independent, and are related by the corresponding trajectory equations (see (5.23) and (5.24) below).  $x^{\infty'}$  is taken to be smaller than  $x^{-\infty}$  by  $O(St)$  since the vorticity displacement  $\Delta x$ , as seen in the previous section, remains  $O(St)$  and negative for all trajectories with  $\theta_t \sim O(1)$ . That this is indeed true even when  $z^{-\infty} \sim O(St^{\frac{1}{2}})$  will be verified in a self-consistent manner.

We have the following relations:

$$x^{\infty'} = x^{-\infty} + St(\Delta \bar{x}), \quad (5.22)$$

$$d'^2 = \int_{\frac{d'}{\sin \theta_t^{d'}}}^{\infty} \exp\left[-\int_{r'}^{\frac{d'}{\sin \theta_t^{d'}}} q(r'') dr''\right] \frac{B' r'}{(1-A')} dr', \quad (5.23)$$

$$d^2 = \int_{\frac{d}{\sin \theta_t^d}}^{\infty} \exp\left[-\int_{r'}^{\frac{d}{\sin \theta_t^d}} q(r'') dr''\right] \frac{B' r'}{(1-A')} dr', \quad (5.24)$$

$$c^2 = St m_1^2 \exp\left[\int_{\frac{c}{\sin \theta_t^c}}^{\infty} q(r') dr'\right] + \int_{\frac{c}{\sin \theta_t^c}}^{\infty} \exp\left[-\int_{r'}^{\frac{c}{\sin \theta_t^c}} q(r'') dr''\right] \frac{B' r'}{(1-A')} dr', \quad (5.25)$$

$$c'^2 = St(m_1 + m_1')^2 \exp\left[\int_{\frac{c'}{\sin \theta_t^{c'}}}^{\infty} q(r') dr'\right] + \int_{\frac{c'}{\sin \theta_t^{c'}}}^{\infty} \exp\left[-\int_{r'}^{\frac{c'}{\sin \theta_t^{c'}}} q(r'') dr''\right] \frac{B' r'}{(1-A')} dr'. \quad (5.26)$$

Equations (5.23) and (5.24) define the relations between the parameters of the respective zero-Stokes separatrices. As seen in (5.25), the  $(c, \theta_t^c)$  zero-Stokes trajectory starts from a gradient offset of  $z^{-\infty} = m_1 St^{\frac{1}{2}}$ . Anticipating that the displacement in the gradient

direction will again be  $O(St)^{\frac{1}{2}}$ , we have taken the gradient offset of the  $(c', \theta_t^{c'})$  trajectory to be  $(m_1 + m'_1)St^{\frac{1}{2}}$  in (5.26). The objective is to determine  $m'_1$  in terms of  $m_1$ ,  $d$  and  $\theta_t^d$ ; the gradient displacement is then given by  $\Delta z = m'_1 St^{\frac{1}{2}}$ .

It is evident that the  $O(St)$  forcing terms in the above equations will lead to relations of the following form

$$\begin{aligned} d' &= d + St a_1, & \theta_t^{d'} &= \theta_t^d + St a_2, \\ c &= d + St b_1, & \theta_t^c &= \theta_t^d + St b_2, \\ c' &= d + St b'_1, & \theta_t^{c'} &= \theta_t^d + St b'_2. \end{aligned}$$

After some cumbersome algebra, one obtains

$$a_1 = -(\Delta \bar{x}) \left( \frac{\cos \theta_t^d}{\sin \theta_t^d} \right) \frac{2A_0 \sin^2 \theta_t^d + B_0(1 - 2 \sin^2 \theta_t^d)}{(2 - B_0)} \exp \left[ \int_{\frac{d}{\sin \theta_t^d}}^{\infty} \frac{q(r')}{2} dr' \right], \quad (5.27)$$

$$a_2 = -\frac{(\Delta \bar{x}) B_0 + 2(1 - B_0) \sin^2 \theta_t^d}{d(2 - B_0)} \exp \left[ \int_{\frac{d}{\sin \theta_t^d}}^{\infty} \frac{q(r')}{2} dr' \right], \quad (5.28)$$

$$b_1 = \frac{m_1^2 (1 - B_0)}{d(2 - B_0)} \left[ 1 + \sin^2 \theta_t^d \frac{(B_0 - A_0)}{(1 - B_0)} \right] \exp \left[ \int_{\frac{d}{\sin \theta_t^d}}^{\infty} q(r') dr' \right], \quad (5.29)$$

$$b_2 = \frac{m_1^2 (\sin \theta_t^d \cos \theta_t^d) (1 - B_0)}{d^2 (2 - B_0)} \exp \left[ \int_{\frac{d}{\sin \theta_t^d}}^{\infty} q(r') dr' \right], \quad (5.30)$$

$$b'_1 = \frac{(m_1 + m'_1)^2 (1 - B_0)}{d(2 - B_0)} \left[ 1 + \sin^2 \theta_t^d \frac{(B_0 - A_0)}{(1 - B_0)} \right] \exp \left[ \int_{\frac{d}{\sin \theta_t^d}}^{\infty} q(r') dr' \right] + a_1, \quad (5.31)$$

$$b'_2 = \frac{(m_1 + m'_1)^2 (\sin \theta_t^d \cos \theta_t^d) (1 - B_0)}{d^2 (2 - B_0)} \exp \left[ \int_{\frac{d}{\sin \theta_t^d}}^{\infty} q(r') dr' \right] + a_2, \quad (5.32)$$

where the subscript '0' now denotes evaluation at  $r = d / \sin \theta_t^d$ .

We now piece together the '+' and '-' branches of the inertial trajectory at

$\phi = \pi/2$ . First matching the radial distances of the two branches, we have

$$r_{\frac{\pi}{2}}^- = r_{\frac{\pi}{2}}^+,$$

where the left-hand side is calculated by perturbing about the  $(c, \theta_t^c)$  trajectory, while the right-hand side is perturbed about the  $(c', \theta_t^{c'})$  trajectory. With an error of  $o(St)$ , the above condition gives

$$\frac{c}{\sin \theta_t^c} = \frac{c'}{\sin \theta_t^{c'}} - 2St k(d, \theta_t^d),$$

where

$$\begin{aligned} k(d, \theta_t^d) = 2 \sin \theta_t^d \frac{(1 - A_0)}{d(2 - B_0)} \int_{\frac{d}{\sin \theta_t^d}}^{\infty} \exp \left[ - \int_{r'}^{\frac{d}{\sin \theta_t^d}} q(r'') dr'' \right] & \left\{ \frac{2r' \cos \theta'_0 \{ (1 - B') \sin^2 \phi'_0 + \frac{B'}{2} \}}{(1 - A') \sin \theta'_0} \theta_{1m}^- + \right. \\ & \left. \frac{r' f_1(r', \theta'_0, \phi'_0)}{(1 - A') \sin \theta'_0} + \frac{\{ (1 - B') \sin^2 \phi'_0 + \frac{B'}{2} \} f_2(r', \theta'_0, \phi'_0)}{(1 - A')^2 \sin^2 \theta'_0 \sin \phi'_0 \cos \phi'_0} \right\} dr'. \end{aligned} \quad (5.33)$$

Using the relations derived above, this finally yields

$$\frac{d(b_2 - b'_2)(1 - A_0)}{\cos \theta_t^d (1 - B_0)} = 2(\Delta \bar{x}) \cos \theta_t^d \frac{(1 - A_0)}{(2 - B_0)} \exp \left[ \int_{\frac{d}{\sin \theta_t^d}}^{\infty} \frac{q(r')}{2} dr' \right] - 2k(d, \theta_t^d) - \frac{d a_2 (1 - A_0)}{\cos \theta_t^d (1 - B_0)}. \quad (5.34)$$

Now equating the angular coordinates of the '+' and '-' branches, we have

$$\begin{aligned} \theta_{\frac{\pi}{2}}^- &= \theta_{\frac{\pi}{2}}^+, \\ \Rightarrow \theta_t^c &= \theta_t^{c'} - 2St \theta_f(d, \theta_t^d), \\ \Rightarrow b_2 - b'_2 &= -2\theta_f(d, \theta_t^d), \end{aligned} \quad (5.35)$$

where

$$\theta_f = \cos \theta_t^d \left( \frac{1 - B_0}{1 - A_0} \right) \frac{k}{d} + \frac{1}{d} \int_{\frac{d}{\sin \theta_t^d}}^{\infty} \exp \left[ - \int_{r'}^{\frac{d}{\sin \theta_t^d}} \frac{q(r'')}{2} dr'' \right] \left\{ \frac{f_3(r', \theta'_0, \phi'_0)}{(1 - A') \sin \theta'_0 \cos \phi'_0 \sin \phi'_0} - \frac{(1 - B') f_2(r', \theta'_0, \phi'_0) \cos \theta'_0}{r' (1 - A')^2 \sin^2 \theta'_0 \cos \phi'_0 \sin \phi'_0} \right\} dr'. \quad (5.36)$$

From (5.34) and (5.35), it can be verified that one obtains the same expression for  $\Delta x = St \Delta \bar{x}$  as that for trajectories with  $O(1)$  gradient offset viz. (5.20). This is consistent with our initial assumption that the non-uniformity is solely with regard to the gradient displacement  $\Delta z$ .

In order to find  $\Delta z$ , we express  $b'_2$  (which contains the unknown  $m'_1$ ) in (5.34) in terms of the other known quantities; thus

$$b'_2 = b_2 + a_2 + \frac{2 \cos \theta_t^d (1 - B_0)}{d(1 - A_0)} k - 2 \frac{\Delta \bar{x}}{d} \cos^2 \theta_t^d \frac{(1 - B_0)}{(2 - B_0)} \exp \left[ \int_{\frac{d}{\sin \theta_t^d}}^{\infty} \frac{q(r')}{2} dr' \right].$$

Using (5.30) and (5.32), we have

$$\begin{aligned} \frac{2m_1 m'_1 + m_1'^2}{d^2} (\sin \theta_t^d \cos \theta_t^d) \frac{(1 - B_0)}{(2 - B_0)} \exp \left[ \int_{\frac{d}{\sin \theta_t^d}}^{\infty} q(r') dr' \right] &= \frac{2 \cos \theta_t^d (1 - B_0)}{d(1 - A_0)} k \\ &- 2 \frac{\Delta \bar{x}}{d} \cos^2 \theta_t^d \frac{(1 - B_0)}{(2 - B_0)} \exp \left[ \int_{\frac{d}{\sin \theta_t^d}}^{\infty} \frac{q(r')}{2} dr' \right], \end{aligned}$$

which leads to a quadratic equation in  $m'_1$  given by

$$m_1'^2 + 2m_1 m'_1 = \frac{2d}{\sin \theta_t^d} \frac{(2 - B_0)}{(1 - A_0)} k \exp \left[ - \int_{\frac{d}{\sin \theta_t^d}}^{\infty} q(r') dr' \right] - 2(\Delta \bar{x}) x^{-\infty}. \quad (5.37)$$

In writing the solution we take the positive root of the equation, the reasoning being the

$x^{-\infty}$	$m_1^c St^{\frac{1}{2}} (St = 0.1)$	$m_1^c St^{\frac{1}{2}} (St = 0.01)$	Ratio
0	0.165	0.05	3.3 (3.162)
0.1	0.163	0.05	3.2 (3.162)
0.2	0.156	0.048	3.25 (3.162)
0.5	0.116	0.036	3.22 (3.162)

Table 5.3: Limiting offsets for off-plane trajectories for small  $x^{-\infty}$ ; the value in brackets in the fourth column gives the ratio  $(St_1/St_2)^{\frac{1}{2}}$  with  $St_1 = 0.1$  and  $St_2 = 0.01$ .

same as that for the in-plane analysis (see Appendix C4). Therefore

$$m_1' = \frac{1}{2} \left( -2m_1 + \left\{ 4m_1^2 + 4 \left[ \frac{2d}{\sin \theta_t^d} \frac{(2 - B_0)}{(1 - A_0)} k \exp \left[ - \int_{\frac{d}{\sin \theta_t^d}}^{\infty} q(r') dr' \right] - 2(\Delta \bar{x}) x^{-\infty} \right] \right\}^{\frac{1}{2}} \right). \quad (5.38)$$

The offset of the limiting finite  $St$  trajectory is then given by  $m_1^c St^{\frac{1}{2}}$ , this being obtained by putting  $m_1' = -m_1$  in (5.38); thus

$$m_1^c = \left( - \frac{2k(d, \theta_t^d)d}{\sin \theta_t^d} \frac{(2 - B_0)}{(1 - A_0)} \exp \left[ - \int_{\frac{d}{\sin \theta_t^d}}^{\infty} q(r') dr' \right] + 2(\Delta \bar{x}) x^{-\infty} \right)^{\frac{1}{2}}. \quad (5.39)$$

In table 5.3 we tabulate the limiting offsets  $m_1^c St^{\frac{1}{2}}$  for off-plane trajectories for small  $x^{-\infty}$  ( $\leq 0.5$ ) and for  $St = 0.1$  and  $0.01$ ; the in-plane limiting offsets correspond to  $x^{-\infty} = 0$ . The values were obtained from numerical integration of the trajectory equations and their ratio for the two Stokes numbers confirms the  $O(St^{\frac{1}{2}})$  scaling predicted by (5.39).

The expression (5.39) is real-valued only for small values of  $x^{-\infty}$ . With increasing  $x^{-\infty}$ , the term  $(2\Delta \bar{x})x^{-\infty}$  remains negative (as argued in the previous section), and the first term in (5.39) reverses sign (see section 5.3.3.4). The argument of the square root then becomes negative, suggesting that limiting finite  $St$  trajectories for large values of  $x^{-\infty}$  no longer originate from a finite gradient offset. In section 5.1 it was seen that this corresponds to the diminishing importance of lubrication interactions in relation to inertial forces and results

in  $\Delta z$  reversing sign, in turn implying the existence of a neutral off-plane trajectory ( $x^{-\infty} = x_c^{-\infty}$ ,  $z^{-\infty} = 0$ ) for which  $\Delta z = 0$ . For this neutral trajectory, the factor multiplying  $1/z^{-\infty}$  in (5.21) goes to zero as  $o(z^{-\infty})$  when  $z^{-\infty} \rightarrow 0$ . From (5.21), we see that  $x_c^{-\infty}$  satisfies

$$2 \int_{\frac{d^c}{\sin \theta_t^{d^c}}}^{\infty} \exp \left[ - \int_{r'}^{\infty} q(r'') dr'' \right] \left\{ \frac{2r' \cos \theta'_0 \left\{ (1-B') \sin^2 \phi'_0 + \frac{B'}{2} \right\}}{(1-A') \sin \theta'_0} \theta_{1m}^- + \frac{r' f_1(r', \theta'_0, \phi'_0)}{(1-A') \sin \theta'_0} \right. \\ \left. + \frac{\left\{ (1-B') \sin^2 \phi'_0 + \frac{B'}{2} \right\} f_2(r', \theta'_0, \phi'_0)}{(1-A')^2 \sin^2 \theta'_0 \sin \phi'_0 \cos \phi'_0} \right\} dr' - (\Delta \bar{x}) |_{x=x_c^{-\infty}} x_c^{-\infty} = 0, \quad (5.40)$$

where  $d^c$  and  $\theta_t^{d^c}$  can be obtained as functions of  $x_c^{-\infty}$  from the zero-Stokes trajectory equations. The value of  $x_c^{-\infty}$  given by the solution of (5.40) is clearly independent of  $St$ , thereby validating the physical arguments put forth in section 5.1. Numerical integration of the trajectory equations gives  $x_c^{-\infty} \approx 0.9$ , and this value is found to be virtually independent of  $St$  for  $St$  ranging from 0.1 to 0.01. Table 5.4 shows similarly obtained values of  $\Delta z$  ( $z^{-\infty}$  ranging from 5 to 0.1) for two values of the off-plane coordinate  $x^{-\infty} > x_c^{-\infty}$ . These values illustrate the reversal in sign of the gradient displacement for small gradient offsets. The  $O(St)$  scaling of  $\Delta z$  for trajectories with large  $z^{-\infty}$  is also evident.

The relation (5.40) is a special case of the more general relation

$$2 \int_{\frac{c}{\sin \theta_t}}^{\infty} \exp \left[ - \int_{r'}^{\infty} q(r'') dr'' \right] \left\{ \frac{2r' \cos \theta'_0 \left\{ (1-B') \sin^2 \phi'_0 + \frac{B'}{2} \right\}}{(1-A') \sin \theta'_0} \theta_{1m}^- + \frac{r' f_1(r', \theta'_0, \phi'_0)}{(1-A') \sin \theta'_0} \right. \\ \left. + \frac{\left\{ (1-B') \sin^2 \phi'_0 + \frac{B'}{2} \right\} f_2(r', \theta'_0, \phi'_0)}{(1-A')^2 \sin^2 \theta'_0 \sin \phi'_0 \cos \phi'_0} \right\} dr' - (\Delta \bar{x}) x^{-\infty} = 0, \quad (5.41)$$

which gives the gradient offset  $z_c^{-\infty}$  for fixed  $x^{-\infty} (\geq x_c^{-\infty})$  at which  $\Delta z$  changes sign; thus for the neutral trajectory,  $z_c^{-\infty} = 0$ ). This value is also seen to be independent of  $St$ , again consistent with arguments in section 5.1. Numerical integration of the trajectory equations shows that  $\Delta z$  in table 5.4 reverses sign at  $z_c^{-\infty} = 0.36$  and  $0.24$ , respectively for the off-plane

$$x^{-\infty} = 1.5$$

$z^{-\infty}$	$\Delta z (St = 0.1)$	$\Delta z (St = 0.01)$
5	$-1.59 \times 10^{-3}$	$-1.589 \times 10^{-4}$
2	$-6.62 \times 10^{-3}$	$-6.593 \times 10^{-4}$
1	$-6.46 \times 10^{-3}$	$-6.397 \times 10^{-4}$
0.5	$-2.444 \times 10^{-3}$	$-2.376 \times 10^{-4}$
0.2	$5.502 \times 10^{-3}$	$5.754 \times 10^{-4}$
0.1	$1.516 \times 10^{-2}$	$1.665 \times 10^{-3}$

$$x^{-\infty} = 5$$

$z^{-\infty}$	$\Delta z (St = 0.1)$	$\Delta z (St = 0.01)$
5	$-3.802 \times 10^{-4}$	$-3.801 \times 10^{-5}$
2	$-2.335 \times 10^{-4}$	$-2.332 \times 10^{-5}$
1	$-8.986 \times 10^{-5}$	$-8.95 \times 10^{-6}$
0.5	$-3.424 \times 10^{-5}$	$-3.371 \times 10^{-6}$
0.2	$1.331 \times 10^{-5}$	$1.418 \times 10^{-6}$
0.1	$1.007 \times 10^{-4}$	$1.022 \times 10^{-5}$

Table 5.4: Values of  $\Delta z$  for  $x^{-\infty} = 1.5$  and 5,  $z^{-\infty}$  ranging from 5 to 0.1;  $St = 0.1, 0.01$ .

coordinates  $x^{-\infty} = 1.5$  and 5. These values of  $z_c^{-\infty}$  remain virtually unchanged for  $St$  ranging from 0.1 to 0.01.

The analysis in this section is also applicable to off-plane trajectories with  $O(St^{\frac{1}{2}})$  or smaller gradient offsets and  $x^{-\infty} \geq x_c^{-\infty}$ , since we have made no assumption regarding the sign of  $m'_1$  upto (5.38). For these values of  $x^{-\infty}$ , (5.21) again loses its validity at a gradient offset of  $O(St^{\frac{1}{2}})$ , and the gradient displacement is given by (5.38). Owing to the change in sign of  $\Delta z$  for small  $z^{-\infty}$ , however, the limiting finite  $St$  trajectory is now coincident with the zero-Stokes separatrix far upstream, i.e.,  $z^{-\infty} = 0$ , and asymptotes to a downstream gradient offset of  $O(St^{\frac{1}{2}})$ . The expression for the (positive) gradient displacement of this limiting trajectory is given by (5.38) with  $m_1 = 0$ . This leads to the same expression as that obtained for  $m_1^c$  viz. (5.39), except that the sign of the argument in the square root is reversed. That such a regime exists is not immediately apparent, since as argued earlier,  $\Delta z = 0$  for  $z^{-\infty} = z_c^{-\infty}$  when  $x \geq x_c^{-\infty}$ , and  $z_c^{-\infty} \ll 1$ ; it is therefore possible that  $m_1$  as given by

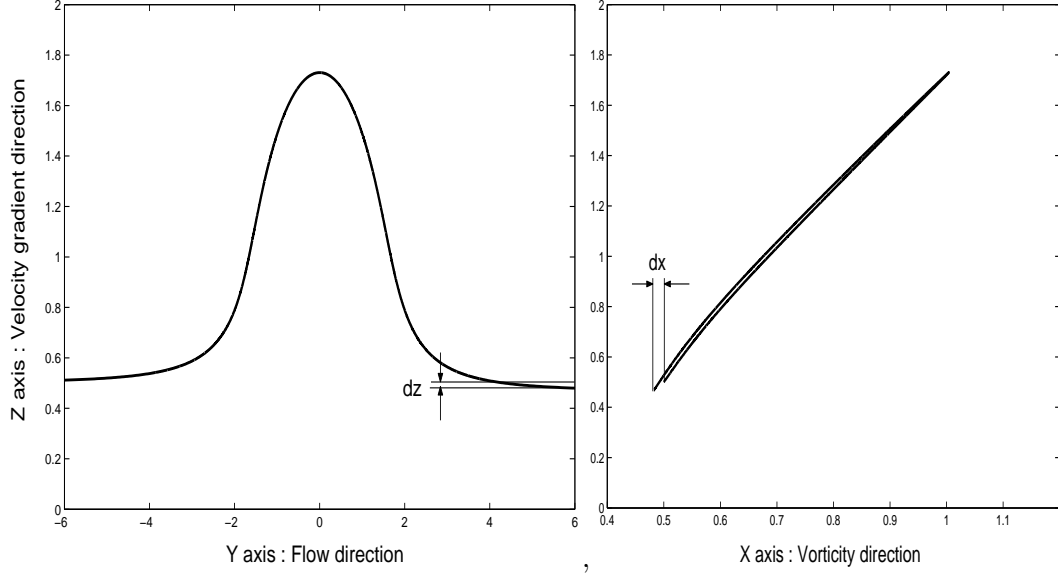


Figure 5.9: Off-plane open trajectory for  $x^{-\infty} = 0.5$  with  $z^{-\infty} = 0.5$ :  $yz$  and  $xz$  projections.

(5.38) is no longer an  $O(1)$  quantity close to the region of non-uniformity ( $z^{-\infty} \leq O(St^{\frac{1}{2}})$ ). However, one must recall that, while (5.38) is valid for trajectories with initial offsets in the range  $(0, bSt^{\frac{1}{2}})$  for  $b \sim O(1)$ , the location of the envelope of trajectories for which  $\Delta z = 0$  is given by (5.41) and is independent of  $St$ . Thus, in principle, one can always go to a  $St$  small enough that  $bSt^{\frac{1}{2}} \ll z_c^{-\infty}$  for  $x^{-\infty} \geq x_c^{-\infty}$ .

In what follows we show off-plane trajectories obtained from numerical integration of the system comprising (5.1) and (5.2) for various values of  $z^{-\infty}$  and  $x^{-\infty}$ . All trajectories shown from here on are for a Stokes number of 0.1. In Figs 5.9 and 5.10 the trajectories start from an off-plane coordinate ( $x^{-\infty}$ ) of 0.5 and have gradient offsets  $z^{-\infty} = 0.5$  and 0.12, respectively; the  $\Delta z$  for these cases is negative. The second trajectory corresponds to the limiting offset ( $z^{-\infty} = 0.12$ ) for this value of  $x^{-\infty}$ , and therefore  $z^{+\infty} \rightarrow 0$  as  $y \rightarrow \infty^4$ . Trajectories with smaller gradient offsets are no longer open. Thus, the nature of the off-plane open trajectories for  $x^{-\infty} = 0.5$  is similar to the in-plane trajectories (see Chapter 3).

<sup>4</sup>Since the figure only shows the portion of the trajectory between  $y = -6$  and  $y = 6$ , that  $z \rightarrow 0$  as  $y \rightarrow \infty$  is not evident. However, this was verified by plotting the trajectory upto a downstream  $y$  coordinate of 300.

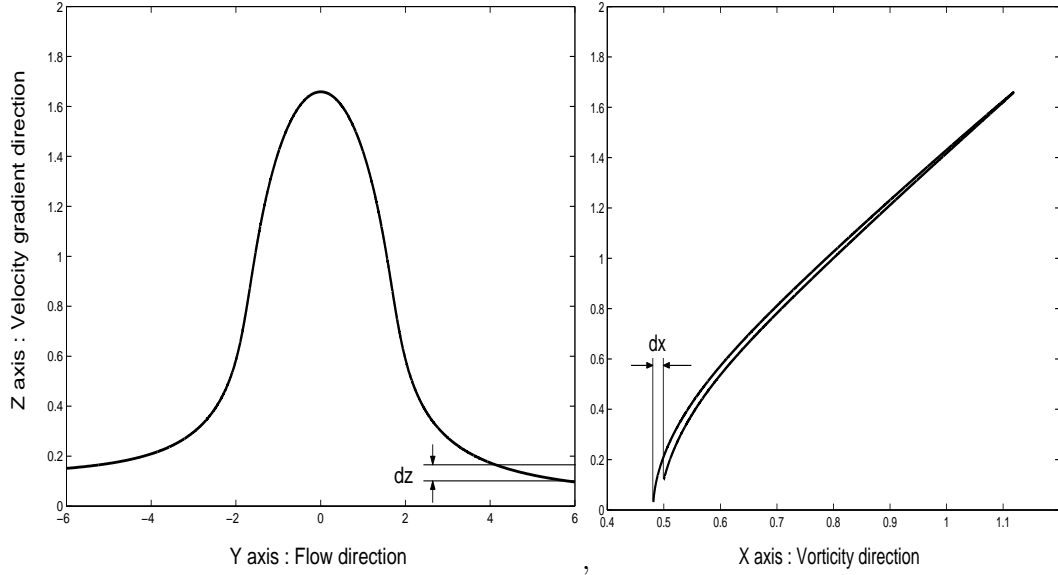


Figure 5.10: Limiting off-plane open trajectory for  $x^{-\infty} = 0.5$  with  $z^{-\infty} = 0.12$ :  $yz$  and  $xz$  projections.

Figs 5.11, 5.12 and 5.13 show trajectories for a larger value of the off-plane coordinate,  $x^{-\infty} = 1.5$ . The projection of the trajectories in the  $yz$  plane shows a hump which is relatively less pronounced and is indicative of weakening interactions. The trajectory starting from the largest gradient offset ( $z^{-\infty} = 0.5$ ) still has a negative  $\Delta z$  similar to the in-plane trajectories; the magnitude of this displacement is, however, 0.0024 for  $St = 0.1$  and therefore not discernible from the figure. The trajectory with  $z^{-\infty} = 0.15$  has a positive  $\Delta z$ . The limiting open trajectory in this case (Fig 5.13) starts from  $z^{-\infty} = 0$  and also has a positive  $\Delta z$ . For still larger values of  $x^{-\infty}$ , the qualitative behavior of the trajectories remains the same as that for  $x^{-\infty} = 1.5$ , except that the inertial effects grow progressively weaker.

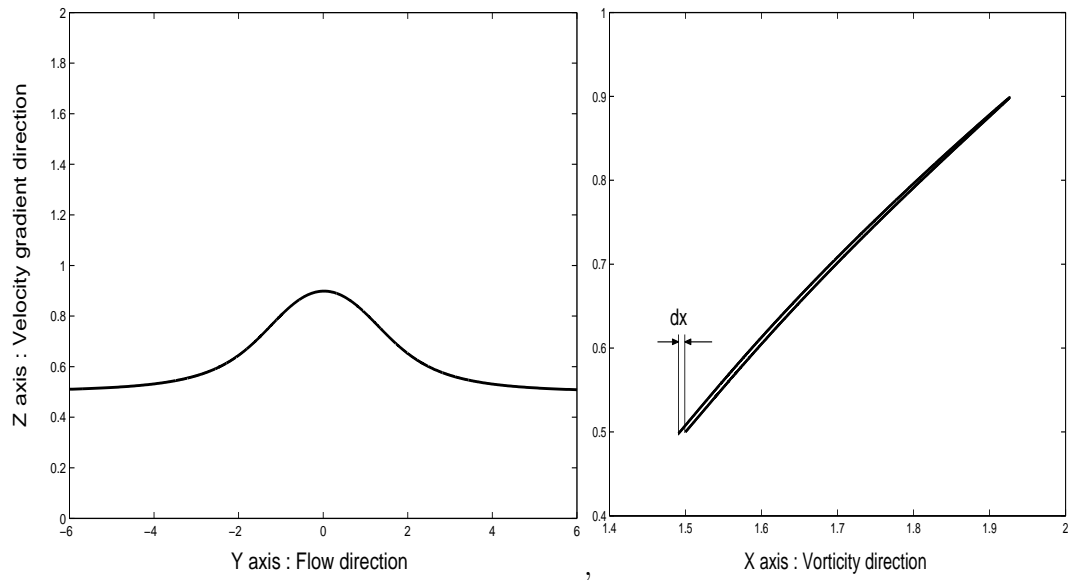


Figure 5.11: Off-plane open trajectory for  $x^{-\infty} = 1.5$  with  $z^{-\infty} = 0.5$ :  $yz$  and  $xz$  projections.

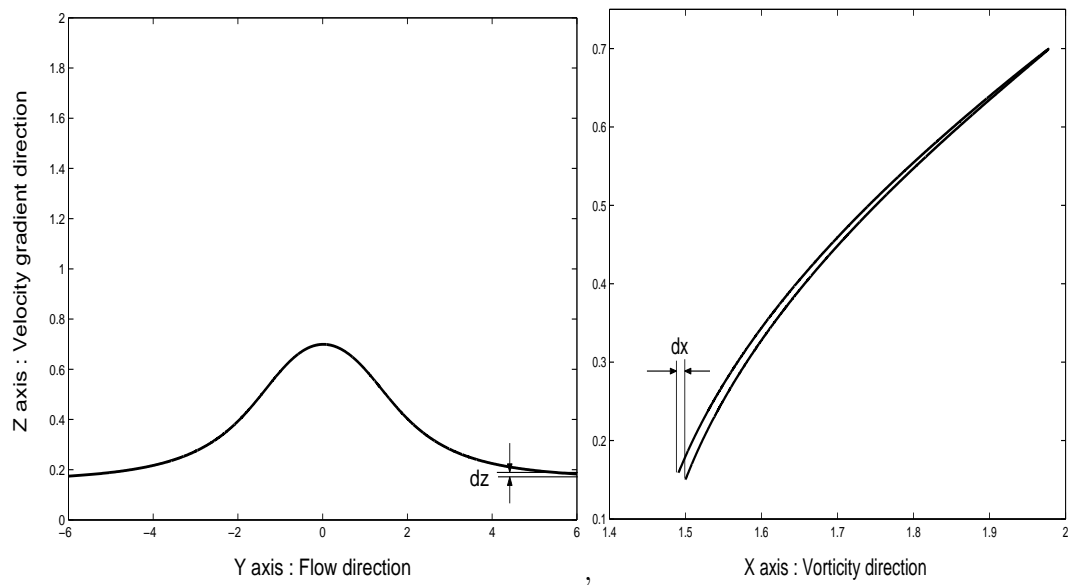


Figure 5.12: Off-plane open trajectory for  $x^{-\infty} = 1.5$  with  $z^{-\infty} = 0.15$ :  $yz$  and  $xz$  projections.

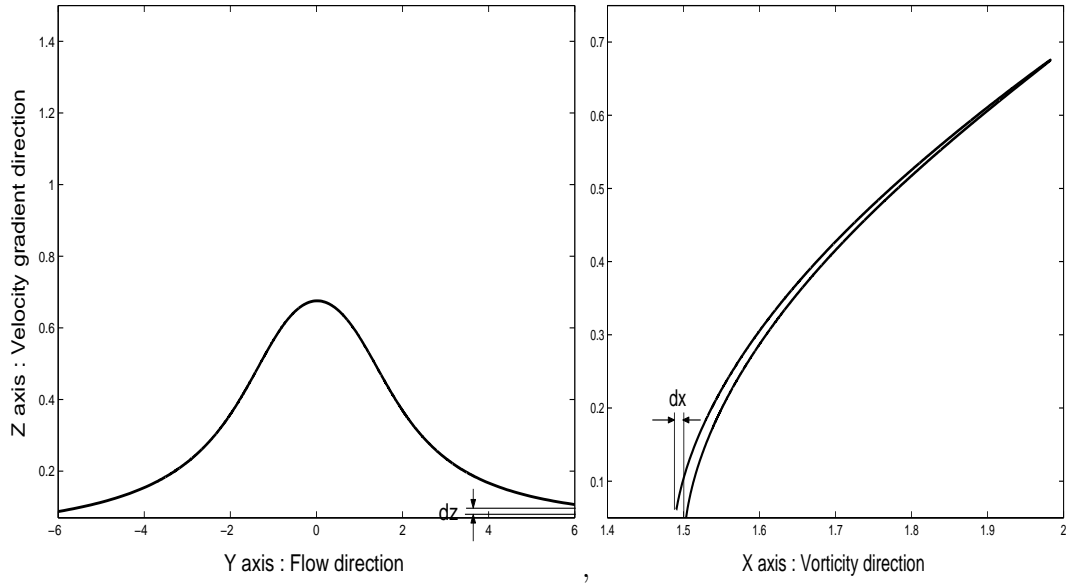


Figure 5.13: Limiting off-plane open trajectory for  $x^{-\infty} = 1.5$  with  $z^{-\infty} = 0$ :  $yz$  and  $xz$  projections.

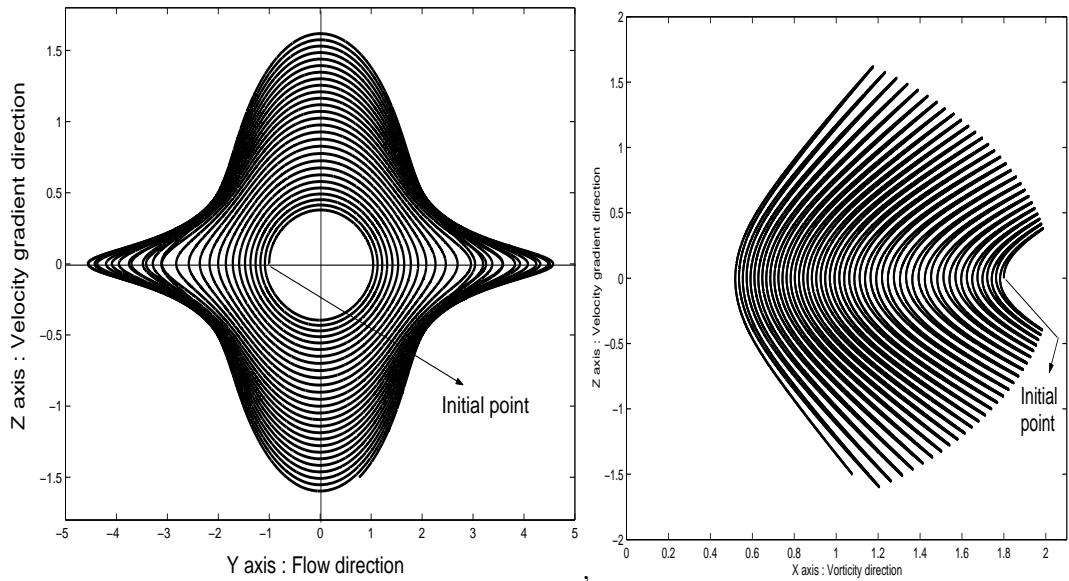


Figure 5.14: Spiralling off-plane trajectory starting from  $(x, y, z) \equiv (1.8, -1, 0)$ :  $yz$  and  $xz$  projections.

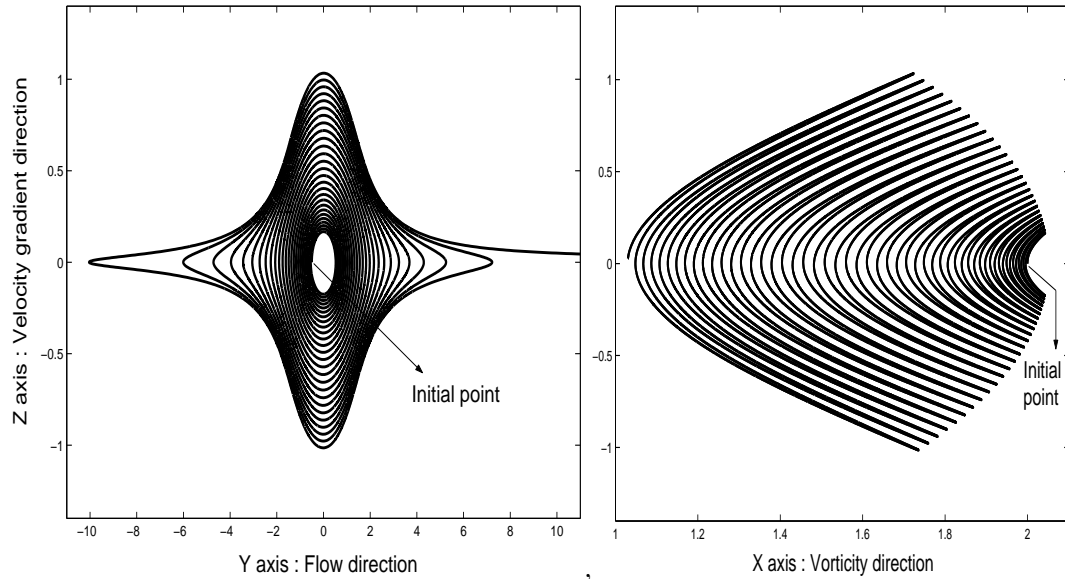


Figure 5.15: Off-plane trajectory starting from  $(x, y, z) \equiv (2, -0.5, 0)$  and spiralling off to infinity:  $yz$  and  $xz$  projections.

An example of a trajectory that spirals in uniformly onto the in-plane limit cycle was shown in Fig 5.4 in section 5.2. Figs 5.14 and 5.15 show other possible spiralling behaviors. The trajectory in Fig 5.14 first spirals outward, but subsequently turns and eventually spirals inward, converging onto the in-plane limit cycle. This can be seen as a retracing of its path in the  $yz$  projection leading to the apparent crossing of trajectories in this view. The trajectory in Fig 5.15 spirals out finally tending to  $y = \infty$ . Although the scale in the figure stops at approximately  $y = 11$ , the trajectory is found to continue along this path upto  $y = 250$  with little change in  $z$ . The above figures again serve to reinforce the physical picture presented in section 5.2.

### 5.3.3 Far-field analytical expressions for lateral displacements $\Delta z$ and $\Delta x$

Here we derive analytical expressions for the gradient and vorticity displacements. Evidently, the resulting approximate expressions for small and large values of the offplane coordinate will be power series in  $x^{-\infty}$  and  $1/x^{-\infty}$ , respectively, for a fixed initial gradient offset. In the former limit, the offplane gradient displacement is expected to approach the inplane displacement  $(\Delta z)_{inplane}$ , and the vorticity displacement, since it tends to zero for  $x^{-\infty} \rightarrow 0$ , is in any event too small to be of any significance. We therefore restrict our attention to the case where  $x^{-\infty} \gg 1$ . In sections 5.3.3.1 and 5.3.3.2 we evaluate  $\Delta x$  and  $\Delta z$  for far-field trajectories located away from the separatrix surface. In sections 5.3.3.3 and 5.3.3.4 we evaluate the  $\Delta x$  and  $\Delta z$  for far-field trajectories that are coincident with the zero-Stokes separatrix surface far upstream, and use these expressions to determine the domain of validity of the perturbation analysis.

#### 5.3.3.1 Vorticity Displacement $\Delta x$ in the limit $x^{-\infty}, z^{-\infty} \gg 1$

The vorticity displacement as given by (5.20) is

$$\Delta x = -2St \int_{\frac{c}{\sin \theta_t}}^{\infty} \exp \left[ -\int_{r'}^{\infty} \frac{q(r'')}{2} dr'' \right] \left\{ \frac{f_3(r', \theta'_0, \phi'_0)}{(1-A') \sin \theta'_0 \cos \phi'_0 \sin \phi'_0} - \frac{(1-B') f_2(r', \theta'_0, \phi'_0) \cos \theta'_0}{r' (1-A')^2 \sin^2 \theta'_0 \cos \phi'_0 \sin \phi'_0} \right\} dr'.$$

We take  $x^{-\infty} = \alpha z^{-\infty}$ , where  $\alpha$  is an  $O(1)$  number. As in the inplane case,  $\Delta x$  will be of the same order as the first deviation of the zero-Stokes trajectory from the ambient streamline (of simple shear flow) due to hydrodynamic interactions. Since this deviation is  $O(1/z^{-\infty})^3$  for  $\alpha \sim O(1)$ , and since we only calculate the leading order term in what would

be an infinite power series, we will use the members of the pairs  $(x^{-\infty}, c \cos \theta_t / \sin \theta_t)$  and  $(z^{-\infty}, c)$  interchangeably in what follows, incurring an error consistent with the order of the neglected terms. With this in mind, we have the following limiting forms for the various quantities in (5.20):

$$\begin{aligned} \cos \theta_0 &\approx \frac{\alpha c}{r}, & \sin \theta_0 &\approx \left(1 - \frac{\alpha^2 c^2}{r^2}\right)^{\frac{1}{2}}, \\ \sin \phi_0 &\approx \frac{c}{r \left(1 - \frac{\alpha^2 c^2}{r^2}\right)^{\frac{1}{2}}}, & \cos \phi_0 &\approx \frac{\left[1 - \frac{(1+\alpha^2)c^2}{r^2}\right]^{\frac{1}{2}}}{\left(1 - \frac{\alpha^2 c^2}{r^2}\right)^{\frac{1}{2}}}, \\ \exp \left[ - \int_{r'}^{\infty} \frac{q(r'')}{2} dr'' \right] &\approx 1, \end{aligned}$$

where the far-field approximations for the hydrodynamic functions are the same as that used in section 4.4.4 when evaluating  $(\Delta z)_{inplane}$ . Again, in a manner exactly analogous to the inplane case, the terms at  $O(1/z^{-\infty})^2$  (corresponding to approximating  $G, H \approx 1$ ) can be shown to cancel out identically. At  $O(1/z^{-\infty})^3$ , we have the following approximate expressions for the terms in the integrand:

$$\begin{aligned} f_3 : & \frac{f_3(r', \theta'_0, \phi'_0)}{(1 - A') \sin \theta'_0 \cos \phi'_0 \sin \phi'_0}, \\ & \approx \frac{2A'(H' - 1) \sin^3 \theta'_0 \cos \theta'_0 \sin^2 \phi'_0 \cos^2 \phi'_0}{\sin \theta'_0 \cos \phi'_0 \sin \phi'_0}, \\ & = -\frac{15\alpha c^2}{2r'^6} \left(1 - \frac{(1 + \alpha^2)c^2}{r'^2}\right)^{\frac{1}{2}}. \\ f_2 : & \frac{(1 - B')f_2(r', \theta'_0, \phi'_0) \cos \theta'_0}{r'(1 - A')^2 \sin^2 \theta'_0 \cos \phi'_0 \sin \phi'_0}, \\ & \approx -\frac{(G' - 1) \cos \theta'_0}{\sin^2 \theta'_0 \cos \phi'_0 \sin \phi'_0} \left[ \sin^4 \theta'_0 \sin^2 \phi'_0 \cos^2 \phi'_0 \left(-r' \frac{dA'}{dr'}\right) - A' \sin^2 \theta'_0 \sin^2 \phi'_0 \right], \\ & = -\frac{\frac{3\alpha c^2}{2r'^6} \left[10 - 15 \frac{(1+\alpha)^2}{r'^2}\right]}{\left[1 - \frac{(1+\alpha)^2}{r'^2}\right]^{\frac{1}{2}}}, \end{aligned}$$

$z^{-\infty}$	$x^{-\infty}$	$(\Delta x)_{numer}$	$(\Delta x)_{far-field}$
5	5	$-3.784 \times 10^{-4}$	$-4.165 \times 10^{-4}$
7	7	$-1.454 \times 10^{-4}$	$-1.518 \times 10^{-4}$
4	8	$-1.563 \times 10^{-4}$	$-1.646 \times 10^{-4}$
5	10	$-8.197 \times 10^{-5}$	$-8.43 \times 10^{-5}$
8	4	$-8.174 \times 10^{-5}$	$-8.43 \times 10^{-5}$
10	5	$-1.555 \times 10^{-4}$	$-1.646 \times 10^{-4}$

Table 5.5: Comparison of numerical and far-field approximation (5.42) for  $\Delta x$  in the limit  $x^{-\infty}, z^{-\infty} \gg 1$  for  $St = 0.1$ .

where  $(G' - 1)$  and  $(H' - 1)$  at this order represent the  $O(1/r)$  corrections to the mobility functions. Therefore, one finally obtains

$$\begin{aligned} \Delta x &= 3(St) \int_{c\sqrt{1+\alpha^2}}^{\infty} \left[ 5 \left\{ 1 - \frac{(1+\alpha)^2}{r'^2} \right\}^{\frac{1}{2}} + \frac{\left\{ 10 - 15 \frac{(1+\alpha)^2}{r'^2} \right\}}{\left\{ 1 - \frac{(1+\alpha)^2}{r'^2} \right\}^{\frac{1}{2}}} \right] \frac{\alpha c^2}{r'^6} dr', \\ &= St \frac{15\alpha}{2c^3(1+\alpha^2)^{\frac{5}{2}}} \int_0^1 \frac{a'^{\frac{3}{2}}(3-4a')}{(1-a')^{\frac{1}{2}}} da', \end{aligned}$$

where we have used  $a' = c^2(1+\alpha^2)/r'^2$ . Evaluating the integral and replacing  $c$  by  $z^{-\infty}$ , one finds

$$\Delta x = -St \frac{15\pi}{16} \frac{\alpha}{(1+\alpha^2)^{\frac{5}{2}} (z^{-\infty})^3}. \quad (5.42)$$

Thus, the vorticity displacement is indeed negative as expected from the arguments in section 5.1. In table 5.5 we compare (5.42) with values obtained from numerical integration, again using an adaptive Runge-Kutta method, of the system of equations (5.1) and (5.2) for  $St = 0.1$ .

### 5.3.3.2 Gradient Displacement $\Delta z$ in the limit $x^{-\infty}, z^{-\infty} \gg 1$

The gradient displacement as given by (5.21) is

$$\Delta z = \frac{St}{z^{-\infty}} \left( 2 \int_{\frac{c}{\sin \theta'_t}}^{\infty} \exp \left[ - \int_{r'}^{\infty} q(r'') dr'' \right] \left\{ \frac{2r' \cos \theta'_0 \{ (1-B') \sin^2 \phi'_0 + \frac{B'}{2} \}}{(1-A') \sin \theta'_0} \theta_{1m}^- + \frac{r' f_1(r', \theta'_0, \phi'_0)}{(1-A') \sin \theta'_0} \right. \right. \\ \left. \left. + \frac{\{ (1-B') \sin^2 \phi'_0 + \frac{B'}{2} \} f_2(r', \theta'_0, \phi'_0)}{(1-A')^2 \sin^2 \theta'_0 \sin \phi'_0 \cos \phi'_0} \right\} dr' \right) - (\Delta x) \frac{x^{-\infty}}{z^{-\infty}}.$$

As for the case of  $\Delta x$ , the terms at  $O(1/z^{-\infty})^2$  can again be shown to cancel out. Again, using  $x^{-\infty} = \alpha z^{-\infty}$  and with the same far-field expressions as in section 5.3.3.1, one obtains the following approximations for the terms in the integrand:

$$f_1 : \frac{r' f_1(r', \theta'_0, \phi'_0)}{(1-A') \sin \theta'_0} \\ \approx - \frac{r' (H' - 1) \sin^2 \theta'_0 \sin \phi'_0 \cos \phi'_0 (2A' \sin^2 \phi'_0 \sin \theta'_0)}{c \sin \theta'_0}, \\ = \frac{15c^3 \left\{ 1 - \frac{(1+\alpha^2)c^2}{r'^2} \right\}^{\frac{1}{2}}}{2r'^6 \left( 1 - \frac{\alpha^2 c^2}{r'^2} \right)}. \\ f_2 : \frac{\{ (1-B') \sin^2 \phi'_0 + \frac{B'}{2} \} f_2(r', \theta'_0, \phi'_0)}{(1-A')^2 \sin^2 \theta'_0 \sin \phi'_0 \cos \phi'_0}, \\ \approx \frac{\sin \phi'_0 (-r') (G' - 1)}{\sin^2 \theta'_0 \cos \phi'_0} \left[ \sin^4 \theta'_0 \sin^2 \phi'_0 \cos^2 \phi'_0 \left( -r' \frac{dA'}{dr'} \right) - A' \sin^2 \theta'_0 \sin^2 \phi'_0 \right], \\ = \frac{3c^3}{2r'^6} \left[ 15 \left\{ 1 - \frac{(1+\alpha^2)c^2}{r'^2} \right\}^{\frac{1}{2}} - \frac{5}{\left\{ 1 - \frac{(1+\alpha^2)c^2}{r'^2} \right\}^{\frac{1}{2}}} \right].$$

$$\begin{aligned}
\theta_{1m}^- &: \frac{2r' \cos \theta'_0 \left\{ (1-B') \sin^2 \phi'_0 + \frac{B'}{2} \right\}}{(1-A') \sin \theta'_0} \theta_{1m}^- \\
&\approx -\frac{2 \cos \theta'_0 \sin^2 \phi'_0}{\sin^2 \theta'_0} \int_{r'}^{\infty} \left( \frac{2A'(H' - 1) \sin^3 \theta'_0 \cos \theta'_0 \sin^2 \phi'_0 \cos^2 \phi'_0}{\sin \theta'_0 \cos \phi'_0 \sin \phi'_0} - \frac{(G' - 1 \cos \theta'_0)}{\sin^2 \theta'_0 \cos \phi'_0 \sin \phi'_0} \right. \\
&\quad \left. \left\{ \sin^4 \theta'_0 \sin^2 \phi'_0 \cos^2 \phi'_0 \left( r' \frac{dA'}{dr'} \right) + A' \sin^2 \theta'_0 \sin^2 \phi'_0 \right\} \right) dr', \\
&= -\frac{\frac{3\alpha c^3}{r'^3}}{\left(1 - \frac{\alpha^2 c^2}{r'^2}\right)^2} \int_{r'}^{\infty} \left[ 5 \left\{ 1 - \frac{(1+\alpha)^2}{r''^2} \right\}^{\frac{1}{2}} + \frac{\left\{ 10 - 15 \frac{(1+\alpha)^2}{r''^2} \right\}}{\left\{ 1 - \frac{(1+\alpha)^2}{r''^2} \right\}^{\frac{1}{2}}} \right] \frac{\alpha c^2}{r''^6} dr'', \\
&= \frac{\frac{3\alpha c^3}{r'^3}}{\left(1 - \frac{\alpha^2 c^2}{r'^2}\right)^2} \frac{5\alpha}{2c^3(1+\alpha^2)^{\frac{5}{2}}} \int_{\left\{ 1 - \frac{(1+\alpha)^2}{r''^2} \right\}}^1 \left( 4a' - \frac{1}{a'} \right) (1-a')^{\frac{3}{2}} da'.
\end{aligned}$$

Changing variables to  $\psi = \sin^{-1} a'$  and integrating, one finally obtains

$$\begin{aligned}
&\frac{2r' \cos \theta'_0 \left\{ (1-B') \sin^2 \phi'_0 + \frac{B'}{2} \right\}}{(1-A') \sin \theta'_0} \theta_{1m}^- \\
&\approx \frac{15\alpha^2}{(1+\alpha^2)^{\frac{5}{2}}} \frac{1}{r'^3 \left(1 - \frac{\alpha^2 c^2}{r'^2}\right)^2} \left[ \frac{1}{8} \sin^{-1} \left\{ 1 - \frac{(1+\alpha^2)c^2}{r'^2} \right\}^{\frac{1}{2}} + \frac{(1+\alpha^2)^{\frac{1}{2}}}{8} \left\{ 1 - \frac{(1+\alpha^2)c^2}{r'^2} \right\}^{\frac{1}{2}} \frac{c}{r'} \right. \\
&\quad \left. + \frac{(1+\alpha^2)^{\frac{3}{2}}}{12} \left\{ 1 - \frac{(1+\alpha^2)c^2}{r'^2} \right\}^{\frac{1}{2}} \frac{c^3}{r'^3} + \frac{2(1+\alpha^2)^{\frac{5}{2}}}{3} \left\{ 1 - \frac{(1+\alpha^2)c^2}{r'^2} \right\}^{\frac{1}{2}} \frac{c^5}{r'^5} - \frac{\pi}{16} \right].
\end{aligned}$$

Using the above approximations in the expression for  $\Delta z$ , we get

$$\begin{aligned}
\Delta z &= \frac{2St}{(z^{-\infty})^3} \left[ \frac{15}{4(1+\alpha^2)^{\frac{5}{2}}} \left\{ 4 \sum_{n=0}^{\infty} \left( \frac{\alpha^2}{1+\alpha^2} \right)^n Be\left(n + \frac{5}{2}, \frac{3}{2}\right) - \sum_{n=0}^{\infty} \left( \frac{\alpha^2}{1+\alpha^2} \right)^n Be\left(n + \frac{5}{2}, \frac{1}{2}\right) \right\} \right. \\
&\quad + \frac{15\pi}{32(1+\alpha^2)^{\frac{3}{2}}} \frac{\sqrt{1+\alpha^2} - 1}{(1+\alpha^2)} + \frac{15\alpha^2}{8(1+\alpha^2)^{\frac{7}{2}}} \sum_{n=0}^{\infty} (n+1) \left( \frac{\alpha^2}{1+\alpha^2} \right)^n Be\left(n + \frac{3}{2}, \frac{3}{2}\right) \\
&\quad + \frac{5\alpha^2}{8(1+\alpha^2)^{\frac{7}{2}}} \sum_{n=0}^{\infty} \left( \frac{\alpha^2}{1+\alpha^2} \right)^n Be\left(n + \frac{5}{2}, \frac{3}{2}\right) + \frac{5\alpha^2}{(1+\alpha^2)^{\frac{7}{2}}} \sum_{n=0}^{\infty} \left( \frac{\alpha^2}{1+\alpha^2} \right)^n Be\left(n + \frac{7}{2}, \frac{3}{2}\right) \\
&\quad \left. - \frac{15\pi\alpha^2}{32(1+\alpha^2)^{\frac{5}{2}}} \right] + St \frac{15\pi\alpha^2}{16(1+\alpha^2)^{\frac{5}{2}}} \frac{1}{(z^{-\infty})^3}, \tag{5.43}
\end{aligned}$$

where the details of the calculation are given in Appendix C5. A comparison of the far-field approximation and the corresponding numerical values is given in table 5.6 for  $St = 0.1$ .

$z^{-\infty}$	$x^{-\infty}$	$(\Delta z)_{numer}$	$(\Delta z)_{far-field}$
5	5	$-3.802 \times 10^{-4}$	$-4.207 \times 10^{-4}$
7	7	$-1.458 \times 10^{-4}$	$-1.518 \times 10^{-4}$
4	8	$-7.9 \times 10^{-5}$	$-8.242 \times 10^{-5}$
5	10	$-4.128 \times 10^{-5}$	$-4.22 \times 10^{-5}$
8	4	$-3.116 \times 10^{-4}$	$-2.846 \times 10^{-4}$
10	5	$-1.637 \times 10^{-4}$	$-1.457 \times 10^{-4}$

Table 5.6: Comparison of numerical values and the far-field approximation (5.43) for  $\Delta z$  in the limit  $x^{-\infty}, z^{-\infty} \gg 1$  for  $St = 0.1$ .

### 5.3.3.3 Vorticity Displacement $\Delta x$ on the finite $St$ separatrix in the limit

$$x^{-\infty} \gg 1$$

We now calculate  $\Delta x$  from (5.20) for large  $x^{-\infty}$  in the limit when the inertial trajectory is coincident with the zero-Stokes separatrix far upstream, i.e., when  $z^{-\infty} = 0$ ; in the notation of the preceding section,  $\alpha$  is no longer an  $O(1)$  quantity. As seen earlier this can only happen when  $x^{-\infty} > x_c^{-\infty}$  and since the latter is  $O(1)$ , the limit  $x^{-\infty} \gg 1$  is consistent with this requirement. It is known that the zero-Stokes separatrix surface is axisymmetric and is described by the relation (Batchelor and Green 1972a)

$$z^2 \sim \frac{16}{9r^3} + O\left(\frac{1}{r^5}\right),$$

for large  $r$ . In the gradient-vorticity  $(xz)$  plane, this gives us

$$d^2 = \frac{16 \sin^3 \theta_t^d}{d^3} \left[ 1 + O(d^{\frac{4}{3}}) \right] = \frac{16 \theta_t^{d^3}}{d^3} \left[ 1 + O(d^{\frac{4}{3}}) \right],$$

where  $d \ll 1$  for large  $x^{-\infty}$ ; the relative error in approximating  $\sin \theta_t^d$  by  $\theta_t^d$  is  $o(d^{\frac{4}{3}})$ . We then have the following approximate expressions for the trigonometric functions appearing

in (5.20):

$$\begin{aligned}\cos \theta_0 &\approx \frac{d \cos \theta_t^d}{\sin \theta_t^d} \frac{1}{r} \approx \frac{1}{\theta_t^d} \frac{d}{r}, & \sin \theta_0 &\approx \left(1 - \frac{\cos^2 \theta_t^d d^2}{\sin^2 \theta_t^d r^2}\right)^{\frac{1}{2}} \approx \left(1 - \frac{1}{\theta_t^{d^2}} \frac{d^2}{r^2}\right)^{\frac{1}{2}}, \\ \cos \phi_0 &\approx \frac{\left(1 - \frac{1}{\sin^2 \theta_t^d} \frac{d^2}{r^2}\right)^{\frac{1}{2}}}{\left(1 - \frac{\cos^2 \theta_t^d d^2}{\sin^2 \theta_t^d r^2}\right)^{\frac{1}{2}}} \approx 1, & \sin \phi_0 &\approx \frac{\left\{\left(d^2 - \frac{16 \sin^3 \theta_t^d}{9d^3}\right) \frac{1}{r^2} + \frac{16}{9r^5}\right\}^{\frac{1}{2}}}{\left(1 - \frac{\cos^2 \theta_t^d d^2}{\sin^2 \theta_t^d r^2}\right)^{\frac{1}{2}}} \approx \frac{4}{3r^{\frac{5}{2}} \left(1 - \frac{1}{\theta_t^{d^2}} \frac{d^2}{r^2}\right)^{\frac{1}{2}}},\end{aligned}$$

where the leading order error is  $O(d^{\frac{4}{3}})$ , this arising from use of the approximate equation for the separatrix surface in simplifying  $\sin \phi_0$ ; the resulting form for  $\sin \phi_0$  is  $O(1/r^{\frac{5}{2}}) = O(d^{\frac{5}{3}})$ . Also note that having replaced  $\cos \theta_t$  in this expression with 1,  $\sin \phi_0$  is no longer bounded in absolute value by unity. The errors incurred, however, are  $O(d^{\frac{10}{3}})$  or smaller. Using these relations it may be verified that the leading order contributions correspond to the approximations:

$$\begin{aligned}f_3(r', \theta'_0, \phi'_0) &\approx \left(1 - \frac{3}{4r'}\right) \frac{B'}{2} \sin \theta'_0 \cos \theta'_0, \\ f_2(r', \theta'_0, \phi'_0) &\approx r' \left(1 - \frac{3}{2r'}\right) \frac{B'}{2'} \cos^2 \phi'_0 \sin^2 \theta'_0,\end{aligned}$$

where the error is again  $O(d^{\frac{4}{3}})$ ; the neglected corrections to the mobility functions  $G$  and  $H$  are of  $O(1/r^3)$  and produce errors of a smaller order. The expression for  $\Delta x$  becomes

$$\Delta x = -2St \int_{\frac{d}{\sin \theta_t^d}}^{\infty} \left\{ \left(1 - \frac{3}{4r'}\right) \frac{B' \cos \theta'_0}{2 \cos \phi'_0 \sin \phi'_0} - \left(1 - \frac{3}{2r'}\right) \frac{B' \cos \phi'_0 \cos \theta'_0}{2 \sin \phi'_0} \right\} dr',$$

where the  $O(d)$  leading order terms are easily seen to cancel out. Since the  $O(1/r)$  terms contribute terms which are  $O(d^{\frac{2}{3}})$  smaller, the original (relative) error of  $O(d^{\frac{4}{3}})$  now becomes

$x^{-\infty}$	$d$	$(\Delta x)_{numer}$	$(\Delta x)_{far-field}$
6	0.0907	$-4.235 \times 10^{-4}$	$-5.44 \times 10^{-4}$
8	0.0589	$-2.149 \times 10^{-4}$	$-2.558 \times 10^{-4}$
10	0.0421	$-1.257 \times 10^{-4}$	$-1.517 \times 10^{-4}$

Table 5.7: Comparison of numerical values and the analytical approximation (5.44) for  $\Delta x$  in the limit  $x^{-\infty} \gg 1, z^{-\infty} = 0$  for  $St = 0.1$ .

$O(d^{\frac{2}{3}})$ ; we obtain

$$\begin{aligned}
\Delta x &= -\frac{3}{4}St \int_{\frac{d}{\theta_t^d}}^{\infty} \frac{B' \cos \theta'_0}{r' \sin \phi'_0} dr', \\
&= -3St \int_{\frac{d}{\theta_t^d}}^{\infty} \frac{1}{r'^{\frac{7}{2}} \theta_t^d r'} \left(1 - \frac{1}{\theta_t^{d^2} r'^2}\right)^{\frac{1}{2}} dr', \\
&= -\frac{3}{2}St \left(\frac{\theta_t^d}{d}\right)^{\frac{5}{2}} Be\left(\frac{7}{4}, \frac{3}{2}\right), \\
&= -0.2967 St d^{\frac{5}{3}} \left[1 + O(d^{\frac{2}{3}})\right], \tag{5.44}
\end{aligned}$$

where the values of the Beta function were obtained from Abramowitz & Stegun 1972. Therefore,  $\Delta x$  on the separatrix still remains  $O(St)$  and negative. For small  $St$ , the relative error in evaluation is  $O(d^{\frac{2}{3}})$ , independent of  $St$ . Since this quantity can be fairly large even for  $d \ll 1$ , we expect a greater discrepancy between (5.44) and the values obtained by numerical integration compared to cases considered in previous sections. These values are given in table 5.7 for  $St = 0.1$ , and appear to capture the variation of  $\Delta x$  at least in a qualitative manner. The above quantities were also calculated for  $St = 0.01$  and the relative discrepancy remains independent of  $St$ .

Using the above far-field approximations, we consider the limiting form of the outer expansion (in layer O1) for the  $\theta$  coordinate (see (5.5) and (5.6)) close to the zero-

Stokes separatrix; it is seen that

$$\theta_t \approx O(d^{\frac{5}{3}}),$$

$$\frac{St}{c} \int_{\frac{c}{\sin \theta_t}}^{\infty} \exp \left[ - \int_{r'}^{\frac{c}{\sin \theta_t}} q(r'') dr'' \right] \left\{ \frac{f_3(r', \theta'_0, \phi'_0)}{(1-A') \sin \theta'_0 \cos \phi'_0 \sin \phi'_0} - \frac{(1-B') f_2(r', \theta'_0, \phi'_0) \cos \theta'_0}{r' (1-A')^2 \sin^2 \theta'_0 \cos \phi'_0 \sin \phi'_0} \right\} dr'$$

$$\approx St d^{\frac{2}{3}},$$

so that the  $O(St)$  perturbation and the leading order term in the expansion are of the same order when  $d \sim O(St)$ , i.e., when  $\theta_t \sim O(St^{\frac{5}{3}})$ . As a result, the perturbation analysis is no longer valid for  $\theta_t^d \leq O(St^{\frac{5}{3}})$ . This perhaps suggests the reason why the discrepancy between the analytical (far-field) and numerical values in table 5.7 does not decrease with increasing  $x^{-\infty}$ . This non-uniformity does not, however, affect the results of the diffusivities to  $O(St^2)$  as shown in section 5.3.4. Neither does it imply any essential change in the nature of the open trajectories since  $\Delta x$  still remains small compared to  $x^{-\infty}$ . Indeed, such a change cannot occur for open trajectories in the limit  $x^{-\infty} \gg 1$  as the interactions and the concomitant inertial effects are extremely weak at these distances. Rather, it shows that spherical polar coordinates are not suited to describe trajectories with  $x^{-\infty} \gg 1, z^{-\infty} \ll 1$ , since the  $\theta$  coordinate becomes asymptotically small close to  $\phi = \pi/2$ .

#### 5.3.3.4 Gradient Displacement $\Delta z$ on the zero-Stokes-separatrix in the limit

$$x^{-\infty} \gg 1$$

Here we examine (5.38) for  $m'_1$  in the limit  $m_1 \rightarrow 0$  for  $x^{-\infty} \gg 1$ ;  $\Delta z = m'_1 St^{\frac{1}{2}}$ . For the approximation derived to be numerically accurate, there must exist an  $O(St^{\frac{1}{2}})$  interval of initial offsets well separated from  $z_c^{-\infty}$  (where  $\Delta z = 0$ ). As seen in section 5.3.2, one may need to go to very small values of Stokes numbers (less than 0.01) for this to be true.

Nevertheless, the resulting approximate expression captures qualitatively the variation in the gradient displacement, showing the change in sign of  $\Delta z$  for large  $x^{-\infty}$ ; it also serves to define the domain of validity of the perturbation analysis, this being consistent with that found above in section 5.3.3.3.

It can be shown that in the above limit, the second term in (5.38) is of  $O(d)$  using the scaling of  $\Delta x$  (see previous section), and is dominant thereby leading to a positive  $\Delta z$ ;  $\Delta z \sim O(St d)^{\frac{1}{2}}$ . We, however, focus on the first term in (5.38) in order to show the sign reversal for large  $x^{-\infty}$  and small gradient offset ( $z^{-\infty}$ ). Using the same far-field approximations as in the previous section, it is found that the term proportional to  $\theta_{1m}^-$  in this term is of a smaller order (see (5.38) and (5.33)). At leading order, the first term is then given by

$$\frac{2k(d, \theta_t^d)d(2-B_0)}{\sin \theta_t^d(1-A_0)} \exp \left[ - \int_{\frac{d}{\sin \theta_t^d}}^{\infty} q(r') dr' \right],$$

where

$$\begin{aligned} k(d, \theta_t^d) &= 2 \sin \theta_t^d \frac{(1-A_0)}{d(2-B_0)} \int_{\frac{d}{\sin \theta_t^d}}^{\infty} \left\{ \frac{r' f_1(r', \theta'_0, \phi'_0)}{(1-A') \sin \theta'_0} + \frac{\{(1-B') \sin^2 \phi'_0 + \frac{B'}{2}\} f_2(r', \theta'_0, \phi'_0)}{(1-A')^2 \sin^2 \theta'_0 \sin \phi'_0 \cos \phi'_0} \right\} dr', \\ &\approx \frac{2\theta_t^d}{d} \int_{\frac{d}{\theta_t^d}}^{\infty} \left\{ \frac{\sin^2 \theta'_0}{2} \cos^3 \phi'_0 \sin \phi'_0 \left( r'^2 \frac{dB'}{dr'} \right) + \frac{B' \cos \phi'_0}{2 \sin \phi'_0} \left( \sin^2 \phi'_0 + \frac{B'}{2} \right) \right\} dr', \\ &= \frac{\theta_t^d}{d} \left[ -\frac{320}{9} \int_{\frac{d}{\theta_t^d}}^{\infty} \frac{dr'}{r'^{\frac{13}{2}}} \left( 1 - \frac{d^2}{r'^2 \sin^2 \theta_t^d} \right)^{\frac{1}{2}} + \frac{64}{9} \int_{\frac{d}{\theta_t^d}}^{\infty} \frac{1}{r'^{\frac{15}{2}} \left( 1 - \frac{d^2}{r'^2 \sin^2 \theta_t^d} \right)^{\frac{1}{2}}} dr' \right. \\ &\quad \left. + \frac{32}{3} \int_{\frac{d}{\theta_t^d}}^{\infty} \frac{dr'}{r'^{\frac{13}{2}}} \left( 1 - \frac{d^2}{r'^2 \sin^2 \theta_t^d} \right)^{\frac{1}{2}} \right], \\ &= d^{\frac{13}{3}} \left[ -\frac{40}{3} Be \left( \frac{11}{4}, \frac{3}{2} \right) + \frac{32}{6} Be \left( \frac{11}{4}, \frac{3}{2} \right) + \frac{32}{9} Be \left( \frac{11}{4}, \frac{1}{2} \right) \right], \\ &= d^{\frac{13}{3}} \frac{48}{39} Be \left( \frac{11}{4}, \frac{1}{2} \right), \end{aligned}$$

and is thus positive in contrast to its value near the shearing plane.

We now reconsider equation (5.26) for  $c'$ . In the limit  $m_1 \ll m'_1$ , and for  $(c', \theta_t^{c'}) \rightarrow (d, \theta_t^d)$ , we have

$$St(m_1 + m'_1)^2 \exp\left[\int_{\frac{c'}{\sin \theta_t^{c'}}}^{\infty} q(r') dr'\right] \approx O(St d),$$

$$\int_{\frac{c'}{\sin \theta_t^{c'}}}^{\infty} \exp\left[-\int_{r'}^{\frac{c'}{\sin \theta_t^{c'}}} q(r'') dr''\right] \frac{B' r'}{(1 - A')} dr' \approx O(d^2),$$

where we have used the scaling of  $\Delta z$  above. The  $O(St)$  and leading order terms are of the same order when  $d \sim O(St)$  or when  $\theta_t^d \sim O(St^{\frac{5}{3}})$ ; thus the perturbation analysis is no longer expected to be valid when  $\theta_t^d \leq O(St^{\frac{5}{3}})$ .

### 5.3.4 Scaling of self-diffusivities $D_{zz}$ and $D_{xx}$

From section 4.4.5, the transverse components of the diffusivity tensor are given as

$$\hat{D}_{zz} = (4) \frac{3}{8\pi} \int_0^{\infty} \int_0^{\infty} dx^{-\infty} dz^{-\infty} z^{-\infty} (\Delta z)^2, \quad (5.45)$$

$$\hat{D}_{xx} = (4) \frac{3}{8\pi} \int_0^{\infty} \int_0^{\infty} dx^{-\infty} dz^{-\infty} z^{-\infty} (\Delta x)^2, \quad (5.46)$$

where owing to symmetry considerations, it suffices to integrate over a quadrant of the whole trajectory space. The analysis in previous sections has shown that the transverse displacements of finite  $St$  trajectories in the gradient and vorticity directions behave very differently. In particular, for small gradient offsets and close to the reference sphere, they no longer scale with  $St$  in the same manner. This leads to an anisotropic inertial diffusivity tensor. Here we show that the scaling of the gradient component of the diffusivity tensor,  $\hat{D}_{zz}$ , remains the same as its in-plane projection ( $\hat{D}_{zz}^{ip}$ ) evaluated in section 4.4.5, and that

the vorticity component,  $\hat{D}_{xx}$ , is  $O(St^2)$ . The relative anisotropy as characterised by the ratio of the diffusivities  $\hat{D}_{zz}/\hat{D}_{xx}$  is then  $O(\ln St)$  and increases as  $St \rightarrow 0$ .

While open trajectories for zero  $St$  cover the entire range of non-zero initial offsets ( $-\infty < z^{-\infty}, x^{-\infty} < \infty$ ;  $z^{-\infty} \neq 0$ ), for finite  $St$  there exists a window of extent  $(\Delta z^{-\infty} \times \Delta x^{-\infty}) \equiv (O(St^{\frac{1}{2}}) \times 2x_c^{-\infty})$  that serves as a trapping zone and will eventually lead to the capture of a given particle by the limit cycle in the shearing plane of a second particle. This effect is not considered here, however, and is expected, on average, to affect the trajectory of any ‘tagged’ particle only at times asymptotically long compared to the flow time for  $St$  small enough. In principle, this provides a sufficient length of time (and thence a sufficient number of interactions) for the particle to start behaving in a diffusive manner. The scaling analysis given below therefore applies to trajectories outside this trapping window.

Since  $\Delta x$  remains  $O(St)$  for all  $z^{-\infty}$  and  $x^{-\infty}$ , and decays rapidly enough (see section 5.3.3) for the integral in (5.46) to be convergent,  $\hat{D}_{xx}$  is expected to be of  $O(St^2)$ . The expression (5.46) evaluated only over the finite  $St$  open trajectories is

$$\begin{aligned} \frac{\hat{D}_{xx}}{4} = \frac{3St^2}{8\pi} & \left( \int_0^{x_c^{-\infty}} dx^{-\infty} \int_{m_1^c(x^{-\infty})St^{\frac{1}{2}}}^{\infty} dz^{-\infty} + \int_{x_c^{-\infty}}^{bSt^{-\frac{2}{3}}} dx^{-\infty} \int_0^{\infty} dz^{-\infty} \right. \\ & \left. + \int_{bSt^{-\frac{2}{3}}}^{\infty} dx^{-\infty} \int_0^{\infty} dz^{-\infty} \right) z^{-\infty} (\Delta \bar{x})^2, \end{aligned} \quad (5.47)$$

where we have explicitly shown the dependence of the limiting offset  $m_1^c$  on  $x_c^{-\infty}$ . Here,  $\Delta x = St \Delta \bar{x}$ . Splitting the integration interval (w.r.t  $x^{-\infty}$ ) across  $x_c^{-\infty}$ , as in the first two integrals, takes into account the change in character of the finite  $St$  separatrix envelope for  $x^{-\infty} \geq x_c^{-\infty}$ ; this is evident from the lower limit of the integration with respect to  $z^{-\infty}$ . The second division at  $bSt^{-\frac{2}{3}}$  ( $b \sim O(1)$ ) serves to isolate the region of non-uniformity (see sections 5.3.3.3 and 5.3.3.4),  $\theta_t \leq O(St^{\frac{5}{3}})$  or equivalently  $x^{-\infty} \geq O(St^{-\frac{2}{3}})$ .

As  $z^{-\infty} \rightarrow 0$ ,  $\Delta x$  remains  $O(St)$  and

$$\int_0^{x_c^{-\infty}} dx^{-\infty} \int_0^{m_1^c St^{\frac{1}{2}}} dz^{-\infty} z^{-\infty} (\Delta x)^2 \sim o(St^2),$$

whence the range of integration respect to  $z^{-\infty}$  in the first term of (5.47) can be extended down to zero. Thus, (5.47) takes the form

$$\frac{\hat{D}_{xx}}{4} = \frac{3St^2}{8\pi} \left( \int_0^{bSt^{-\frac{2}{3}}} dx^{-\infty} + \int_{bSt^{-\frac{2}{3}}}^{\infty} dx^{-\infty} \right) \int_0^{\infty} dz^{-\infty} z^{-\infty} (\Delta \bar{x})^2,$$

where  $\Delta x$  is given by (5.20) in the first term. In the second term,  $\theta_t \sim O(St^{\frac{5}{3}})$ , which implies  $\Delta \bar{x} \sim St^{-1} O(d^{\frac{5}{3}}) \sim O(St^{\frac{2}{3}})$  (see section 5.3.3.3);  $\Delta x$  will certainly be smaller for larger  $x^{-\infty}$  since the perturbation analysis predicts erroneously large values of  $\Delta x$  for smaller values of  $\theta_t$ . Therefore (5.47) reduces to

$$\frac{\hat{D}_{xx}}{4} = \frac{3St^2}{8\pi} \int_0^{\infty} dx^{-\infty} \int_0^{\infty} dz^{-\infty} z^{-\infty} (\Delta \bar{x})^2, \quad (5.48)$$

with an error of  $o(St^2)$ , thereby yielding the expected  $O(St^2)$  scaling.

For  $\hat{D}_{zz}$ , (5.45) when evaluated over the open finite  $St$  trajectories, can similarly be written as

$$\begin{aligned} \frac{\hat{D}_{zz}}{4} = \frac{3St^2}{8\pi} & \left( \int_0^{x_c^{-\infty}} dx^{-\infty} \int_{m_1^c St^{\frac{1}{2}}}^{\infty} dz^{-\infty} + \int_{x_c^{-\infty}}^{bSt^{-\frac{2}{3}}} dx^{-\infty} \int_0^{\infty} dz^{-\infty} \right. \\ & \left. + \int_{bSt^{-\frac{2}{3}}}^{\infty} dx^{-\infty} \int_0^{\infty} dz^{-\infty} \right) z^{-\infty} (\Delta \bar{z})^2, \end{aligned} \quad (5.49)$$

For the purposes of analytical evaluation, the integrals over  $z^{-\infty}$  in the first two  $x^{-\infty}$  sub-intervals above will be further split, as in section 4.4.5, into an outer layer where  $\Delta z$  is given

by (5.21) and a singular layer of  $O(St^{\frac{1}{2}})$  where it is given by (5.38).

In order to deduce the scaling of the leading order contribution to  $\hat{D}_{zz}$ , however, this will not be necessary. Since  $\Delta z$ , like  $\Delta x$ , decays away rapidly for large  $x^{-\infty}$  and  $z^{-\infty}$ , one can again neglect the region of non-uniformity viz.  $x^{-\infty} \in (bSt^{-\frac{2}{3}}, \infty)$ . Therefore, the largest contributions come from the first and second terms where the singular layer scales as  $O(St^{\frac{1}{2}})$ , and as in the in-plane case, the logarithmic singularity in (5.21) results in an  $O(St^2 \ln St)$  leading order term. The scaling for  $\hat{D}_{zz}$  remains the same even with the added integration with respect to  $x^{-\infty}$  because  $x_c^{-\infty}$  is independent of  $St$ , and therefore the range of integration with respect to  $x^{-\infty}$  in the first and second terms is, to leading order, independent of  $St$ .

## 5.4 Comparison with direct numerical simulation of pair trajectories

In this section we simulate pair-particle trajectories in simple shear flow by numerically integrating the exact equations of motion for small Stokes numbers. The values of the transverse displacements obtained are compared to those obtained by numerical integration of the  $O(St)$  trajectory equations (5.1) and (5.2) (these latter values were used to support the conclusions of the perturbation analysis in Chapter 4 and in section 5.3 of this chapter).

The equations of relative translational and rotational motion (the appropriate variable being the sum of the individual angular velocities) are solved below using an adaptive step fourth order Runge Kutta routine. The values of the hydrodynamic functions required for the numerical integration (and for the trajectory calculations performed earlier) were obtained as follows. For separations less than 4 particle radii, the values of the hydrodynamic functions were obtained by interpolating between tabulated values obtained from the twin multipole expansions given in Jeffrey & Onishi (1984) and Jeffrey (1992); the number of terms included

in the expansion was 300. For separations greater than 4 particle radii, the approximate far-field expressions given in the same references were used (also see Kim & Miffllin 1985, Kim & Karrila 1992). The equations of motion are given by

$$\begin{aligned} St \frac{d\mathbf{V}}{dt} &= -(\mathbf{R}_{FU}^{11} - \mathbf{R}_{FU}^{12}) \cdot (\mathbf{V} - \mathbf{\Gamma} \cdot \mathbf{r}) + (\mathbf{R}_{F\Omega}^{11} + \mathbf{R}_{F\Omega}^{12}) \cdot (\mathbf{\Omega}^s - 2\mathbf{\Omega}^\infty) - 2(\mathbf{R}_{FE}^{11} + \mathbf{R}_{FE}^{12}) : \mathbf{E}^\infty, \\ \frac{2}{5} \frac{d\mathbf{\Omega}^s}{dt} &= (\mathbf{R}_{F\Omega}^{11} + \mathbf{R}_{F\Omega}^{12})^\dagger \cdot (\mathbf{V} - \mathbf{\Gamma} \cdot \mathbf{r}) - (\mathbf{R}_{L\Omega}^{11} + \mathbf{R}_{L\Omega}^{12}) \cdot (\mathbf{\Omega}^s - 2\mathbf{\Omega}^\infty) + 2(\mathbf{R}_{LE}^{11} + \mathbf{R}_{LE}^{12}) : \mathbf{E}^\infty, \end{aligned} \quad (5.50)$$

where  $\mathbf{\Omega}^s = \mathbf{\Omega}_1 + \mathbf{\Omega}_2$  and are solved in spherical coordinates together with the set of equations relating the spatial coordinates to the respective velocities, viz.  $d\mathbf{x}/dt = \mathbf{v}$ . The numerical integration is carried out starting from far upstream. The initial translational ( $\mathbf{V}_{t=0}$ ) and angular velocities ( $\mathbf{\Omega}_{t=0}^s$ ) are taken to be that induced by the ambient simple shear flow at the initial position of the particle.

In tables 5.8 to 5.13, we compare the values of  $\Delta x$  and  $\Delta z$  obtained by integrating the system (5.50) (denoted by  $(\Delta x, \Delta z)_{dirnum}$ ) to that obtained by numerical integration of the  $O(St)$  trajectory equations (denoted by  $(\Delta x, \Delta z)_{traj}$ ) in section 5.3 for various values of the off-plane coordinate, varying the gradient offset  $z^{-\infty}$  in each case from 5 down to 0.1; the Stokes number for all cases considered is 0.1. In general the values of  $\Delta x$  and  $\Delta z$  show good agreement. There is a relatively large discrepancy between the values of  $\Delta z$  near the zero-crossing ( $z^{-\infty} = z_c^{-\infty}$ ) which is to be expected.

The direct numerical simulation gives the value of  $x_c^{-\infty}$ , the off-plane coordinate defining the neutral trajectory, as approximately 0.95, in close agreement with earlier  $O(St)$  trajectory calculations (see section 5.3, where  $x_c^{-\infty}$  was found to be close to 0.9). This value is found to be virtually independent of  $St$  for  $St$  ranging from 0.1 to 0.01, thereby confirming the theoretical prediction (5.40). Further, the values of  $z_c^{-\infty}$ , the gradient offsets at which  $\Delta z$

$z^{-\infty}$	$(\Delta x)_{dirnum}$	$(\Delta x)_{traj}$	$(\Delta z)_{dirnum}$	$(\Delta z)_{traj}$
5	0	0	$-1.855 \times 10^{-3}$	$-1.941 \times 10^{-3}$
2	0	0	$-1.565 \times 10^{-2}$	$-1.587 \times 10^{-2}$
1	0	0	$-3.834 \times 10^{-2}$	$-3.838 \times 10^{-2}$
0.5	0	0	$-4.802 \times 10^{-2}$	$-4.806 \times 10^{-2}$
0.2	0	0	$-9.341 \times 10^{-2}$	$-9.353 \times 10^{-2}$
0.1	0	0	spirals	spirals

Table 5.8:  $\Delta x$  and  $\Delta z$  values for  $x^{-\infty} = 0$  and  $z^{-\infty}$  ranging from 5 to 0.1.

$z^{-\infty}$	$(\Delta x)_{dirnum}$	$(\Delta x)_{traj}$	$(\Delta z)_{dirnum}$	$(\Delta z)_{traj}$
5	$-7.733 \times 10^{-5}$	$-7.716 \times 10^{-5}$	$-1.848 \times 10^{-3}$	$-1.933 \times 10^{-3}$
2	$-1.485 \times 10^{-3}$	$-1.557 \times 10^{-3}$	$-1.536 \times 10^{-2}$	$-1.557 \times 10^{-2}$
1	$-5.963 \times 10^{-3}$	$-6.295 \times 10^{-3}$	$-3.685 \times 10^{-2}$	$-3.684 \times 10^{-2}$
0.5	$-8.373 \times 10^{-3}$	$-8.784 \times 10^{-3}$	$-4.514 \times 10^{-2}$	$-4.503 \times 10^{-2}$
0.2	$-9.048 \times 10^{-3}$	$-9.424 \times 10^{-3}$	$-8.272 \times 10^{-2}$	$-8.222 \times 10^{-2}$
0.1	spirals	spirals	spirals	spirals

Table 5.9:  $\Delta x$  and  $\Delta z$  values for  $x^{-\infty} = 0.2$  and  $z^{-\infty}$  ranging from 5 to 0.1.

$z^{-\infty}$	$(\Delta x)_{dirnum}$	$(\Delta x)_{traj}$	$(\Delta z)_{dirnum}$	$(\Delta z)_{traj}$
5	$-1.798 \times 10^{-4}$	$-1.892 \times 10^{-4}$	$-1.813 \times 10^{-3}$	$-1.897 \times 10^{-3}$
2	$-3.371 \times 10^{-3}$	$-3.533 \times 10^{-3}$	$-1.395 \times 10^{-2}$	$-1.413 \times 10^{-2}$
1	$-1.244 \times 10^{-2}$	$-1.309 \times 10^{-2}$	$-3.008 \times 10^{-2}$	$-2.991 \times 10^{-2}$
0.5	$-1.686 \times 10^{-2}$	$-1.756 \times 10^{-2}$	$-3.301 \times 10^{-2}$	$-3.24 \times 10^{-2}$
0.2	$-1.831 \times 10^{-2}$	$-1.779 \times 10^{-2}$	$-4.694 \times 10^{-2}$	$-4.496 \times 10^{-2}$
0.1	spirals	spirals	spirals	spirals

Table 5.10:  $\Delta x$  and  $\Delta z$  values for  $x^{-\infty} = 0.5$  and  $z^{-\infty}$  ranging from 5 to 0.1.

$z^{-\infty}$	$(\Delta x)_{dirnum}$	$(\Delta x)_{traj}$	$(\Delta z)_{dirnum}$	$(\Delta z)_{traj}$
5	$-3.363 \times 10^{-4}$	$-3.536 \times 10^{-4}$	$-1.772 \times 10^{-3}$	$-1.696 \times 10^{-3}$
2	$-4.921 \times 10^{-3}$	$-5.146 \times 10^{-3}$	$-1.018 \times 10^{-2}$	$-1.031 \times 10^{-2}$
1	$-1.37 \times 10^{-2}$	$-1.427 \times 10^{-2}$	$-1.558 \times 10^{-2}$	$-1.524 \times 10^{-2}$
0.5	$-1.686 \times 10^{-2}$	$-1.719 \times 10^{-2}$	$-1.183 \times 10^{-2}$	$-1.094 \times 10^{-2}$
0.2	$-1.709 \times 10^{-2}$	$-1.697 \times 10^{-2}$	$-4.755 \times 10^{-2}$	$-2.573 \times 10^{-2}$
0.1	$-1.725 \times 10^{-2}$	$-1.704 \times 10^{-2}$	$3.605 \times 10^{-4}$	$4.512 \times 10^{-3}$

Table 5.11:  $\Delta x$  and  $\Delta z$  values for  $x^{-\infty} = 1$  and  $z^{-\infty}$  ranging from 5 to 0.1.

$z^{-\infty}$	$(\Delta x)_{dirnum}$	$(\Delta x)_{traj}$	$(\Delta z)_{dirnum}$	$(\Delta z)_{traj}$
5	$-5.23 \times 10^{-4}$	$-5.486 \times 10^{-4}$	$-1.318 \times 10^{-3}$	$-1.376 \times 10^{-3}$
2	$-3.801 \times 10^{-3}$	$-3.954 \times 10^{-3}$	$-3.942 \times 10^{-3}$	$-4.003 \times 10^{-3}$
1	$-5.457 \times 10^{-3}$	$-5.562 \times 10^{-3}$	$-2.855 \times 10^{-3}$	$-2.943 \times 10^{-3}$
0.5	$-5.043 \times 10^{-3}$	$-4.896 \times 10^{-3}$	$-9.471 \times 10^{-4}$	$-7.601 \times 10^{-4}$
0.2	$-4.981 \times 10^{-3}$	$-4.512 \times 10^{-3}$	$2.699 \times 10^{-3}$	$3.121 \times 10^{-3}$
0.1	$-5.276 \times 10^{-3}$	$-4.707 \times 10^{-3}$	$7.759 \times 10^{-3}$	$8.541 \times 10^{-3}$

Table 5.12:  $\Delta x$  and  $\Delta z$  values for  $x^{-\infty} = 2$  and  $z^{-\infty}$  ranging from 5 to 0.1.

$z^{-\infty}$	$(\Delta x)_{dirnum}$	$(\Delta x)_{traj}$	$(\Delta z)_{dirnum}$	$(\Delta z)_{traj}$
5	$-3.643 \times 10^{-4}$	$-3.784 \times 10^{-4}$	$-3.675 \times 10^{-4}$	$-3.803 \times 10^{-4}$
2	$-5.496 \times 10^{-4}$	$-5.613 \times 10^{-4}$	$-2.307 \times 10^{-4}$	$-2.336 \times 10^{-4}$
1	$-3.91 \times 10^{-4}$	$-3.909 \times 10^{-4}$	$-9.097 \times 10^{-5}$	$-8.988 \times 10^{-5}$
0.5	$-2.854 \times 10^{-4}$	$-2.708 \times 10^{-4}$	$-3.771 \times 10^{-5}$	$-3.425 \times 10^{-5}$
0.2	$-3.182 \times 10^{-4}$	$-2.744 \times 10^{-4}$	$6.903 \times 10^{-6}$	$1.325 \times 10^{-5}$
0.1	$-4.496 \times 10^{-4}$	$-3.754 \times 10^{-4}$	$9.068 \times 10^{-5}$	$1.007 \times 10^{-4}$

Table 5.13:  $\Delta x$  and  $\Delta z$  values for  $x^{-\infty} = 5$  and  $z^{-\infty}$  ranging from 5 to 0.1.

changes sign for fixed  $x^{-\infty}$ , are also in good agreement with the  $O(St)$  trajectory calculations and independent of  $St$  for  $St$  in the same range.

A vivid instance of how the small  $St$  theory formulated in this Chapter and in Chapter 4 fails when  $St \sim O(1)$  is seen from plotting an in-plane spiralling trajectory obtained by integrating the equations of motion (5.50) with  $St = 2$ . The trajectory (see Fig 5.16) shows crossing of paths. In contrast, that obtained from integrating the  $O(St)$  trajectory equation (4.25) shows the same qualitative character as that for  $St \ll 1$  (see Fig 4.18) and is found to spiral in to unrealistically small separations. The crossing of paths clearly suggests that for  $St \ll 1$  one cannot reduce the full phase space to only the three positional degrees of freedom as in the  $O(St)$  trajectory equations. This would then justify the apparent crossing of paths in Fig 5.16, since it is always possible for the actual trajectories in the six-dimensional  $(\mathbf{x}, \mathbf{V})$  phase space to intersect when projected onto subspaces of lower dimensions. The qualitative difference between the two cases is not related to neglecting corrections of  $o(St)$

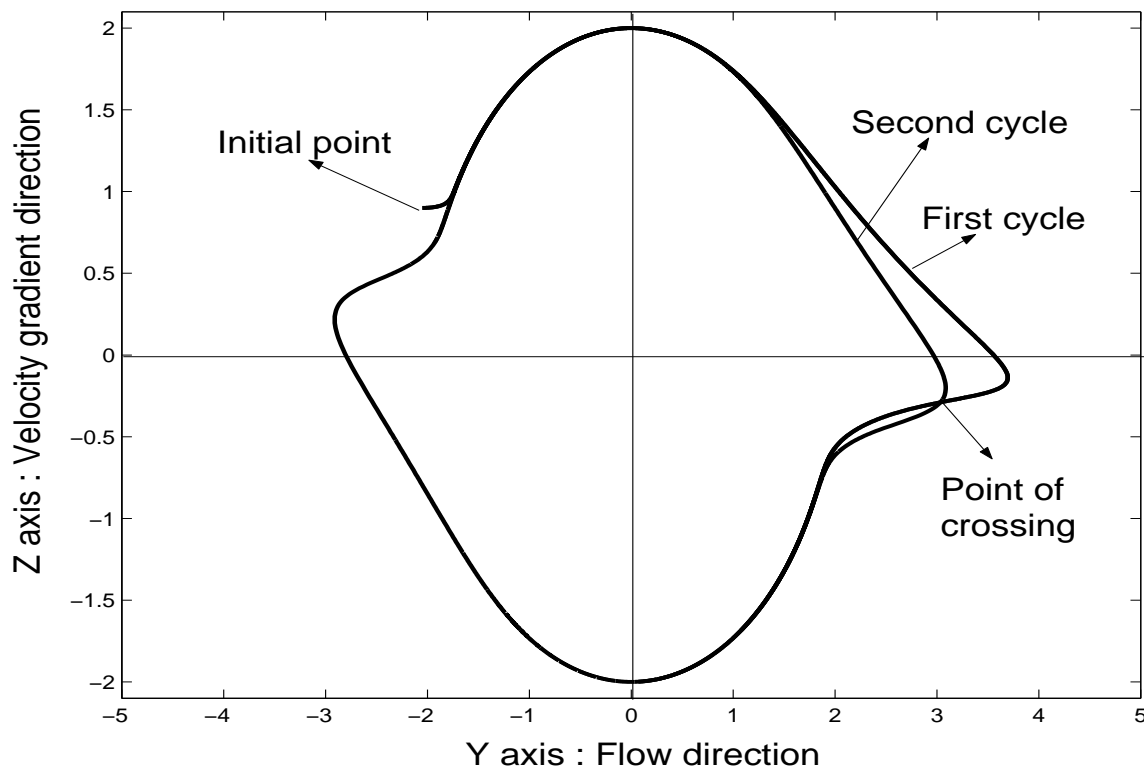


Figure 5.16: In-Plane trajectory starting from  $(x, y) \equiv (-2.03, 0.9)$  for  $St = 2$ .

in the trajectory equations. Incorporating any finite number of such corrections will still yield a single valued inertial velocity field and thence non-intersecting paths. It must be emphasised, however, that even for  $St = 2$  there seems to exist an attracting limit cycle in the shearing plane.

## 5.5 Microstructure and rheology

As seen in previous sections, the effect of particle inertia in the absence of Brownian motion is to destroy the fore-aft symmetry of the zero-Stokes trajectory space in simple shear flow. This is expected to affect the macroscopic rheological properties of the suspension. The equation governing the pair-distribution function  $g$ , to  $O(St)$ , is the corrected Smoluchowski

equation in the limit  $Pe \rightarrow \infty$  (see (4.9)):

$$\frac{\partial g}{\partial t} + \nabla_{\mathbf{r}} \cdot \left[ \left( \mathbf{V}^{(0)} + St \mathbf{V}^{(1)} + \dots \right) g \right] = 0. \quad (5.51)$$

Equation (5.51) for  $g$  does not admit a steady solution, however. The analysis of finite  $St$  trajectories revealed, for small  $St$ , the existence of a stable limit cycle in the shearing plane that is a local attractor, and whose domain of attraction is infinite in extent. Thus, a constant flux at infinity will lead to a progressive accumulation of particles, and therefore to a temporally growing density in the vicinity of the limit cycle. This may be compared to the case  $St = 0$ , where any non-singular initial condition leads to a bounded distribution for all time. Even in this case, however, a steady solution exists only for open pathlines; the distribution of particles in a region of closed pathlines depends on the particular initial condition imposed and is in general a periodic function of time (Wilson & Davis 2000). This makes the rheology of an inertialess suspension in simple shear flow indeterminate (Batchelor & Green 1972b). The above discussion shows that the rheology of a finite  $St$  suspension under pairwise interactions is still indeterminate. The resolution, of course, lies in either incorporating three-particle effects or in recognizing that other non-hydrodynamic mechanisms such as Brownian motion or short-range interparticle forces come into play in regions close to the limit cycle where particles come into close contact.

Not considering the domain of attraction of the in-plane limit cycle, the asymmetry of the finite  $St$  open trajectories in itself should induce a similar asymmetry in the pair-distribution function  $g$ . This microstructural asymmetry in turn should manifest itself in a non-Newtonian rheology. However, we still need to look at equation (5.51) in order to establish this in a more rigorous manner, because in extensional flow at zero Stokes number,  $g(\mathbf{r}) = g(r)$ , and is thus isotropic despite the relative translational velocity of the two spheres

exhibiting an angular dependence (Batchelor & Green 1972b). In order to ensure that a similar coincidence does not occur for simple shear flow at finite  $St$ , we again examine (5.51).

At leading order, one has

$$\frac{\partial g_0}{\partial t} + \mathbf{V}^{(0)} \cdot \nabla_{\mathbf{x}} g_0 = -g_0 \nabla_{\mathbf{r}} \cdot \mathbf{V}^{(0)}. \quad (5.52)$$

The crucial property of the leading order velocity  $\mathbf{V}^{(0)}$  which allows for an isotropic distribution as a possible steady solution is that the divergence of  $\mathbf{V}^{(0)}$  is related to its radial component via a function that only depends on the scalar distance  $r$ , given by

$$\nabla_{\mathbf{r}} \cdot \mathbf{V}^{(0)} = \left\{ \frac{3(A-B)}{r(1-A)} + \frac{1}{(1-A)} \frac{dA}{dr} \right\} V_r^{(0)}. \quad (5.53)$$

This then allows one to rewrite (5.52) as

$$\frac{\partial g_0}{\partial t} + \mathbf{V}^{(0)} \cdot \nabla_{\mathbf{r}} \left( \frac{g(r)}{\Phi(r)} \right) = 0,$$

where

$$\Phi(r) = \frac{1}{1-A} \exp \left[ \int_r^\infty \frac{3q(r')}{2} dr' \right],$$

and which states that the ratio  $g(r)/\Phi(r)$  is a conserved quantity along particle pathlines, from which the inference of an isotropic distribution on open pathlines follows.

The property (5.53) no longer holds for the inertial velocity  $\mathbf{V}^{(0)} + St \mathbf{V}^{(1)}$ , as can easily be seen by taking the divergence of (4.11), implying that the resulting distribution will be anisotropic and hence asymmetric in view of the different angular dependencies in the upstream and downstream regions.

## Bibliography

- [1] Abramowitz, M. & Stegun, I.A. 1972 *Handbook of Mathematical Functions*. Dover.
- [2] Batchelor, G.K. & Green, J.T. 1972a The hydrodynamic interaction of two small freely-moving spheres in a linear flow field. *J. Fluid Mech.* **56**, 375-400.
- [3] Batchelor, G.K. & Green, J.T. 1972b The determination of the bulk stress in a suspension of spherical particles to  $O(c^2)$ . *J. Fluid Mech.* **56**, 401-427.
- [4] Brady, J.F. & Bossis, G. 1988 Stokesian dynamics. *Ann. Rev. Fluid Mech.* **20**, 111-157.
- [5] daCunha, F.R. & Hinch, E.J. 1996 Shear-induced dispersion in a dilute suspension of rough spheres. *J. Fluid Mech.* **309**, 211-223.
- [6] Davis, R.H. 1996 Hydrodynamic diffusion of suspended particles: A symposium. *J. Fluid Mech.* **310**, 325-335.
- [7] Gradshteyn, I.S. & Ryzhik, I.M. 2000 *Table of Integrals, Series and Products*. Academic Press.
- [8] Guckenheimer, J. & Holmes, P. 1983 *Nonlinear oscillations, dynamical systems, and bifurcations of vector fields*. Springer-Verlag.
- [9] Jeffrey, D.J. & Onishi, Y. 1984 Calculation of the resistance and mobility functions for two unequal rigid spheres in low Reynolds number flow. *J. Fluid Mech.* **139**, 261-290.
- [10] Jeffrey, D.J. 1992 The calculation of the low Reynolds number resistance functions for two unequal spheres. *Phys. Fluids* **A4**(1), 16-29.

- [11] Kevorkian, J. & Cole, J.D. 1996 *Multiple Scale and Singular Perturbation Methods*. Springer-Verlag.
- [12] Kim, S. & Karrila, S.J. 1991 *Microhydrodynamics: Principles and Selected Applications*. Butterworth-Heinemann.
- [13] Kim, S. & Mifflin, R.T. 1985 The resistance and mobility functions of two equal spheres in low-Reynolds-number flow. *Phys. Fluids* **28**(7), 2033-2045.
- [14] Koch, D.L. 1990 Kinetic theory for a monodisperse gas-solid suspension. *Phys. Fluids* **A2**(10), 1711-1723.
- [15] Kumaran, V. & Koch, D.L. 1993a Properties of a bidisperse particle-gas suspension. 1. collision time small compared with viscous relaxation time. *J. Fluid Mech.* **247**, 623-641.
- [16] Kumaran, V. & Koch, D.L. 1993b Properties of a bidisperse particle-gas suspension. 2. viscous relaxation time small compared with collision time. *J. Fluid Mech.* **247**, 643-660.
- [17] Lagerstrom, P.A. & Casten, R.G. 1972 Basic concepts underlying singular perturbation techniques. *SIAM Rev.* **14**, 63-120.
- [18] Leighton, D. & Acrivos, A. 1987a Measurement of shear-induced self-diffusion in concentrated suspensions. *J. Fluid Mech.* **177**, 109-131.
- [19] Leighton, D. & Acrivos, A. 1987b The shear-induced migration of particles in concentrated suspensions. *J. Fluid Mech.* **181**, 415-439.
- [20] Sangani, A.S., Mo, G., Tsao, H.K. & Koch, D.L. 1996 Simple shear flow of dense gas-solid suspensions at finite Stokes numbers. *J. Fluid Mech.* **313**, 309-341.
- [21] Sundararajakumar, R.R. & Koch, D.L. 1996 Non-continuum lubrication flows between particles colliding in a gas. *J. Fluid Mech.* **313**, 283-308.

- [22] Tsao, H.K. & Koch, D.L. 1995 Simple shear flows of dilute gas-solid suspensions. *J. Fluid Mech.* **296**, 211-245.
- [23] Van Dyke, M. 1975 *Perturbation Methods in Fluid Mechanics*. Academic Press.
- [24] Wiggins, S. 1990 *Introduction to applied nonlinear dynamical systems and chaos*. Springer-Verlag.
- [25] Wilson, H.J. & Davis, R.H. 2000 The viscosity of a dilute suspension of rough spheres. *J. Fluid Mech.* **421**, 339-367.
- [26] Zarraga, I.E. & Leighton, D.T. 2001a Shear-induced diffusivity in a dilute bidisperse suspension of hard spheres. *J. Colloid Interf. Sci.* **243**, 503-514.
- [27] Zarraga, I.E. & Leighton, D.T. 2001b Normal stress and diffusion in a dilute suspension of hard spheres undergoing simple shear. *Phys. Fluids* **13**(3), 565-577.

## Chapter 6

### Conclusions

We have developed a Chapman-Enskog-like formalism in order to solve the Fokker-Planck equation characterizing the particle statistics in finite  $St$  suspensions. The formalism was then used to derive an inertially corrected Smoluchowski equation (Chapter 3), which determines the spatial microstructure of a finite  $St$  suspension. The structure of the final formalism, in particular the form of the rapid momentum relaxations, was motivated from that of a multiple scales procedure, the latter being used to analyse the model problem of a single Brownian particle in simple shear flow (Chapter 2). The Chapman-Enskog method can, in principle, be used to derive inertial corrections to the Smoluchowski equation to any desired order. We gave the explicit form of the  $O(St)$  correction that represents the first effect of particle inertia, while indicating the general structure of the higher order terms. The  $O(St)$  terms include corrections to both the leading order (inertialess) hydrodynamic velocity field and the Brownian diffusivity, the latter correction being flow dependent. In addition, they contain a non-Fickian term at  $O(St/Pe^2)$  that involves fourth-order derivatives; the coefficients of the fourth-order derivatives characterize higher-order transport effects, i.e., they affect the higher-order moments of the spatial probability distribution. Such effects have previously been encountered in the analysis of the linear Boltzmann equation (used to describe the behavior of ion swarms), where the Chapman-Enskog procedure again gives rise to a generalized diffusion equation containing non-Fickian terms at higher orders (Kumar and Robson 1974, Skullerud 1974).

Explicit analytical results were obtained by using the aforementioned formalism to perform a trajectory analysis for a dilute non-Brownian suspension of (inertial) spherical particles in simple shear flow (Chapters 4 and 5). The analysis considered pair-wise interactions, and the trajectories determined therefore corresponded to the finite  $St$  modification of the inertialess pair-trajectories found originally by Batchelor and Green (1972ab). Particle inertia was found to break the fore-aft symmetry of the zero-Stokes trajectory space (and thence, of the microstructure), and the transverse displacements suffered during each pair-interaction led to shear-induced diffusivities in the velocity gradient and vorticity directions that scaled as  $St^2 \ln St$  and  $St^2$ , respectively. Particle inertia, though a possible mechanism for microstructural asymmetry, was, however, found to result in an indeterminate rheology. The latter was due to the absence of a steady state spatial microstructure for finite  $St$  (considering only pair-wise interactions), this in turn arising from the existence of an attractive limit cycle in the inertially modified trajectory space. The qualitative modifications of the zero-Stokes trajectories, for instance, the destruction of the zero-Stokes closed orbits, the location of the finite  $St$  neutral offplane trajectory, the relative proportions of finite  $St$  trajectories spiralling onto the limit cycle and those spiralling off to infinity etc., were virtually independent of  $St$  for small  $St$ . Thus, the inclusion of particle inertia fundamentally altered the nature of pair-interactions in simple shear flow.

Although we have obtained explicit results only for a dilute non-Brownian system of spherical particles in simple shear flow, the inertially corrected Smoluchowski equation derived in chapter 3 is generally valid. Thus, while one can certainly include the residual effects of Brownian motion in the above deterministic limit, thereby yielding a well-posed rheological problem, the corrected Smoluchowski equation with the appropriate hydrodynamic velocity field (to account for the possibly differing nature of hydrodynamic interactions) also applies

to other situations, for instance, in examining the effects of particle inertia in sedimentation. Indeed, a sedimenting suspension of one micron particles in air falls in the parameter regime of interest (taking  $\rho_p/\rho_f \approx 1000$ ,  $St = 0.1$ ,  $Re = 10^{-4}$ ,  $Pe = 45$ ). It is our hope that the range of problems which can be addressed with the formalism developed in this thesis will be quite extensive.

## Bibliography

- [1] Batchelor, G.K. & Green, J.T. 1972a The hydrodynamic interaction of two small freely-moving spheres in a linear flow field. *J. Fluid Mech.* **56**, 375-400.
- [2] Batchelor, G.K. & Green, J.T. 1972b The determination of the bulk stress in a suspension of spherical particles to  $O(c^2)$ . *J. Fluid Mech.* **56**, 401-427.
- [3] Kumar, K. & Robson, R.E. 1973 Mobility and Diffusion I. Boltzmann equation treatment for charged particles in a neutral gas. *Aust. J. Phys.* **26**, 157-186.
- [4] Skullerud, H.R. 1974 On the theory of electron diffusion in electrostatic fields in gases. *Aust. J. Phys.* **27**, 195-209.

## Appendix A

# Appendices for Chapter 2

### A.1 Free Brownian motion

We compare the exact and multiple scales solutions for free Brownian motion to second order in the appropriate small parameter for a delta function initial condition. The comparison is carried out for one dimension; the generalization to any number of dimensions is straightforward. For free Brownian motion in one dimension, equation (2.1) becomes

$$\frac{\partial P}{\partial \bar{t}} + u \frac{\partial P}{\partial y} = \frac{6\pi\eta a}{m} \frac{\partial}{\partial u}(uP) + \frac{kT}{m} \left( \frac{6\pi\eta a}{m} \right) \frac{\partial^2 P}{\partial u^2}, \quad (\text{A.1})$$

which in non-dimensional form is

$$\frac{\partial P}{\partial \bar{t}} + \epsilon v \frac{\partial P}{\partial x} = \frac{\partial}{\partial v}(vP) + \frac{\partial^2 P}{\partial v^2}, \quad (\text{A.2})$$

where  $\bar{t} = \tau_p t$ ,  $y = ax$ ,  $u = (kT/m)^{\frac{1}{2}}v$  and  $\epsilon = (mkT)^{\frac{1}{2}}/(6\pi\eta a^2) = (\tau_p/\tau_D)^{\frac{1}{2}} \ll 1$ . A third time scale  $\tau_{th} = a/(kT/m)^{\frac{1}{2}}$  can be constructed and represents the time taken for the particle to travel a distance of order its own size when moving ballistically with the thermal velocity. This time scale is, however, of little physical relevance since for all length scales of  $O(a)$  or greater, the motion of the particle becomes diffusive. Indeed, free Brownian motion is characterized by relaxation of the velocity distribution towards a Maxwellian on the scale of  $\tau_p$  leading to diffusive motion on longer time scales characterized by  $\tau_d = \tau_p/\epsilon^2$ , where

$D = kT/(6\pi\eta a)$  is the Stokes-Einstein diffusivity. Thus, the two relevant time scales for the multiple scales expansion are  $t_1 = t$  and  $t_2 = \epsilon^2 t_1$ .

### A.1.1 Exact solution

For an initial condition which is a delta function centered at the origin of phase space (i.e.

$P(x, v, 0) = \delta(x)\delta(v)$ ), the exact solution is (Chandrasekhar 1943)

$$P_E(x, v, t) = G(x, v, t|0, 0, 0) = \frac{1}{(2\pi)(FG - H^2)^{\frac{1}{2}}} \exp\left[-\frac{(Fv^2 - 2\epsilon Hxv + Gx^2)}{2(FG - H^2)}\right], \quad (\text{A.3})$$

where

$$F = (2t - 3 + 4e^{-t} - e^{-2t}),$$

$$G = (1 - e^{-2t}),$$

$$H = (1 - e^{-t})^2.$$

This can be expressed uniquely in terms of  $t_1$  and  $t_2$  provided only that one recognizes the linear term in  $F$  to characterise diffusive growth and scales it with  $\tau_d$ . The two-time-scale expansion of  $P(x, v, t)$  is therefore given by

$$P_E(x, v, t_1, t_2; \epsilon) = \frac{1}{(2\pi)(a + \epsilon^2 b)^{\frac{1}{2}}} \exp\left[-\frac{cx^2 - 2\epsilon f xv + (d + \epsilon^2 e)v^2}{2(a + \epsilon^2 b)}\right], \quad (\text{A.4})$$

where  $a, b, c, d, e$  and  $f$  are functions of  $t_1$  and  $t_2$ :

$$a(t_1, t_2) = 2t_2(1 - e^{-2t_1}),$$

$$b(t_1, t_2) = -4 - 4e^{-2t_1} + 8e^{-t_1},$$

$$c(t_1, t_2) = (1 - e^{-2t_1}),$$

$$d(t_1, t_2) = 2t_2,$$

$$e(t_1, t_2) = -3 + 4e^{-t_1} - e^{-2t_1},$$

$$f(t_1, t_2) = (1 - e^{-t_1})^2.$$

The expression (A.4) can in turn be expanded as a power series in  $\epsilon$ ,

$$P_E(x, v, t_1, t_2; \epsilon) = P_E^{(0)}(x, v, t_1, t_2) + \epsilon P_E^{(1)}(x, v, t_1, t_2) + \epsilon^2 P_E^{(2)}(x, v, t_1, t_2) + \dots, \quad (\text{A.5})$$

where

$$P_E^{(0)}(x, v, t_1, t_2) = \frac{1}{(2\pi)\{(2t_2)(1 - e^{-2t_1})\}^{\frac{1}{2}}} \exp\left[-\frac{x^2}{4t_2}\right] \exp\left[-\frac{v^2}{2(1 - e^{-2t_1})}\right], \quad (\text{A.6})$$

$$P_E^{(1)}(x, v, t_1, t_2) = \frac{(1 - e^{-t_1})^2}{2t_2(1 - e^{-2t_1})} (xv) P_E^{(0)}, \quad (\text{A.7})$$

$$P_E^{(2)}(x, v, t_1, t_2) = \left[ \frac{(1 - e^{-t_1})^2}{t_2(1 - e^{-2t_1})} - \frac{(1 - e^{-t_1})^2}{2t_2^2(1 - e^{-2t_1})} x^2 + \frac{(1 - e^{-t_1})^4}{8t_2^2(1 - e^{-2t_1})^2} (xv)^2 - \frac{(1 - e^{-t_1})^4}{4t_2(1 - e^{-2t_1})^2} v^2 \right] P_E^{(0)}. \quad (\text{A.8})$$

It was noted earlier (Wycoff & Balazs 1987a) that the multiple scales expansion is an implicit expansion in the (inverse) length scale characterising the initial positional distribution. Since a delta function has zero variance, the multiple scales expansion gives rise to a divergent series.

This can be seen by expressing  $t_1$  and  $t_2$  in terms of  $t$  in which case,  $P_E^{(i)} \sim O(1/\epsilon^{2i})P^{(0)}$

and the expansion becomes a series in  $1/\epsilon$  for  $\epsilon \ll 1$ . As we shall see in the next section, the multiple scales procedure nevertheless reproduces (A.5) with terms to  $O(\epsilon^2)$  given by (A.6), (A.7) and (A.8), thus validating the correctness of the formalism.

### A.1.2 Multiple scales analysis

For the case of free Brownian motion, rather than use equation (2.10), it is more convenient to apply the multiple scales procedure directly to the governing equation. Considering (A.2) and splitting  $t$  into the two relevant time scales  $t_1$  (fast) and  $t_2$  (slow), we obtain

$$\frac{\partial P}{\partial t_1} + \epsilon^2 \frac{\partial P}{\partial t_2} + \epsilon v \frac{\partial P}{\partial x} = \frac{\partial}{\partial v}(vP) + \frac{\partial^2 P}{\partial v^2}, \quad (\text{A.9})$$

where  $t_1$  and  $t_2$  are now treated as independent variables. Expanding  $P$  as a power series in  $\epsilon$ , we get the following equations at successive orders,

$$O(1) : \quad \frac{\partial P^{(0)}}{\partial t_1} - \left[ \frac{\partial}{\partial v}(vP^{(0)}) + \frac{\partial^2 P^{(0)}}{\partial v^2} \right] = 0, \quad (\text{A.10})$$

$$O(\epsilon) : \quad \frac{\partial P^{(1)}}{\partial t_1} - \left[ \frac{\partial}{\partial v}(vP^{(1)}) + \frac{\partial^2 P^{(1)}}{\partial v^2} \right] = -v \frac{\partial P^{(0)}}{\partial x}, \quad (\text{A.11})$$

$$O(\epsilon^2) : \quad \frac{\partial P^{(2)}}{\partial t_1} - \left[ \frac{\partial}{\partial v}(vP^{(2)}) + \frac{\partial^2 P^{(2)}}{\partial v^2} \right] = -\frac{\partial P^{(0)}}{\partial t_2} - v \frac{\partial P^{(1)}}{\partial x}. \quad (\text{A.12})$$

Considering the general initial condition

$$P(x, v, 0) = \frac{1}{(2\pi)^{\frac{1}{2}}} \sum_{n=0}^{\infty} \tilde{a}_n(x) \bar{H}_n \left( \frac{v}{2^{\frac{1}{2}}} \right),$$

where  $\tilde{a}_0(x) = 1$  (to satisfy the normalization constraint), we obtain

$$O(1) : \quad P^{(0)}(x, v, 0) = \sum_{n=0}^{\infty} \tilde{a}_n(x) \bar{H}_n \left( \frac{v}{2^{\frac{1}{2}}} \right), \quad (\text{A.13})$$

$$O(\epsilon) : \quad P^{(1)}(x, v, 0) = 0, \quad (\text{A.14})$$

$$O(\epsilon^2) : \quad P^{(2)}(x, v, 0) = 0. \quad (\text{A.15})$$

The general solution to the  $O(1)$  equation is

$$P^{(0)} = \frac{1}{(2\pi)^{\frac{1}{2}}} \sum_{n=0}^{\infty} b_n(x, t_2) \bar{H}_n \left( \frac{v}{2^{\frac{1}{2}}} \right) e^{-nt_1}, \quad (\text{A.16})$$

where  $b_n(x, 0) = \tilde{a}_n(x)$ ; its dependence on  $t_2$  is left unspecified and will be determined from suitable constraints at higher orders. The solution to (A.11) for  $P^{(1)}$  satisfying (A.14) is

$$P^{(1)} = \int_0^{t_1} dt'_1 \int_{-\infty}^{\infty} dv' G(v, t_1 | v', t'_1) \left[ -\frac{v'}{(2\pi)^{\frac{1}{2}}} \sum_{n=0}^{\infty} \frac{\partial b_n}{\partial x} \bar{H}_n \left( \frac{v'}{2^{\frac{1}{2}}} \right) e^{-nt'_1} \right], \quad (\text{A.17})$$

where the Green's function  $G$  is (Chandrasekhar 1943)

$$G(v, t_1 | v', t'_1) = \frac{1}{\{(2\pi)(1 - e^{-2(t_1 - t'_1)})\}^{\frac{1}{2}}} \exp \left[ -\frac{\{v - v' e^{-(t_1 - t'_1)}\}^2}{2(1 - e^{-2(t_1 - t'_1)})} \right]. \quad (\text{A.18})$$

Equation (A.17) can be written in the form

$$P^{(1)} = -\frac{e^{-\frac{v^2}{2}}}{(2\pi)^{\frac{1}{2}}} \sum_{n=0}^{\infty} \frac{\partial b_n}{\partial x} \int_0^{t_1} \frac{dt'_1 e^{-nt'_1}}{\pi^{\frac{1}{2}}} \int_{-\infty}^{\infty} dp e^{-(p-k)^2} \left[ \frac{H_{n+1}(\alpha p)}{2^{\frac{1}{2}}} + 2^{\frac{1}{2}} n H_{n-1}(\alpha p) \right],$$

where  $\alpha = (1 - e^{-2(t_1 - t'_1)})^{\frac{1}{2}}$ ,  $k = \frac{v' e^{-(t_1 - t'_1)}}{2^{\frac{1}{2}}(1 - e^{-2(t_1 - t'_1)})^{\frac{1}{2}}}$ ,  $p = \frac{v'}{2^{\frac{1}{2}}(1 - e^{-2(t_1 - t'_1)})^{\frac{1}{2}}}$  and

$$J_n = \int_{-\infty}^{\infty} dp e^{-(p-k)^2} H_n(\alpha p) = \pi^{\frac{1}{2}} (1 - \alpha^2)^{\frac{n}{2}} H_n \left( \frac{\alpha k}{\sqrt{1 - \alpha^2}} \right).$$

Using this, one obtains

$$P^{(1)} = \frac{1}{\pi^{\frac{1}{2}}} \sum_{n=0}^{\infty} \left[ \left\{ (n+1)e^{-(n+1)t_1} \frac{\partial b_{n+1}}{\partial x} - \frac{e^{-(n-1)t_1}}{2} \frac{\partial b_{n-1}}{\partial x} \right\} + \left\{ \frac{1}{2} \frac{\partial b_{n-1}}{\partial x} - (n+1) \frac{\partial b_{n+1}}{\partial x} \right\} e^{-nt_1} \right] \bar{H}_n \left( \frac{v}{2^{\frac{1}{2}}} \right). \quad (\text{A.19})$$

The solution at  $O(\epsilon^2)$  can be written as

$$P^{(2)} = I_1 + I_2,$$

where

$$I_1 = -\frac{1}{(2\pi)^{\frac{1}{2}}} \int_0^{t_1} dt'_1 \int_{-\infty}^{\infty} dv' G(v, t_1 | v', t'_1) \sum_{n=0}^{\infty} \frac{\partial b_n}{\partial t_2} \bar{H}_n \left( \frac{v'}{2^{\frac{1}{2}}} \right),$$

$$I_2 = -\frac{1}{\pi^{\frac{1}{2}}} \int_0^{t_1} dt'_1 \int_{-\infty}^{\infty} dv' G(v, t_1 | v', t'_1) \sum_{n=0}^{\infty} \left[ \left\{ (n+1) \frac{\partial^2 b_{n+1}}{\partial x^2} e^{-(n+1)t_1} - \frac{e^{-(n-1)t'_1}}{2} \frac{\partial^2 b_{n-1}}{\partial x^2} \right\} + \left\{ \frac{1}{2} \frac{\partial^2 b_{n-1}}{\partial x^2} - (n+1) \frac{\partial^2 b_{n+1}}{\partial x^2} \right\} e^{-nt'_1} \right] v' \bar{H}_n \left( \frac{v'}{2^{\frac{1}{2}}} \right).$$

On evaluating these integrals, one finds

$$I_1 = -\frac{1}{(2\pi)^{\frac{1}{2}}} \sum_{n=0}^{\infty} \frac{\partial b_n}{\partial t_2} e^{-nt_1} \bar{H}_n \left( \frac{v}{2^{\frac{1}{2}}} \right),$$

$$I_2 = \frac{1}{(2\pi)^{\frac{1}{2}}} \left[ \sum_{n=0}^{\infty} \frac{\partial^2 b_n}{\partial x^2} e^{-nt_1} \bar{H}_n \left( \frac{v}{2^{\frac{1}{2}}} \right) + \sum_{n=0}^{\infty} \left\{ \frac{(e^{t_1} - 1)^2}{4} \frac{\partial^2 b_{n-2}}{\partial x^2} - \{(2n+1) - (n+1)e^{-t_1} - ne^{-t_1}\} \frac{\partial^2 b_n}{\partial x^2} + (n+1)(n+2)(1 - e^{-t_1})^2 \frac{\partial^2 b_{n+2}}{\partial x^2} \right\} e^{-nt_1} \bar{H}_n \left( \frac{v}{2^{\frac{1}{2}}} \right) \right].$$

Therefore,  $P^{(2)}$  contains terms of the form

$$-\frac{1}{(2\pi)^{\frac{1}{2}}} \sum_{n=0}^{\infty} \left( \frac{\partial b_n}{\partial t_2} - \frac{\partial^2 b_n}{\partial x^2} \right) t_1 e^{-nt_1} \bar{H}_n \left( \frac{v}{2^{\frac{1}{2}}} \right),$$

which have an algebraic dependence on  $t_1$  in addition to the exponential decay (note that except for  $n = 0$ , the terms do not become unbounded as  $t_1 \rightarrow \infty$ ). Eliminating the algebraic dependence for each  $n$  gives the consistency condition for the corresponding  $b_n$  as<sup>1</sup>

$$\frac{\partial b_n}{\partial t_2} = \frac{\partial^2 b_n}{\partial x^2}. \quad (\text{A.20})$$

Thus, the  $b_n$ 's satisfy the Smoluchowski equation for the diffusion of a free Brownian particle and are given by

$$b_n(x, t_2) = \int_{-\infty}^{\infty} \frac{dx'}{(4\pi t_2)^{\frac{1}{2}}} \exp \left[ -\frac{(x-x')^2}{4t_2} \right] \tilde{a}_n(x'). \quad (\text{A.21})$$

The solution at  $O(\epsilon^2)$  may now be written as

$$P^{(2)} = \frac{1}{(2\pi)^{\frac{1}{2}}} \sum_{n=0}^{\infty} \left[ \frac{(e^{t_1} - 1)^2}{4} \frac{\partial^2 b_{n-2}}{\partial x^2} - \{(2n+1) - (n+1)e^{-t_1} - ne^{-t_1}\} \frac{\partial^2 b_n}{\partial x^2} + (n+1)(n+2)(1 - e^{-t_1})^2 \frac{\partial^2 b_{n+2}}{\partial x^2} \right] e^{-nt_1} \bar{H}_n \left( \frac{v}{2^{\frac{1}{2}}} \right). \quad (\text{A.22})$$

Determining  $P$  to  $O(\epsilon^2)$  requires knowing  $b_n$  to  $O(\epsilon^2)$ , which in turn implies knowledge of the consistency condition (given by (A.20) to leading order) to the same order. By considering the  $O(\epsilon^3)$  and  $O(\epsilon^4)$  contributions, it may be verified that (A.20) is correct at least to  $O(\epsilon^2)$  so that the probability density is given by

$$P = P^{(0)} + \epsilon P^{(1)} + \epsilon^2 P^{(2)} + O(\epsilon^3). \quad (\text{A.23})$$

---

<sup>1</sup>This step is motivated by the fact that the coefficients identified with the spatial relaxation processes must satisfy diffusion-like equations.

Using equations (3),(25),(26),(32) and (40) of Wycoff & Balazs (1987a) together with the consistency conditions (equation (30) and its analogs in Wycoff & Balazs (1987a)), it may be verified that their expression for  $f(x, v, t)$  to  $O(\epsilon^2)$  is identical to (A.23) above. The structure of the above hierarchy strongly suggests that (A.20) is correct to all orders (that this is true for  $b_0$  has already been shown by Titulaer (1978)). For a delta function initial condition, it can be shown that (A.20) for  $b_n$  is, in fact, exact and that the general form of the  $O(\epsilon^n)$  solution is

$$P^{(n)}(x, v, t_1, t_2) = \frac{2^{\frac{n-3}{2}}}{\pi n!} \frac{(1 - e^{-t_1})^n}{t_2^{\frac{n+1}{2}} (1 - e^{-2t_1})^{\frac{n+1}{2}}} \tilde{H}_n \left[ \frac{v(1 - e^{-t_1})}{2(1 - e^{-2t_1})^{\frac{1}{2}}} \right] \tilde{H}_n \left[ \frac{x}{(2t_2)^{\frac{1}{2}}} \right]. \quad (\text{A.24})$$

For  $n = 0, 1, 2$ , the above expression matches up to (A.6), (A.7) and (A.8), respectively, thus proving the identity of the exact and multiple scales solutions to  $O(\epsilon^2)$ . This then shows that the consistency condition (A.20) is indeed exact to all orders in  $\epsilon$ , since (A.20) is evidently independent of the specific form of the initial distribution.

### A.1.3 Failure of the naive multiple scales scheme

The approach described above works only for the case of free Brownian motion. Even for the harmonic potential in one dimension, the simplest possibility of a non-trivial force field while still retaining the well-posedness of the problem in an infinite domain, the method does not give the correct form of the inertial relaxations. The reason for this can be understood by considering the complete Fokker-Planck operator for a single Brownian particle in an arbitrary (dimensionless) position dependent force field,

$$L_{FP}(\mathbf{x}, \mathbf{v}, t) \equiv \frac{\partial}{\partial t} + St\mathbf{v} \cdot \frac{\partial}{\partial \mathbf{x}} + (St)^k \mathbf{F}^o(\mathbf{x}) \cdot \frac{\partial}{\partial \mathbf{v}} - \frac{1}{PeSt} \left( \frac{\partial}{\partial \mathbf{v}} (\mathbf{v} + \nabla_{\mathbf{v}}^2) \right), \quad (\text{A.25})$$

where  $k$  is 0 for a hydrodynamic force field and 1 otherwise. The presence of the spatial derivative ensures that  $L_{FP}$  does not commute with any position dependent function  $h(\mathbf{x})$ , i.e.,  $L_{FP}(h(\mathbf{x})) \neq h(\mathbf{x})L_{FP}$ . Similarly, the position dependent force field gives rise to a non-trivial commutator for the operators  $\partial/\partial\mathbf{x}$  and  $L_{FP}$ , i.e.,  $[\frac{\partial}{\partial\mathbf{x}}, L_{FP}] \neq 0$ . In the direct approach above, the operator at leading order becomes

$$L_{FP}^V(\mathbf{v}, t) \equiv \frac{\partial}{\partial t} - \frac{1}{PeSt} \left( \frac{\partial}{\partial \mathbf{v}} (\mathbf{v} + \nabla_{\mathbf{v}}^2) \right),$$

for a non-hydrodynamic force field and

$$L_{FP}^W(\mathbf{w}, t) \equiv \frac{\partial}{\partial t} - \frac{1}{PeSt} \left( \frac{\partial}{\partial \mathbf{w}} (\mathbf{w} + \nabla_{\mathbf{w}}^2) \right),$$

for a hydrodynamic force field where  $\mathbf{w} = \mathbf{v} - \mathbf{F}^o(\mathbf{x})$ . Unlike  $L_{FP}$ , however, the operator  $L_{FP}^V$  commutes both with functions of the form  $h(\mathbf{x})$  and the gradient operator  $\partial/\partial\mathbf{x}$ . This leads to spurious terms at higher orders; for instance, assuming the fast and slow time scales to be  $t_1 = t$  and  $t_2 = (St)t$ , one obtains at  $O(St)$ ,

$$L_{FP}^V P^{(1)} = -\frac{\partial P^{(0)}}{\partial t_2} - \mathbf{v} \cdot \frac{\partial P^{(0)}}{\partial \mathbf{x}} - \mathbf{F}^o(\mathbf{x}) \cdot \frac{\partial P^{(0)}}{\partial \mathbf{v}}.$$

The solutions corresponding to the second and third forcing functions can be obtained as  $\partial/\partial\mathbf{x} \cdot (\mathbf{P}_{II}^{(1)})$  and  $\mathbf{F}^o(\mathbf{x}) \cdot \mathbf{P}_{III}^{(1)}$ , where  $\mathbf{P}_{II}^{(1)}$  and  $\mathbf{P}_{III}^{(1)}$  are the particular solutions for the forcing functions  $\mathbf{v}P^{(0)}$  and  $\partial P^{(0)}/\partial\mathbf{v}$  respectively. This has the effect that spatial gradients and position-dependent prefactors in the initial condition are propagated without modification for all time thereby giving rise to erroneous terms at  $O(St)$  and higher. Hence, the direct approach does not work for the case of a non-hydrodynamic force field. The above arguments

also follow for  $L_{FP}^W$ , and therefore for a hydrodynamic force field, in terms of the variables  $(\mathbf{x}, \mathbf{w})$ . Free Brownian motion is the special case wherein  $[\frac{\partial}{\partial \mathbf{x}}, L_{FP}] = 0$ ; thus,  $L_{FP}$ , like  $L_{FP}^V$ , commutes with the gradient operator, and there is no distinction between the direct and indirect approaches.

The indirect approach adopted in the text works in the general case because it assumes a form for the momentum space functions (in terms of the Hermite polynomials), and thereby circumvents the simultaneous consideration of both position and momentum variables.

## A.2 Two-time-scale expansions of the exact solutions

In this appendix we consider the two-time-scale expansions of  $P^m$  and  $P^d$  (see section 2.3.1). Since the exact solutions for both initial conditions are multivariate Gaussians in phase space of the form  $\Delta^{-\frac{1}{2}} e^{-c_{ij} X_i X_j}$ , we tabulate to  $O(St)$ , the small  $St$  expansions for the  $c_{ij}$ 's and  $(1/\Delta)$  for the two cases.

1. Maxwellian initial condition:

$$\begin{aligned}
 c_{xx}^{(0)} &= \frac{3Pe}{t_2(t_2^2 + 12)}, \\
 c_{xx}^{(1)} &= Pe St \frac{3(t_2^2 + 4) + 4e^{-t_1}(3t_2^2 - 4) + 9e^{-2t_1}(4 - 3t_2^2 + t_2^4)}{2t_2^2(t_2^2 + 12)^2}, \\
 c_{xy}^{(0)} &= -\frac{3Pe}{t_2^2 + 12}, \\
 c_{xy}^{(1)} &= -3Pe St \frac{(t_2^2 - 24) - e^{-t_1}(t_2^4 - 6t_2^2 + 24) + e^{-2t_1}(t_2^4 - 10t_2^2 + 24)}{t_2(t_2^2 + 12)^2}, \\
 c_{yy}^{(0)} &= \frac{Pe(t_2^2 + 3)}{t_2(t_2^2 + 12)},
 \end{aligned}$$

$$c_{yy}^{(1)} = PeSt \left[ \frac{(t_2^6 + 21t_2^4 + 63t_2^2 + 108) - 2e^{-t_1}(t_2^6 - 7t_2^4 - 42t_2^2 + 72)}{2t_2^2(t_2^2 + 12)^2} + \frac{e^{-2t_1}(t_2^6 - 17t_2^4 + 69t_2^2 + 36)}{2t_2^2(t_2^2 + 12)^2} \right],$$

$$c_{uu}^{(0)} = \frac{PeSt}{2},$$

$$c_{vv}^{(0)} = \frac{PeSt}{2},$$

$$c_{ux}^{(0)} = -3PeSt \frac{2 + e^{-t_1}(t_2^2 - 2)}{t_2(t_2^2 + 12)},$$

$$c_{vx}^{(0)} = PeSt \frac{3 + 3e^{-t_1}}{t_2^2 + 12},$$

$$c_{uy}^{(0)} = -PeSt \frac{(t_2^2 + 9) + e^{-t_1}(9 - t_2^2)}{t_2^2 + 12},$$

$$c_{vy}^{(0)} = -PeSt \frac{2(t_2^2 + 3) + e^{-t_1}(t_2^2 - 6)}{t_2(t_2^2 + 12)},$$

$$\frac{1}{\Delta} = \frac{3Pe^4St^2}{t_2^2(t_2^2 + 12)} + 3Pe^4St^3 \frac{6(t_2^2 + 6) + 16e^{-t_1}(t_2^2 - 3) + e^{-2t_1}(3t_2^4 + 14t_2^2 + 12)}{t_2^3(t_2^2 + 12)^2}.$$

In the above,  $c_{ij}^{(0)}$  and  $c_{ij}^{(1)}$  denote the zeroth and first order terms respectively, in the expansion of  $c_{ij}$  in powers of  $St$ . The terms not included at these orders, viz.  $c_{uu}^{(1)}$ ,  $c_{uv}^{(0)}$ ,  $c_{vv}^{(1)}$ ,  $c_{ux}^{(1)}$ ,  $c_{uy}^{(1)}$ ,  $c_{vx}^{(1)}$  and  $c_{vy}^{(1)}$ , are all  $O(St^2)$  and therefore need not be considered for the  $O(St)$  corrections. None of the terms at higher orders viz.  $c_{ij}^{(k)}$  ( $k \geq 2$ ) contributes at  $O(St)$ .

## 2. Delta function initial condition:

In this case we restrict the comparison of the exact and multiple scales solutions to velocity dependent corrections at  $O(St)$  (see section 2.4.2);  $c_{xx}^{(1)}$ ,  $c_{xy}^{(1)}$ ,  $c_{yy}^{(1)}$  and  $\Delta^{(1)}$  need not be considered. As a result, we are only concerned with the leading order expressions

for all coefficients (and  $\Delta$ ) and the superscripts ‘0’ and ‘1’ are omitted.

$$\begin{aligned}
c_{xx} &= \frac{3Pe}{t_2(t_2^2 + 12)}, \\
c_{xy} &= -\frac{3Pe}{t_2^2 + 12}, \\
c_{yy} &= \frac{Pe(t_2^2 + 3)}{t_2(t_2^2 + 12)}, \\
c_{uu} &= \frac{PeSt(1 - e^{-2t_1})}{2(1 - e^{-2t_1}(t_2^2 + 2) + e^{-4t_1})}, \\
c_{uv} &= -\frac{PeSt(t_2e^{-2t_1})}{(1 - e^{-2t_1}(t_2^2 + 2) + e^{-4t_1})}, \\
c_{vv} &= \frac{PeSt[1 - (t_2^2 + 1)e^{-2t_1}]}{2(1 - e^{-2t_1}(t_2^2 + 2) + e^{-4t_1})}, \\
c_{ux} &= -6PeSt \frac{1 + e^{-t_1}(t_2^2 - 2) + 2e^{-2t_1}t_2^2 + 2e^{-3t_1} - e^{-4t_1}}{t_2(t_2^2 + 12)(1 - e^{-2t_1}(t_2^2 + 2) + e^{-4t_1})}, \\
c_{vx} &= 3PeSt \frac{1 + 2e^{-t_1} - e^{-2t_1}(t_2^2 - 4) - 6e^{-3t_1} - e^{-4t_1}}{(t_2^2 + 12)(1 - e^{-2t_1}(t_2^2 + 2) + e^{-4t_1})}, \\
c_{uy} &= -PeSt \frac{(t_2^2 + 9) - 2e^{-t_1}(t_2^2 - 9) - 8e^{-2t_1}(t_2^2 + 3) - 6e^{-3t_1} + 3e^{-4t_1}}{(t_2^2 + 12)(1 - e^{-2t_1}(t_2^2 + 2) + e^{-4t_1})}, \\
c_{vy} &= -PeSt \left[ \frac{-2(t_2^2 + 3) - 2e^{-t_1}(t_2^2 - 6) + 3e^{-2t_1}t_2^2(t_2^2 + 4) + 4e^{-3t_1}(2t_2^2 - 3)}{t_2(t_2^2 + 12)(1 - e^{-2t_1}(t_2^2 + 2) + e^{-4t_1})} \right. \\
&\quad \left. + \frac{2e^{-4t_1}(t_2^2 + 3)}{t_2(t_2^2 + 12)(1 - e^{-2t_1}(t_2^2 + 2) + e^{-4t_1})} \right], \\
\frac{1}{\Delta} &= \frac{3Pe^4St^2}{t_2^2(t_2^2 + 12)(1 - e^{-2t_1}(t_2^2 + 2) + e^{-4t_1})}.
\end{aligned}$$

For the Maxwellian initial condition, the form of the coefficients suggests that, to leading order, the solution is the product of a steady Maxwellian about the ambient flow field and a positional distribution. For the delta function initial condition, however, the leading order solution is more complicated; the expressions for  $c_{uu}$ ,  $c_{vv}$  and  $c_{uv}$  indicate coupling of the  $u$  and  $v$  components of velocity and dependence of the leading order velocity distribution on the  $t_2$  scale (see below).

The exact solution for the Maxwellian case is written in the form

$$P^m(\mathbf{x}, \mathbf{v}, t_1, t_2) = \frac{1}{(2\pi)^2 \Delta_0^{\frac{1}{2}}} \left(1 - \frac{St \Delta_1}{2 \Delta_0}\right) \exp[-(c_{xx}^{(0)} x^2 + c_{yy}^{(0)} y^2 + c_{xy}^{(0)} xy)] \exp[-(c_{uu}^{(0)} u^2 + c_{vv}^{(0)} v^2)] \\ \exp[-(c_{xx}^{(1)} x^2 + c_{yy}^{(1)} y^2 + c_{xy}^{(1)} xy + c_{ux}^{(0)} ux + c_{vx}^{(0)} vx + c_{uy}^{(0)} uy + c_{vy}^{(0)} vy)],$$

where  $\Delta = \Delta_0 + St \Delta_1$ . Rewriting the above in terms of the fluctuation velocity  $(u - y, v)$ , we obtain

$$P^m(\mathbf{x}, \mathbf{v}, t_1, t_2) = \frac{1}{(2\pi)^2 \Delta_0^{\frac{1}{2}}} \left(1 - \frac{St \Delta_1}{2 \Delta_0}\right) \exp[-(c_{xx}^{(0)} x^2 + c_{yy}^{(0)} y^2 + c_{xy}^{(0)} xy)] \exp[-\{c_{uu}^{(0)} (u - y)^2 \\ + c_{vv}^{(0)} v^2\}] \exp[-\{c_{xx}^{(1)} x^2 + (c_{yy}^{(1)} + c_{uu}^{(0)} + c_{uy}^{(0)}) y^2 + (c_{xy}^{(1)} + c_{ux}^{(0)}) xy \\ + c_{ux}^{(0)} (u - y)x + c_{vx}^{(0)} vx + (c_{uy}^{(0)} + 2c_{uu}^{(0)}) (u - y)y + c_{vy}^{(0)} vy\}].$$

The first two exponentials with the factor  $(2\pi)^{-2} \Delta_0^{-\frac{1}{2}}$  constitute the leading order term; we expand the third exponential to linear order for small  $St$  to obtain

$$P^m(\mathbf{x}, \mathbf{v}, t_1, t_2) = P^{m(0)} \left(1 - \frac{St \Delta_1}{2 \Delta_0}\right) \left\{1 - (c_{xx}^{(1)} x^2 + (c_{yy}^{(1)} + c_{uu}^{(0)} + c_{uy}^{(0)}) y^2 + (c_{xy}^{(1)} + c_{ux}^{(0)}) xy \\ + c_{ux}^{(0)} (u - y)x + c_{vx}^{(0)} vx + (c_{uy}^{(0)} + 2c_{uu}^{(0)}) (u - y)y + c_{vy}^{(0)} vy) \\ + O(Pe St^2) + O(Pe^2 St^2)\right\}, \\ = P^{m(0)} \left\{1 - (c_{xx}^{(1)} x^2 + (c_{yy}^{(1)} + c_{uu}^{(0)} + c_{uy}^{(0)}) y^2 + (c_{xy}^{(1)} + c_{ux}^{(0)}) xy + c_{ux}^{(0)} (u - y)x \\ + c_{vx}^{(0)} vx + (c_{uy}^{(0)} + 2c_{uu}^{(0)}) (u - y)y + c_{vy}^{(0)} vy) - \frac{St \Delta_1}{2 \Delta_0} \\ + O(Pe St^2) + O(Pe^2 St^2)\right\}, \quad (\text{A.26})$$

where the leading order solution is given by

$$\begin{aligned} P^{m(0)} &= \frac{(Pe St)}{(2\pi)^2 \Delta_0^{\frac{1}{2}}} \exp\left[-Pe St \frac{(u-y)^2 + v^2}{2}\right] \exp\left[-(c_{xx}^{(0)} x^2 + c_{yy}^{(0)} y^2 + c_{xy}^{(0)} xy)\right] \\ &= \frac{(Pe St)}{(2\pi)} \exp\left[-Pe St \frac{(u-y)^2 + v^2}{2}\right] G_0(x, y, t_2), \end{aligned} \quad (\text{A.27})$$

$G_0$  being the Green's function for the Smoluchowski equation as defined in Appendix A5.

For the delta function case, including only the terms linear in the fluctuation velocity at  $O(St)$ , we similarly have

$$\begin{aligned} P^d(\mathbf{x}, \mathbf{v}, t_1, t_2) &= P^{d(0)} \left\{ 1 - (c_{ux}(u-y)x + c_{vx}vx + (c_{uy} + 2c_{uu})(u-y)y + (c_{vy} + c_{uv})vy) \right. \\ &\quad \left. + O(Pe St^2) + O(Pe^2 St^2) \right\}, \end{aligned} \quad (\text{A.28})$$

where

$$\begin{aligned} P^{d(0)} &= \frac{1}{(2\pi)^2 \Delta^{\frac{1}{2}}} \exp[-(c_{xx}x^2 + c_{yy}y^2 + c_{xy}xy)] \exp[-(c_{uu}(u-y)^2 + c_{uv}uv + c_{vv}v^2)], \\ &= \frac{(Pe St) G_0(x, y, t_2)}{2\pi\{1 - (t_2^2 + 2)e^{-2t_1} + e^{-4t_1}\}^{\frac{1}{2}}} \exp\left[-Pe St \frac{(1 - e^{-2t_1})(u-y)^2 + (1 - (t_2^2 + 1)e^{-2t_1})v^2}{2\{1 - (t_2^2 + 2)e^{-2t_1} + e^{-4t_1}\}} \right. \\ &\quad \left. - \frac{t_2 e^{-2t_1}(u-y)v}{\{1 - (t_2^2 + 2)e^{-2t_1} + e^{-4t_1}\}}\right]. \end{aligned} \quad (\text{A.29})$$

In order for an expansion in terms of Hermite functions to be possible, we have retained to leading order the  $O(St)$  coefficients of terms quadratic in the fluctuation velocity in the above manipulations. The expressions (A.26) and (A.28) with  $P^{m(0)}$  and  $P^{d(0)}$  defined by (A.27) and (A.29) are used for comparison with the multiple scales solutions given by (2.58) and (2.69) respectively.

### A.3 Inertial corrections to equation (2.36) for $b_{m,n}^{(0)}$

Here, we derive the expressions for the operators  $\partial/\partial t_4$  and  $\partial/\partial t_5$ . For  $i = 3$ , equation (2.18)

becomes

$$\begin{aligned} & \frac{\partial}{\partial t_4} \phi_{m,n,s}^{(0)} + \frac{\partial}{\partial t_3} \phi_{m,n,s}^{(1)} + \frac{\partial}{\partial t_2} \phi_{m,n,s}^{(2)} + (m+n-s)\phi_{m,n,s}^{(3)} + \frac{1}{2^{\frac{1}{2}}} \left( \frac{\partial \phi_{m-1,n,s}^{(2)}}{\partial \hat{x}} + \frac{\partial \phi_{m,n-1,s}^{(2)}}{\partial \hat{y}} \right) \\ & + \hat{y} \frac{\partial \phi_{m,n,s}^{(2)}}{\partial \hat{x}} + 2^{\frac{1}{2}} \left\{ (m+1) \frac{\partial \phi_{m+1,n,s}^{(2)}}{\partial \hat{x}} + (n+1) \frac{\partial \phi_{m,n+1,s}^{(2)}}{\partial \hat{y}} \right\} + \frac{\phi_{m-1,n-1,s}^{(2)}}{2} + (n+1)\phi_{m-1,n+1,s}^{(2)} = 0. \end{aligned} \quad (\text{A.30})$$

For  $s = m + n$ , using the expressions for the  $\phi^{(2)}$ 's given in (2.32), this simplifies to

$$\begin{aligned} \frac{\partial b_{m,n}^{(2)}}{\partial t_2} + \hat{y} \frac{\partial b_{m,n}^{(2)}}{\partial \hat{x}} + (n+1)b_{m-1,n+1}^{(2)} &= \left[ \frac{\partial b_{m,n}^{(1)}}{\partial t_3} - \left( \frac{\partial^2 b_{m,n}^{(1)}}{\partial \hat{x}^2} + \frac{\partial^2 b_{m,n}^{(1)}}{\partial \hat{y}^2} \right) \right] \\ &+ \left[ -\frac{\partial b_{m,n}^{(0)}}{\partial t_4} - \frac{1}{2^{\frac{1}{2}}} \left( \frac{\partial}{\partial \hat{x}} [\phi_{m-1,n,m+n}^{(2)}]_{b_0} + \frac{\partial}{\partial \hat{y}} [\phi_{m,n-1,m+n}^{(2)}]_{b_0} \right) \right. \\ &\left. - 2^{\frac{1}{2}} \left\{ (m+1) \frac{\partial}{\partial \hat{x}} [\phi_{m+1,n,m+n}^{(2)}]_{b_0} + (n+1) \frac{\partial}{\partial \hat{y}} [\phi_{m,n+1,m+n}^{(2)}]_{b_0} \right\} \right. \\ &\quad \left. - \frac{[\phi_{m-1,n-1,m+n}^{(2)}]_{b_0}}{2} \right], \end{aligned} \quad (\text{A.31})$$

where  $[\cdot]_{b_0}$  denotes the part of the argument that depends on  $b_{m,n}^{(0)}$ , and is used because we need only consider the part of  $\phi_{m,n,s}^{(2)}$  that involves  $b_{m,n}^{(0)}$  for the purposes of evaluating  $\partial/\partial t_4$  (acting on  $b_{m,n}^{(0)}$ ). Using the definitions of the operators  $\partial/\partial t_2$  and  $\partial/\partial t_3$  as given by (2.30) and (2.31), (A.31) can be separated into the following individual consistency conditions,

$$\frac{\partial b_{m,n}^{(2)}}{\partial t_2} + \hat{y} \frac{\partial b_{m,n}^{(2)}}{\partial \hat{x}} + (n+1)b_{m-1,n+1}^{(2)} = 0, \quad (\text{A.32})$$

$$\frac{\partial b_{m,n}^{(1)}}{\partial t_3} = \frac{\partial^2 b_{m,n}^{(1)}}{\partial \hat{x}^2} + \frac{\partial^2 b_{m,n}^{(1)}}{\partial \hat{y}^2}, \quad (\text{A.33})$$

$$\begin{aligned} \frac{\partial b_{m,n}^{(0)}}{\partial t_4} = & -\frac{1}{2^{\frac{1}{2}}}\left(\frac{\partial}{\partial \hat{x}}[\phi_{m-1,n,m+n}^{(2)}]_{b_0} + \frac{\partial}{\partial \hat{y}}[\phi_{m,n-1,m+n}^{(2)}]_{b_0}\right) - 2^{\frac{1}{2}}\left\{(m+1)\frac{\partial}{\partial \hat{x}}[\phi_{m+1,n,m+n}^{(2)}]_{b_0}\right. \\ & \left.+ (n+1)\frac{\partial}{\partial \hat{y}}[\phi_{m,n+1,m+n}^{(2)}]_{b_0}\right\} - \frac{[\phi_{m-1,n-1,m+n}^{(2)}]_{b_0}}{2}. \end{aligned} \quad (\text{A.34})$$

From (A.34) we see that  $\partial/\partial t_4$  involves derivatives of  $\phi_{m,n,m+n\pm 1}^{(2)}$  (which contains first order derivatives of  $b_{m,n}^{(0)}$ ) and  $\phi_{m-1,n-1,m+n}^{(2)}$  (which contains second-order derivatives of  $b_{m,n}^{(0)}$ ), and therefore consists entirely of second-order derivatives of  $b_{m,n}^{(0)}$ . Using the expressions for the  $\phi^{(2)}$ 's from (2.32), (A.34) reduces to

$$\frac{\partial b_{m,n}^{(0)}}{\partial t_4} = 2(n+1)\frac{\partial^2 b_{m-1,n+1}^{(0)}}{\partial \hat{x}^2} - (n+1)\frac{\partial^2 b_{m-1,n+1}^{(0)}}{\partial \hat{y}^2} + (m+1)\frac{\partial^2 b_{m+1,n-1}^{(0)}}{\partial \hat{x}^2} + (3n-m-1)\frac{\partial^2 b_{m,n}^{(0)}}{\partial \hat{x}\partial \hat{y}}. \quad (\text{A.35})$$

Thus, (2.36) represents the complete leading order equation for  $b_{m,n}^{(0)}$ . Combining equations (2.30) and (A.33), we observe that  $b_{m,n}^{(1)}$  satisfies an identical equation to leading order. This will, in fact, be true for all  $b_{m,n}^{(i)}$ 's and indicates the recurrent structure of the hierarchy.

Now, consider equation (2.18) for  $i = 4$ ,

$$\begin{aligned} & \frac{\partial}{\partial t_5}\phi_{m,n,s}^{(0)} + \frac{\partial}{\partial t_4}\phi_{m,n,s}^{(1)} + \frac{\partial}{\partial t_3}\phi_{m,n,s}^{(2)} + \frac{\partial}{\partial t_2}\phi_{m,n,s}^{(3)} + (m+n-s)\phi_{m,n,s}^{(4)} + \frac{1}{2^{\frac{1}{2}}}\left(\frac{\partial \phi_{m-1,n,s}^{(3)}}{\partial \hat{x}}\right. \\ & \left. + \frac{\partial \phi_{m,n-1,s}^{(3)}}{\partial \hat{y}}\right) + \hat{y}\frac{\partial \phi_{m,n,s}^{(3)}}{\partial \hat{x}} + 2^{\frac{1}{2}}\left\{(m+1)\frac{\partial \phi_{m+1,n,s}^{(3)}}{\partial \hat{x}} + (n+1)\frac{\partial \phi_{m,n+1,s}^{(3)}}{\partial \hat{y}}\right\} + \frac{\phi_{m-1,n-1,s}^{(3)}}{2} \\ & + (n+1)\phi_{m-1,n+1,s}^{(3)} = 0. \end{aligned} \quad (\text{A.36})$$

Putting  $s = m+n$  we see that  $\partial b_{m,n}^{(0)}/\partial t_5$  will involve  $[\phi_{m,n,m+n\pm 1}^{(3)}]_{b_0}$  and  $[\phi_{m,n,m+n+2}^{(3)}]_{b_0}$ , where we need only look at contributions containing the highest order derivatives. In order to obtain expressions for the  $\phi_{m,n}^{(3)}$ 's, we again consider equation (A.30). For  $s = m+n+1$ ,

we have

$$\begin{aligned}
& L\phi_{m,n,m+n+1}^{(2)} + (n+1)\phi_{m-1,n+1,m+n+1}^{(2)} + \frac{\partial}{\partial t_3}\phi_{m,n,m+n+1}^{(1)} - \phi_{m,n,m+n+1}^{(3)} + \frac{\phi_{m-1,n-1,m+n+1}^{(2)}}{2} \\
&= -\frac{1}{2^{\frac{1}{2}}}\left(\frac{\partial\phi_{m-1,n,m+n+1}^{(2)}}{\partial\hat{x}} + \frac{\partial\phi_{m,n-1,m+n+1}^{(2)}}{\partial\hat{y}}\right) + 2^{\frac{1}{2}}\left\{(m+1)\frac{\partial\phi_{m+1,n,m+n+1}^{(2)}}{\partial\hat{x}}\right. \\
&\quad \left.+ (n+1)\frac{\partial\phi_{m,n+1,m+n+1}^{(2)}}{\partial\hat{y}}\right\}.
\end{aligned}$$

When use of (2.22) is made for  $L(= \partial/\partial t_2 + \hat{y}\partial/\partial\hat{x})$  acting on  $\phi^{(2)}$ , all terms on the left-hand side except the  $\phi^{(1)}$  term involve only first-order derivatives of  $b_{m,n}^{(0)}$  (note that  $\phi_{m-1,n-1,m+n+1}^{(2)} = 0$ ). On the right-hand side,  $\phi_{m+1,n,m+n+1}^{(2)}$  and  $\phi_{m,n+1,m+n+1}^{(2)}$  involve only the corresponding  $b_{m,n}^{(2)}$ 's. Thus, the terms relevant to the  $O(St)$  correction to  $b_{m,n}^{(0)}$  are those involving derivatives of  $\phi_{m-1,n,m+n+1}^{(2)}$  and  $\phi_{m,n-1,m+n+1}^{(2)}$ , that themselves contain second-order derivatives of  $b_{m,n}^{(0)}$  (see (2.32)), and  $\partial/\partial t_3(\phi_{m,n,m+n+1}^{(1)})$  (where the operator  $\partial/\partial t_3$  has been defined in terms of second-order spatial derivatives in (2.31)). After some manipulation, one obtains

$$\begin{aligned}
[\phi_{m,n,m+n+1}^{(3)}]_{b_0} &= 2^{\frac{1}{2}}\left[(m+1)\frac{\partial}{\partial\hat{x}}\left(\frac{\partial^2}{\partial\hat{x}^2} + \frac{\partial^2}{\partial\hat{y}^2}\right)b_{m+1,n}^{(0)} + (n+1)\frac{\partial}{\partial\hat{y}}\left(\frac{\partial^2}{\partial\hat{x}^2} + \frac{\partial^2}{\partial\hat{y}^2}\right)b_{m,n+1}^{(0)}\right] \\
&\quad + \frac{1}{2^{\frac{1}{2}}}\left[m(m+1)\frac{\partial^3 b_{m+1,n}^{(0)}}{\partial\hat{x}^3} + (n+1)(n+2)\frac{\partial^3 b_{m-1,n+1}^{(0)}}{\partial\hat{x}^2\partial\hat{y}} + 2m(n+1)\frac{\partial^3 b_{m,n+1}^{(0)}}{\partial\hat{x}^2\partial\hat{y}}\right. \\
&\quad \left.+ (m+1)(m+2)\frac{\partial^3 b_{m+2,n-1}^{(0)}}{\partial\hat{x}^2\partial\hat{y}} + n(n+1)\frac{\partial^3 b_{m,n+1}^{(0)}}{\partial\hat{y}^3} + 2n(m+1)\frac{\partial^3 b_{m+1,n}^{(0)}}{\partial\hat{x}\partial\hat{y}^2}\right].
\end{aligned} \tag{A.37}$$

In a similar manner, for  $s = m + n - 1$

$$[\phi_{m,n,m+n-1}^{(3)}]_{b_0} = -\frac{\partial}{\partial t_3}\phi_{m,n,m+n-1}^{(1)} - 2^{\frac{1}{2}}\left[(m+1)\frac{\partial\phi_{m+1,n,m+n-1}^{(2d)}}{\partial\hat{x}} + (n+1)\frac{\partial\phi_{m,n+1,m+n-1}^{(2d)}}{\partial\hat{y}}\right],$$

$$\begin{aligned}
&= \frac{1}{2^{\frac{1}{2}}} \left[ \frac{\partial}{\partial \hat{x}} \left( \frac{\partial^2}{\partial \hat{x}^2} + \frac{\partial^2}{\partial \hat{y}^2} \right) b_{m-1,n}^{(0)} + \frac{\partial}{\partial \hat{y}} \left( \frac{\partial^2}{\partial \hat{x}^2} + \frac{\partial^2}{\partial \hat{y}^2} \right) b_{m,n-1}^{(0)} \right] \\
&\quad - \frac{2^{\frac{1}{2}}}{4} \left[ (m+1) \frac{\partial}{\partial \hat{x}} \left( \frac{\partial^2 b_{m-1,n}^{(0)}}{\partial \hat{x}^2} + 2 \frac{\partial^2 b_{m,n-1}^{(0)}}{\partial \hat{x} \partial \hat{y}} + \frac{\partial^2 b_{m+1,n-2}^{(0)}}{\partial \hat{y}^2} \right) \right. \\
&\quad \left. + (n+1) \frac{\partial}{\partial \hat{y}} \left( \frac{\partial^2 b_{m-2,n+1}^{(0)}}{\partial \hat{x}^2} + 2 \frac{\partial^2 b_{m-1,n}^{(0)}}{\partial \hat{x} \partial \hat{y}} + \frac{\partial^2 b_{m,n-1}^{(0)}}{\partial \hat{y}^2} \right) \right], \tag{A.38}
\end{aligned}$$

where the superscript ‘2d’ is used to denote the part involving second-order derivatives.

For  $s = m + n + 2$ , we have

$$\begin{aligned}
L\phi_{m,n,m+n+2}^{(2)} - 2\phi_{m,n,m+n+2}^{(3)} + (n+1)\phi_{m-1,n+1,m+n+2}^{(2)} = \\
- 2^{\frac{1}{2}} \left[ (m+1) \frac{\partial \phi_{m+1,n,m+n+2}}{\partial \hat{x}} + (n+1) \frac{\partial \phi_{m,n+1,m+n+2}}{\partial \hat{y}} \right]. \tag{A.39}
\end{aligned}$$

If one again uses equation (2.22) to simplify  $L\phi_{m,n,m+n+2}^{(2)}$ , then  $\phi_{m,n,m+n+2}^{(3)}$  is found to involve only second-order derivatives and is therefore not relevant to the  $O(St)$  correction of  $b_{m,n}^{(0)}$ . The expressions (A.37) and (A.38) when substituted (with appropriate change of indices) into the consistency condition for  $b_{m,n}^{(0)}$  obtained from (A.36), the resulting fourth-order derivatives identically cancel out. Thus equation (2.37) represents the entire  $O(St)$  correction.

## A.4 Identity of exact and multiple scales solutions of section

### 2.4.2

#### A.4.1 Identity of leading order solutions

From (A.29), the leading order term in the expansion of the rescaled (exact) probability density is

$$\begin{aligned}
 & (\bar{P}^d)^{(0)}(\hat{\mathbf{x}}, \mathbf{w}, t_1, t_2) \\
 &= \frac{\bar{G}_0(x, y, t_2)}{2\pi\{1 - (t_2^2 + 2)e^{-2t_1} + e^{-4t_1}\}^{\frac{1}{2}}} \exp\left[-\frac{(1 - e^{-2t_1})w_1^2 + (1 - (t_2^2 + 1)e^{-2t_1})w_2^2 - 2t_2e^{-2t_1}w_1w_2}{2\{1 - (t_2^2 + 2)e^{-2t_1} + e^{-4t_1}\}}\right],
 \end{aligned} \tag{A.40}$$

where  $\mathbf{w}$  is the scaled fluctuation velocity (see section 2.2). We find the series coefficients  $\tilde{b}_{m,n}$  when (A.40) is expanded in terms of Hermite functions; they are defined as

$$\tilde{b}_{m,n} = \frac{1}{(2\pi)^{2m+n}m!n!} \int_{-\infty}^{\infty} \int_{-\infty}^{\infty} P^d{}^{(0)} H_m\left(\frac{w_1}{2^{\frac{1}{2}}}\right) H_n\left(\frac{w_2}{2^{\frac{1}{2}}}\right) dw_1 dw_2.$$

The identity of the exact and multiple scales solutions at this order holds provided  $\tilde{b}_{m,n} = b_{m,n}^{(0)}e^{-(m+n)t_1}$  for all  $m$  and  $n$  where the  $b_{m,n}^{(0)}$ 's are as defined in equations (2.59), (2.60), (2.61) and (2.62). It is easily seen that there are no terms in the expansion proportional to  $\bar{H}_{2m}(w_1/2^{\frac{1}{2}})\bar{H}_{2n+1}(w_2/2^{\frac{1}{2}})$  and  $\bar{H}_{2m+1}(w_1/2^{\frac{1}{2}})\bar{H}_{2n}(w_2/2^{\frac{1}{2}})$  because these terms would change sign under the transformation  $(w_1, w_2) \rightarrow (-w_1, -w_2)$  while (A.40) being a homogeneous quadratic function of  $w_1$  and  $w_2$ , remains unchanged. Thus,  $\tilde{b}_{2m,2n+1} = b_{2m,2n+1}^{(0)} = 0$  and  $\tilde{b}_{2m+1,2n} = b_{2m+1,2n}^{(0)} = 0$ . For the terms proportional to  $\bar{H}_{2m}\bar{H}_{2n}$  and  $\bar{H}_{2m+1}\bar{H}_{2n+1}$ , we use induction with respect to  $m$ ; we assume that the coefficients  $\tilde{b}_{j,n}$  are given by  $b_{j,n}^{(0)}e^{-(j+n)t_1}$  for  $j \leq 2m + 1$  and  $n$  arbitrary (even or odd depending on  $j$ ); we then prove that the same

holds for  $\tilde{b}_{2m+2,2n}$  and  $\tilde{b}_{2m+3,2n+1}$ . Consider

$$\begin{aligned}\tilde{b}_{2m+2,2n} &= \frac{1}{(2\pi)2^{2m+2}2^{2n}(2n)!(2m+2)!} \int_{-\infty}^{\infty} \int_{-\infty}^{\infty} dw_1 dw_2 P^{d(0)} H_{2m+2} \left( \frac{w_1}{2^{\frac{1}{2}}} \right) H_{2n} \left( \frac{w_2}{2^{\frac{1}{2}}} \right), \\ &= \frac{1}{(2\pi)2^{2m+2}2^{2n}(2n)!(2m+2)!} \int_{-\infty}^{\infty} \int_{-\infty}^{\infty} dw_1 dw_2 P^{d(0)} \left[ -2^{\frac{1}{2}} \frac{d}{dw_1} H_{2m+1} \left( \frac{w_1}{2^{\frac{1}{2}}} \right) \right. \\ &\quad \left. + H_{2m+2} \left( \frac{w_1}{2^{\frac{1}{2}}} \right) + 2(2m+1) H_{2m} \left( \frac{w_1}{2^{\frac{1}{2}}} \right) \right] H_{2n} \left( \frac{w_2}{2^{\frac{1}{2}}} \right),\end{aligned}$$

where we have used the recurrence relation between Hermite polynomials. Integrating by parts,

$$\begin{aligned}\tilde{b}_{2m+2,2n} &= \frac{1}{(2\pi)2^{2m+2}2^{2n}(2n)!(2m+2)!} \left[ 2^{\frac{1}{2}} \int_{-\infty}^{\infty} \int_{-\infty}^{\infty} dw_1 dw_2 \frac{d}{dw_1} (P^{d(0)}) H_{2m+1} \left( \frac{w_1}{2^{\frac{1}{2}}} \right) H_{2n} \left( \frac{w_2}{2^{\frac{1}{2}}} \right) \right. \\ &\quad \left. + \int_{-\infty}^{\infty} \int_{-\infty}^{\infty} dw_1 dw_2 P^{d(0)} \left\{ H_{2m+2} \left( \frac{w_1}{2^{\frac{1}{2}}} \right) + 2(2m+1) \bar{H}_{2m} \left( \frac{w_1}{2^{\frac{1}{2}}} \right) \right\} H_{2n} \left( \frac{w_2}{2^{\frac{1}{2}}} \right) \right].\end{aligned}$$

Differentiating (A.40) and using the resulting expression in the above relation, one obtains after some manipulation

$$\begin{aligned}\tilde{b}_{2m+2,2n} &= \frac{1}{(2\pi)2^{2m+2}2^{2n}(2n)!(2m+2)! \{1 - e^{-2t_1}(t_2^2 + 2) + e^{-4t_1}\}} \left[ \{e^{-4t_1} - e^{-2t_1}(t_2^2 + 1)\} \right. \\ &\quad \int_{-\infty}^{\infty} \int_{-\infty}^{\infty} dw_1 dw_2 \left\{ H_{2m+2} \left( \frac{w_1}{2^{\frac{1}{2}}} \right) + 2(2m+1) H_{2m} \left( \frac{w_1}{2^{\frac{1}{2}}} \right) \right\} H_{2n} \left( \frac{w_2}{2^{\frac{1}{2}}} \right) P^{d(0)} \\ &\quad + e^{-2t_1} t_2 \int_{-\infty}^{\infty} \int_{-\infty}^{\infty} dw_1 dw_2 \left\{ H_{2m+1} \left( \frac{w_1}{2^{\frac{1}{2}}} \right) H_{2n+1} \left( \frac{w_2}{2^{\frac{1}{2}}} \right) \right. \\ &\quad \left. + 4n H_{2n-1} \left( \frac{w_2}{2^{\frac{1}{2}}} \right) H_{2m+1} \left( \frac{w_1}{2^{\frac{1}{2}}} \right) \right\} P^{d(0)} \left. \right],\end{aligned}$$

from which, using the definition of the coefficients  $\tilde{b}_{m,n}$ , we obtain

$$\begin{aligned} & \tilde{b}_{2m+2,2n} \left[ 1 - \frac{e^{-4t_1} - e^{-2t_1}(t_2^2 + 1)}{1 - e^{-2t_1}(t_2^2 + 2) + e^{-4t_1}} \right] \\ &= \frac{1}{\{1 - e^{-2t_1}(t_2^2 + 2) + e^{-4t_1}\}} \left[ \frac{e^{-4t_1} - e^{-2t_1}(t_2^2 + 1)}{2(2m+2)} \tilde{b}_{2m,2n} + \frac{e^{-2t_1}t_2(2n+1)}{(2m+2)} \tilde{b}_{2m+1,2n+1} \right. \\ & \quad \left. + \frac{e^{-2t_1}t_2}{2(2m+2)} \tilde{b}_{2m+1,2n-1} \right], \\ \Rightarrow \tilde{b}_{2m+2,2n}(1 - e^{-2t_1}) &= \frac{e^{-4t_1} - e^{-2t_1}(t_2^2 + 1)}{2(2m+2)} \tilde{b}_{2m,2n} + \frac{e^{-2t_1}t_2(2n+1)}{(2m+2)} \tilde{b}_{2m+1,2n+1} \\ & \quad + \frac{e^{-2t_1}t_2}{2(2m+2)} \tilde{b}_{2m+1,2n-1}. \end{aligned}$$

Therefore

$$\begin{aligned} \tilde{b}_{2m+2,2n}(1 - e^{-2t_1}) &= \left[ \frac{e^{-4t_1}}{2(2m+2)} \tilde{b}_{2m,2n} + e^{-2t_1}t_2 \frac{(2n+1)}{(2m+2)} \tilde{b}_{2m+1,2n+1} \right] \\ & \quad + \left[ \frac{e^{-2t_1}t_2}{2(2m+2)} \tilde{b}_{2m+1,2n-1} - \frac{\tilde{e}^{-2t_1}(t_2^2 + 1)}{2(2m+2)} \tilde{b}_{2m,2n} \right], \\ &= T_1 + T_2. \end{aligned}$$

In accordance with our assumption, we use the expressions (2.61) and (2.62) for  $\tilde{b}_{2m,2n}$  and  $\tilde{b}_{2m+1,2n+1}$  while  $\tilde{b}_{2m+1,2n-1}$  is similarly given by

$$\tilde{b}_{2m+1,2n-1} = \frac{(-1)^{m+n-1}}{(2\pi)2^{2n+m-1}(n-1)!} \sum_{k=0}^m \frac{t_2^{2m+1-2k} \prod_{l=k}^{m-1} (2n+2m-1-2l)}{2^k k! (2m+1-2k)!} \bar{G}_0.$$

Using these,

$$\begin{aligned} T_1 &= \frac{(-1)^{m+n} e^{-(2m+2n+4)t_1} \bar{G}_0}{(2\pi)(2m+2)2^{2n+m+1}n!} \left[ \sum_{k=0}^m \frac{t_2^{2m-2k} \prod_{l=k}^{m-1} (2n+2m-1-2l)}{2^k k! (2m-2k)!} \right. \\ & \quad \left. + \sum_{k=0}^m \frac{t_2^{2m+2-2k} \prod_{l=k}^m (2n+2m+1-2l)}{2^k k! (2m+1-2k)!} \right], \end{aligned}$$

$$\begin{aligned}
&= \frac{(-1)^{m+n} e^{-(2m+2n+4)t_1} \bar{G}_0}{(2\pi)(2m+2)2^{2n+2m+1}n!} \left[ \sum_{k=0}^m \frac{t_2^{2m-2k} \prod_{l=k}^{m-1} (2n+2m-1-2l)}{2^k k! (2m-2k)!} \right. \\
&\quad \left. + (2m+2) \sum_{k=0}^m \frac{t_2^{2m+2-2k} \prod_{l=k}^m (2n+2m+1-2l)}{2^k k! (2m+2-2k)!} - \sum_{k=1}^m \frac{t_2^{2m+2-2k} \prod_{l=k}^m (2n+2m+1-2l)}{2^{k-1} (k-1)! (2m+2-2k)!} \right], \\
&= \frac{(-1)^{m+n} e^{-(2m+2n+4)t_1} \bar{G}_0}{(2\pi)(2m+2)2^{2n+2m+1}n!} \left[ \sum_{k=0}^m \frac{t_2^{2m-2k} \prod_{l=k}^{m-1} (2n+2m-1-2l)}{2^k k! (2m-2k)!} \right. \\
&\quad \left. + (2m+2) \sum_{k=0}^m \frac{t_2^{2m+2-2k} \prod_{l=k}^m (2n+2m+1-2l)}{2^k k! (2m+2-2k)!} - \sum_{k=0}^{m-1} \frac{t_2^{2m-2k} \prod_{l=k}^{m-1} (2n+2m-1-2l)}{2^k k! (2m-2k)!} \right], \\
&= \frac{(-1)^{m+n} e^{-(2m+2n+4)t_1} \bar{G}_0}{(2\pi)2^{2n+2m+1}n!} \left[ \sum_{k=0}^m \frac{t_2^{2m+2-2k} \prod_{l=k}^m (2n+2m+1-2l)}{2^k k! (2m+2-2k)!} + \frac{1}{2^{m+1}(m+1)!} \right], \\
&= \frac{(-1)^{m+n}}{(2\pi)2^{2n+2m+1}n!} \sum_{k=0}^{m+1} \frac{t_2^{2m+2-2k} \prod_{l=k}^m (2n+2m+1-2l)}{2^k k! (2m+2-2k)!} \bar{G}_0 e^{-(2m+2n+4)t_1}, \tag{A.41}
\end{aligned}$$

and

$$\begin{aligned}
T_2 &= \frac{(-1)^{m+n+1} e^{-(2m+2n+2)t_1} \bar{G}_0}{(2\pi)(2m+2)2^{2n+m+1}n!} \left[ (2n) \sum_{k=0}^m \frac{t_2^{2m+2-2k} \prod_{l=k}^{m-1} (2n+2m-1-2l)}{2^k k! (2m+1-2k)!} \right. \\
&\quad \left. + (t_2^2 + 1) \sum_{k=0}^m \frac{t_2^{2m-2k} \prod_{l=k}^{m-1} (2n+2m-1-2l)}{2^k k! (2m-2k)!} \right], \\
&= \frac{(-1)^{m+n+1} e^{-(2m+2n+2)t_1} \bar{G}_0}{(2\pi)(2m+2)2^{2n+m+1}n!} \left[ \sum_{k=0}^m \frac{t_2^{2m+2-2k} (2n+2m+1-2k) \prod_{l=k}^{m-1} (2n+2m-1-2l)}{2^k k! (2m+1-2k)!} \right. \\
&\quad \left. + \sum_{k=0}^m \frac{t_2^{2m-2k} \prod_{l=k}^{m-1} (2n+2m-1-2l)}{2^k k! (2m-2k)!} \right], \\
&= \frac{(-1)^{m+n+1} e^{-(2m+2n+2)t_1} \bar{G}_0}{(2\pi)(2m+2)2^{2n+m+1}n!} \left[ \sum_{k=0}^m \frac{t_2^{2m+2-2k} \prod_{l=k-1}^{m-1} (2n+2m-1-2l)}{2^k k! (2m+1-2k)!} \right. \\
&\quad \left. + \sum_{k=0}^m \frac{t_2^{2m-2k} \prod_{l=k}^{m-1} (2n+2m-1-2l)}{2^k k! (2m-2k)!} \right], \\
&= \frac{(-1)^{m+n+1} e^{-(2m+2n+2)t_1} \bar{G}_0}{(2\pi)(2m+2)2^{2n+m+1}n!} \left[ (2m+2) \sum_{k=0}^m \frac{t_2^{2m+2-2k} \prod_{l=k}^m (2n+2m+1-2l)}{2^k k! (2m+2-2k)!} \right. \\
&\quad \left. - \sum_{k=1}^m \frac{t_2^{2m+2-2k} \prod_{l=k}^m (2n+2m+1-2l)}{2^{k-1} (k-1)! (2m+2-2k)!} + \sum_{k=0}^m \frac{t_2^{2m-2k} \prod_{l=k}^{m-1} (2n+2m-1-2l)}{2^k k! (2m-2k)!} \right],
\end{aligned}$$

$$\begin{aligned}
&= \frac{(-1)^{m+n+1} e^{-(2m+2n+2)t_1} \bar{G}_0}{(2\pi)(2m+2)2^{2n+m+1}n!} \left[ (2m+2) \sum_{k=0}^m \frac{t_2^{2m+2-2k} \prod_{l=k}^m (2n+2m+1-2l)}{2^k k! (2m+2-2k)!} \right. \\
&\quad \left. - \sum_{k=0}^{m-1} \frac{t_2^{2m-2k} \prod_{l=k}^{m-1} (2n+2m-1-2l)}{2^k k! (2m-2k)!} + \sum_{k=0}^m \frac{t_2^{2m-2k} \prod_{l=k}^{m-1} (2n+2m-1-2l)}{2^k k! (2m-2k)!} \right], \\
&= \frac{(-1)^{m+n+1} e^{-(2m+2n+2)t_1} \bar{G}_0}{(2\pi)2^{2n+m+1}n!} \left[ \sum_{k=0}^m \frac{t_2^{2m+2-2k} \prod_{l=k}^m (2n+2m+1-2l)}{2^k k! (2m+2-2k)!} + \frac{1}{2^{m+1}(m+1)!} \right], \\
&= \frac{(-1)^{m+n+1}}{(2\pi)2^{2n+m+1}n!} \sum_{k=0}^{m+1} \frac{t_2^{2m+2-2k} \prod_{l=k}^m (2n+2m+1-2l)}{2^k k! (2m+2-2k)!} \bar{G}_0 e^{-(2m+2n+2)t_1}. \tag{A.42}
\end{aligned}$$

Adding (A.41) and (A.42), we have

$$\begin{aligned}
\tilde{b}_{2m+2,2n} &= \frac{(-1)^{m+n+1}}{(2\pi)2^{2n+m+1}n!} \sum_{k=0}^{m+1} \frac{t_2^{2m+2-2k} \prod_{l=k}^m (2n+2m+1-2l)}{2^k k! (2m+2-2k)!} e^{-(2m+2n+2)t_1}, \\
&= b_{2m+2,2n}^{(0)} e^{-(2m+2n+2)t_1}. \tag{A.43}
\end{aligned}$$

Similarly for  $\tilde{b}_{2m+3,2n+1}$ , one can derive the recurrence relation

$$\begin{aligned}
\tilde{b}_{2m+3,2n+1} (1 - e^{-2t_1}) &= \frac{e^{-4t_1} - (t_2^2 + 1)e^{-2t_1}}{2(2m+3)} \tilde{b}_{2m+1,2n+1} + \frac{e^{-2t_1} t_2}{2(2m+3)} \tilde{b}_{2m+2,2n} \\
&\quad + e^{-2t_1} t_2 \frac{(2n+2)}{(2m+3)} \tilde{b}_{2m+2,2n+2}, \tag{A.44}
\end{aligned}$$

where we now use (A.43) (changing  $n$  to  $n+1$ ) for  $\tilde{b}_{2m+2,2n+2}$ . Carrying out similar manipulations, one obtains

$$\begin{aligned}
\tilde{b}_{2m+3,2n+1} &= \frac{(-1)^{m+n+1}}{(2\pi)2^{2n+m+2}n!} \sum_{k=0}^{m+1} \frac{t_2^{2m+3-2k} \prod_{l=k}^m (2n+2m+3-2l)}{2^k k! (2m+3-2k)!} e^{-(2m+2n+4)t_1}, \\
&= b_{2m+3,2n+1}^{(0)} e^{-(2m+2n+4)t_1}. \tag{A.45}
\end{aligned}$$

Thus, provided one proves  $\tilde{b}_{m,n} = b_{m,n}^{(0)} e^{-(m+n)t_1}$  for  $(m = 0, \text{ even } n)$  and  $(m = 1, \text{ odd } n)$ , one has the identity of the two for all  $m$  and  $n$ . For  $(m, n) \equiv (0, 2n)$ , we have

$$\begin{aligned} \tilde{b}_{0,2n} &= \frac{1}{(2\pi)^2 2^{2n} (2n)!} \int_{-\infty}^{\infty} \int_{-\infty}^{\infty} dw_1 dw_2 P^{d(0)} H_{2n} \left( \frac{w_2}{2^{\frac{1}{2}}} \right), \\ &= \frac{1}{(2\pi)^2 2^{2n} (2n)!} \frac{\bar{G}_0}{[1 - e^{-2t_1}(t_2^2 + 2) + e^{-4t_1}]^{\frac{1}{2}}} \int_{-\infty}^{\infty} \int_{-\infty}^{\infty} dw_1 dw_2 \exp \left[ -\frac{w_2^2}{2(1 - e^{-2t_1})} \right] \\ &\quad \exp \left[ -\frac{1}{2[1 - e^{-2t_1}(t_2^2 + 2) + e^{-4t_1}]} \left\{ w_1(1 - e^{-2t_1})^{\frac{1}{2}} - \frac{w_2 e^{-2t_1} t_2}{(1 - e^{-2t_1})^{\frac{1}{2}}} \right\}^2 \right] H_{2n} \left( \frac{w_2}{2^{\frac{1}{2}}} \right), \\ &= \frac{1}{2^{2n} (2n)!} \frac{\bar{G}_0}{2^{\frac{3}{2}} \pi^2 (1 - e^{-2t_1})^{\frac{1}{2}}} \int_{-\infty}^{\infty} dw_2 \exp \left[ -\frac{w_2^2}{2(1 - e^{-2t_1})} \right] H_{2n} \left( \frac{w_2}{2^{\frac{1}{2}}} \right) \int_{-\infty}^{\infty} dp \exp[-(p - K)^2], \end{aligned}$$

where we have expressed the exact solution alternately as the product of two exponentials.

Using the relation derived in Appendix F

$$\begin{aligned} \tilde{b}_{0,2n} &= \frac{\bar{G}_0}{2^{2n} (2n)! (2\pi)^{\frac{3}{2}}} \sum_{m=0}^{\infty} \frac{(-1)^m e^{-2mt_1}}{2^{2m} m!} \int_{-\infty}^{\infty} \bar{H}_{2m} \left( \frac{w_2}{2^{\frac{1}{2}}} \right) H_{2n} \left( \frac{w_2}{2^{\frac{1}{2}}} \right) dw_2, \\ &= \frac{(-1)^n \bar{G}_0}{(2\pi)^2 2^{2n} n!} e^{-2nt_1}, \end{aligned} \tag{A.46}$$

from the orthogonality of the Hermite polynomials with respect to  $e^{-\frac{w^2}{2}}$ . For  $(m, n) \equiv (1, 2n + 1)$ ,

$$\begin{aligned} \tilde{b}_{1,2n+1} &= \frac{1}{(2\pi)^2 2^{2n+2} (2n + 1)!} \frac{\bar{G}_0}{[1 - e^{-2t_1}(t_2^2 + 2) + e^{-4t_1}]^{\frac{1}{2}}} \int_{-\infty}^{\infty} \int_{-\infty}^{\infty} dw_1 dw_2 \exp \left[ -\frac{w_2^2}{2(1 - e^{-2t_1})} \right] \\ &\quad \exp \left[ -\frac{1}{2[1 - e^{-2t_1}(t_2^2 + 2) + e^{-4t_1}]} \left\{ w_1(1 - e^{-2t_1})^{\frac{1}{2}} - \frac{w_2 e^{-2t_1} t_2}{(1 - e^{-2t_1})^{\frac{1}{2}}} \right\}^2 \right] 2^{\frac{1}{2}} w_1 H_{2n+1} \left( \frac{w_2}{2^{\frac{1}{2}}} \right), \\ &= \frac{2^{\frac{3}{2}}}{(2\pi)^2 2^{2n+2} (2n + 1)!} \frac{\bar{G}_0 [1 - e^{-2t_1}(t_2^2 + 2) + e^{-4t_1}]^{\frac{1}{2}}}{(1 - e^{-2t_1})} \\ &\quad \int_{-\infty}^{\infty} dw_2 \exp \left[ -\frac{w_2^2}{2(1 - e^{-2t_1})} \right] H_{2n+1} \left( \frac{w_2}{2^{\frac{1}{2}}} \right) \int_{-\infty}^{\infty} dp p \exp[-(p - K)^2], \end{aligned}$$

where

$$K = \frac{w_2 t_2 e^{-2t_1}}{2^{\frac{1}{2}}(1 - e^{-2t_1})^{\frac{1}{2}}[1 - e^{-2t_1}(t_2^2 + 2) + e^{-4t_1}]^{\frac{1}{2}}}.$$

Therefore

$$\begin{aligned} \tilde{b}_{1,2n+1} &= \frac{1}{2^2 \pi^{\frac{3}{2}} 2^{2n+1} (2n+1)! (1 - e^{-2t_1})^{\frac{3}{2}}} \int_{-\infty}^{\infty} dw_2 w_2 \exp\left[-\frac{w_2^2}{2(1 - e^{-2t_1})}\right] H_{2n+1}\left(\frac{w_2}{2^{\frac{1}{2}}}\right), \\ &= \frac{-\bar{G}_0 e^{-2t_1} t_2}{2^{2n+2} (2n+1)! (2\pi)^{\frac{3}{2}}} \int_{-\infty}^{\infty} dw_2 \sum_{m=0}^{\infty} \frac{(-1)^m \bar{H}'_{2m}\left(\frac{w_2}{2^{\frac{1}{2}}}\right) e^{-2mt_1}}{2^{2m} m!} H_{2n+1}\left(\frac{w_2}{2^{\frac{1}{2}}}\right). \end{aligned}$$

Using  $\bar{H}'_m(z) = -\bar{H}_{m+1}(z)$  and integrating, we obtain

$$\tilde{b}_{1,2n+1} = \frac{(-1)^n \bar{G}_0 t_2 e^{-(2n+2)t_1}}{(2\pi) 2^{2n+1} n!}. \quad (\text{A.47})$$

Equations (A.46) and (A.47) are of the form  $b_{m,n}^{(0)} e^{-(m+n)t_1}$  for  $m = 0$  and  $m = 1$  respectively, which completes the proof.

#### A.4.2 Identity of $O(St)$ velocity-dependent corrections

From (A.28) and (A.40), the exact solution at  $O(St)$ , including only velocity-dependent corrections, can be written as

$$\begin{aligned} &(\bar{P}^d)^{(1)}(\hat{\mathbf{x}}, \mathbf{w}, t_1, t_2) \\ &= (c_{w_1 x} w_1 \hat{x} + c_{w_2 x} w_2 \hat{x} + c_{w_1 y} w_1 \hat{y} + c_{w_2 y} w_2 \hat{y}) (\bar{P}^d)^{(0)}, \\ &= (c_{w_1 x} w_1 \hat{x} + c_{w_2 x} w_2 \hat{x} + c_{w_1 y} w_1 \hat{y} + c_{w_2 y} w_2 \hat{y}) \sum_{m+n=2k} b_{m,n}^{(0)} e^{-(m+n)t_1} \bar{H}_m\left(\frac{w_1}{2^{\frac{1}{2}}}\right) \bar{H}_n\left(\frac{w_2}{2^{\frac{1}{2}}}\right), \end{aligned}$$

where

$$\begin{aligned} (PeSt)c_{w_1x} &= c_{ux}, & (PeSt)c_{w_2x} &= c_{vx}, \\ (PeSt)c_{w_1y} &= 2c_{uu} + c_{uy}, & (PeSt)c_{w_2y} &= c_{vy} + c_{uv}. \end{aligned}$$

Using the recurrence relation between Hermite functions,

$$\begin{aligned} (\bar{P}^d)^{(1)} &= \sum_{m+n=2k+1} \left[ (c_{w_1x}\hat{x} + c_{w_1y}\hat{y}) \left\{ \frac{b_{m-1,n}^{(0)}}{2^{\frac{1}{2}}} e^{-(m+n-1)t_1} + 2^{\frac{1}{2}}(m+1)b_{m+1,n}^{(0)} e^{-(m+n+1)t_1} \right\} + \right. \\ &\quad \left. (c_{w_2x}\hat{x} + c_{w_2y}\hat{y}) \left\{ \frac{b_{m,n-1}^{(0)}}{2^{\frac{1}{2}}} e^{-(m+n-1)t_1} + 2^{\frac{1}{2}}(n+1)b_{m,n+1}^{(0)} e^{-(m+n+1)t_1} \right\} \right] \bar{H}_m\left(\frac{w_1}{2^{\frac{1}{2}}}\right) \bar{H}_n\left(\frac{w_2}{2^{\frac{1}{2}}}\right), \\ (\bar{P}^d)^{(1)} &= \sum_{m,n=0}^{\infty} \left\{ [C^{(1)}]_{2m,2n+1} \bar{H}_{2m}\left(\frac{w_1}{2^{\frac{1}{2}}}\right) \bar{H}_{2n+1}\left(\frac{w_2}{2^{\frac{1}{2}}}\right) + [C^{(1)}]_{2m+1,2n} \bar{H}_{2m+1}\left(\frac{w_1}{2^{\frac{1}{2}}}\right) \bar{H}_{2n}\left(\frac{w_2}{2^{\frac{1}{2}}}\right) \right\}, \end{aligned}$$

where we have used  $b_{2m+1,2n}^{(0)} = b_{2m,2n+1}^{(0)} = 0$  (see section A.4.1). In the above expression,

$$\begin{aligned} [C^{(1)}]_{2m,2n+1} &= (c_{w_1x}\hat{x} + c_{w_1y}\hat{y}) \left[ \frac{b_{2m-1,2n+1}^{(0)}}{2^{\frac{1}{2}}} e^{-(2m+2n)t_1} + 2^{\frac{1}{2}}(2m+1)b_{2m+1,2n+1}^{(0)} e^{-(2m+2n+2)t_1} \right] \\ &\quad + (c_{w_2x}\hat{x} + c_{w_2y}\hat{y}) \left[ \frac{b_{2m,2n}^{(0)}}{2^{\frac{1}{2}}} e^{-(2m+2n)t_1} + 2^{\frac{1}{2}}(2n+2)b_{2m,2n+2}^{(0)} e^{-(2m+2n+2)t_1} \right], \\ &= \frac{2^{\frac{1}{2}} e^{-2(m+n)t_1} (-1)^{m+n} \bar{G}_0}{(2\pi)2^{2n+m+1}n!} [(c_{w_1x}\hat{x} + c_{w_1y}\hat{y}) W_1 + (c_{w_2x}\hat{x} + c_{w_2y}\hat{y}) W_2]. \end{aligned}$$

From (2.61) and (2.62),

$$\begin{aligned} W_1 &= - \sum_{k=0}^{m-1} \frac{t_2^{2m-2k-1} \prod_{l=k}^{m-2} (2n+2m-1-2l)}{2^k k! (2m-1-2k)!} \\ &\quad + (2m+1) e^{-2t_1} \sum_{k=0}^m \frac{t_2^{2m+1-2k} \prod_{l=k}^{m-1} (2n+2m+1-2l)}{2^k k! (2m+1-2k)!}, \end{aligned}$$

$$\begin{aligned}
&= - \sum_{k=0}^{m-1} \frac{t_2^{2m-2k-1} \prod_{l=k}^{m-2} (2n+2m-1-2l)}{2^k k! (2m-1-2k)!} \\
&\quad + e^{-2t_1} \left[ \sum_{k=0}^m \frac{t_2^{2m+1-2k} \prod_{l=k}^{m-1} (2n+2m+1-2l)}{2^k k! (2m-2k)!} + \sum_{k=1}^m \frac{t_2^{2m+1-2k} \prod_{l=k}^{m-1} (2n+2m+1-2l)}{2^{k-1} (k-1)! (2m+1-2k)!} \right], \\
&= -(1-e^{-2t_1}) \sum_{k=0}^{m-1} \frac{t_2^{2m-2k-1} \prod_{l=k}^{m-2} (2n+2m-1-2l)}{2^k k! (2m-1-2k)!} \\
&\quad + t_2 e^{-2t_1} \sum_{k=0}^m \frac{t_2^{2m-2k} \prod_{l=k}^{m-1} (2n+2m+1-2l)}{2^k k! (2m-2k)!},
\end{aligned}$$

and

$$\begin{aligned}
W_2 &= \sum_{k=0}^m \frac{t_2^{2m-2k} \prod_{l=k}^{m-1} (2n+2m-1-2l)}{2^k k! (2m-2k)!} - e^{-2t_1} \sum_{k=0}^m \frac{t_2^{2m-2k} \prod_{l=k}^{m-1} (2n+2m+1-2l)}{2^k k! (2m-2k)!}, \\
&= \sum_{k=0}^m \frac{t_2^{2m-2k} [\{2n+2m-2(m-1)-1\} - (2n+2m+1-2k)] \prod_{l=k}^{m-2} (2n+2m-1-2l)}{2^k k! (2m-2k)!} \\
&\quad + (1-e^{-2t_1}) \sum_{k=0}^m \frac{t_2^{2m-2k} \prod_{l=k}^{m-1} (2n+2m+1-2l)}{2^k k! (2m-2k)!}, \\
&= -t_2 \sum_{k=0}^{m-1} \frac{t_2^{2m-1-2k} \prod_{l=k}^{m-2} (2n+2m-1-2l)}{2^k k! (2m-1-2k)!} \\
&\quad + (1-e^{-2t_1}) \sum_{k=0}^m \frac{t_2^{2m-2k} \prod_{l=k}^{m-1} (2n+2m+1-2l)}{2^k k! (2m-2k)!}.
\end{aligned}$$

Using the expressions for  $W_1$  and  $W_2$ ,

$$\begin{aligned}
[C^{(1)}]_{2m,2n+1} &= \frac{2^{\frac{1}{2}} e^{-2(m+n)t_1} (-1)^{m+n} \bar{G}_0}{(2\pi) 2^{2n+m+1} n!} \left[ S_2^{\prime(m,n)} \{ (c_{w_1x} \hat{x} + c_{w_1y} \hat{y}) t_2 e^{-2t_1} + (c_{w_2x} \hat{x} + c_{w_2y} \hat{y}) \right. \\
&\quad \left. (1 - e^{-2t_1}) \} - S_1^{\prime(m,n)} \{ (c_{w_1x} \hat{x} + c_{w_1y} \hat{y}) (1 - e^{-2t_1}) + t_2 (c_{w_2x} \hat{x} + c_{w_2y} \hat{y}) \} \right], \\
&= \frac{2^{\frac{1}{2}} e^{-2(m+n)t_1} (-1)^{m+n} \bar{G}_0}{(2\pi) 2^{2n+m+1} n!} \left[ S_2^{\prime(m,n)} \left\{ - \frac{3(2e^{-t_1} + 1 + 3e^{-2t_1})}{(t_2^2 + 12)} \hat{x} \right. \right. \\
&\quad \left. \left. + \frac{2e^{-t_1}(t_2^2 - 6) + 2(t_2^2 + 3) + e^{-2t_1}(5t_2^2 + 6)}{t_2(t_2^2 + 12)} \hat{y} \right\} - \right. \\
&\quad \left. S_1^{\prime(m,n)} \left\{ \frac{3\{-(t_2^2 - 2) + 2e^{-2t_1} - 4e^{-t_1}\}}{t_2(t_2^2 + 12)} \hat{x} + \frac{(2t_2^2 + 3) - 3e^{-2t_1} + 6e^{-t_1}}{(t_2^2 + 12)} \hat{y} \right\} \right].
\end{aligned}$$

(A.48)

In an exactly analogous manner, one also obtains

$$\begin{aligned}
[C^{(1)}]_{2m+1,2n} &= (c_{w_1x}\hat{x} + c_{w_1y}\hat{y}) \left[ \frac{b_{2m,2n}^{(0)}}{2^{\frac{1}{2}}} e^{-(2m+2n)t_1} + 2^{\frac{1}{2}}(2m+2)b_{2m+1,2n+1}^{(0)} e^{-(2m+2n+2)t_1} \right] \\
&\quad + (c_{w_2x}\hat{x} + c_{w_2y}\hat{y}) \left[ \frac{b_{2m+1,2n-1}^{(0)}}{2^{\frac{1}{2}}} e^{-(2m+2n)t_1} + 2^{\frac{1}{2}}(2n+1)b_{2m+1,2n+1}^{(0)} e^{-(2m+2n+2)t_1} \right], \\
&= \frac{2^{\frac{1}{2}} e^{-2(m+n)t_1} (-1)^{m+n} \bar{G}_0}{(2\pi)2^{2n+m+1}n!} \left[ -S_2^{(m,n)} \{ (c_{w_1x}\hat{x} + c_{w_1y}\hat{y})t_2 e^{-2t_1} + (c_{w_2x}\hat{x} + c_{w_2y}\hat{y}) \right. \\
&\quad \left. (1 - e^{-2t_1}) \} + S_1^{(m,n)} \{ (c_{w_1x}\hat{x} + c_{w_1y}\hat{y})(1 - e^{-2t_1}) + t_2(c_{w_2x}\hat{x} + c_{w_2y}\hat{y}) \} \right], \\
&= \frac{2^{\frac{1}{2}} e^{-2(m+n)t_1} (-1)^{m+n} \bar{G}_0}{(2\pi)2^{2n+m+1}n!} \left[ -S_2^{(m,n)} \left\{ -\frac{3(2e^{-t_1} + 1 + 3e^{-2t_1})}{(t_2^2 + 12)} \hat{x} \right. \right. \\
&\quad \left. \left. + \frac{2e^{-t_1}(t_2^2 - 6) + 2(t_2^2 + 3) + e^{-2t_1}(5t_2^2 + 6)}{t_2(t_2^2 + 12)} \hat{y} \right\} + \right. \\
&\quad \left. S_1^{(m,n)} \left\{ \frac{3\{-(t_2^2 - 2) + 2e^{-2t_1} - 4e^{-t_1}\}}{t_2(t_2^2 + 12)} \hat{x} + \frac{(2t_2^2 + 3) - 3e^{-2t_1} + 6e^{-t_1}}{(t_2^2 + 12)} \hat{y} \right\} \right]. \tag{A.49}
\end{aligned}$$

(A.50)

where  $S_i^{(m,n)}$  and  $S_i^{\prime(m,n)}$  ( $i = 1, 2$ ) are as defined in section 2.4.2. (A.48) and (A.50) will be used for comparison with the first order multiple scales solution.

From (2.16), the multiple scales series at  $O(St)$ , including only velocity-dependent corrections, is given by

$$\begin{aligned}
\bar{P}^{(1)}(\hat{\mathbf{x}}, \bar{w}, t_1, t_2) &= St \sum_{m,n}^{\infty} \left[ b_{m,n}^{(1)} e^{-(m+n)t_1} + 2^{\frac{1}{2}} \left\{ (m+1) \frac{\partial b_{m+1,n}^{(0)}}{\partial \hat{x}} + (n+1) \frac{\partial b_{m,n+1}^{(0)}}{\partial \hat{y}} \right\} e^{-(m+n+1)t_1} \right. \\
&\quad \left. - \frac{1}{2^{\frac{1}{2}}} \left\{ \frac{\partial b_{m-1,n}^{(0)}}{\partial \hat{x}} + \frac{\partial b_{m,n-1}^{(0)}}{\partial \hat{y}} \right\} e^{-(m+n-1)t_1} - \frac{b_{m-1,n-1}^{(0)}}{4} e^{-(m+n-2)t_1} \right] \bar{H}_m\left(\frac{w_1}{2^{\frac{1}{2}}}\right) \bar{H}_n\left(\frac{w_2}{2^{\frac{1}{2}}}\right),
\end{aligned}$$

where we have used the expressions for the  $\phi^{(1)}$ 's from (2.24). It suffices to compare the coefficients of  $\bar{H}_m \bar{H}_n$  for  $m+n$  odd, with (A.48) and (A.50). As argued in section 2.4.2,

terms with  $m+n$  even, do not contribute at  $O(St)$ . The coefficient of  $H_{2m}H_{2n+1}$  is given by

$$[D^{(1)}]_{2m,2n+1} = St \left\{ b_{2m,2n+1}^{(1)} e^{-(2m+2n+1)t_1} + 2^{\frac{1}{2}} \left[ (2m+1) \frac{\partial b_{2m+1,2n+1}^{(0)}}{\partial \hat{x}} + (2n+2) \frac{\partial b_{2m,2n+2}^{(0)}}{\partial \hat{y}} \right] e^{-(2m+2n+2)t_1} - \frac{1}{2^{\frac{1}{2}}} \left[ \frac{\partial b_{2m-1,2n+1}^{(0)}}{\partial \hat{x}} + \frac{\partial b_{2m,2n}^{(0)}}{\partial \hat{y}} \right] e^{-(2m+2n)t_1} \right\},$$

where we have again used that  $b_{2m+1,2n}^{(0)} = 0$ . Using (2.61) and (2.62),

$$[D^{(1)}]_{2m,2n+1} = (St) b_{2m,2n+1}^{(1)} e^{-(2m+2n+1)t_1} + \frac{2^{\frac{1}{2}}(St) e^{-2(m+n)t_1} (-1)^{m+n}}{(2\pi) 2^{2n+m+1} n!} \left[ e^{-2t_1} \left\{ \frac{\partial \bar{G}_0}{\partial \hat{x}} \frac{(2m+1)}{(2n+1)} S_2^{(m,n)} - \frac{\partial \bar{G}_0}{\partial \hat{y}} S_2^{\prime(m,n)} \right\} + \left\{ \frac{\partial \bar{G}_0}{\partial \hat{x}} S_1^{\prime(m,n)} - \frac{\partial \bar{G}_0}{\partial \hat{y}} S_1^{(m,n)} \right\} \right].$$

It may be shown that

$$S_1^{(m,n)} = S_2^{\prime(m,n)} - t_2 S_1^{\prime(m,n)},$$

$$S_2^{(m,n)} \frac{(2m+1)}{(2n+1)} = t_2 S_2^{\prime(m,n)} + S_1^{\prime(m,n)}.$$

Using these, we obtain

$$[D^{(1)}]_{2m,2n+1} = (St) b_{2m,2n+1}^{(1)} e^{-(2m+2n+1)t_1} + \frac{2^{\frac{1}{2}}(St) e^{-2(m+n)t_1} (-1)^{m+n}}{(2\pi) 2^{2n+m+1} n!} \left[ S_1^{\prime(m,n)} \left( (1 + e^{-2t_1}) \frac{\partial \bar{G}_0}{\partial \hat{x}} + t_2 \frac{\partial \bar{G}_0}{\partial \hat{y}} \right) + S_2^{\prime(m,n)} \left( t_2 e^{-2t_1} \frac{\partial \bar{G}_0}{\partial \hat{x}} - (1 + e^{-2t_1}) \frac{\partial \bar{G}_0}{\partial \hat{y}} \right) \right].$$

On substituting the expression for  $\bar{G}_0$  from Appendix E,

$$\begin{aligned}
[D^{(1)}]_{2m,2n+1} = St b_{2m,2n+1}^{(1)} e^{-(2m+2n+1)t_1} + \frac{2^{\frac{1}{2}} e^{-2(m+n)t_1} (-1)^{m+n} \bar{G}_0}{(2\pi) 2^{2n+m+1} n!} \left[ \right. \\
- S_1^{(m,n)} \left\{ \frac{3\{-(t_2^2 - 2) + 2e^{-2t_1}\}}{t_2(t_2^2 + 12)} \hat{x} + \frac{(2t_2^2 + 3) - 3e^{-2t_1}}{(t_2^2 + 12)} \hat{y} \right\} \\
\left. + S_2^{(m,n)} \left\{ -\frac{3(1 + 3e^{-2t_1})}{(t_2^2 + 12)} \hat{x} + \frac{2(t_2^2 + 3) + e^{-2t_1}(5t_2^2 + 6)}{t_2(t_2^2 + 12)} \hat{y} \right\} \right]. \quad (\text{A.51})
\end{aligned}$$

In a similar manner,

$$\begin{aligned}
[D^{(1)}]_{2m+1,2n} = St b_{2m+1,2n}^{(1)} e^{-(2m+2n+1)t_1} + \frac{2^{\frac{1}{2}} (St) e^{-2(m+n)t_1} (-1)^{m+n}}{(2\pi) 2^{2n+m+1} n!} \left[ -S_1^{(m,n)} \right. \\
\left. \left( (1 + e^{-2t_1}) \frac{\partial \bar{G}_0}{\partial \hat{x}} + t_2 \frac{\partial \bar{G}_0}{\partial \hat{y}} \right) + S_2^{(m,n)} \left( -t_2 e^{-2t_1} \frac{\partial \bar{G}_0}{\partial \hat{x}} + (1 + e^{-2t_1}) \frac{\partial \bar{G}_0}{\partial \hat{y}} \right) \right], \\
= St b_{2m+1,2n}^{(1)} e^{-(2m+2n+1)t_1} + \frac{2^{\frac{1}{2}} e^{-2(m+n)t_1} (-1)^{m+n} \bar{G}_0}{(2\pi) 2^{2n+m+1} n!} \left[ S_1^{(m,n)} \left\{ \frac{-3(t_2^2 - 2) + 6e^{-2t_1}}{t_2(t_2^2 + 12)} \hat{x} \right. \right. \\
\left. \left. + \frac{(2t_2^2 + 3) - 3e^{-2t_1}}{(t_2^2 + 12)} \hat{y} \right\} + S_2^{(m,n)} \left\{ \frac{3(1 + 3e^{-2t_1})}{(t_2^2 + 12)} \hat{x} - \frac{2(t_2^2 + 3) + (5t_2^2 + 6)e^{-2t_1}}{t_2(t_2^2 + 12)} \hat{y} \right\} \right]. \quad (\text{A.52})
\end{aligned}$$

Comparing the sets of equations (A.48), (A.50) and (A.51), (A.52), we see that the bracketed terms constant on the  $t_1$  scale and those proportional to  $e^{-2t_1}$  match up exactly, and the coefficients  $[C]_{i,j}$  and  $[D]_{i,j}$  will therefore be identical provided  $b_{m,n}^{(1)}$  equals the factor multiplying  $e^{-t_1}$ . In other words, the identity of the exact and multiple scales solutions at  $O(St)$  holds provided

$$\begin{aligned}
b_{2m,2n+1}^{(1)} = \frac{2^{\frac{1}{2}} (-1)^{m+n} \bar{G}_0}{(2\pi) 2^{2n+m+1} n! (St)} \left[ S_2^{(m,n)} \left\{ \frac{2(t_2^2 - 6)}{t_2(t_2^2 + 12)} \hat{y} - \frac{6}{(t_2^2 + 12)} \hat{x} \right\} \right. \\
\left. + S_1^{(m,n)} \left\{ \frac{12}{t_2(t_2^2 + 12)} \hat{x} - \frac{6}{(t_2^2 + 12)} \hat{y} \right\} \right],
\end{aligned}$$

$$b_{2m+1,2n}^{(1)} = \frac{2^{\frac{1}{2}}(-1)^{m+n}\bar{G}_0}{(2\pi)2^{2n+m+1}n!(St)} \left[ S_1^{(m,n)} \left\{ \frac{6}{(t_2^2+12)}\hat{y} - \frac{12}{t_2(t_2^2+12)}\hat{x} \right\} \right. \\ \left. + S_2^{(m,n)} \left\{ \frac{6}{(t_2^2+12)}\hat{x} - \frac{2(t_2^2-6)}{t_2(t_2^2+12)}\hat{y} \right\} \right].$$

These may be rewritten as

$$b_{2m,2n+1}^{(1)} = \frac{2^{\frac{1}{2}}(-1)^{m+n}}{(2\pi)2^{2n+m}n!} \left[ S_2^{\prime(m,n)} \left( \frac{\partial\bar{G}_0}{\partial\hat{y}} + t_2 \frac{\partial\bar{G}_0}{\partial\hat{x}} \right) - S_1^{\prime(m,n)} \frac{\partial\bar{G}_0}{\partial\hat{x}} \right], \quad (\text{A.53})$$

$$b_{2m+1,2n}^{(1)} = \frac{2^{\frac{1}{2}}(-1)^{m+n}}{(2\pi)2^{2n+m}n!} \left[ S_1^{(m,n)} \frac{\partial\bar{G}_0}{\partial\hat{x}} - S_2^{(m,n)} \left( \frac{\partial\bar{G}_0}{\partial\hat{y}} + t_2 \frac{\partial\bar{G}_0}{\partial\hat{x}} \right) \right]. \quad (\text{A.54})$$

These identities may be proven by induction w.r.t  $m$ . As in section A.4.1, we assume that the  $b_{i,j}^{(1)}$ 's are given by (A.53) and (A.54) for  $i \leq 2m$ ,  $j$  even or odd so that  $i+j = 2k+1$ , and show that the same holds for  $i = 2m+1$  and  $2m+2$ . The equation for  $b_{2m+1,2n}^{(1)}$  is

$$Db_{2m+1,2n}^{(1)} = -(2n+1)b_{2m,2n+1}^{(1)},$$

with the initial condition given by (2.64). The operator  $D$  is as defined in section 2.4.1. Using (A.53) and (2.61), we have

$$Db_{2m+1,2n}^{(1)} = \frac{2^{\frac{1}{2}}(-1)^{m+n}(2n+1)}{(2\pi)2^{2n+m}n!} \left[ S_1^{\prime(m,n)} \frac{\partial\bar{G}_0}{\partial\hat{x}} - S_2^{\prime(m,n)} \left( \frac{\partial\bar{G}_0}{\partial\hat{y}} + t_2 \frac{\partial\bar{G}_0}{\partial\hat{x}} \right) \right],$$

with the initial condition

$$b_{2m+1,2n}^{(1)}(\hat{x}, \hat{y}, 0) = \frac{2^{\frac{1}{2}}(-1)^{m+n}}{(2\pi)2^{2(m+n)}m!n!} \delta'(\hat{x})\delta(\hat{y}).$$

The solution to the above system is given by

$$\begin{aligned}
& b_{2m+1,2n}^{(1)}(\hat{x}, \hat{y}, t_2) \\
&= b_{2m+1,2n}^{(1)h} + b_{2m+1,2n}^{(1)p}, \\
&= \frac{2^{\frac{1}{2}}(-1)^{m+n}}{(2\pi)2^{2(m+n)}m!n!} \frac{\partial \bar{G}_0}{\partial \hat{x}} + \frac{2^{\frac{1}{2}}(-1)^{m+n}(2n+1)}{(2\pi)2^{2n+m}n!} D^{-1} \left[ S_1^{(m,n)} \frac{\partial \bar{G}_0}{\partial \hat{x}} - S_2^{(m,n)} \left( \frac{\partial \bar{G}_0}{\partial \hat{y}} + t_2 \frac{\partial \bar{G}_0}{\partial \hat{x}} \right) \right], \\
&= \frac{2^{\frac{1}{2}}(-1)^{m+n}}{(2\pi)2^{2(m+n)}m!n!} \frac{\partial \bar{G}_0}{\partial \hat{x}} + \frac{2^{\frac{1}{2}}(-1)^{m+n}(2n+1)}{(2\pi)2^{2n+m}n!} \left[ \frac{\partial \bar{G}_0}{\partial \hat{x}} \int_0^{t_2} S_1^{(m,n)} dt'_2 \right. \\
&\quad \left. - \left( \frac{\partial \bar{G}_0}{\partial \hat{y}} + t_2 \frac{\partial \bar{G}_0}{\partial \hat{x}} \right) \int_0^{t_2} S_2^{(m,n)} dt'_2 \right], \\
&= \frac{2^{\frac{1}{2}}(-1)^{m+n}}{(2\pi)2^{2(m+n)}m!n!} \frac{\partial \bar{G}_0}{\partial \hat{x}} + \frac{2^{\frac{1}{2}}(-1)^{m+n}(2n+1)}{(2\pi)2^{2n+m}n!} \left[ \frac{\partial \bar{G}_0}{\partial \hat{x}} \sum_{k=0}^{m-1} \frac{t_2^{2m-2k} \prod_{l=k}^{m-2} (2n+2m-1-2l)}{2^k k! (2m-2k)!} \right. \\
&\quad \left. - \left( \frac{\partial \bar{G}_0}{\partial \hat{y}} + t_2 \frac{\partial \bar{G}_0}{\partial \hat{x}} \right) \sum_{k=0}^m \frac{t_2^{2m-2k+1} \prod_{l=k}^{m-1} (2n+2m-1-2l)}{2^k k! (2m+1-2k)!} \right], \\
&= \frac{2^{\frac{1}{2}}(-1)^{m+n}}{(2\pi)2^{2n+m}n!} \frac{\partial \bar{G}_0}{\partial \hat{x}} \left[ \frac{1}{2^m m!} + \sum_{k=0}^{m-1} \frac{t_2^{2m-2k} \prod_{l=k}^{m-1} (2n+2m-1-2l)}{2^k k! (2m-2k)!} \right] \\
&\quad + \frac{2^{\frac{1}{2}}(-1)^{m+n}}{(2\pi)2^{2n+m}n!} \left( \frac{\partial \bar{G}_0}{\partial \hat{y}} + t_2 \frac{\partial \bar{G}_0}{\partial \hat{x}} \right) \sum_{k=0}^m \frac{t_2^{2m+1-2k} \prod_{l=k}^m (2n+2m-1-2l)}{2^k k! (2m-2k)!}, \\
&= \frac{2^{\frac{1}{2}}(-1)^{m+n}}{(2\pi)2^{2n+m}n!} \left[ S_1^{(m,n)} \frac{\partial \bar{G}_0}{\partial \hat{x}} - S_2^{(m,n)} \left( \frac{\partial \bar{G}_0}{\partial \hat{y}} + t_2 \frac{\partial \bar{G}_0}{\partial \hat{x}} \right) \right], \tag{A.55}
\end{aligned}$$

where the superscripts ‘*h*’ and ‘*p*’ denote the homogeneous and particular solutions, respectively.

At the next order, we have using (A.55)

$$\begin{aligned}
Db_{2m+2,2n+1}^{(1)} &= -(2n+2)b_{2m+1,2n+2}^{(1)}, \\
&= \frac{2^{\frac{1}{2}}(-1)^{m+n+1}(2n+2)}{(2\pi)2^{2n+m+2}(n+1)!} \left[ S_1^{(m,n+1)} \frac{\partial \bar{G}_0}{\partial \hat{x}} - S_2^{(m,n+1)} \left( \frac{\partial \bar{G}_0}{\partial \hat{y}} + t_2 \frac{\partial \bar{G}_0}{\partial \hat{x}} \right) \right],
\end{aligned}$$

with the initial condition

$$b_{2m+2,2n+1}^{(1)}(\hat{x}, \hat{y}, 0) = \frac{2^{\frac{1}{2}}(-1)^{m+n}}{(2\pi)2^{2(m+n+1)}(m+1)!n!} \delta(\hat{x})\delta'(\hat{y}).$$

Therefore

$$\begin{aligned} & b_{2m+2,2n+1}^{(1)}(\hat{x}, \hat{y}, t_2) \\ &= b_{2m+2,2n+1}^{(1)h} + b_{2m+2,2n+1}^{(1)p}, \\ &= \frac{2^{\frac{1}{2}}(-1)^{m+n+1}}{(2\pi)2^{2(m+n+1)}(m+1)!n!} \left( \frac{\partial \bar{G}_0}{\partial \hat{y}} + t_2 \frac{\partial \bar{G}_0}{\partial \hat{x}} \right) \\ &\quad + \frac{2^{\frac{1}{2}}(-1)^{m+n}(2n+2)}{(2\pi)2^{2n+m+2}(n+1)!} D^{-1} \left[ S_1^{(m,n+1)} \frac{\partial \bar{G}_0}{\partial \hat{x}} - S_2^{(m,n+1)} \left( \frac{\partial \bar{G}_0}{\partial \hat{y}} + t_2 \frac{\partial \bar{G}_0}{\partial \hat{x}} \right) \right], \\ &= \frac{2^{\frac{1}{2}}(-1)^{m+n+1}}{(2\pi)2^{2(m+n+1)}(m+1)!n!} \left( \frac{\partial \bar{G}_0}{\partial \hat{y}} + t_2 \frac{\partial \bar{G}_0}{\partial \hat{x}} \right) \\ &\quad + \frac{2^{\frac{1}{2}}(-1)^{m+n}(2n+2)}{(2\pi)2^{2n+m+2}(n+1)!} \left[ \frac{\partial \bar{G}_0}{\partial \hat{x}} \int_0^{t_2} S_1^{(m,n+1)} dt'_2 - \left( \frac{\partial \bar{G}_0}{\partial \hat{y}} + t_2 \frac{\partial \bar{G}_0}{\partial \hat{x}} \right) \int_0^{t_2} S_2^{(m,n+1)} dt'_2 \right], \\ &= \frac{2^{\frac{1}{2}}(-1)^{m+n+1}}{(2\pi)2^{2(m+n+1)}(m+1)!n!} \left( \frac{\partial \bar{G}_0}{\partial \hat{y}} + t_2 \frac{\partial \bar{G}_0}{\partial \hat{x}} \right) \\ &\quad + \frac{2^{\frac{1}{2}}(-1)^{m+n}}{(2\pi)2^{2n+m+1}n!} \left[ \frac{\partial \bar{G}_0}{\partial \hat{x}} \sum_{k=0}^m \frac{t_2^{2m+1-2k} \prod_{l=k}^{m-1} (2n+2m+1-2l)}{2^k k! (2m+1-2k)!} \right. \\ &\quad \quad \left. - \left( \frac{\partial \bar{G}_0}{\partial \hat{y}} + t_2 \frac{\partial \bar{G}_0}{\partial \hat{x}} \right) \sum_{k=0}^m \frac{t_2^{2m+2-2k} \prod_{l=k}^m (2n+2m+3-2l)}{2^k k! (2m+2-2k)!} \right], \\ &= \frac{2^{\frac{1}{2}}(-1)^{m+n}}{(2\pi)2^{2n+m+1}n!} \frac{\partial \bar{G}_0}{\partial \hat{x}} \sum_{k=0}^m \frac{t_2^{2m+1-2k} \prod_{l=k}^{m-1} (2n+2m+1-2l)}{2^k k! (2m+1-2k)!} \\ &\quad - \frac{2^{\frac{1}{2}}(-1)^{m+n}}{2^{2n+m+1}n!} \left( \frac{\partial \bar{G}_0}{\partial \hat{y}} + t_2 \frac{\partial \bar{G}_0}{\partial \hat{x}} \right) \left[ \frac{1}{2^{m+1}(m+1)!} + \sum_{k=0}^m \frac{t_2^{2m+2-2k} \prod_{l=k}^m (2n+2m+3-2l)}{2^k k! (2m+2-2k)!} \right], \\ &= \frac{2^{\frac{1}{2}}(-1)^{m+n+1}}{(2\pi)2^{2n+m+1}n!} \left[ S_2^{(m+1,n)} \left( \frac{\partial \bar{G}_0}{\partial \hat{y}} + t_2 \frac{\partial \bar{G}_0}{\partial \hat{x}} \right) - S_1^{(m+1,n)} \frac{\partial \bar{G}_0}{\partial \hat{x}} \right]. \tag{A.56} \end{aligned}$$

From (A.55) and (A.56), it follows that (A.53) and (A.54) hold for all  $m$  and  $n$  provided (A.53) is true for  $m = 0$  and arbitrary  $n$ . This can easily be verified by direct solution of the corresponding equation viz.  $Db_{0,2n+1}^{(1)} = 0$ , the initial condition being given by (2.65) with

$m = 0$ .

## A.5 Solution to the inhomogeneous Smoluchowski equation

### A.5.1 Green's function for the Smoluchowski equation

The Green's function for the equation<sup>2</sup>

$$\frac{\partial P}{\partial t} + y \frac{\partial P}{\partial x} = \frac{\partial^2 P}{\partial x^2} + \frac{\partial^2 P}{\partial y^2}, \quad (\text{A.57})$$

satisfying

$$G(x, y, 0|x', y', 0) = \delta(x)\delta(y),$$

$$G(x, y, t|x', y', 0) = 0 \quad \forall t < 0,$$

is given by [5]

$$G(x, y, t|0, 0, 0) = G_0(x, y, t) = \frac{1}{(2\pi) \left[4t^2(1 + \frac{t^2}{12})\right]^{\frac{1}{2}}} \exp\left[-\frac{x^2 + y^2(1 + \frac{t^2}{3}) - xy(t)}{4t(1 + \frac{t^2}{12})}\right], \quad (\text{A.58})$$

whence

$$\langle xx \rangle_{G_0} = 2t \left(1 + \frac{t^2}{3}\right),$$

$$\langle yy \rangle_{G_0} = 2t,$$

$$\langle xy \rangle_{G_0} = t^2.$$

---

<sup>2</sup>Here, the variables  $x$  and  $y$  have been rescaled by a factor of  $Pe^{1/2}$  to eliminate the parametric dependence.

The Green's function  $G(x, y, t|x', y', t')$  for the general case satisfies

$$G(x, y, t|x', y', t') = \delta(x - x')\delta(y - y'), \quad (\text{A.59})$$

$$G(x, y, t|x', y', t') = 0 \quad \forall t < t', \quad (\text{A.60})$$

To find  $G$ , one transforms to the variables  $s = t - t'$ ,  $\tilde{y} = y - y'$  and  $\tilde{x} = x - x' - y'(t - t')$

and uses

$$\frac{\partial}{\partial t} = \frac{\partial}{\partial s} - y' \frac{\partial}{\partial \tilde{x}}, \quad \frac{\partial}{\partial x} = \frac{\partial}{\partial \tilde{x}}, \quad \frac{\partial}{\partial y} = \frac{\partial}{\partial \tilde{y}},$$

so that equation (A.57) in the new variables becomes

$$\frac{\partial P}{\partial s} + \tilde{y} \frac{\partial P}{\partial \tilde{x}} = \frac{\partial^2 P}{\partial \tilde{x}^2} + \frac{\partial^2 P}{\partial \tilde{y}^2}.$$

Clearly,  $G_0(\tilde{x}, \tilde{y}, s)$  is a solution of the transformed equation with

$$G_0(\tilde{x}, \tilde{y}, 0) = \delta(\tilde{x})\delta(\tilde{y}),$$

$$G_0(\tilde{x}, \tilde{y}, s) = 0 \quad \forall s < 0,$$

these being the transformed initial conditions. Hence, the Green's function for the case where the Brownian particle is at  $(x', y')$  at  $t = t'$  is given by

$$G(x, y, t|x', y', t') = G_0(x - x' - y'(t - t'), y - y', t - t'). \quad (\text{A.61})$$

### A.5.2 A Green's function identity

In this section we give a formal proof for a Green's function identity which proves useful in deriving particular integrals for the inhomogeneous Smoluchowski equation. Equation (A.57)

can be written in the form

$$\frac{\partial u}{\partial t} = L_{SM}(x, y)u, \quad (\text{A.62})$$

where the operator  $L_{SM}$  is defined to be

$$L_{SM}(x, y) = -y \frac{\partial}{\partial x} + \left( \frac{\partial^2}{\partial x^2} + \frac{\partial^2}{\partial y^2} \right).$$

If  $u(x, y, 0) = \delta(x - x')\delta(y - y')$ , then the formal solution of the above equation is given by

$$u(x, y, t) = G_0(x - x' - y't, y - y', t) = e^{L_{SM}(x, y)t} \{\delta(x - x')\delta(y - y')\},$$

where the operator  $e^{At}$  is defined in the usual manner. Consider

$$\begin{aligned} & \int_{-\infty}^{\infty} \int_{-\infty}^{\infty} G_0(x - x' - y'(t - t'), y - y', t - t') G_0(x', y', t') dx' dy', \\ &= \int_{-\infty}^{\infty} \int_{-\infty}^{\infty} e^{L_{SM}(x, y)(t-t')} \{\delta(x - x')\delta(y - y')\} e^{L_{SM}(x', y')t'} \{\delta(x')\delta(y')\} dx' dy', \\ &= e^{L_{SM}(x, y)(t-t')} \int_{-\infty}^{\infty} \int_{-\infty}^{\infty} \delta(x - x')\delta(y - y') e^{L_{SM}(x', y')t'} \{\delta(x')\delta(y')\} dx' dy', \\ &= e^{L_{SM}(x, y)(t-t')} e^{L_{SM}(x, y)t'} \{\delta(x)\delta(y)\}, \\ &= e^{L_{SM}(x, y)t} \{\delta(x)\delta(y)\}, \\ &= G_0(x, y, t). \end{aligned}$$

which is the required identity. We now use the above identity to obtain the solution of the inhomogeneous Smoluchowski equation for two canonical cases.

1. When the forcing function is  $\partial G_0/\partial x$ , the particular integral is given by

$$\begin{aligned}
 I_x &= \int_0^t dt' \int_{-\infty}^{\infty} \int_{-\infty}^{\infty} G_0(x-x'-y'(t-t'), y-y', t-t') \frac{\partial}{\partial x'} G_0(x', y', t') dx' dy', \\
 &= - \int_0^t dt' \int_{-\infty}^{\infty} \int_{-\infty}^{\infty} G_0(x', y', t') \frac{\partial}{\partial x'} G_0(x-x'-y'(t-t'), y-y', t-t') dx' dy', \\
 &= \int_0^t dt' \frac{\partial}{\partial x} \int_{-\infty}^{\infty} \int_{-\infty}^{\infty} G_0(x', y', t') G_0(x-x'-y'(t-t'), y-y', t-t') dx' dy', \\
 &= \int_0^t dt' \frac{\partial}{\partial x} G_0(x, y, t), \\
 &= t \frac{\partial G_0}{\partial x}.
 \end{aligned}$$

2. When the forcing function is  $\partial G_0/\partial y$ ,

$$\begin{aligned}
 I_y &= \int_0^t dt' \int_{-\infty}^{\infty} \int_{-\infty}^{\infty} G_0(x-x'-y'(t-t'), y-y', t-t') \frac{\partial}{\partial y'} G_0(x', y', t') dx' dy', \\
 &= - \int_0^t dt' \int_{-\infty}^{\infty} \int_{-\infty}^{\infty} G_0(x', y', t') \frac{\partial}{\partial y'} G_0(x-x'-y'(t-t'), y-y', t-t') dx' dy', \\
 &= - \int_0^t dt' \int_{-\infty}^{\infty} \int_{-\infty}^{\infty} G_0(x', y', t') \left[ -(t-t') \frac{\partial}{\partial x} - \frac{\partial}{\partial y} \right] G_0(x-x'-y'(t-t'), y-y', t-t') dx' dy', \\
 &= \int_0^t dt' \left[ (t-t') \frac{\partial}{\partial x} + \frac{\partial}{\partial y} \right] \int_{-\infty}^{\infty} \int_{-\infty}^{\infty} G_0(x-x'-y'(t-t'), y-y', t-t') G_0(x', y', t') dx' dy', \\
 &= \int_0^t dt' \left[ (t-t') \frac{\partial}{\partial x} G_0(x, y, t) + \frac{\partial}{\partial y} G_0(x, y, t) \right], \\
 &= \frac{t^2}{2} \frac{\partial G_0}{\partial x} + t \frac{\partial G_0}{\partial y}.
 \end{aligned}$$

The solution for a general forcing function of the form  $\partial^{i+j} G_0/\partial x^i \partial y^j$  will proceed in an analogous manner.

## Appendix B

### Appendices for Chapter 3

#### B.1 The $O(St)$ Chapman-Enskog solution, $\bar{P}_M^{(1)}$ , for general $M$

Here we derive an expression for the general solution  $\bar{P}_M^{(1)}$  at  $O(St)$ , including only the non-flow contributions that generate the diffusive term in the Smoluchowski equation (3.18) at leading order. Using  $i = 1$  in (3.28), one obtains

$$\begin{aligned} \mathbf{L}_H^{(M)}(\bar{\mathbf{w}})(\bar{P}_M^{(1)})^{diff} &= \frac{1}{(PeSt)^{\frac{1}{2}}} \left[ \frac{1}{2} (m^{\frac{1}{2}})_{ij}^{-1} \bar{w}_j \bar{P}_M^{(0)} \frac{\partial}{\partial x_i} \{ \ln(\det m_{ab}) \} + \bar{w}_j (m^{\frac{1}{2}})_{ij}^{-1} \frac{\partial \bar{P}_M^{(0)}}{\partial x_i} \right] \\ &\quad - \frac{1}{(PeSt)^{\frac{1}{2}}} \{ (m^{\frac{1}{2}})_{lk}^{-1} (m^{\frac{1}{2}})_{mj}^{-1} + (m^{\frac{1}{2}})_{lj}^{-1} (m^{\frac{1}{2}})_{mk}^{-1} \} \frac{\partial m_{km}^{\frac{1}{2}}}{\partial x_l} \bar{w}_j \bar{P}_M^{(0)} \\ &\quad + \frac{1}{(PeSt)^{\frac{1}{2}}} (m^{\frac{1}{2}})_{kj}^{-1} (m^{\frac{1}{2}})_{lb}^{-1} \left( \frac{\partial m_{al}^{\frac{1}{2}}}{\partial x_k} - \frac{\partial m_{ak}^{\frac{1}{2}}}{\partial x_l} \right) \frac{\partial}{\partial \bar{w}_j} (\bar{w}_a \bar{w}_b \bar{P}_M^{(0)}), \quad (\text{B.1}) \end{aligned}$$

where we have not included  $\partial_M^{(0)}$  in (B.1), since it is defined solely in terms of flow terms in (3.30); the superscript ‘*diff*’ has been used for the aforementioned reason. Using  $P_M^{(0)} = a_{i_1 i_2 \dots i_M}^M \{ \bar{H}_M \}_{i_1 i_2 \dots i_M}$ , (3.32) reduces to

$$\begin{aligned} \mathbf{L}_H^{(M)}(\bar{\mathbf{w}})(\bar{P}_M^{(1)})^{diff} &= \frac{1}{(PeSt)^{\frac{1}{2}}} \left[ \{ c_{M+1}^{(1)} \}_{i_1 i_2 \dots i_{M+1}} \{ \bar{H}_{M+1} \}_{i_1 i_2 \dots i_{M+1}} + \{ c_{M-1}^{(1)} \}_{i_1 i_2 \dots i_{M-1}} \right. \\ &\quad \left. \{ \bar{H}_{M-1} \}_{i_1 i_2 \dots i_{M-1}} + \{ c_{M+3}^{(1)} \}_{i_1 i_2 \dots i_{M+3}} \{ \bar{H}_{M+3} \}_{i_1 i_2 \dots i_{M+3}} \right], \quad (\text{B.2}) \end{aligned}$$

where

$$\begin{aligned}
\{c_{M+1}^{(1)}\}_{i_1 i_2 \dots i_{M+1}} &= \frac{1}{2^{\frac{1}{2}}} \left\{ (m^{\frac{1}{2}})_{ii_{M+1}}^{-1} \frac{\partial}{\partial x_i} (a_{i_1 i_2 \dots i_M}^M) - a_{i_1 i_2 \dots i_M}^M \{ (m^{\frac{1}{2}})_{lk}^{-1} (m^{\frac{1}{2}})_{mi_{M+1}}^{-1} \right. \\
&\quad \left. + (m^{\frac{1}{2}})_{li_{M+1}}^{-1} (m^{\frac{1}{2}})_{mk}^{-1} \frac{\partial m_{km}^{\frac{1}{2}}}{\partial x_l} \right\} + \frac{1}{2^{\frac{3}{2}}} (m^{\frac{1}{2}})_{ii_{M+1}}^{-1} \frac{\partial}{\partial x_i} \{ \ln(\det m_{ab}) \} a_{i_1 i_2 \dots i_M}^M \\
&\quad - \frac{M}{2^{\frac{1}{2}}} (m^{\frac{1}{2}})_{ki_{M+1}}^{-1} (m^{\frac{1}{2}})_{li_M}^{-1} \left( \frac{\partial m_{al}^{\frac{1}{2}}}{\partial x_k} - \frac{\partial m_{ak}^{\frac{1}{2}}}{\partial x_l} \right) a_{ai_1 i_2 \dots i_{M-1}}^M \\
&\quad - \frac{1}{2^{\frac{1}{2}}} (m^{\frac{1}{2}})_{ki_{M+1}}^{-1} (m^{\frac{1}{2}})_{la}^{-1} \left( \frac{\partial m_{al}^{\frac{1}{2}}}{\partial x_k} - \frac{\partial m_{ak}^{\frac{1}{2}}}{\partial x_l} \right) a_{i_1 i_2 \dots i_M}^M \\
&\quad - \frac{M}{2^{\frac{1}{2}}} (m^{\frac{1}{2}})_{ki_{M+1}}^{-1} (m^{\frac{1}{2}})_{lb}^{-1} \left( \frac{\partial m_{i_M l}^{\frac{1}{2}}}{\partial x_k} - \frac{\partial m_{i_M k}^{\frac{1}{2}}}{\partial x_l} \right) a_{bi_1 i_2 \dots i_{M-1}}^M, \tag{B.3}
\end{aligned}$$

$$\begin{aligned}
\{c_{M-1}^{(1)}\}_{i_1 i_2 \dots i_{M-1}} &= 2^{\frac{1}{2}} M \left\{ (m^{\frac{1}{2}})_{ia}^{-1} \frac{\partial}{\partial x_i} (a_{ai_1 i_2 \dots i_{M-1}}^M) - a_{ai_1 i_2 \dots i_{M-1}}^M \{ (m^{\frac{1}{2}})_{lk}^{-1} (m^{\frac{1}{2}})_{ma}^{-1} + (m^{\frac{1}{2}})_{la}^{-1} \right. \\
&\quad \left. (m^{\frac{1}{2}})_{mk}^{-1} \frac{\partial m_{lm}^{\frac{1}{2}}}{\partial x_l} \right\} - 2^{\frac{1}{2}} M (M-1) (m^{\frac{1}{2}})_{ki_{M-1}}^{-1} (m^{\frac{1}{2}})_{lb}^{-1} \left( \frac{\partial m_{al}^{\frac{1}{2}}}{\partial x_k} - \frac{\partial m_{ak}^{\frac{1}{2}}}{\partial x_l} \right) a_{abi_1 i_2 \dots i_{M-2}}^M, \tag{B.4}
\end{aligned}$$

$$\{c_{M+3}^{(1)}\}_{i_1 i_2 \dots i_{M+3}} = -\frac{1}{2^{\frac{3}{2}}} a_{i_1 i_2 \dots i_M}^M (m^{\frac{1}{2}})_{ki_{M+3}}^{-1} (m^{\frac{1}{2}})_{li_{M+2}}^{-1} \left( \frac{\partial m_{i_{M+1} l}^{\frac{1}{2}}}{\partial x_k} - \frac{\partial m_{i_{M+1} k}^{\frac{1}{2}}}{\partial x_l} \right). \tag{B.5}$$

This then suggests a solution of the form

$$\begin{aligned}
(\bar{P}_M^{(1)})^{diff} &= \{b_{M, M+1}^{(1)}\}_{i_1 i_2 \dots i_{M+1}} \{\bar{H}_{M+1}\}_{i_1 i_2 \dots i_{M+1}} + \{b_{M, M-1}^{(1)}\}_{i_1 i_2 \dots i_{M-1}} \{\bar{H}_{M-1}\}_{i_1 i_2 \dots i_{M-1}} \\
&\quad + \{b_{M, M+3}^{(1)}\}_{i_1 i_2 \dots i_{M+3}} \{\bar{H}_{M+3}\}_{i_1 i_2 \dots i_{M+3}}, \tag{B.6}
\end{aligned}$$

where the  $\mathbf{b}_{M, M_1}^{(1)}$ 's can again be chosen as symmetric in their indices. Substituting this, we

obtain the following linear relations for the coefficients:

$$\begin{aligned}
R_{jk}^{FU} (m^{\frac{1}{2}})_{ki}^{-1} \left\{ \{b_{M, M+1}^{(1)}\}_{i_1 i_2 \dots i_M} (m^{\frac{1}{2}})_{j i_{M+1}}^{-1} \right\}_s &= -\{c_{M+1}^{(1)}\}_{i_1 i_2 \dots i_{M+1}}, \\
R_{jk}^{FU} (m^{\frac{1}{2}})_{ki}^{-1} \left\{ \{b_{M, M-1}^{(1)}\}_{i_1 i_2 \dots i_{M-2}} (m^{\frac{1}{2}})_{j i_{M-1}}^{-1} \right\}_s &= \{c_{M-1}^{(1)}\}_{i_1 i_2 \dots i_{M-1}}, \tag{B.7}
\end{aligned}$$

$$R_{jk}^{FU} (m^{\frac{1}{2}})_{ki}^{-1} \left\{ \{b_{M,M+3}^{(1)}\}_{i_1 i_2 \dots i_{M+2} i} (m^{\frac{1}{2}})_{j i_{M+3}}^{-1} \right\}_s = -\frac{1}{3} \{c_{M+1}^{(1)}\}_{i_1 i_2 \dots i_{M+3}},$$

which determines  $(\bar{P}_M^{(1)})^{diff}$ .

## Appendix C

### Appendices for Chapter 4

#### C.1 The $O(1)$ and $O(St)$ velocity fields

Here we derive the explicit forms of the terms involving the  $O(1)$  and  $O(St)$  hydrodynamic velocity fields, in the Smoluchowski equation (4.7). The former is given by

$$\begin{aligned} & \nabla_{\mathbf{x}} \cdot (\mathbf{R}_{FU}^{-1} \cdot \mathbf{F}^o g) \\ &= (\nabla_{\mathbf{x}}, \mathbf{0}) \cdot \left[ \left( \begin{array}{cc} \mathbf{R}_{FU} & \mathbf{R}_{F\Omega} \\ \mathbf{R}_{LU} & \mathbf{R}_{L\Omega} \end{array} \right)^{-1} \cdot \left\{ \left( \begin{array}{cc} \mathbf{R}_{FU} & \mathbf{R}_{F\Omega} \\ \mathbf{R}_{LU} & \mathbf{R}_{L\Omega} \end{array} \right) \cdot \begin{pmatrix} \mathbf{U}^\infty \\ \boldsymbol{\Omega}^\infty \end{pmatrix} + \begin{pmatrix} \mathbf{R}_{FE} \\ \mathbf{R}_{LE} \end{pmatrix} : \mathbf{E}^\infty \right\} g \right], \\ &= \nabla_{\mathbf{x}} \cdot [\{\mathbf{U}^\infty + (\mathbf{M}_{UF} \cdot \mathbf{R}_{FE} + \mathbf{M}_{UL} \cdot \mathbf{R}_{LE}) : \mathbf{E}^\infty\} g], \end{aligned}$$

where we have used the expression for  $\mathbf{F}^o$  in terms of the resistance tensors (Brady and Bossis 1988), and the fact that orientation constitutes a degenerate degree of freedom for spherical particles. When  $\mathbf{x} \equiv (\mathbf{x}_1, \mathbf{x}_2)$ , this takes the form

$$\begin{aligned} & \nabla_{\mathbf{x}_1} \cdot [\{\mathbf{U}_1^\infty + (\mathbf{M}_{UF}^{11} \cdot (\mathbf{R}_{FE}^{11} + \mathbf{R}_{FE}^{12}) + \mathbf{M}_{UF}^{12} \cdot (\mathbf{R}_{FE}^{21} + \mathbf{R}_{FE}^{22}) + \mathbf{M}_{UL}^{11} \cdot (\mathbf{R}_{LE}^{11} + \mathbf{R}_{LE}^{12}) + \mathbf{M}_{UL}^{12} \cdot (\mathbf{R}_{LE}^{21} \\ & + \mathbf{R}_{LE}^{22})) : \mathbf{E}^\infty\} g] + \nabla_{\mathbf{x}_2} \cdot [\{\mathbf{U}_2^\infty + (\mathbf{M}_{UF}^{21} \cdot (\mathbf{R}_{FE}^{11} + \mathbf{R}_{FE}^{12}) + \mathbf{M}_{UF}^{22} \cdot (\mathbf{R}_{FE}^{21} + \mathbf{R}_{FE}^{22}) + \mathbf{M}_{UL}^{21} \cdot (\mathbf{R}_{LE}^{11} \\ & + \mathbf{R}_{LE}^{12}) + \mathbf{M}_{UL}^{22} \cdot (\mathbf{R}_{LE}^{21} + \mathbf{R}_{LE}^{22})) : \mathbf{E}^\infty\} g]. \end{aligned}$$

In a statistically homogeneous suspension, the various mobility and resistance tensors and the pair distribution function are only functions of  $\mathbf{r}$ , and we therefore change to relative

coordinates using  $\mathbf{r} = \mathbf{x}_2 - \mathbf{x}_1$ ,  $\nabla_{\mathbf{x}_1} = -\nabla_{\mathbf{r}}$ ,  $\nabla_{\mathbf{x}_2} = \nabla_{\mathbf{r}}$ . In addition, for equal sized spherical particles

$$\begin{aligned}
\mathbf{M}_{UF}^{11} &= \mathbf{M}_{UF}^{22}, & \mathbf{M}_{UF}^{12} &= \mathbf{M}_{UF}^{21}, \\
\mathbf{M}_{UL}^{11} &= -\mathbf{M}_{UL}^{22}, & \mathbf{M}_{UL}^{12} &= -\mathbf{M}_{UL}^{21}, \\
\mathbf{R}_{FE}^{11} &= -\mathbf{R}_{FE}^{22}, & \mathbf{R}_{FE}^{12} &= -\mathbf{R}_{FE}^{21}, \\
\mathbf{R}_{LE}^{11} &= \mathbf{R}_{LE}^{22}, & \mathbf{R}_{LE}^{12} &= \mathbf{R}_{LE}^{21}.
\end{aligned} \tag{C.1}$$

Therefore,

$$\nabla_{\mathbf{x}} \cdot (\mathbf{R}_{FU}^{-1} \cdot \mathbf{F}^o g) = \nabla_{\mathbf{r}} \cdot \{[(\mathbf{U}_2^\infty - \mathbf{U}_1^\infty) - 2(\mathbf{M}_{UF}^{11} - \mathbf{M}_{UF}^{12}) \cdot (\mathbf{R}_{FE}^{11} + \mathbf{R}_{FE}^{12}) : \mathbf{E}^\infty] \tag{C.2}$$

$$-2(\mathbf{M}_{UL}^{11} + \mathbf{M}_{UL}^{12}) \cdot (\mathbf{R}_{LE}^{11} + \mathbf{R}_{LE}^{12}) : \mathbf{E}^\infty] g\}. \tag{C.3}$$

We now examine the term involving the  $O(St)$  velocity field viz.

$\nabla_{\mathbf{x}} \cdot [\mathbf{R}_{FU}^{-1} \cdot \{(\mathbf{R}_{FU}^{-1} \cdot \mathbf{F}^o) \cdot \nabla_{\mathbf{x}}(\mathbf{R}_{FU}^{-1} \cdot \mathbf{F}^o) \cdot \mathbf{m}\} g]$ . First consider

$$\begin{aligned}
& \nabla_{\mathbf{x}}(\mathbf{R}_{FU}^{-1} \cdot \mathbf{F}^o) \\
&= \left[ \begin{array}{c} \nabla_{\mathbf{x}}(\mathbf{U}^\infty + \mathbf{M}_{UF} \cdot \mathbf{R}_{FE} : \mathbf{E}^\infty + \mathbf{M}_{UL} \cdot \mathbf{R}_{LE} : \mathbf{E}^\infty) \nabla_{\mathbf{x}}(\boldsymbol{\Omega}^\infty + \mathbf{M}_{\Omega F} \cdot \mathbf{R}_{FE} : \mathbf{E}^\infty + \mathbf{M}_{\Omega L} \cdot \mathbf{R}_{LE} : \mathbf{E}^\infty) \\ \mathbf{0} \qquad \qquad \qquad \mathbf{0} \end{array} \right]. \\
&\Rightarrow \nabla_{\mathbf{x}}(\mathbf{R}_{FU}^{-1} \cdot \mathbf{F}^o) \cdot \mathbf{m} \\
&= \left[ \begin{array}{c} \nabla_{\mathbf{x}}(\mathbf{U}^\infty + \mathbf{M}_{UF} \cdot \mathbf{R}_{FE} : \mathbf{E}^\infty + \mathbf{M}_{UL} \cdot \mathbf{R}_{LE} : \mathbf{E}^\infty) \frac{2}{5} \nabla_{\mathbf{x}}(\boldsymbol{\Omega}^\infty + \mathbf{M}_{\Omega F} \cdot \mathbf{R}_{FE} : \mathbf{E}^\infty + \mathbf{M}_{\Omega L} \cdot \mathbf{R}_{LE} : \mathbf{E}^\infty) \\ \mathbf{0} \qquad \qquad \qquad \mathbf{0} \end{array} \right],
\end{aligned}$$

where we have used the inertia tensor for solid spherical particles (the moment of inertia of a

solid sphere is  $2/5ma^2$ ,  $m$  being its mass and  $a$  its radius).

$$\begin{aligned}
&\Rightarrow (\mathbf{R}_{FU}^{-1} \cdot \mathbf{F}^o) \cdot \nabla_{\mathbf{x}} (\mathbf{R}_{FU}^{-1} \cdot \mathbf{F}^o) \cdot \mathbf{m} \\
&= [(\mathbf{U}^\infty + \mathbf{M}_{UF} \cdot \mathbf{R}_{FE} : \mathbf{E}^\infty + \mathbf{M}_{UL} \cdot \mathbf{R}_{LE} : \mathbf{E}^\infty) \cdot \nabla_{\mathbf{x}} (\mathbf{U}^\infty + \mathbf{M}_{UF} \cdot \mathbf{R}_{FE} : \mathbf{E}^\infty + \mathbf{M}_{UL} \cdot \mathbf{R}_{LE} : \mathbf{E}^\infty), \\
&\quad \frac{2}{5} (\mathbf{U}^\infty + \mathbf{M}_{UF} \cdot \mathbf{R}_{FE} : \mathbf{E}^\infty + \mathbf{M}_{UL} \cdot \mathbf{R}_{LE} : \mathbf{E}^\infty) \cdot \nabla_{\mathbf{x}} (\boldsymbol{\Omega}^\infty + \mathbf{M}_{\Omega F} \cdot \mathbf{R}_{FE} : \mathbf{E}^\infty + \mathbf{M}_{\Omega L} \cdot \mathbf{R}_{LE} : \mathbf{E}^\infty)]. \\
&\Rightarrow \mathbf{R}_{FU}^{-1} \cdot \{ (\mathbf{R}_{FU}^{-1} \cdot \mathbf{F}^o) \cdot \nabla_{\mathbf{x}} (\mathbf{R}_{FU}^{-1} \cdot \mathbf{F}^o) \cdot \mathbf{m} \} \\
&= \left[ \begin{aligned} &\mathbf{M}_{UF} \cdot \{ (\mathbf{U}^\infty + (\mathbf{M}_{UF} \cdot \mathbf{R}_{FE} + \mathbf{M}_{UL} \cdot \mathbf{R}_{LE}) : \mathbf{E}^\infty) \cdot \nabla_{\mathbf{x}} (\mathbf{U}^\infty + (\mathbf{M}_{UF} \cdot \mathbf{R}_{FE} + \mathbf{M}_{UL} \cdot \mathbf{R}_{LE}) : \mathbf{E}^\infty) \} + \\ &\frac{2}{5} \mathbf{M}_{UL} \cdot \{ (\mathbf{U}^\infty + (\mathbf{M}_{UF} \cdot \mathbf{R}_{FE} + \mathbf{M}_{UL} \cdot \mathbf{R}_{LE}) : \mathbf{E}^\infty) \cdot \nabla_{\mathbf{x}} (\boldsymbol{\Omega}^\infty + (\mathbf{M}_{\Omega F} \cdot \mathbf{R}_{FE} + \mathbf{M}_{\Omega L} \cdot \mathbf{R}_{LE}) : \mathbf{E}^\infty) \} \\ &\mathbf{M}_{\Omega F} \cdot \{ (\mathbf{U}^\infty + (\mathbf{M}_{UF} \cdot \mathbf{R}_{FE} + \mathbf{M}_{UL} \cdot \mathbf{R}_{LE}) : \mathbf{E}^\infty) \cdot \nabla_{\mathbf{x}} (\mathbf{U}^\infty + (\mathbf{M}_{UF} \cdot \mathbf{R}_{FE} + \mathbf{M}_{UL} \cdot \mathbf{R}_{LE}) : \mathbf{E}^\infty) \} + \\ &\frac{2}{5} \mathbf{M}_{\Omega L} \cdot \{ (\mathbf{U}^\infty + (\mathbf{M}_{UF} \cdot \mathbf{R}_{FE} + \mathbf{M}_{UL} \cdot \mathbf{R}_{LE}) : \mathbf{E}^\infty) \cdot \nabla_{\mathbf{x}} (\boldsymbol{\Omega}^\infty + (\mathbf{M}_{\Omega F} \cdot \mathbf{R}_{FE} + \mathbf{M}_{\Omega L} \cdot \mathbf{R}_{LE}) : \mathbf{E}^\infty) \} \end{aligned} \right].
\end{aligned}$$

Finally,

$$\begin{aligned}
&\nabla_{\mathbf{x}} \cdot \mathbf{R}_{FU}^{-1} \cdot \{ (\mathbf{R}_{FU}^{-1} \cdot \mathbf{F}^o) \cdot \nabla_{\mathbf{x}} (\mathbf{R}_{FU}^{-1} \cdot \mathbf{F}^o) \cdot \mathbf{m} \} g \\
&= \nabla_{\mathbf{x}} \cdot g [\mathbf{M}_{UF} \cdot \{ (\mathbf{U}^\infty + (\mathbf{M}_{UF} \cdot \mathbf{R}_{FE} + \mathbf{M}_{UL} \cdot \mathbf{R}_{LE}) : \mathbf{E}^\infty) \cdot \nabla_{\mathbf{x}} (\mathbf{U}^\infty + (\mathbf{M}_{UF} \cdot \mathbf{R}_{FE} \\
&\quad + \mathbf{M}_{UL} \cdot \mathbf{R}_{LE}) : \mathbf{E}^\infty) \} + \frac{2}{5} \mathbf{M}_{UL} \cdot \{ (\mathbf{U}^\infty + (\mathbf{M}_{UF} \cdot \mathbf{R}_{FE} + \mathbf{M}_{UL} \cdot \mathbf{R}_{LE}) : \mathbf{E}^\infty) \cdot \\
&\quad \nabla_{\mathbf{x}} (\boldsymbol{\Omega}^\infty + (\mathbf{M}_{\Omega F} \cdot \mathbf{R}_{FE} + \mathbf{M}_{\Omega L} \cdot \mathbf{R}_{LE}) : \mathbf{E}^\infty) \}].
\end{aligned}$$

In relative coordinates for equal sized spheres, using the symmetry properties of the resistance

tensors given in (C.1), this becomes

$$\begin{aligned}
& \nabla_{\mathbf{r}} \cdot [(\mathbf{M}_{UF}^{11} - \mathbf{M}_{UF}^{12}) \cdot \{(\mathbf{U}_2^\infty - \mathbf{U}_1^\infty) - 2(\mathbf{M}_{UF}^{11} - \mathbf{M}_{UF}^{12}) \cdot (\mathbf{R}_{FE}^{11} + \mathbf{R}_{FE}^{12}) : \mathbf{E}^\infty - 2(\mathbf{M}_{UL}^{11} \\
& \quad + \mathbf{M}_{UL}^{12}) \cdot (\mathbf{R}_{LE}^{11} + \mathbf{R}_{LE}^{12}) : \mathbf{E}^\infty\} \cdot \nabla_{\mathbf{r}} \{(\mathbf{U}_2^\infty - \mathbf{U}_1^\infty) - 2(\mathbf{M}_{UF}^{11} - \mathbf{M}_{UF}^{12}) \cdot (\mathbf{R}_{FE}^{11} + \mathbf{R}_{FE}^{12}) : \mathbf{E}^\infty \\
& \quad - 2(\mathbf{M}_{UL}^{11} + \mathbf{M}_{UL}^{12}) \cdot (\mathbf{R}_{LE}^{11} + \mathbf{R}_{LE}^{12}) : \mathbf{E}^\infty\}] g \\
& - \frac{2}{5} \nabla_{\mathbf{r}} \cdot [(\mathbf{M}_{UL}^{11} + \mathbf{M}_{UL}^{12}) \cdot \{(\mathbf{U}_2^\infty - \mathbf{U}_1^\infty) - 2(\mathbf{M}_{UF}^{11} - \mathbf{M}_{UF}^{12}) \cdot (\mathbf{R}_{FE}^{11} + \mathbf{R}_{FE}^{12}) : \mathbf{E}^\infty - 2(\mathbf{M}_{UL}^{11} \\
& \quad + \mathbf{M}_{UL}^{12}) \cdot (\mathbf{R}_{LE}^{11} + \mathbf{R}_{LE}^{12}) : \mathbf{E}^\infty\} \cdot \nabla_{\mathbf{r}} \{2(\mathbf{M}_{\Omega F}^{11} - \mathbf{M}_{\Omega F}^{12}) \cdot (\mathbf{R}_{FE}^{11} + \mathbf{R}_{FE}^{12}) : \mathbf{E}^\infty + 2(\mathbf{M}_{\Omega L}^{11} \\
& \quad + \mathbf{M}_{\Omega L}^{12}) \cdot (\mathbf{R}_{LE}^{11} + \mathbf{R}_{LE}^{12}) : \mathbf{E}^\infty\}] g, \tag{C.4}
\end{aligned}$$

where we have used that the ambient angular velocity  $\boldsymbol{\Omega}^\infty$  is a constant in simple shear.

Using the explicit expressions for the resistance and mobility tensors in (C.4), we get

$$\begin{aligned}
V_i^{(1)} &= (E_{jk}^\infty r_j r_k)^2 r_i \left[ (G - H) \left\{ \frac{(A - B)^2}{r^4} - \frac{(1 - A)}{r^3} \frac{dA}{dr} \right\} + H \left\{ \frac{(A - 3B + 2)(A - B)}{r^4} \right. \right. \\
& \quad \left. \left. - \frac{(1 - A)}{r^3} \left( \frac{dA}{dr} - \frac{dB}{dr} \right) \right\} \right] + Hr_j [\Gamma_{il}^\infty \Gamma_{lj}^\infty - B \Gamma_{il}^\infty E_{lj}^\infty - B E_{il}^\infty \Gamma_{lj}^\infty + B^2 E_{il}^\infty E_{lj}^\infty] \\
& \quad + \frac{r_i r_j r_k}{r^2} [(G - H) \{ \Gamma_{jl}^\infty \Gamma_{lk}^\infty - B \Gamma_{jl}^\infty E_{lk}^\infty + (B - 2A) E_{jl}^\infty \Gamma_{lk}^\infty - B(B - 2A) E_{jl}^\infty E_{lk}^\infty \} \\
& \quad + H \{ 2B(A - B) E_{jl}^\infty E_{lk}^\infty - 2(A - B) E_{jl}^\infty \Gamma_{lk}^\infty \}] + Hr_l r_j r_k \left[ \left\{ \frac{2B(A - B)}{r^2} \right. \right. \\
& \quad \left. \left. - \frac{(1 - A)}{r} \frac{dB}{dr} \right\} E_{il}^\infty E_{jk}^\infty - \frac{2(A - B)}{r^2} \Gamma_{il}^\infty E_{jk}^\infty \right], \tag{C.5}
\end{aligned}$$

$$\begin{aligned}
\Rightarrow V_r^{(1)} &= Gr \left[ \frac{(E_{jk}^\infty r_j r_k)^2}{r^4} \left\{ (A - B)^2 - r(1 - A) \frac{dA}{dr} \right\} + \Gamma_{ik}^\infty \Gamma_{kj}^\infty \frac{r_i r_j}{r^2} + (B - 2A) E_{ik}^\infty \Gamma_{kj}^\infty \frac{r_i r_j}{r^2} \right. \\
& \quad \left. - B \Gamma_{ik}^\infty E_{kj}^\infty \frac{r_i r_j}{r^2} - B(B - 2A) E_{ik}^\infty E_{kj}^\infty \frac{r_i r_j}{r^2} \right], \tag{C.6}
\end{aligned}$$

$$\begin{aligned}
\lim_{r \rightarrow 2} V_r^{(1)} &= 4(r - 2) [0.3528(E_{jk}^\infty n_j n_k)^2 + n_i n_j \{ \Gamma_{ik}^\infty \Gamma_{kj}^\infty - 1.594 E_{ik}^\infty \Gamma_{kj}^\infty - 0.406 \Gamma_{ik}^\infty E_{kj}^\infty \\
& \quad - 0.6472 E_{ik}^\infty E_{kj}^\infty \}]. \tag{C.7}
\end{aligned}$$

## C.2 $O(St)$ solution in the outer layer O1

The expression for the  $O(St)$  solution as given in section 4.4.1.1 is

$$r\phi_1^- = - \int_r^\infty \exp \left[ - \int_{r'}^r \left\{ \frac{\sin^2 \phi_0'' - \frac{B''}{2}}{r'' \sin^2 \phi_0'' \cos^2 \phi_0'' (1 - A'')} - \frac{1}{r''} \right\} dr'' \right] \left\{ \frac{f_1(r', \phi_0')}{(1 - A') \sin \phi_0' \cos \phi_0'} \right. \\ \left. + \frac{\{(1 - B') \sin^2 \phi_0' + \frac{B'}{2}\} f_2(r', \phi_0')}{r'(1 - A')^2 \sin^2 \phi_0' \cos^2 \phi_0'} \right\} dr'.$$

Using the leading order equation in layer O1 viz. (4.27), we obtain

$$\begin{aligned} & \exp \left[ - \int_{r'}^r \left\{ \frac{\sin^2 \phi_0'' - \frac{B''}{2}}{r'' \sin^2 \phi_0'' \cos^2 \phi_0'' (1 - A'')} - \frac{1}{r''} \right\} dr'' \right] \\ &= \exp \left[ - \int_{r'}^r dr'' \frac{d\phi_0'' \sin \phi_0''}{dr'' \cos \phi_0''} \right] \exp \left[ - \int_{r'}^r \left\{ \frac{(1 - B'') \sin^2 \phi_0'' - \frac{B''}{2}}{r'' \sin^2 \phi_0'' (1 - A'')} - \frac{1}{r''} \right\} dr'' \right], \\ &= \exp \left[ \int_{r'}^r d \ln(\cos \phi_0') \right] \exp \left[ - \int_{r'}^r \left\{ \frac{(1 - B'') \sin^2 \phi_0'' - \frac{B''}{2}}{r'' \sin^2 \phi_0'' (1 - A'')} - \frac{1}{r''} \right\} dr'' \right], \\ &= \frac{\cos \phi_0'}{\cos \phi_0} \exp \left[ - \int_{r'}^r \left\{ \frac{(1 - B'') \sin^2 \phi_0'' - \frac{B''}{2}}{r'' \sin^2 \phi_0'' (1 - A'')} - \frac{1}{r''} \right\} dr'' \right]. \end{aligned} \quad (C.8)$$

This can be further simplified by first noting that

$$\begin{aligned} \frac{d(r \sin \phi_0)}{r \sin \phi_0} &= \frac{dr}{r \sin \phi_0} \left[ \frac{d\phi_0}{dr} (r \cos \phi_0) + \sin \phi_0 \right], \\ &= dr \left[ -\frac{1}{r} \frac{(A - B)}{(1 - A)} - \frac{B}{2r \sin^2 \phi_0 (1 - A)} \right], \\ \Rightarrow \frac{B dr}{2r \sin^2 \phi_0 (1 - A)} &= -\frac{dr}{r} \frac{(A - B)}{(1 - A)} - \frac{d(r \sin \phi_0)}{r \sin \phi_0}. \end{aligned} \quad (C.9)$$

Therefore, one can write

$$\begin{aligned} & \exp\left[-\int_{r'}^r \left\{ \frac{(1-B'') \sin^2 \phi_0'' - \frac{B''}{2}}{r'' \sin^2 \phi_0'' (1-A'')} - \frac{1}{r''} \right\} dr''\right] \\ &= \exp\left[\int_{r'}^r \left\{ \frac{B''}{2 r'' \sin^2 \phi_0'' (1-A'')} \right\} dr''\right] \exp\left[-\int_{r'}^r \frac{(A''-B'')}{(1-A'')r''} dr''\right], \end{aligned}$$

and using (C.9), this becomes

$$\begin{aligned} & \exp\left[-\int_{r'}^r \left\{ \frac{(1-B'') \sin^2 \phi_0'' - \frac{B''}{2}}{r'' \sin^2 \phi_0'' (1-A'')} - \frac{1}{r''} \right\} dr''\right] \\ &= \exp\left[-\int_{r'}^r \frac{d(r'' \sin \phi_0'')}{r'' \sin \phi_0''}\right] \exp\left[-\int_{r'}^r \frac{2(A''-B'')}{(1-A'')r''} dr''\right], \\ &= \frac{r' \sin \phi_0'}{r \sin \phi_0} \exp\left[-\int_{r'}^r \frac{2(A''-B'')}{(1-A'')r''} dr''\right], \end{aligned} \tag{C.10}$$

whence

$$\exp\left[-\int_{r'}^r \left\{ \frac{\sin^2 \phi_0'' - \frac{B''}{2}}{r'' \sin^2 \phi_0'' \cos^2 \phi_0'' (1-A'')} - \frac{1}{r''} \right\} dr''\right] = \frac{r' \sin \phi_0' \cos \phi_0'}{r \sin \phi_0 \cos \phi_0} \exp\left[-\int_{r'}^r \frac{2(A''-B'')}{(1-A'')r''} dr''\right]. \tag{C.11}$$

Substituting (C.11) in (4.32), the solution satisfying the upstream boundary condition is finally given by

$$\begin{aligned} r\phi_1^- = & -\frac{1}{r \cos \phi_0 \sin \phi_0} \int_r^\infty \exp\left[-\int_{r'}^r \frac{2(A''-B'')}{(1-A'')r''} dr''\right] \left\{ \frac{r' f_1(r', \phi_0')}{(1-A')} \right. \\ & \left. + \frac{\{(1-B') \sin^2 \phi_0' + \frac{B'}{2}\} f_2(r', \phi_0')}{(1-A')^2 \sin \phi_0' \cos \phi_0'} \right\} dr', \end{aligned}$$

which is the same as (4.34) in section 4.4.1.1.

### C.3 Non-uniform nature of the $O(St)$ corrections for zero-Stokes closed trajectories

Since the entire family of in-plane closed trajectories intersecting the  $y$  axis in the interval  $(-\infty, -2)$  is squeezed into a very narrow interval at  $\phi = \pi/2$ , one expects a tiny change in the radial distance at  $\phi = \pi/2$  to have a large effect on the subsequent point of intersection with the  $y$ -axis. In particular, for  $\phi \rightarrow 0$  and for sufficiently large radial distances, the finite Stokes trajectory may deviate by a large amount from a zero-Stokes trajectory having the same point of intersection at  $\phi = \pi/2$ . This in turn would imply that the  $O(St)$  inertial corrections do not remain uniformly small for such a perturbative formulation. This non-uniformity on account of the cumulative effect of inertial corrections is explicitly shown for the spiralling trajectories in what follows.

We perturb the inertial trajectory about a zero-Stokes closed orbit whose points of intersection the  $y$  and  $z$  axes are  $(\pm R_2, 0)$  and  $(0, \pm R_1)$  respectively. The inertial trajectory is assumed to pass through  $(0, R_1)$ , which therefore serves as the boundary condition in the inner layer around  $\phi = \pi/2$ . Without going into the details (which remain the same as that for open trajectories discussed earlier and as that in section 4.4.6.1), it can be verified that the solutions in the outer layer which match up to the inner solution close to  $\phi = \pi/2$ , are given by

$$r^2 \sin^2 \phi_0 = \int_r^{R_2} \exp \left[ - \int_{r'}^r q(r'') dr'' \right] \frac{B' r'}{(1 - A')} dr',$$

$$r \phi_1 = \frac{1}{r \cos \phi_0 \sin \phi_0} \int_{R_1}^r \exp \left[ - \int_{r'}^r q(r') dr' \right] \left\{ \frac{r' f_1(r', \phi'_0)}{(1 - A')} + \frac{\{(1 - B') \sin^2 \phi'_0 + \frac{B'}{2}\} f_2(r', \phi'_0)}{(1 - A')^2 \sin \phi'_0 \cos \phi'_0} \right\} dr',$$

For zero-Stokes closed orbits  $R_1$  remains  $O(1)$  (infact, it ranges over values very close to the contact value), while  $R_2$  can be arbitrarily large. Considering the limit  $r \gg 1$  ( $R_2 - r \approx O(1)$ ), and using that  $\sin \phi_0 \approx \phi_0 \approx O(r^{-\frac{5}{2}})$ , one obtains

$$\lim_{r \gg 1} \phi_0 \approx \frac{1}{r^{\frac{5}{2}}}, \quad (\text{C.12})$$

$$\lim_{r \gg 1} St \phi_1 \approx \lim_{r \gg 1} \frac{St}{r^{-\frac{1}{2}}} \int_{R_1}^r \exp \left[ - \int_{r'}^r q(r') dr' \right] \left\{ \frac{r' f_1(r', \phi'_0)}{(1 - A')} + \frac{\{(1 - B') \sin^2 \phi'_0 + \frac{B'}{2}\} f_2(r', \phi'_0)}{(1 - A')^2 \sin \phi'_0 \cos \phi'_0} \right\} dr'.$$

The integral is an  $O(1)$  quantity, and one obtains an estimate by replacing  $r$  by  $R_2$  in the upper limit and the integrand. Thus,  $St \phi_1 \approx \phi_0$  for  $r \sim O(St^{-\frac{1}{3}})$ . This implies that for closed trajectories with points of intersection (with the  $y$ -axis) sufficiently far from the origin, to be precise  $R_2 > r \geq O(St^{-\frac{1}{3}})$ , the outer expansion is no longer valid. This is true for large  $r$  regardless of how close  $r$  is to  $R_2$ , and therefore the outer expansion loses its validity before one reaches the inner layer around  $\phi = 0$  (where  $R_2 - r \ll R_2$ ).

The above non-uniformity manifests itself even though one is able to carry out the matching based on the formal magnitude of terms. The solution in the vicinity of  $\phi = 0$  is given by  $\phi = St \tilde{\phi}$ , and

$$\tilde{\phi} = \frac{G_0 B_0 (B_0 - 2A_0 + 2)}{4(1 - A_0)} \left[ 1 + \left\{ 1 + \frac{16(1 - A_0)(\tilde{r} + I_i)}{G_0^2 (B_0 - 2A_0 + 2)^2 R_2 B_0} \right\}^{\frac{1}{2}} \right],$$

where  $r = R_2 + St k' + St^2 \tilde{r}$  and the subscript '0' denotes evaluation of the relevant function

at  $r = R_2$ . Matching gives us

$$k' = -\frac{2(1-A_0)}{R_2 B_0} \int_{R_1}^{R_2} \exp \left[ -\int_{r'}^{R_2} \frac{2(A'' - B'')}{(1-A'')r''} dr'' \right] \left\{ \frac{r' f_1(r', \phi'_0)}{(1-A')} + \frac{\{(1-B') \sin^2 \phi'_0 + \frac{B'}{2}\} f_2(r', \phi'_0)}{(1-A')^2 \sin \phi'_0 \cos \phi'_0} \right\} dr'. \quad (\text{C.13})$$

However, the above procedure remains valid provided  $St k'$  given by the above expression remains small compared to  $R_2$ . For  $R_2 \gg 1$ ,  $(1-A_0) \sim 1$  and  $B_0 \sim O(1/R_2^5)$ . The condition  $St k' \ll R_2$  holds only when  $R_2 \ll O(St^{-\frac{1}{3}})$ , which is consistent with the conclusion above.

Though the perturbation about a zero-Stokes trajectory starting from the same radial distance at  $\phi = \pi/2$  fails, we can carry out a perturbation starting from  $\phi = 0$  as in section 4.4.6.1, and the latter works since the trajectories come closer together as we go towards  $\phi = \pi/2$ . The non-uniformity in the former case is the same as that encountered far downstream for trajectories with  $O(St^{\frac{1}{2}})$  offsets (see section 4.4.3) and is also seen for the off-plane spiralling trajectories in Chapter 5. It has the consequence that for finite  $St$ , and at large distances (along the  $y$  axis) from the reference sphere, the  $y$  coordinates of successive points of intersection of the inward spiralling trajectory no longer differ by an infinitesimal amount.

## C.4 In-plane open trajectories with initial offsets of $O(St^\beta)$

$$(0 < \beta \leq 1/2)$$

We first consider the set of in-plane open trajectories with initial offsets  $z^{-\infty} = m_1 St^\beta$  where  $\beta < 1/2$ , so that they lie within the trajectories with  $O(1)$  offsets, but are asymptotically away the limiting  $O(St^{\frac{1}{2}})$  trajectory. The in-plane gradient displacement for these trajectories is determined in a manner exactly analogous to that for the limiting finite  $St$  trajectory (see

section 4.4.3), i.e., we perturb the ‘-’ branch of the actual trajectory about a zero-Stokes trajectory having the same initial offset, and the ‘+’ branch about a different zero-Stokes trajectory with offset  $z^{-\infty'}$ ;  $z^{-\infty'} < z^{-\infty}$  because all in-plane open trajectories suffer a negative gradient displacement.

If  $c$  be the distance of nearest approach for the trajectory with offset  $z^{-\infty}$ , then

$$c^2 = m_1^2 St^{2\beta} \exp \left[ \int_c^\infty q(r') dr' \right] + \int_c^\infty \exp \left[ - \int_{r'}^c q(r'') dr'' \right] \frac{B'r'}{(1-A')} dr', \quad (\text{C.14})$$

which implies a solution of the form

$$c = d + St^{2\beta} p_1 + St^{4\beta} p_2 + \dots + St^{2n\beta} p_n + o(St) \quad (\text{C.15})$$

for small  $St$ , where  $2n\beta$  is the greatest integer less than or equal to 1, and  $d$ , the distance of nearest approach for the limiting zero-Stokes trajectory, satisfies equation (4.49). Proceeding as in section 4.4.3, one obtains

$$c' = c + 2 St k(d) = d + St^{2\beta} p_1 + \dots + St^{2n\beta} p_n + 2 St k(d) + o(St), \quad (\text{C.16})$$

where  $k(d)$  is defined in (4.40) and  $c'$  is the distance of nearest approach for the zero-Stokes trajectory with offset  $z^{-\infty'}$ . To find the gradient displacement  $(\Delta z)_{inplane}$ , we need to find a small  $St$  expansion for  $c'$  in terms of  $(\Delta z)_{inplane}$ , which in turn necessitates assuming a suitable form for  $z^{-\infty'}$ . As for the case of trajectories with  $O(1)$  initial offsets, we expect the gradient displacement to be much smaller than  $z^{-\infty}$ , that is,  $(\Delta z)_{inplane} \sim O(St^\delta)$  where  $\delta > \beta$ . Accordingly we assume  $z^{\infty'} = m_1 St^\beta + m_1' St^\delta$ , whence  $c'$  satisfies a relation similar

to (C.14) given as

$$c'^2 = \int_{c'}^{\infty} \exp \left\{ - \int_{r'}^{c'} q(r'') dr'' \right\} \frac{B'r'}{(1-A')} dr' + (m_1^2 St^{2\beta} + 2m_1 m_1' St^{\beta+\delta} + m_1'^2 St^{2\delta}) \exp \left\{ \int_{c'}^{\infty} q(r') dr' \right\}. \quad (\text{C.17})$$

The above equation contains additional forcing terms at  $O(St^{\beta+\delta})$  and  $O(St^{2\delta})$ . From (C.16), we see that  $c$  and  $c'$  differ at  $O(St)$  which suggests that the leading order forcing term in (C.17) must be  $O(St)$ . This implies  $\beta + \delta = 1 \Rightarrow \delta = 1 - \beta$ . Hence,  $\delta > \frac{1}{2}$  for  $\beta < \frac{1}{2}$ . This also implies  $O(St^{2\delta}) \sim o(St)$ , and can therefore be neglected. Thus for trajectories with initial offset  $St^\beta$ , the in-plane gradient displacement scales like  $St^{1-\beta}$  and (C.17) becomes

$$c'^2 = \int_{c'}^{\infty} \exp \left[ - \int_{r'}^{c'} q(r'') dr'' \right] \frac{B'r'}{(1-A')} dr' + (m_1^2 St^{2\beta} + 2m_1 m_1' St) \exp \left[ \int_{c'}^{\infty} q(r') dr' \right]. \quad (\text{C.18})$$

The solution of (C.18), to  $O(St)$ , is

$$c' = d + St^{2\beta} p_1 + St^{4\beta} p_2 + \dots + St^{2n\beta} p_n + St p'. \quad (\text{C.19})$$

where  $St p'$  is the correction owing to the forcing term ( $\propto 2m_1 m_1'$ ) in (C.18). Comparing (C.16) and (C.19) gives  $p' = 2St k(d)$ ; now using (C.19) in (C.18) with this value of  $p'$ , one gets

$$p' d \frac{(2-B_0)}{(1-A_0)} = 2m_1 m_1' \exp \left[ \int_d^{\infty} q(r') dr' \right].$$

The in-plane gradient displacement is finally given by

$$(\Delta z)_{inplane} = z^{\infty'} - z^{\infty} = m_1' St^{1-\beta}, \quad (\text{C.20})$$

where

$$m'_1 = \frac{k(d)d(2-B_0)}{m_1(1-A_0)} \exp \left[ - \int_d^\infty q(r') dr' \right]. \quad (\text{C.21})$$

Referring back to (4.45) for  $(\Delta z)_{inplane}$  in section 4.4.1.4, we find that for trajectories with offset  $O(St^\beta)$ ,  $c$  and  $d$  differ by  $o(1)$ , and one can replace  $c$  in (4.45) by  $d$  with an error of  $o(St)$ ; this together with the expression for  $k(d)$  (given by (4.40)) shows that, to  $O(St)$ , the above expression for the gradient displacement is identical to that given by equation (4.45), as should be the case.

For the case when  $\beta = 1/2$ , (C.17) takes the form

$$c'^2 = \int_{c'}^\infty \exp \left[ - \int_{r'}^{c'} q(r'') dr'' \right] \frac{B'r'}{(1-A')} dr' + St(m_1 + m'_1)^2 \exp \left[ \int_{c'}^\infty q(r') dr' \right]. \quad (\text{C.22})$$

Writing  $c' = d + Stp'$ , we obtain in a similar manner

$$p' = \frac{1}{2d} \left[ (2m_1m'_1 + m_1'^2) \exp \left( \int_d^\infty q(r') dr' \right) - p'd \left\{ \frac{2(A_0 - B_0)}{(1 - A_0)} - \frac{B_0}{(1 - A_0)} \right\} \right].$$

and in terms of  $k(d)$ ,

$$m_1'^2 + 2m_1m'_1 - 2k(d)d \frac{(2-B_0)}{(1-A_0)} \exp \left[ - \int_d^\infty q(r') dr' \right] = 0.$$

Solving the quadratic in  $m'_1$ , one gets

$$m'_1 = \frac{1}{2} \left( -2m_1 \pm \left[ 4m_1^2 + 8k(d)d \frac{(2-B_0)}{(1-A_0)} \exp \left\{ - \int_d^\infty q(r') dr' \right\} \right]^{\frac{1}{2}} \right). \quad (\text{C.23})$$

The above expression for  $m'_1$  must tend to (C.21) for trajectories with  $O(St^\beta)$  ( $\beta < 1/2$ )

offsets in the limit  $m_1 \gg 1$ ; this implies choice of the positive sign in (C.23). Indeed, we have

$$\begin{aligned}
\lim_{m_1 \gg 1} m'_1 &= \lim_{m_1 \gg 1} \frac{1}{2} \left( -2m_1 + \left\{ 4m_1^2 + 8k(d)d \frac{(2-B_0)}{(1-A_0)} \exp \left[ - \int_d^\infty q(r') dr' \right] \right\}^{\frac{1}{2}} \right), \\
&= \lim_{m_1 \gg 1} \left( -m_1 + m_1 \left\{ 1 + \frac{2k(d)d(2-B_0)}{m_1^2(1-A_0)} \exp \left[ - \int_d^\infty q(r') dr' \right] \right\}^{\frac{1}{2}} \right), \\
&= \left( -m_1 + m_1 \left\{ 1 + \frac{k(d)d(2-B_0)}{m_1^2(1-A_0)} \exp \left[ - \int_d^\infty q(r') dr' \right] \right\} \right) + o(St), \\
&= \frac{k(d)d(2-B_0)}{\bar{m}_1(1-A_0)} \exp \left[ - \int_d^\infty q(r') dr' \right],
\end{aligned}$$

identical to (C.21).

Therefore, the in-plane gradient displacement for open trajectories with  $O(St^{\frac{1}{2}})$  initial offsets, lying above the limiting open trajectory, is given by

$$(\Delta z)_{inplane} = m'_1 St^{\frac{1}{2}},$$

where

$$m'_1 = \frac{1}{2} \left( -2m_1 + \left[ 4m_1^2 + 8k(d)d \frac{(2-B_0)}{(1-A_0)} \exp \left\{ - \int_d^\infty q(r') dr' \right\} \right]^{\frac{1}{2}} \right).$$

The case  $m'_1 = -m_1$  corresponds to the limiting open trajectory (see (4.53)).

## Appendix D

### Appendices for Chapter 5

#### D.1 Gradient displacement $\Delta z$ in the limit $x^{-\infty}, z^{-\infty} \gg 1$

Using the approximate expressions in section 5.3.3.2, the expression for  $\Delta z$  to be evaluated in this limit can be written as

$$\Delta z = \frac{2St}{z^{-\infty}}(I_1 + I_2 + I_3 + I_4 + I_5 + I_6 - I_7) + St \frac{I_{\theta_1^+} x^{-\infty}}{z^{-\infty}}, \quad (\text{D.1})$$

where

$$\begin{aligned} I_1 &= \int_{c\sqrt{1+\alpha^2}}^{\infty} \frac{15c^3}{2r'^6} \frac{\left\{1 - \frac{(1+\alpha^2)c^2}{r'^2}\right\}^{\frac{1}{2}}}{\left(1 - \frac{\alpha^2 c^2}{r'^2}\right)} dr', \\ &= \frac{15}{4c^2(1+\alpha^2)^{\frac{5}{2}}} \int_0^1 a'^{\frac{3}{2}} \frac{(1-a')^{\frac{1}{2}}}{\left(1 - \frac{\alpha^2}{1+\alpha^2} a'\right)} da', \\ &= \frac{15}{4c^2(1+\alpha^2)^{\frac{5}{2}}} \sum_{n=0}^{\infty} \left(\frac{\alpha^2}{1+\alpha^2}\right)^n \int_0^1 a'^{n+\frac{3}{2}} (1-a')^{\frac{1}{2}} da', \\ &= \frac{15}{4c^2(1+\alpha^2)^{\frac{5}{2}}} \sum_{n=0}^{\infty} \left(\frac{\alpha^2}{1+\alpha^2}\right)^n Be\left(n + \frac{5}{2}, \frac{3}{2}\right). \\ I_2 &= \int_{c\sqrt{1+\alpha^2}}^{\infty} \frac{3c^3}{2r'^6} \frac{1}{\left(1 - \frac{\alpha^2 c^2}{r'^2}\right)} \left[ 15 \left\{1 - \frac{(1+\alpha^2)c^2}{r'^2}\right\}^{\frac{1}{2}} - \frac{5}{\left\{1 - \frac{(1+\alpha^2)c^2}{r'^2}\right\}^{\frac{1}{2}}} \right] dr', \\ &= \frac{15}{4c^2(1+\alpha^2)^{\frac{5}{2}}} \int_0^1 \left[ 3a'^{\frac{3}{2}} \frac{(1-a')^{\frac{1}{2}}}{\left(1 - \frac{\alpha^2}{1+\alpha^2} a'\right)} - \frac{a'^{\frac{3}{2}}}{(1-a')^{\frac{1}{2}} \left(1 - \frac{\alpha^2}{1+\alpha^2} a'\right)} \right] da', \\ &= \frac{15}{4c^2(1+\alpha^2)^{\frac{5}{2}}} \left[ 3 \sum_{n=0}^{\infty} \left(\frac{\alpha^2}{1+\alpha^2}\right)^n Be\left(n + \frac{5}{2}, \frac{3}{2}\right) - \sum_{n=0}^{\infty} \left(\frac{\alpha^2}{1+\alpha^2}\right)^n Be\left(n + \frac{5}{2}, \frac{1}{2}\right) \right]. \end{aligned}$$

$$\begin{aligned}
I_3 &= \frac{15\alpha^2}{8(1+\alpha^2)^{\frac{5}{2}}} \int_{c\sqrt{1+\alpha^2}}^{\infty} \sin^{-1} \left\{ 1 - \frac{(1+\alpha^2)c^2}{r'^2} \right\}^{\frac{1}{2}} \frac{dr'}{r'^3 \left( 1 - \frac{\alpha^2 c^2}{r'^2} \right)^2}, \\
&= \frac{15\alpha^2}{8c^2(1+\alpha^2)^{\frac{3}{2}}} \int_0^1 \frac{b' \sin^{-1} b'}{(1+\alpha^2 b'^2)^2} db', \\
&= \frac{15\pi}{32c^2(1+\alpha^2)^{\frac{3}{2}}} \frac{\sqrt{1+\alpha^2}-1}{(1+\alpha^2)}.
\end{aligned}$$

$$\begin{aligned}
I_4 &= \frac{15\alpha^2}{8(1+\alpha^2)^2} \int_{c\sqrt{1+\alpha^2}}^{\infty} \left\{ 1 - \frac{(1+\alpha^2)c^2}{r'^2} \right\}^{\frac{1}{2}} \frac{c dr'}{r'^4 \left( 1 - \frac{\alpha^2 c^2}{r'^2} \right)^2}, \\
&= \frac{15\alpha^2}{8c^2(1+\alpha^2)^{\frac{7}{2}}} \int_0^1 a'^{\frac{1}{2}} \frac{(1-a')^{\frac{1}{2}}}{\left( 1 - \frac{\alpha^2}{1+\alpha^2} a' \right)^2} da', \\
&= \frac{15\alpha^2}{8c^2(1+\alpha^2)^{\frac{7}{2}} c} \sum_{n=0}^{\infty} (n+1) \left( \frac{\alpha^2}{1+\alpha^2} \right)^n Be\left(n + \frac{3}{2}, \frac{3}{2}\right).
\end{aligned}$$

$$\begin{aligned}
I_5 &= \frac{5\alpha^2}{4(1+\alpha^2)} \int_{c\sqrt{1+\alpha^2}}^{\infty} \left\{ 1 - \frac{(1+\alpha^2)c^2}{r'^2} \right\}^{\frac{1}{2}} \frac{c^3 dr'}{r'^6 \left( 1 - \frac{\alpha^2 c^2}{r'^2} \right)^2}, \\
&= \frac{5\alpha^2}{8c^2(1+\alpha^2)^{\frac{7}{2}}} \int_0^1 a'^{\frac{3}{2}} \frac{(1-a')^{\frac{1}{2}}}{\left( 1 - \frac{\alpha^2}{1+\alpha^2} a' \right)^2} da', \\
&= \frac{5\alpha^2}{8c^2(1+\alpha^2)^{\frac{7}{2}}} \sum_{n=0}^{\infty} \left( \frac{\alpha^2}{1+\alpha^2} \right)^n Be\left(n + \frac{5}{2}, \frac{3}{2}\right).
\end{aligned}$$

$$\begin{aligned}
I_6 &= 5\alpha^2 \int_{c\sqrt{1+\alpha^2}}^{\infty} \left\{ 1 - \frac{(1+\alpha^2)c^2}{r'^2} \right\}^{\frac{1}{2}} \frac{c^5 dr'}{r'^8 \left( 1 - \frac{\alpha^2 c^2}{r'^2} \right)^2}, \\
&= \frac{5\alpha^2}{c^2(1+\alpha^2)^{\frac{7}{2}}} \int_0^1 a'^{\frac{5}{2}} \frac{(1-a')^{\frac{1}{2}}}{\left( 1 - \frac{\alpha^2}{1+\alpha^2} a' \right)^2} da', \\
&= \frac{5\alpha^2}{c^2(1+\alpha^2)^{\frac{7}{2}}} \sum_{n=0}^{\infty} \left( \frac{\alpha^2}{1+\alpha^2} \right)^n Be\left(n + \frac{7}{2}, \frac{3}{2}\right).
\end{aligned}$$

$$\begin{aligned}
I_7 &= \frac{15\alpha^2}{16(1+\alpha^2)^{\frac{5}{2}}} \int_{c\sqrt{1+\alpha^2}}^{\infty} \frac{dr'}{r'^3 \left(1 - \frac{\alpha^2 c^2}{r'^2}\right)^2}, \\
&= \frac{15\alpha^2}{32c^2(1+\alpha^2)^{\frac{5}{2}}} \int_0^1 \frac{da'}{\left(1 - \frac{\alpha^2}{1+\alpha^2} a'\right)^2} da', \\
&= \frac{15\pi\alpha^2}{32c^2(1+\alpha^2)^{\frac{5}{2}}}.
\end{aligned}$$

We have used  $a' = (1+\alpha^2)c^2/r'^2$  as the intermediate variable of integration. In the evaluation of  $I_3$ ,  $b' = a'^{\frac{1}{2}}$ . The final expression for  $I_3$  was looked up from [7]. Using the above integrals and the corresponding far-field approximation of  $\Delta x$  (which contributes to  $\Delta y$  through  $I_{\theta_1^+}$ ), and replacing  $c$  by  $z^{-\infty}$ , one obtains the expression given in section 5.3.3.2 viz. (5.43).